UTILIZATION OF WASTE MATERIALS IN SUBGRADE OF PAVEMENT

Ph.D. THESIS

by

ADITYA KUMAR ANUPAM

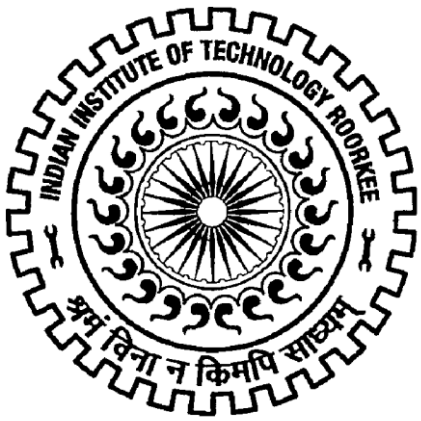

DEPARTMENT OF CIVIL ENGINEERING
INDIAN INSTITUTE OF TECHNOLOGY ROORKEE
ROORKEE – 247667 (INDIA)
JULY, 2013

UTILIZATION OF WASTE MATERIALS IN SUBGRADE OF PAVEMENT

A THESIS

Submitted in partial fulfilment of the requirements for the award of the degree of
DOCTOR OF PHILOSOPHY
in
CIVIL ENGINEERING

by

ADITYA KUMAR ANUPAM

DEPARTMENT OF CIVIL ENGINEERING
INDIAN INSTITUTE OF TECHNOLOGY ROORKEE
ROORKEE – 247 667 (INDIA)
JULY, 2013

©INDIAN INSTITUTE OF TECHNOLOGY ROORKEE, ROORKEE-2013
ALL RIGHTS RESERVED

INDIAN INSTITUTE OF TECHNOLOGY ROORKEE
ROORKEE

CANDIDATE'S DECLARATION

I hereby certify that the work which is being presented in the thesis entitled "**UTILIZATION OF WASTE MATERIALS IN SUBGRADE OF PAVEMENT"** in partial fulfilment of the requirements for the award of the Degree of Doctor of Philosophy and submitted in the Department of Civil Engineering of the Indian Institute of Technology Roorkee, Roorkee, is an authentic record of my own work carried out during the period from July, 2010 to July, 2013 under the supervision of Dr. Praveen Kumar, Professor, and Dr. G. D. Ransinchung R. N., Assistant Professor, Civil Engineering Department, Indian Institute of Technology Roorkee, Roorkee, India.

The matter presented in this thesis has not been submitted by me for the award of any other degree of this or any other Institute.

(ADITYA KUMAR ANUPAM)

This is to certify that the above statement made by the candidate is correct to the best of our knowledge.

(G. D. RANSINCHUNG R. N.)
Supervisor

(PRAVEEN KUMAR)
Supervisor

Date:

The Ph.D. Viva-Voce Examination of **Mr. Aditya Kumar Anupam,** Research Scholar, has been held on…….. …….

Supervisors Chairman, SRC External Examiner

Head of Department/Chairman,ODC

ABSTRACT

A shortage of construction materials and the subsequent rise in their rates has lead to an increase in the cost of road construction in many folds. The shortage of construction material is across the country due to a ban on mining and scarcity of open land for borrows areas. On the other hand, construction of flexible pavement demands enormous quantities of raw materials including soils.

In the coming decades the design, construction and maintenance of roads will face a range of new challenges and as such will require a number of new approaches. Such challenges will result from a growing number of interconnected environmental, social, and economic factors, which are set to apply significant pressure on the future of roads. Natural materials are exhaustible in nature. Hence, their quantity is declining gradually day by day. Concerned about this, highway engineers and scientists have started looking for alternative materials for highway construction, and waste product is one such category. Enormous quantities of domestic, industrial, agricultural and mining wastes are generated annually in the world. Therefore, authorities face the challenges of reinforcing their available infrastructure for efficient waste management and ensuring a scientific disposal of the wastes. If these materials can be suitably utilized in highway construction, the pollution and disposal problems may be partly reduced. Huge amount of construction materials are required to meet the demands of the increasing road network in India. The use of conventional material like soil for a large road network may result in scarcity of naturally available materials; hence an alternative is required to fulfill these demands. Use of locally available materials, including marginal and industrial waste materials could be one of the possible solutions to reduce the consumption of conventional materials. Studies have been conducted in several forms using waste materials in subgrade construction. However, the use of new waste materials and technologies is not becoming popular owing to certain procedural constraints as well as lack of awareness and therefore appropriate steps may have to be taken for popularizing the waste materials for building sustainable roads. This may also result in the conservation of natural resources, thus protecting the environment.

One of the major causes for flexible pavement failure is the weak foundation due to the presence of soft clay particles in soil subgrade. In recent time, one of the topics that have recently received much attention from highway engineers is the study on problematic soils. Basically, a soil is problematic when it exhibits an unexpected behavior under specific conditions and this unpredicted behavior will, in many cases, cause problems during road construction. As clay soils are highly expansive in nature in presence of moisture; clay soil is considered among these problematic soils. India is one of the countries where expansive soil is prevalent in most of its region. Therefore, more of such problems are frequently encountered during construction of highways. Hence, with the perspective to upgrade clayey soil as a construction material using various waste materials like fly ash, bagasse ash, rice straw ash, rice husk ash, bagasse fiber, and recycled fines obtained from demolished concrete slabs to explicitly recommend the most suitable stabilizers in terms of their effectiveness and economy, the present research work has been taken up. It is more important as India produces a huge amount of waste materials as byproducts from different sectors like industrial, agricultural, construction etc. The quantities of wastes (such as cement and lime kiln dusts, quarry waste, slags, fly ash, construction & demolition wastes, rice husk ash bagasse ash, etc.) accumulating throughout the world are causing disposal problems that are both financially and environmentally expensive. To deal with the growing disposal problem of such waste materials is an issue that requires co-ordination and commitment on the part of all parties involved such as government agencies, companies, the public and professionals. One of the most effective ways to overcome such problem is by recycling and utilizing these waste materials in the construction of highways. Therefore, the present research is aimed at investigating the soil engineering properties with and without stabilizers to check their suitability and make maximum utilization of these waste materials in highway construction.

In the present study, the influence of different waste materials on the geotechnical characteristics of soil were investigated by conducting various laboratory tests. Tests were performed for various combinations of soil-waste materials as 0, 5, 10, 15, 20, 25, 30, & 35% of fly ash (FA), bagasse ash (BA), rice straw ash (RSA), rice husk ash (RHA) & fines obtained from demolished concrete slab (FDCS) and 0, 0.5, 1.0, 1.5, 2.0, 2.5, 3.0, & 3.5% of bagasse fiber (BF). The tests were conducted in accordance with IS and ASTM standard codes.

Chosen additives were subjected to the thermo gravimetric analysis (TGA) in a dry air atmosphere by maintaining heating rate of 10°C/min. Samples weighing 80 mg were heated at preselected heating rates from ambient temperature to 850°C in a Mettler thermal analyzer. The TGA curve showed that the mass loss for FA & RHA was 1.0-1.5% even after heating at a temperature of 650°C, whereas in case of BA & RSA it was 8-10%.

Initially, physical and chemical properties of clayey soil and waste materials were analyzed and compared. Then wet grain size analysis was conducted for clayey soil to accrue the details of particle size distribution, and soil classification was done in accordance with IS: 1498. Tests like Atterberg limits, shrinkage limits; maximum dry density (MDD) & optimum moisture content (OMC), California bearing ratio (CBR), unconfined compressive strength (UCS), static triaxial and cyclic triaxial tests were conducted to study the soil engineering properties with and without waste materials (stabilizers). Also, investigations on microstructures of clay soil and stabilized soils were carried out to elucidate their changes in relation to consequent improvement on engineering properties such as strength and permeability. Effort was also made to study the deformation behavior of different compacted layers of pavement in a model tank under repeated applications of load.

Admixing of FA, BA, RHA RSA and FDCS increased the shrinkage limits remarkably. This increase was more pronounced for RHA and FA admixed with soil samples. Similar behavior was also observed for soil admixed with BA and RSA, BF and FDCS. Highest CBR value was observed for FDCS admixed soil sample amongst all the selected soil mixtures irrespective of days of curing. No significant improvement on CBR was observed for BF reinforced soil sample. However, BF reinforced soil sample produced remarkable unconfined compressive strength irrespective of days of curing and which has proven to be the best in all the additives used. Reinforcing BF into clayey soil not only improved split tensile strength but also improved the modulus of subgrade reaction and ultimate strength considerably. However, as far as modulus of subgrade reaction is concerned, FDCS is more effective by offering the highest k-value in comparison to the rest of the mixes.

Based on the cyclic triaxial test, substantial improvements in resilient modulus were noted on admixing of FA, BA, RHA, RSA, FDCS and BF irrespective of confining pressure applied. Resilient modulus increased with the percentage increase of additives. In overall, lower permanent strains were observed on admixing of FA, BA, RHA, RSA, FDCS and BF in comparison to clayey soil. However, the least permanent strain was observed for BF admixed soil sample followed by FDCS, RSA, RHA, BA and FA admixed soil samples respectively.

SEM micrographs were determined to analyze the significant changes in mineralogical phases of stabilizers in presence of moisture. Calcium silicate hydrates (CSH) developed at early stage in case of the RHA, RSA, FA and BA admixed soil. Whereas in case of BF admixed soil, fibrous materials tend to reinforce the soil mass.

Efforts were made to establish correlation between different strength parameters, additives content and days of curing for FA, RSA, RHA, BA, FDCS and BF. The correlation between strength parameters, percent additives and curing days was developed by multiple linear regression analysis using 7, 14, 28 & 56 days results. The validation of the developed relation was done using the results of 128 days strength parameters results. Validation results were compared between the predicted values from developed equation and results obtained in laboratory.

The behaviour of pavement under repeated load has been studied by model tank test which was constructed with a subgrade (natural and treated stabilized soil), sub base, base layer of wet mix macadam (WMM), dense grade bituminous macadam and bituminous concrete (BC). The total deflection on surface of specimen was determined and vertical stress was evaluated at each interface of layer and bottom to better understand the dynamic behaviour of a portion of natural soil subgrade and treated soil subgrade by LVDT and pressure cell. In same manner, the vertical stresses at each interface of layer and bottom of subgrade were determined by KENPAVE software. Three magnitude of pressure 0.57 MPa, 0.40 MPa and 0.20 MPa were applied to determine stress and strain for model tank test as well as KENPAVE analysis.

For the cost benefit analysis of the stabilized soil by different types of additives, it is pertinent to evaluate the pavement thickness reduction in different layers based on its CBR value. The pavement structure was designed based on the CBR value and the cost analysis was done to compare the cost of flexible pavements having stabilized and non-stabilized subgrade. The total thickness of pavement was 805 mm with natural subgrade soil and minimum value was 555 mm after admixing of FDCS or RSA. This reduction in thickness leads to reduction in cost by 30.90%. It was seen that all waste materials used for subgrade soil at their optimum content of admixing not only improve the strength but also reduce the total cost of pavement.

ACKNOWLEDGEMENT

First and foremost, I thank the almighty God who showered his blessings, without which it would have not been possible for me to complete the dissertation in the present form.

Today when I am intended to attain another milestone of my life in the form of this thesis, it will be simple to name all those people who helped me to get this done, but it will be tough to thank them appropriately. I would like to thank God for blessing me the company of such nice people around me.

I wish to express my deep and sincere gratitude to **Dr. Praveen Kumar**, Professor, Department of Civil Engineering, Indian Institute of Technology Roorkee, who was gracious enough for esteemed guidance and keen interest at various stages of this work. His painstaking effort in going through the manuscript and giving precious advice and suggestions for its improvement are gratefully acknowledged. I am also thankful to his wife **Mrs. Ruchi Agrawal** and children **Divyakshi** and **Prakhar** for welcoming me at their home at times.

I express my heartfelt thanks and indebtness towards **Dr. G. D. Ransinchung R. N.**, Assistant Professor, Department of Civil Engineering, Indian Institute of Technology Roorkee, for all the enlightening discussions with him and for the motivation he instilled to give my full best for this research. I would also like to thank him for his generous help, encouragement and suggestions for improvement. A very special note of thanks is due to his wife **Mrs. G.D. Shweta** and children **Spandan** and **Elbert** for the hospitality they rendered upon me each time I visited them.

I express my thanks to **Dr. D. Kashyap**, Professor and Head, Department of Civil Engineering, Indian Institute of Technology Roorkee, for making available the departmental facilities during this research.

I wish to place on record my gratitude to **Dr. Satish Chandra,** DRC Chairman, **Dr. Akhil Upadhyay** SRC Chairman, **Dr. Mahendra Singh,** Member SRC, Professor, Department of Civil Engineering and **Dr. M. R. Maurya**, Member SRC, Professor, Department of Chemistry, Indian Institute of Technology Roorkee, for their valuable suggestions and recommendations during my research work.

I would like to express my sincere thanks to **Dr. S. S. Jain** and **Dr. M. Parida**, Professor, Indian institute of Technology Roorkee, for their advice, concern and good wishes during the course of this research work. I would also like to express my sincere thanks to **Dr. Rajat Rastogi,** Associate Professor and **Dr. Indrajit Ghosh**, Assistant Professor, Department of Civil Engineering and other faculty members of Civil Engineering Department for their good wishes and moral support during the course of this research work.

I wish to convey my sincere thanks to **Mr. Pradeep Kumar**, Lab Incharge Transportation Engineering laboratory and **Mr. Praveen Ahuja**, Lab Incharge, Environment Laboratory for their wholehearted cooperation and friendly research environment.

My thanks are also due to **Mr. Rakesh Kumar, Mr. J. P. Mishra, Mr. Raj Pal, Mr. Bhopal Singh, Mr. Dal Singh, Mr. Mukesh, Mr. Pushpendra, Mr. Gyanendra** and **Mr. Manish** for providing their assistance during laboratory investigations.

I am extremely thankful to **Mr. Yogesh U Shah, Research Scholar,** CTRANS, Department of Civil Engineering, Indian Institute of Technology Roorkee, and **Dr. Maninder Singh,** Assistant Professor, Punjabi University Patiyala, who supported me and helped me constantly for the improvement of my research work. I will always cherish the time spent with them during my stay at IIT Roorkee.

I wish to convey my thanks to my friends **Dr. Sanjeev Suman, Dr. Ankit Gupta, Dr. Sushil Kumar Singh, Mr. R. P. Singh, Mr. Kunal Jain, Lokpriya, Arpan Mehar, Haider, C. Naveen, Shashi Kant, Nikhil** and **Amardeep** for their support and encouragement during this research.

I would also like to thanks my close friends **Ankit Chakrawarti, Divyesh Patel, Kamlesh Jangid, Himanshu Panjiar** and **Ajay Lodhi** for wonderful company they gave me during my stay in Azad Bhawan IIT Roorkee. They have always given me tremendous moral support and I thank them for their constant support and friendship.

I convey with my heartiest feeling, the never ending heartfelt stream of caring and blessings of my respected parents **Shri Yugal Kishor Pathak and Smt. Sharda Devi** for their encouragement and moral support during the course of this study. Their foresight and valuable paved the way of a privileged education since my childhood. They are pillars of my strength, motivation and inspiration. I give my heartfelt gratitude and thanks to my sister **Snigdha Gautam** and brother-in-law **Mr. Rahul Gautam** along with their daughter **Ishanvi,** who have always been an inspiration for my success.

Last but not least, I am extremely thankful to those people who directly and indirectly helped me during this research and for the moral support given to me.

(**ADITYA KUMAR ANUPAM**)

CONTENTS

LIST OF FIGURES

LIST OF TABLES

NOMENCLATURE

AASHTO	American Association of State Highway and Transportation Officials
ASTM	American Society for Testing and Materials
BA	Bagasse Ash
BC	Bituminous Concrete
BF	Bagasse Fiber
c	Cohesion
CBR	California Bearing Ratio
CCRs	Coal Combustion Residues
CD	Consolidated Drained
CU	Consolidated Undrained
DBM	Dense Graded Bituminous Macadam
DOT	Department of Transportation
DSL	Deviator Stress Levels
E	Modulus of Elasticity
ER	Expansion Ratio
FA	Fly Ash
FDCS	Fines Obtained from Demolished Concrete Slab
FSI	Free Swell Index
GSB	Granular Sub Base
ICAR	Indian Council of Agricultural Research
IRC	Indian Roads Congress
IS	Indian Standard
k	Modulus of Subgrade Reaction
LL	Liquid Limit
LVDT	Linear Variable Differential Transformers
MDD	Maximum Dry Density
MoRT&H	Ministry of Shipping, Road Transport & Highways
M_R	Resilient Modulus
MSW	Municipal Solid Wastes
Mt	Million Tonne
NHAI	National Highways Authority of India
NHDP	National Highways Development Programme
OBC	Optimum Binder Content
OMC	Optimum Moisture Contents
PI	Plasticity Index
PL	Plastic Limit
PMGSY	Pradhan Mantri Gram Sadak Yojana
PWD	Public Works Department
RHA	Rice Husk Ash
RSA	Rice Straw Ash
SEM	Scanning Electron Microscope

SHIPs	State Highways Improvement Programmes
SL	Shrinkage Limit
STS	Split Tensile Strength
TGA	Thermo Gravimetric Analysis
UCS	Unconfined Compressive Strength
USCS	Unified Soil Classification System
UU	Unconsolidated Undrained
υ	Poisson Ratio
WMM	Wet Mix Macadam
ε_r	Resilient Strain
σ_d	Deviator Stress
φ	Angle of Internal Friction

CHAPTER 1

INTRODUCTION

1.1 GENERAL

Tremendous increase in road infrastructure has been achieved during the last century. Road network in India increases in manifolds under various development schemes like National Highways Development Programme (NHDP), State Highways Improvement Programmes (SHIPs), Pradhan Mantri Gram Sadak Yojana (PMGSY), Bharat Nirman etc. India's road network is considered to be one of the largest in the world, with the total road length of 46.90 lakh kilometers as on 31st March 2011, which constituted 0.70 lakh km of National Highways, 11.69 lakh km of State Highways & Public Works Department (PWD) Roads, 27.49 lakh km of Rural Roads, 4.11 lakh km of Urban Roads and 2.88 lakh km of Project Roads. Total road length increased from 3.99 lakh km as on 31st March 1951 to 46.90 lakh km as on 31st March 2011 and the growth trend is presented in Figure 1.1. This increase is more than 11 times during the 60 years period from 1951 to 2011. The growth trend of the road length for different road categories is shown in Figure 1.2. In order to cater the heavy traffic conditions on the main corridors, a high quality pavement structure is required. The road network has been quantitatively significant under the Golden Quadrilateral project and the North-South and East-West corridors project of National Highways Authority of India (NHAI).

Huge amount of construction materials are required to meet the demands of the increasing road network. The use of conventional materials for such a large network may result in scarcity of naturally available materials; hence an alternative is required to fulfil these demands. The use of conventional materials can be reduced by making use of locally available marginal and industrial waste materials. Researchers have tried to test the efficiency of various types of new waste materials in road construction. The standard procedural constraints and lack of awareness results in use of waste materials not being so popular. This leads to take immediate measures to popularize the new technologies using waste materials for building better cost effective roads. Conservation of natural resources, energy and environment are the added advantage of these.

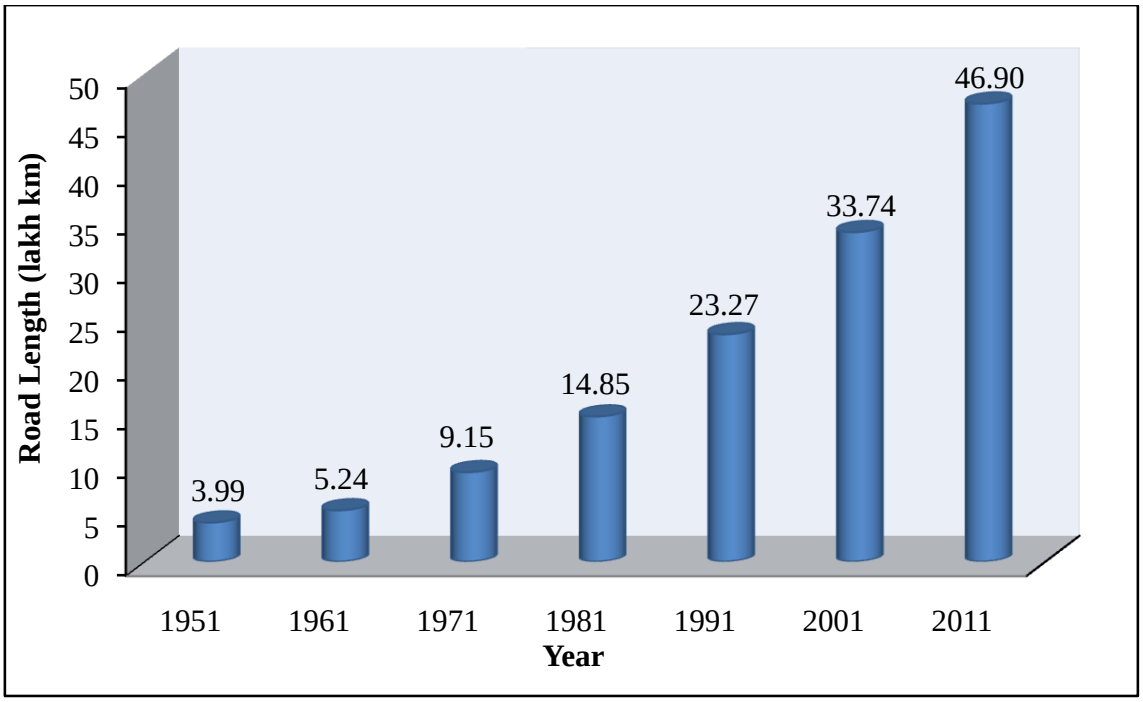

(Source: Basic Road Statistics of India, MoRT&H, 2012)

Figure 1.1 Growth Trend of Total Road Length

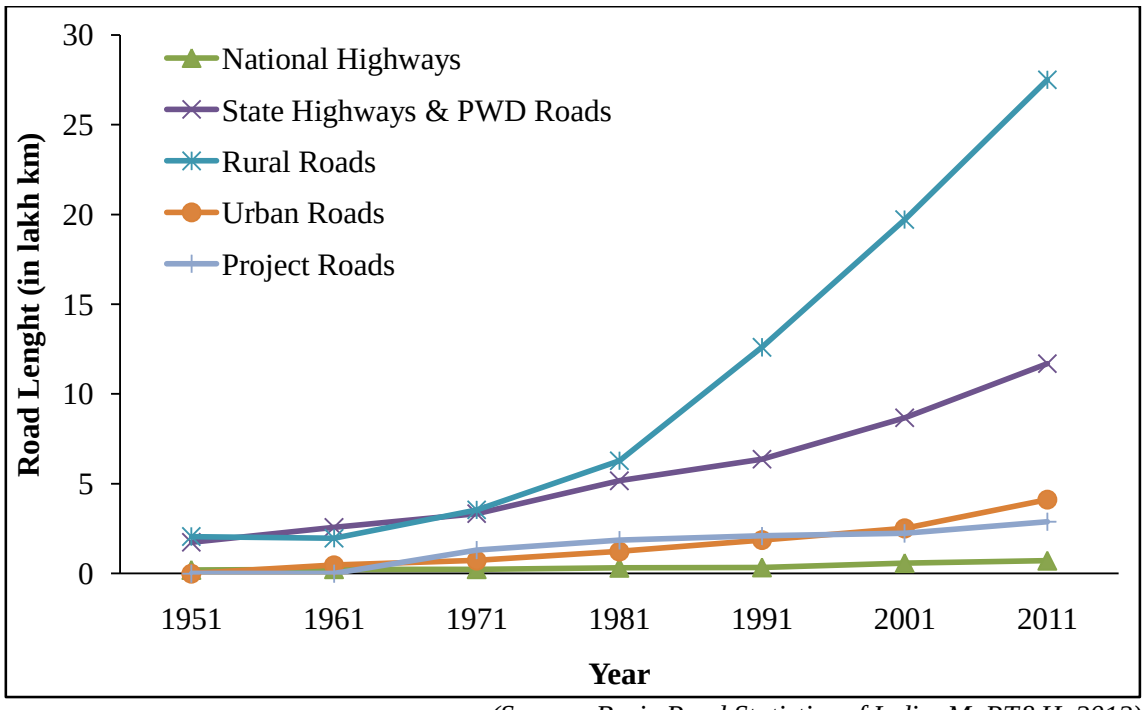

(Source: Basic Road Statistics of India, MoRT&H, 2012)

Figure 1.2 Trend Growth in Road Length by Categories: 1951 to 2011

1.2 BACKGROUND

Generation of waste increases with the growth of population and remains un-decomposed in the environment for several years. Waste disposal crisis arise due to these non-decaying waste materials along with growing population. The best solution to overcome this is its utilization in productive manner.

Enormous quantities of domestic, industrial, agricultural and mining waste are generated annually in India. Factors that have reduced the implication of waste management are lack of financial resources, institutional weaknesses, improper choice of technology and community indifference towards waste. Serious environmental and public health problems have been resulted due to uncontrolled dumping of waste on the outskirts of towns and cities. Industrialization in India has rapidly increased the waste generation. Hence it is a challenging job for the authorities to utilize this waste efficiently and ensure safe disposal of these waste. Implementing new technologies to recover resources from waste management is the only optimal solution for this.

Research projects checking the suitability, performance and environmental sustainability of using recycled waste materials in highway construction have been undertaken by various highway agencies, institutes, government organizations and individuals (Collins and Ciesielski, 1993; Ghaman, R.S. et al. 2004). Research results gave better solutions for safe and economic disposal of waste materials and its use in more cost-effective manner in highway construction sector.

1.3 EXPANSIVE SOILS AND THEIR TREATMENTS

Soil is a very important material for pavement construction. In most cases, poor soil posses a challenge to the pavement engineer and as a way out, he might try to change the design to suit the soil type, improve the soil mass or better it, or abandon the site for a better one. Soil treatment or stabilization is recognized by engineers as a very important process in improving the performance of weak or marginal soils and make perform better as pavement material. Areas with igneous rocks like basalt containing calcium rich feldspars and dark minerals are

found to be source for highly clayey soils. These constituents weather to form amorphous hydrous oxides and clay minerals. The fine-grained, mostly clay size, plastic soil which is highly impermeable, and easily becomes waterlogged, are formed due to absence of quartz leads. Formation of black cotton soil results due to presence of rich magnesium and calcium present in the rock creating swelling problems. Alluvial soil in the gangetic plains has prominence of such highly clayey soils. Expansive soils are clays or very fine silts that have a tendency for volume changes, to swell and soften or shrink and dry-crack, depending on the increase or decrease in moisture content respectively. There are many correlations that identify the potential expansive soils. It may also be possible to identify them visually. Visual indications include wide and deep shrinkage cracks occurring during dry periods, soil rock-hard when dry, but very sticky and soft when wet and damages on the surrounding structures due to expansion of soil (Wayne et al., 1984). These swell-shrink movements in expansive soils have historically caused frequent problems because of the unpredicted upward movements of the structures or cracks in the pavements resting on them. In addition, they also affect the serviceability performance of lightweight structures supported on shallow and relatively flexible footing systems and pavements thereby resulting in road accidents (Furlonge, R. J., 1996 and Taneerananon, P. et al, 2005).

1.4 DISTRIBUTION OF EXPANSIVE SOIL IN INDIA

Expansive soils which include black soil and alluvial soil are widespread throughout India. The main region of black soils is the Deccan plateau and its periphery extending from 8°45'to 26° north latitude and 68° to 83°45' east longitude. The soils are characterised by dark grey to black colour with 35-60% clay, neutral to slightly alkaline reaction, high swelling and shrinkage, plasticity, deep cracks during summer and poor status of organic matter, nitrogen and phosphorus. Mainly found in the Deccan region which includes the major part of Maharashtra, Gujarat and part of Tamil Nadu, Andhra Pradesh and Madhya Pradesh as shown in Figure 1.3. The percentage coverage of black soil is around 29.69 % of total area (ICAR 2010).

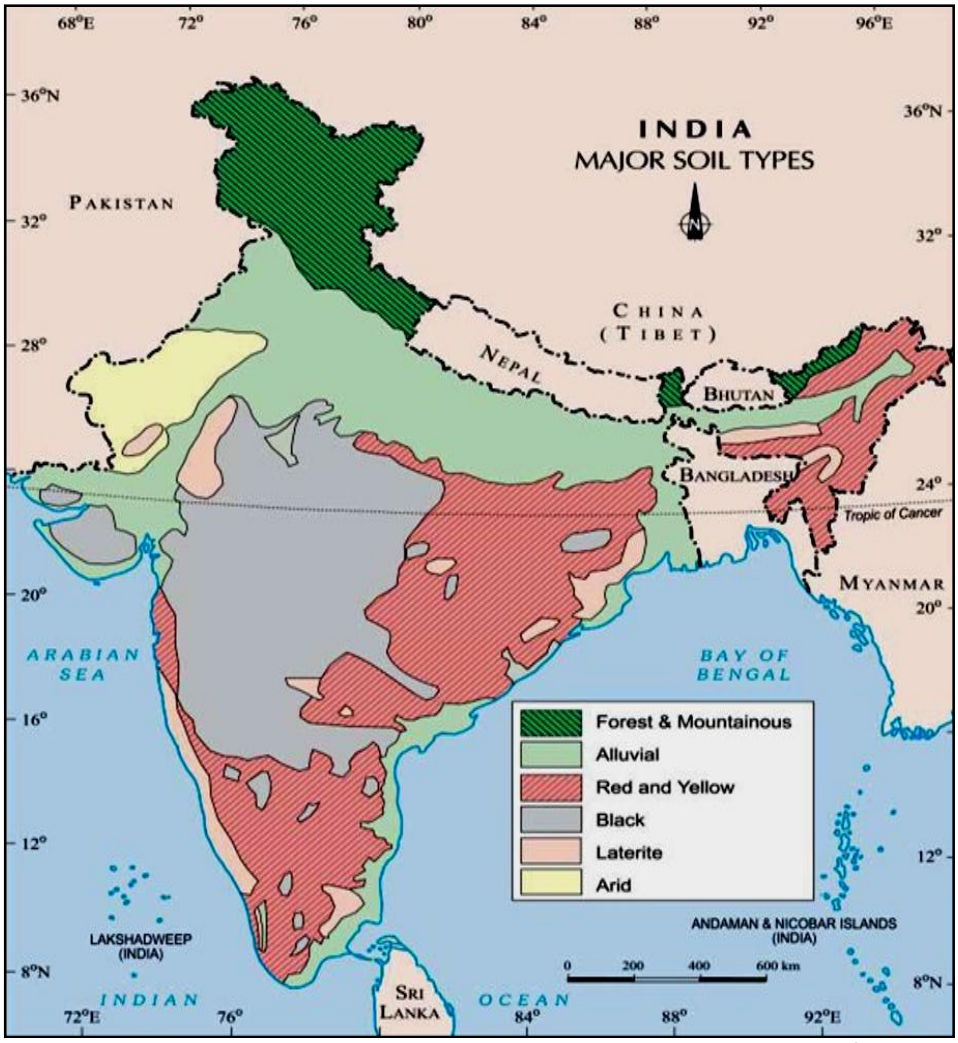

(Source: http://www.docstoc.com/docs/3765459/GEOGRAPHY-Outline-Political-Map-of-India-Identification-only-Major-soil)

Figure 1.3 Distribution of Soil in India

Alluvial soil, cover the largest area in India (approximately 7 lakh km^2) and these are the most important soils from agricultural point of view. The main features of alluvial soils have been derived as silt deposition laid down by the Indian river systems like the Indus, the Ganges, the Brahmaputra and the rivers like Narmada, Tapti, Mahanadi, Godavari, Krishna and Cauvery. These rivers carry the products of weathering of rocks constituting the mountains and deposit them along their path as they flow down the plain land towards the sea. Geologically, the alluvium is divided into recent alluvium which is known as Khadar and old alluvium, as Bhangar. The newer alluvium is sandy and light coloured whereas older alluvium is more clayey, dark coloured and contains lime concretions. The soils have a wide range in soil

characteristics viz. acid to alkaline, sandy to clay, normal to saline, sodic and calcareous, shallow to very deep found in Punjab, Assam, Haryana, Bihar, Uttaranchal, West Bengal, & U.P. In south it is found in the plains and deltas in Tamil Nadu, Orissa and Andhra Pradesh. The percentage coverage of alluvial soils is around 22.16 % of total area (ICAR 2010).

1.5 FACTORS INFLUENCING MECHANISMS IN EXPANSIVE SOILS

There are many factors that govern the expansion behaviour of soil. The mechanism of shrinkage and swelling in expansive soils is rather complex and is influenced by several physical and chemical properties such as clay content, type of clay mineral, crystal lattice structure, cation exchange capacity, ability of water absorption and environmental factors like moisture conditions of the site, magnitude of surcharge load. Nelson and Miller (1992) summarized various factors into three groups, viz., soil characteristics, environmental factors and state of stresses.

Soil characteristics influence the basic nature of the internal force field, which depend on the negative surface charges of clay particles and the electrochemistry related reaction with water. In addition, the swelling capacity of an entire soil mass depends on the amount and type of clay minerals in the soil, the arrangement and specific surface area of the clay particles. Furthermore, on a macro scale, the dry unit weight and physical arrangement of particles will also affect the swell potential (Nelson and Miller, 1992). Environmental factors influence the change of the soil-water system that affects the internal stress equilibrium, the state of stress influences the changes in particle spacing, which in turn influences internal stress equilibrium (Punthutaecha, 2002).

1.6 WASTE MATERIAL GENERATION IN INDIA

Worldwide the quantity of wastes generation was projected to be 12.6 billion tonnes in the year 2002, which constitutes of 11 billion tonnes industrial wastes and 1.6 billion tonnes municipal solid wastes (MSW). About 19 billion tonnes of solid wastes are expected to be generated annually by the year 2025. About 4.4 billion tonnes of solid wastes is generated in Asia; with 3.61 billion tonnes of industrial wastes and 0.790 billion tonnes of MSW (Yoshizawa, et al., 2004). Figure 1.4 shows the sources of solid waste (non-hazardous and hazardous waste)

generation in India. Sugarcane baggase, paddy and wheat straw and husk, oil production, jute fibre, wooden mill waste, coconut husk, groundnut shell, wastes of vegetables, food products, tea, cotton stalk etc. are the major quantity of wastes generated from agricultural sources. Coal combustion residues (CCRs), bauxite red mud, tailings from aluminum, iron, copper and zinc primary extraction processes are the major industrial non-hazardous inorganic solid wastes. About 290 Mt per annum of inorganic industrial wastes are estimated to be generated in India (Ramachandra and Saira, 2004). It has now become the most important to have a technical, economic, eco-friendly solution to maintain the environment green and clear.

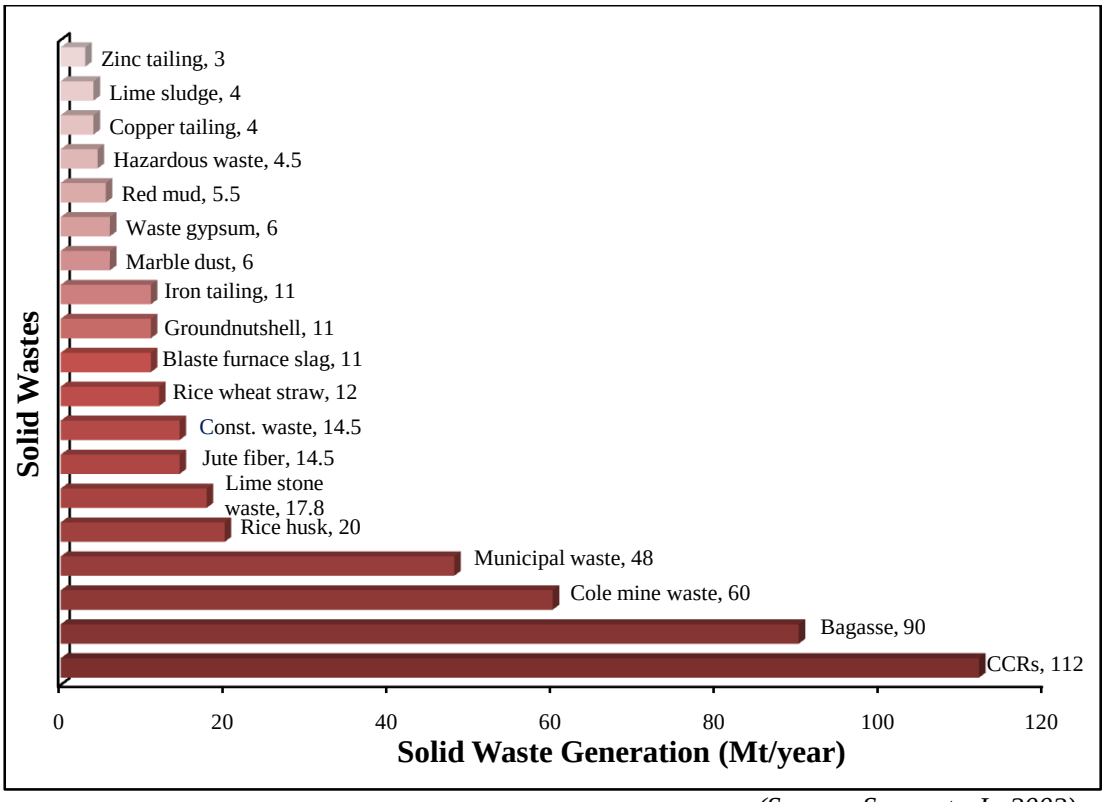

(Source: Sengupta J., 2002)

Figure 1.4 Solid Waste Generation in India (Million Tonne/Year)

India is considered to be largest in production of agricultural products. Agricultural activities such as crop production, crop harvest, saw milling, agro-industrial processing and others are main sources of production of agricultural wastes. Sugar industries in India alone produces about 90 Mt of baggase per year and is used in manufacturing of insulation boards, wall panels,

printing paper and corrugating medium (Sengupta, 2002, Haque et al., 2000). The burning of the agricultural wastes contributes to global warming. Table 1.1 presents the applications of different organic wastes.

Table 1.1 Types and Nature of Solid Wastes and Their Recycling and Utilization Potentials

Type of solid wastes	Source details	Recycling and utilization potentials
Agro-waste (organic)	Bagasse, rice and wheat straw and husk, saw mill waste, ground nut shell, jute, sisal, cotton stalk, vegetable residues	Cement boards, particle boards, insulation boards, wall panels, roof sheets, binder, fibrous building panels, bricks, acid-proof cement, coir fiber, reinforced composites, polymer composites
Industrial waste (inorganic)	Coal combustion residues, steel slag, bauxite red mud, construction debris	Bricks, blocks, tiles, cement, paint, fine and coarse aggregates, concrete, wood substitute products, ceramic products
Mining/mineral waste	Coal washeries waste; mining waste tailing from iron, copper, zinc, gold and aluminium industries	Bricks, fine and coarse lightweight aggregates, tiles
Non hazardous waste	Waste gypsum, lime sludge, lime stone waste, broken glass and ceramics, marble processing residues, kiln dust	Blocks, bricks, cement clinker, hydraulic binder, fibrous gypsum boards, gypsum plaster, super-sulfated cement
Hazardous waste	Contaminated blasting materials, galvanizing waste, metallurgical residues, sludge from waste water and waste treatment plants, tannery waste	Boards, bricks, cement, ceramics, tiles

(Source: Pappu et al., 2007)

1.7 THE USE OF WASTE MATERIALS IN HIGHWAY CONSTRUCTION

Road construction industry in India is at a great boom due to various road construction programmes launched by Indian government. NHDP and PMGSY is two major programmes under which thousands of kilometers of roads are in progress or constructed in a decade and will require huge quantities of road construction materials. In order to execute the road projects which meet the sustainable development needs, many industries are looking forward for a substitute to materials and construction technology. These result in eco-friendly, energy efficient and cost reduction for construction and maintenance of roads.

Enormous studies have been done to improve the pavement strength by using modified bitumen (Awanti, S. S.et al. 2008; Panda, M and Mazumdar, M. 1999 and many others). Alternative option is to improve the subgrade soil strength using waste materials. Use of waste materials which are available locally and in enough quantity is highly emphasized for road construction directly or after treatment. Various combinations of local materials like soil, gravel, moorum, laterite, sand, and waste materials like industrial slag, mine waste, municipal waste, waste plastic, jute geo-textile, soil-enzymes etc. are effectively used as an alternative to conventional materials. Use of steel slag in bituminous to improve its bearing capacity has been presented by Fwa et al. (2004). Bio-Enzyme namely Terra Zyme has been used as stabilizer for improving the geotechnical properties of lateritic and shedi soils. The laboratory results revealed the improvements in its fatigue behavior (Ravi Shankar, A.U et al., 2010). Sahoo et al. (2010) used thin recycles plastic sheets to construct cell filled pavements. The behavior of pavements constructed by filling the cells with (i) cement concrete (ii) soil cement (iii) sand cement laid over two different types of subbase was studied in the field. The problem of disposing used high density polyethylene sheet can be overcome to a large extent by such use. Similarly applications of these materials in road section after studying their engineering properties are as shown in Table 1.2.

1.8 MECHANISMS OF STABILIZATION

The selection of chemical or mechanical stabilization for geo-materials such as soils and rocks, used for construction and maintenance of road networks, is based on the properties of natural soil. Most commonly, mechanical and chemical stabilization techniques are employed.

Table 1.2 Applications of Waste Materials in Highway Construction

Waste material	Sources	Current and past highway uses
Fly ash **(**bottom ash and pond ash)	Thermal power station	Bulk fill in embankment, in subgrade soil, filler in bituminous mix, artificial aggregates
Cement kiln dust	Cement industry	Stabilization of subgrade and base, binder in bituminous mix
Waste glass	Municipal solid waste	Use of glass in asphalt pavements, in Portland cement concrete, in unbound aggregate base layers and embankment construction
Blast furnace slag	Steel industry	concrete aggregate, base/ sub-base material, binder in soil stabilization
Rubber tires	Municipal solid waste	Rubber modified asphalt saving products, use of tires in subgrade/embankment
Rice husk ash	Rice mill	Stabilization of subgrade and base,
Marble dust	Marble industry	Concrete pavement, filler in bituminous mix
Construction and demolition waste	Construction industry	Concrete pavement , base/sub-base material, bulk-fill, recycling

(Source: Schroeder, 1994)

1.8.1 Mechanical Stabilization

Mechanical stabilization is the process of improving the properties of the soil by changing its gradations without any chemical additives. Two or more types of natural soils are mixed to obtain a composite material which is superior to any of its components. To achieve the desired grading, sometimes the soils with coarse particles are added to the soils with fine particles. Sometimes mechanical stabilization is also known as granular stabilization. Soil strength is improved by compaction, use of fibrous and non biodegradable reinforcement geo-materials in case of mechanical stabilization. The properties of stabilized geo-materials and their mixtures should not change by such stabilization techniques.

1.8.2 Chemical Stabilization

Chemical stabilization is the process of modification of the properties of a natural soil to improve its engineering performance. Several additives like lime, cement, fly ash, bitumen etc are considered for soil stabilization. Of all these, the most preferred soil stabilizers are lime and cement. This is true especially for clayey soils. Besides these additions, rise husk ash rich silica material is also considered one of the prominent materials suitable for soil stabilization along with certain amount of cement or lime to further enhance the properties of the stabilized soil. On other hand, a few additives are admixed with clayey soil just enough to make it workable, better in texture and compatibility regardless the strength and durability, then it is referred to as modification (Indiana DOT, 2008). Admixing of certain amount of lime with clayey soils is a good example just to make it pulverize the soil grain better then followed by cement admixing to enhance the soil engineering properties.

Chen (1988) and Nelson et al. (1992) gave various methods for stabilizing expansive soils. "Remove and replace" technique is one of them. In this technique, expansive soil is removed and non – expansive soil brought from selected borrow areas is used for rebuilding the excavated road section. This removal is done for the entire layer if the soil stratum is thin. But if stratum extends to a great depth would be uneconomical. In such situation, excavation is made to an acceptable depth approximately upto 500 mm and the same is rebuilt with selected earth. This strategy is accepted only when good quality earth is abundantly available in local area. Depending upon the severity of site condition, suitable stabilization techniques can be employed. Otherwise, there is a method which can also be implemented by way of pre wetting the site to increase moisture content level. The expansive soil problem can be overcome if high moisture content is maintained by prewetting. Soils with high permeability may never sufficiently wet and that with low permeability may take years to prewet. In such dire situation, either lime stabilization or cement stabilization technique is commonly adopted. However, the most effective measures for clayey soil stabilization are combination of both lime and cement. Stabilization using lime has been extensively used in highway projects and it results in various reactions. Higher pH environment increased the solubility of silica and behaves as a cementing agent. Soil strength is increased due to a divalent cation that can form Casilicates and Ca-Al hydrates due lime addition. Lime stabilization reactions can be slowed down by the presence of

organics, sulfates, and iron compounds. An alternative to lime is fly ash (product of coal combustion). Mixing of fly ash with soil results in flocculation which reduces swell potential in expansive soils; the (Ferguson, 1993).

Furthermore, the effectiveness of the stabilizer can be measured by its ability to provide enough calcium to chemical reaction. Lime, Portland cement and fly ash materials are the most frequently used chemical stabilizers. Fly ash that possesses self-cementing property that can stabilize/treat soil without cement or lime are called class C fly ash, whereas that often used either with lime or cement in order to make it more reactive are called class F or non-cementing fly ash. The mechanism of stabilization for these stabilizers is almost similar regardless of few different processes. Soil improvement by means of chemical stabilization can be grouped into four chemical reactions; cation exchange, flocculation - agglomeration, Cementitious hydration, and pozzolanic reactions. (Prusinski and Bhattacharja, 1999; Mallela et al. 2004).

***Cation exchange*:** The excess of ions of opposite charge (to that of the surface) over those of like charge present in the diffuse double layer are called exchangeable ions. These ions can be replaced by a group of different ions having the same total charge by altering the chemical composition of the equilibrium electrolyte solution (Winterkorn and Pamukcu, 1990). Cation exchange includes an immediate reaction of the clay with the stabilizer within few minutes of mixing, resulting in a soil with improved texture. The tetrahedral (T) and octahedral (O) combination of clay minerals in 1:1 (1T and 1O) or 2:1 (2T and 1O) have charge deficiency that results in the attraction of the cations or water molecule. Generally, sodium or potassium (Na^+ or K^+) are prevalent in clay minerals along with water. However, these cations can be replaced by the higher valance cations like Al^{+3}, Ca^{+2}, Mg^{+2} etc. so called cation exchange. During this process calcium rich chemical stabilizer provides enough cations to replace the monovalent cations resulting in a reduced thickness of diffused double layer (Geiman et al., 2005). The calcium is released in suspension of stabilizer-soil-water and will be available for the stabilization of soil. The exchangeable cations may be present in the surrounding water or be gained from the stabilizers. An example of the cation exchange (Sivapullaiah, 1996) is given below;

$$Ca^{2+} + Na^{+}\text{-Clay} \rightarrow Ca^{2+}\ Clay + (Na^{+})$$

The thickness of the diffused double layer decreases as replacing the divalent ions (Ca^{2+}) from stabilizers with monovalent ions (Na^{+}) of clay. Thus, swelling potential decreases.

***Flocculation and agglomeration*:** Flocculation and agglomeration is the rearrangement of the clay particles from face to face orientation to more compact edge-face orientation. The fine grained soil changes to the more coarse grained with much more improved strength/stiffness as well as workability (Al-Mukhtar et al., 2010; Brooks et al., 2011). As cation exchange, flocculation and agglomeration is also a short-term process, which takes place within few hours of mixing the stabilizer and water with subgrade soil.

***Cementitious hydration*:** In addition to lime, cement contains calcium-aluminate-hydrate (C-A-H) that takes part in the further stabilization of the flocculated clay particles by yielding the glue like structure with calcium-silicate-hydrate (C-S-H). The strength provided by cementitious hydration in cement treated soil is extra strength as compared to the lime treated soils that is the main reason why cement treated/stabilized soil have better strength compared to any other treated/stabilized soils. The rapid gain in strength continues from the day of mixing till a month and may continue up to few years (Prusinski and Bhattacharja, 1999). Sometimes, carbonation occurs in lime treated soils that is undesirable reaction at the start of stabilization because of formation of relatively insoluble carbonates rather than hydrates (Mallela et al., 2004).

***Pozzolanic reaction*:** Time depending pozzolanic reactions play a major role in the stabilization of the soil, since they are responsible for the improvement in the various soil properties (Show et al., 2003). Pozzolanic constituents produces calcium silicate hydrate (CSH) and calcium aluminate hydrate (CAH).

$$Ca^{2+} + 2(OH)^{-} + SiO_2\ (\text{Clay Silica}) \rightarrow CSH$$
$$Ca^{2+} + 2(OH)^{-} + Al_2O_3\ (\text{Clay Alumina}) \rightarrow CAH$$

The calcium silicate gel formed initially coats and binds lumps of clay together. The gel then crystallizes to form an interlocking structure thus, strength of the soils increases (Hadi et al, 2008; Sivapullaiah, 2006).

Fly ash stabilization of the soil is similar to cement; however the strength provided is less than the cement. Depending upon the reactivity, the fly ashes are classified as self-cementing (C-class) and/or non-self-cementing (F-class). Generally, C-class fly ash is applied with either cement or lime, whereas F-class does not include any activating stabilizers.

1.9 NEED OF THE RESEARCH

India produces large quantity of waste materials annually mainly from various sectors like industrial, construction/infrastructure, agricultural etc. These waste materials can be hazardous to human life if not utilized timely. Road construction is one sector, where many of these waste materials can be used after laboratory investigation and judging their suitability for the use in different pavement layers. The study was taken up with an aim to use some of these waste materials in subgrade of pavement construction, thereby creating a sustainable environment.

One of the major causes for pavement failure is the week foundation due to the presence of soft clay in soil subgrade. Various materials like cement, lime, synthetic fiber reinforcement etc. have been used to improve the weak foundation of soft clay soil which are very costly and have handling problem in utilization. About seventy percent of the total electricity is produced using pulverized coal as fuel in thermal power generation units. This process generates huge quantities of coal ashes, in the form of fly ash and bottom ash. In India the production of fly ash was about 131.09 Mt in the year 2010-11. The disposal of this ash is a problem creating environmental pollution. Scientists and engineers in India and abroad are working on increasing its use but still the consumption is far less than its production.

Bagasse ash, rice straw ash and rice husk ash are the waste products produced in huge quantities in different parts of the country. Since their disposal has become severe environmental problem, its use in pavement constructions is one of the suitable alternatives for the safe disposal.

India being one of the largest producers of sugarcane in the world to a tune of average 300 Mt per year, large quantity of sugarcane bagasse is generated by sugar mills. Sugarcane contains about 30-35% bagasse fibers, out of which about 20-30 % is being used as fuel at the sugar mills and very small quantity less than 2% is being used for paper mill packing etc. The remaining bagasse fiber is being left out as waste material of the sugar mills. Their disposal has become a severe social and environmental problem especially in the northern part of India. As a result of which these fibrous materials have been chosen as a soil stabilizer for improvement of soil subgrade properties in the present research work. Besides bagasse fibers and bagasse ash other waste material identified for the study is cement mortar obtained from demolished concrete slabs. Demolished concrete slabs were collected from Roorkee Sabzi Mandi that got removed for renovation of the same. It is estimated the construction industry in India generates about 10-12 Mt of waste annually (Ministry of urban development, Government of India). Reclaimed concrete aggregate is a popular substitute for natural stone aggregate especially in metropolitan areas that are finding their aggregate sources to be increasingly distance. Processing generally involves crushing the concrete and screening it to separate out fine particles from course particles. Generally, the fine fraction is disposed off as waste material. This being the material of rich cement content concrete, there is a possibility of presence of certain amount of slaked lime (calcium hydroxide) in the fines. In order to judge its sutability as soil stabilizer, material passing 1.18 mm IS sieve was considered in the present research work.

1.10 OBJECTIVES OF THE RESEARCH

The main objective of the study is to investigate the use of waste fly ash (FA), bagasse ash (BA), rice straw ash (RSA), rice husk ash (RHA), bagasse fiber (BF), and recycled fines obtained from demolished concrete slabs (FDCS) in subgrade soil stabilization for pavement construction and to evaluate the effect of these waste materials of soil engineering properties. Following are the sub objectives framed to achieve the main objective:

(i) Determination of physical and chemical properties of fly ash, bagasse ash, rice straw ash, rice husk ash, bagasse fiber, fines obtained from demolished concrete slabs and clayey soil.

(ii) Study on thermal analysis of fly ash, bagasse ash, rice straw ash and rice husk ash using TGA.

(iii) Determination of performance related tests like unconfined compressive strength, split tensile strength, triaxial, modulus of elasticity and California bearing ratio value for soil samples with or without waste materials under static loading condition.

(iv) Microstructural study of clay soil and stabilized soils to elucidate their changes in relation to consequent improvement on engineering properties such as strength and permeability.

(v) Determination of resilient strain, permanent strain and resilient modulus using repeated triaxial test under dynamic loading condition for soil samples with or without stabilizers.

(vi) Determination of modulus of sugrade reaction and ultimate bearing capacity of soil samples with or without stabilizers using plate load test.

(vii) Study on distribution of vertical stresses at the interface of different pavement layers using model tank and KENPAVE analysis.

(viii) Development of regression models for subgrade soil strength parameters.

(ix) Economic analysis Cost comparison.

1.11 SCOPE OF THE PRESENT WORK

Scope of the present study is confined to following area:

- Only six waste materials were used to determine its efficacy for subgrade construction.
- The mix was isolated to determine the engineering properties of admixed soil.
- Only CL type of expansive soil was used for stabilization.
- All tests were conducted in laboratory at room temperature.
- All conclusions and recommendations drawn based on only laboratory work.

1.12 ORGANIZATION OF THE THESIS

This thesis includes a total of eight chapters. Chapter 1 contains introduction part that presents total growth of road network, distribution of expansive soil, waste generation in India, mechanisms of soil stabilization, need, objectives and scope of present work.

Chapter 2 summarizes the review of literature related to the engineering behaviour of different types of waste materials like fly ash, bagasse ash, rice straw ash, rice husk ash, bagasse fiber,

and recycled fines obtained from demolished concrete slabs. Influence of these materials on geotechnical properties of soil is also discussed. Various applications of these waste materials in construction field are presented in this chapter.

Chapter 3 highlights the various combinations of soil-waste materials mix considered in present study. The influence of various combinations of soil-waste materials on the geotechnical characteristics of soil were investigated by conducting various tests in the laboratory as per the standards and the detailed tests procedures are described in this chapter.

Chapter 4 presents the material characterization of expansive soil and different additives. Details of sources, physical & chemical and other basic properties of all materials like soil, FA, RHA, RSA, BA, BF and FDCS are discussed.

Chapter 5 describes the test results and their interpretation, for all laboratory tests that were performed on the natural and treated subgrade soils. The tests were performed for various combinations of soil with waste materials as soil-FA, soil-RHA, soil-BA, soil-RSA, soil-FDCS and soil-BF, mixtures. In addition, the regression correlations developed between different strength parameters, days of curing and different percent of waste additive are presented.

Chapter 6 highlights the behaviour of pavement under repeated load studied by model tank test. The total deflection on surface of specimen was determined and the vertical stress was evaluated at each interface layer and bottom to study the dynamic behaviour of natural soil and treated soil subgrade. The vertical stress, strain and deflection at each interface layer and bottom of subgrade, evaluated using KENPAVE software is also described in this chapter.

Chapter 7 gives the summary of the cost analysis for flexible pavement with stabilized and non-stabilized subgrade soil. The pavement thickness was designed based on the CBR value and the comparative cost analysis was carried out.

Chapter 8 presents the conclusions derived from this study and shows the efficacy of different waste materials like FA, RHA, BA, RSA, FDCS and BF admixed with soil for subgrade construction. The recommendations for future research in this area are also summarized.

CHAPTER 2

LITERATURE REVIEW

2.1 GENERAL

The amount and type of waste generated increases with increase in population. These wastes remain in the environment for longer duration since it is unused. The waste disposal crisis arose due to the creation of non decaying waste materials. Recycling of this waste disposal into useful products is the only solution through which this crisis may be dealt with. Now days, a number of new and innovative methods and techniques are being worked upon to find the uses of waste materials. For the utilization of waste products in highway construction, many private organizations including highway agencies and researchers have initiated the processes and reported various studies which prove that use of these waste materials is environmental sustainable and viable. Soil subgrade layer is one such layer where large quintiles of waste materials can be used to strengthen the mechanical properties of problematic soils.

This chapter synthesizes the information on the use of industrial and agricultural waste materials in highway construction. The mechanism of soil stabilization using different waste materials is explained. The applications of selected waste materials including fly ash, rice husk ash, bagasse ash, rice straw ash, bagasse fiber and fine C&D debris are critically reviewed.
Studies based on economic, environmental and technical factors indicate that the use of these waste materials as full or partial replacement to the conventional materials being used in the highway construction prove to be much more economical and should be projected for future construction.

2.2 APPLICATION OF FLY ASH

Coal/Lignite based Thermal Power Generation has been the backbone of capacity addition in the country. Indian coal is of low grade having high ash content up to 40% in comparison to imported coals which have ash content of the order of 10-15%. Thermal Power Stations

utilizing coal/lignite generate large quantity of ash in the country, which has been one of the source of pollution of both air and water.

Fly ash generation & utilization data for the year 2010-11 as obtained from 88 thermal power stations using coal/lignite of different power utilities in India having a total capacity of approx. 80,458 MW are as shown in Table 2.1.

Table 2.1 Summary of Fly Ash Production and Utilization

Components	Values
Installed capacity	80458 MW
Coal consumed	407.61 Mt
Average Ash content	32.16%
Total Ash generated	131.09 Mt
Total Ash utilized	73.13 Mt
Percentage Utilization	55.79%

(Source: Central Electricity Authority, 2011)

In year 2010-11 total ash generated was 131.09 Mt of which 55.79% was utilized in different modes and 44.21% was unutilized in India as shown in Figure 2.1. The various modes used for utilizing the ash during the year 2010-11 along with utilization in each mode are shown in Figure 2.2. It can be seen from Figure 2.2 that the maximum utilization of fly ash is 48.50% in cement sector, followed by 12.73% in reclamation of low lying area, 11.65% in roads & embankments. Utilization of fly ash in road and embankment is a lesser amount (only 6.50% of total production during the year 2010-11) and it can be increased.

The progressive total ash utilization and its utilization in road and embankment for the period from 1998-99 to 2010-11 are given in Figure 2.3. As compared to total fly ash utilization every year, fly ash utilization in road and embankment is quite low which indicates its use in other modes. Hence efforts should be made to utilize more fly ash in sector of road and embankment.

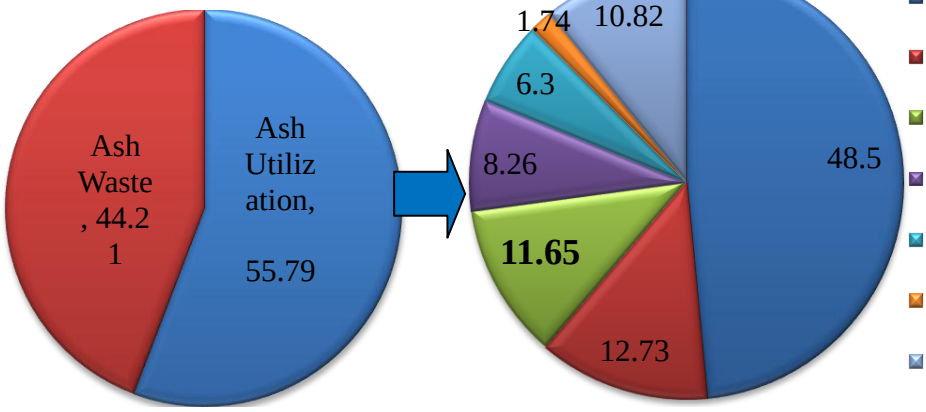

Figure 2.1 Percentage Ash Utilization and Waste during the Year 2010-11

(Source: Central Electricity Authority, 2011)

Figure 2.2 Percentage Ash Utilization in Each Mode during the Year 2010-11

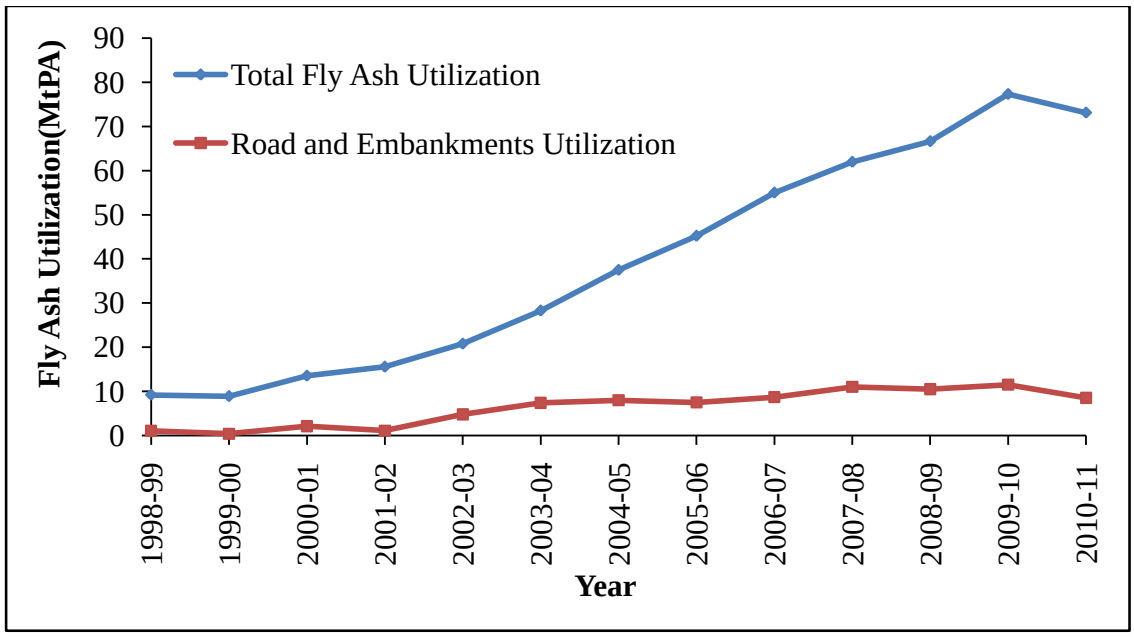

(Source: Central Electricity Authority, 2011)

Figure 2.3 Progressive Utilization of Fly Ash in Road and Embankment

Indian coals, though low in sulfur, contain higher amount of ash, resulting in huge quantities of fly ash in India. Under ionized conditions, fly ash can produce an adequate range of trivalent and divalent cations (Al^{3+}, Fe^{3+}, Ca^{2+}, etc.) which promote flocculation of dispersed clay particles. Thus, expansive soils can be potentially stabilized by cation exchange using fly ash

(Kumar, A. et al., 2007). As per IRC: SP: 58-2001 fly ash is acceptable for embankment with typical values for different geotechnical properties as given in Table 2.2.

Table 2.2 Typical Geotechnical Properties of Fly Ash

Parameter	Range
Specific Gravity	1.90-2.55
Plasticity	Non-Plastic
Maximum Dry Density (g/cc)	0.9-1.6
Optimum Moisture Contant (%)	38.0-18.0
Cohesion (kN/m^2)	Negligible
Angle of Internal Friction (φ)	30°-40°
Coefficient of Consolidation C_v (cm^2/sec)	1.75×10^{-5}-2.01×10^{-3}
Compression Index C_c	0.05-0.4
Permeability (cm/sec)	8×10^{-6}-7×10^{-4}
Particle Size Distribution (% of materials)	
Clay size friction	1-10
Silt size friction	8-85
Sand size friction	7-90
Gravel size friction	0-10
Coefficient of Uniformity	3.1-10.7

(Source: IRC: SP: 58-2001)

Dhawan, P. K. et al. (1994) explored the feasibility of ash utilization in bulk for road construction. They considered three types of ashes as fly ash, bottom ash & pond ash admixed with different types of soil as CL, ML & CH for laboratory investigation. Data revealed that the maximum dry density of soil-coal ash mixes decrease with increase in coal ash content as compared with the density of neat soils. The result CBR values indicated that improvement of CBR values of the soil with the coal ash from thermal power station I as compared to soil-coal ash mixes from other three (II, III & IV) thermal power station was more. Based on the improvement of the CBR values of soil-coal-ash mixes authors concluded that soil-bottom ash/pond ash mix from thermal power station I can be used as a sub base materials. The soil-fly-ash mixes from thermal power stations I & III, and soil-fly ash/pond ash mixes from thermal power station II could be used as embankment materials and/or for improving the subgrade soils.

FA-soil mixtures were stabilized using 3.0-9.0% cement, the baumineral FA taken from Bochum, Germany. Kaniraj, S.R. and Havanagi, V. G. (1999) mixed Rajghat FA from Delhi, India, and silty and sandy soils in different proportions. These samples were then subjected to unconfined compression tests. Results of UCS values and secant modulus in terms of FA content, curing period, and cement content were used to establish correlations. Correlations between cement content, water content and curing period have also been developed and shown in Table 2.3.

Table 2.3 Summary of Correlations Established

S N	Test name	Relations	R^2
1.	Unconfined compressive strength(q_c)	$q_c = q_{co} + \frac{t}{mt + c}$ Where, $m = 0.00292 \times 1.0113^{FA} \times 0.686^{C}$ $c = 0.0292 \times 1.014^{FA} \times 0.724^{C}$	0.91 0.87
2.	Secant modulus(E_s)	$E_S = E_{SO} + \frac{t}{nt + d}$ Where, $n = 1.487 \times 10^{-5} \times 1.016^{FA} \times 0.771^{C}$ $d = 0.00116 \times 1.0041^{FA} \times 0.603^{C}$	0.93 0.74
3.	Change in water content(w)	$w = 37.52 - 0.0834t - 0.563C$ $w = 37.64 \times 0.9975^{t} \times 0.9836^{C}$	0.92 0.92

(Source: Kaniraj, S.R. and Havanagi, V. G., 1999)

Where, q_{co} = Measured initial unconfined compressive strength

E_{so} = Measured initial secant modulus

t = Curing time

FA = % Fly Ash

C = % Cement

The authors assumed the hyperbolic nature of gain in secant modulus of FA-soil mixtures and UCS with time. The results indicate that strength and modulus increases with increase in cement content and decreases with increase in FA content. High influence of cement content was observed than the FA content. The water content of a FA-soil mixture depends on the curing period and cement content. As the curing time and cement content increases, the water content decreases. Cement content has much more effect than that of the curing time.

Shirazi, H. (1999) observed the performance of lime and FA-stabilized base as an alternative to soil-cement-stabilized base for flexible pavement systems on reconstructed highways in Louisiana. He tested two combinations one with 2% lime and 4% FA, and another with 3% lime and 6% FA and soil-cement base at 8% cement by volume. The analysis was based on cracking, rutting and unconfined compression strengths tests. Both field and laboratory samples were tested for unconfined compression at 7 days, 28 days, and 56 days interval. The results revealed that the sections stabilized with soil-cement cracked more extensively and earlier than the lime and FA test sections. It was concluded after experimentation that the soil-cement stabilized base are more prone to shrinkage compared to lime and FA. No significant rutting occurred on both FA-stabilized and cement-stabilized test lanes and control sections in any of the test or control section monitoring strips as indicated by the dynaflect results. Soil-cement bases have much higher unconfined compression strengths compared to lime and FA bases. The above fact did not result in long-term performance or reduced structural numbers.

Zia, N. and Fox, P. J. (2000) used Class C FA to improve the engineering properties of Indiana loess soils. FA was mixed in various percentages with loess soil and then the specimens were allowed to cure for 3 h to 28 days. Pure loess also was tested for comparison. Changes in unconfined compression strength Atterberg limits, swell potential and moisture-density relationships were presented. The maximum dry unit weight decreases abruptly at 11 to 15% FA content and then decreases slightly thereafter. The OMC generally increased with increasing FA content. The increase in FA content results in increase in finer particles, which in turn results in higher specific surfaces in the loess-FA mixtures and thus increases in hydration of loess and FA mixtures. 9% FA content results in optimum moisture content and maximum dry unit weight of the loess–FA mixture. UCS increased with FA content up to 11% for specimens cured up to 14 days. The strength of specimens that contained higher FA contents (15 and 20%) increased up to 7 days of curing. Most strength development occurred within 7 days for all mixtures. Unconfined compression strength decreased for all the mixtures after 7 to 14 days, reaching the level consistent with the pure loess specimen at 28 days when FA contains more than 11%. CBR values for pure loess and two mixtures containing 10 and 15% FA were presented. The CBR increased for the mixture containing FA upto 10%, and then

further addition of FA decreased CBR. The maximum swell magnitude for the mixture containing 10% FA decreased by 55% compared with the pure loess soil, whereas values for the mixture containing 15% FA were 255% higher than those for pure loess soil.

Sobhan, K. and Mashnad, M. (2003) evaluated the mechanical performance of a soil–cement–FA mix, reinforced with recycled plastic waste. They determined the flexural strength, compressive strength, toughness and split tensile strength characteristics of the composite recycled plastic strips. Laboratory results revealed that the soil–cement matrix stabilized with 4 to 10% by weight of FA and reinforced with 0.25 to 0.5% by weight plastic waste. Split tensile strength and compressive strengths achieved are 1000 kPa and 7000 kPa by using soil–cement mix in base course 10% FA, 10% cement and 0.5% of 38 mm long fibers. Reinforcing the same mix by 0.8% fibers results in approximately 1200kPa increased flexural strength. Reinforcement provided by using fiber resulted in considerable improvement in toughness index (TI) compared to unreinforced specimens.

Jain, P. K. et al. (2004) stabilized the fly ash with fine sand and observed the change in its Proctor's density and CBR values. Various percentage of sand as 10, 20, 30, 40 and 50% admixed with fly ash for experimental program and founded that MDD is increasing with increase in proportion of the sand and OMC is decreasing with increase in the proportion of sand. CBR test were conducted on samples of fly ash and its combination with sand for both soaked and unsoaked condition. They observed that CBR value increases in both soaked and unsoaked condition. The unsoaked and soaked CBR values of fly ash were 17.5% and 2.16% respectively. These values increased to 28.22 and 6.22 respectively when 50% of fly ash is replaced by the sand.

Prabakar, J. et al. (2004) described that the load bearing capacity of the soil is improved by the introduction of FA. Engineering behavioral aspects of three soil types have been studied with different percentage of FA viz. 9, 20, 28.5, 33.5, 41.2 and 46% by weight of soil. These aspects cover the swelling characteristics, settlement and compaction behavior, California bearing ratio, shear strength parameters for admixed soil with FA. For all samples of FA addition into the soils, the dry density decreased at optimum moisture content beyond which the increase in

water content reduced further dry density. They observed that the value of cohesion increases, while increasing the amount of FA for all types of soil. A non linear relation was observed between the friction angle and FA content. Introduction of FA resulted in improved deviator stress of all types of soils. For soils mixed with 46% FA, deviator stress increases with an increase in confining pressure, and thus FA has been effectively utilized to get soil with improved shear strength. Increasing the FA content upto 46% in soil resulted in improved CBR values of soil. As the amount of FA increases swelling decreases and as we keep on increasing the amount of FA in soils the swelling in soil keeps on reducing.

Kumar, A. et al. (2007) studied the effects of lime stabilization and addition of polyester fiber on the geotechnical properties of soil-FA mixtures. FA and Lime were added to an expansive soil at varying amount, ranging from 1–20% and 1–10%, respectively with 0, 0.5, 1.0, 1.5, and 2% of crimped and plain polyester fibers by dry weight of randomly oriented fibers. The results indicate that maximum dry density of soil-lime admixes decreases with increase in the lime proportion, and optimum moisture content increased. With the addition of FA, there is further decrease in maximum dry density and increase in optimum moisture content. There was no significant effect on maximum dry density and optimum moisture content of inclusion of fiber in FA-soil-lime-fiber mixtures. The increase in UCS with curing period upto 8% of lime after this result showed a decrease in strength. In addition, the strength of FA-soil-lime mixtures increases with increasing curing time with 15% of FA. The optimum value of FA and lime may be adopted as 15 and 8%, respectively. The addition of 1.0% of 6 mm crimped fibers or 1.5% of 6 mm plain fibers to FA-soil-lime-fiber mixtures (at 15% FA content and 8% lime content) increases split tensile strength and UCS and by about 100% and 74% respectively, as compared to that of same mixture without fibers. Also, with the addition of 1% of 12 mm plain fibers and 1.5% of 6 mm crimped fibers, the gain in split tensile strength and UCS was about 135% and 100%, respectively, compared to that of the same mixture without fibers. The ratio of split tensile strength and UCS increased with increase in fiber portion, which shows that polyester fibers are more efficient when soil is subjected to tension rather than compression.

Altun, S. and Goktepe, A. B. (2008) studied the mechanical performance of silty soils stabilized with 10% and 30% of FA and 2% and 8% of cement by conducting the freezing and

thawing tests. The silty samples were subjected to uniaxial test after the compacting through proctor densification at different freezing and thawing cycles (one, three and seven) under varying curing conditions. Curing had very little effect on natural soil sample. A slight change in strength of natural soil sample was observed with the change in the curing period. Whereas in case of cement added samples, the strength increases with increase in the curing time, nevertheless, the rate of the increase was less compared to those of FA added samples. In case of silty soils, it was concluded that the adding 10%, 20% and 30% FA is more beneficial than adding 2%, 5% and 8% cement. In case only FA and cement content is increased, it was observed that as the amount of additive increases, the strength increases. Sample with 30% FA and 8% exhibited maximum unconfined compressive strength, thus proving that increase in additive content results in increased compressive strength. The experimental results indicated higher compressive strengths for both natural and mixed soils subjected to freezing/thawing phenomena demonstrating brittle and crisp behavior. This was due to excessive loss of water content from the specimens during curing.

Soni, D. K. and Jain, A. (2008) described the strength behavior of black cotton soil treated with the lime and FA. Lime percentages in the soil have been varied from 0 to 10% with FA percentage ranging from 0 to 20%. For comparing the strength and durability of the various soil-stabilizer mixtures, split tensile strength tests have been conducted on cylindrical samples prepared for each mixture. The 28-day cured specimens have been subjected to 14 cycles of freezing-thawing and wetting-drying in an open-ended system to study the durability characteristics of stabilized soil. It was observed that at a particular lime-FA percentage; increase in amount of lime and FA in soil increases the strength. Initially, this increase is quite high, but as the total content increases, percentage increase is on the lower side. From the experimental study, it was concluded that due to stabilizing of the cohesive soil, its tensile strength increases. Maximum strength gain is obtained when 8% of lime and 20% of FA are mixed with black cotton soil. It was observed that when FA is added to soil-lime; its durability to freezing and thawing increases and in the optimum range of 8% lime and 20% FA, the soil shows more resistance to weathering. The same trend was seen from the results of wet-dry cycles also.

Kumar, P. and Singh, S. P. (2008) utilized fiber-reinforced fly ash as a subbase material. Fly ash as such has CBR value of 8.5%, so it cannot be used in subbase as such. After mixing 25% soil, CBR value becomes 14.6%, which still is less than 15% and so not suitable for subbases. Fly ash with 0.2% fiber content has CBR value 16.6%. Therefore fly ash with 0.2% fiber content is suitable for rural road subbases. Also, after mixing 25% soil with fly ash with 0.1% fiber content is sufficient. For rural roads with higher traffic, IRC 37 (2001) is to be followed, which states the CBR requirement of 20 and 30% depending upon the traffic. Fiber reinforcement of 0.3 and 0.4% will make the fly ash suitable for these conditions. Resilient modulus (M_R), modulus of subgrade reaction (k), and field CBR value of fly ash increase due to reinforcement and mixing of soil.

Kamel, M. A. et al. (2011) took six different groups of stabilizers to improve the engineering properties of two different types of soils. Cement, Lime, a combination of cement & polystyrene fibers, a combination of lime & polystyrene fibers, a combination of lime & fly ash and finally a combination of lime, cement & fly ash were used as a stabilizer. It was found that cement content of 7% by dry weight of the soil is the best stabilizing combination and the mixture of 7% lime and 15% fly ash is the poorest combination amongst the selected combination of stabilizers.

2.3 APPLICATION OF RICE HUSK ASH

Rice husk is available in huge quantities in rice producing countries like China, India, Indonesia, Bangladesh, Brazil and South East Asia. Rice husk is mainly used as a fuel in industries in boilers for process energy requirements and for power generations. Rice husk is a fuel having high ash content, having 80-90% of silica. Much of the husk produced from the processing of rice is either burnt for heat or dumped as a waste in the majority of rice producing countries. India alone produces around 120 Mt of rice paddy per year, giving around 24 Mt of rice husk and 4.4 Mt of RHA every year (Govindarao, V. M. H., 1980).

Noor, M. J. M. M. et al. (1993) investigated the effect of various RHA-cement proportions for road construction of a lateritic soil. The mix samples were subjected to various tests like compaction, tensile strength, unsoaked and soaked unconfined compressive strength, and

durability. Compaction properties were determined of soil with various percentage of RHA with constant 10% of cement mixes. It was seen that the optimum moisture content increase while the maximum dry density decreases with increase in RHA contents. It was seen that dry strength of soil without any stabilizing agent achieved 0.2 MN/m^2 while at 10% cement content significant improvement in strength of above 1.5 MN/m^2 was observed. Addition of RHA at 5% showed a slight increase to approximate 2.6 MN/m^2 and with further increase in RHA, there was no significant in strength development. The maximum soaked UCS is achieved at 1.4 MN/m^2 for a 10% addition of RHA. Improvement in strength is not significant when RHA content is increased above 10%. The admixing of RHA did not affect the tensile strength of soil.

Mantohar, A. S. and Hantoro, G. (1999) investigated the influence of lime mixed with rice husk ash (LRHA) on clayey soils. Practically, the effective lime content blended in between 2% to 6% Lime and 4% to 10% Rice Husk Ash. Plasticity index (PI) of admixed soil decreased from 41.25% to 0.96% when subjected to a LRHA blend of 12 to 12.5%. At the same blending swell potential reduced from 19.23% to 0.019% and CBR value improved from 3.03% to 16.3% at a LRHA blend of 6-12.5%. The shear strength parameters like internal friction improved from 5.36 to 23.85 and cohesion from 54.32 kN/m^2 to 157.19 kN/m^2. This in turn increased the bearing capacity from 391.12 kN/m^2 to 413.1 kN/m^2. At LRHA 6-10%, consolidation settlement reduced from 0.03 to 0.006. Authors concluded that mixing of LRHA with clayey soil improves the engineering properties of admixed clayey soils and can be used for construction.

Basha, E.A. et al. (2005) studied the chemical aspect of stabilization of residual soils by using RHA and cement. They evaluated compaction, X-ray diffraction and strength characteristics of the soil. It was observed that RHA and cement reduced the plasticity of soils. In general, 10–15% RHA and 6–8% of cement is the optimum amount to reduce the plasticity of soil. It was observed after experimentation that addition of RHA and cement results in increased OMC and diminishes the amount of the MDD corresponding to the increased percentage of RHA and cement content. Optimum cement content was observed to be 8% without RHA. Maximum CBR value was determined at cement content of 4% and RHA mixture content of 5% with soil.

According to PI and compressive strength, 15–20% RHA and 6–8% of cement was determined to be the optimum amount for improving the properties of soils.

Chandra, S. et al. (2005) used two industrial wastes RHA & lime sludge, one from rice mill and other from paper factory respectively for stabilization of clayey soil. The different percentage of RHA as 5, 10, 15 & 20% and lime sludge of 4, 8, 12 & 16% were tried with clayey soil to stabilize. Proctor's test results showed that MDD of soil decreases and OMC increases with increase in the proportion of RHA and lime sludge in soil. It was also observed that the liquid limit and plastic limit both shows an increase on addition of RHA and lime sludge and plasticity index was lowest at combination of 10% of RHA and 16% of lime sludge with soil. Results of UCS test showed that value increases at marginal rate with only RHA upto 10% but rate of increase was higher with addition of lime sludge in soil-RHA and it was the highest at 10% of RHA and 16% of lime sludge with soil. Improvement of soaked CBR values was also found and it was maximum for mix of 20% of RHA and 16% RHA with soil.

Jha, J. N. and Gill, K. S. (2006) evaluated the effectiveness of RHA to enhance the lime treatment of soil. The paper presents the influence of different mix proportions of lime as 3, 5, 7% and RHA as 0, 6 12, 18% with soils. Addition of lime with soil increased the optimum moisture content but decreased the maximum dry density when lime content increased. This trend does not change even after the addition of RHA in soil – lime mixture. The compressive strength properties of soil are improved on addition of lime. These strength characteristics of the lime-stabilized soil get further improved with the addition of RHA upto12% in all the cases. Curing temperature has a significant effect on the strength characteristics. Samples cured at 30°C developed half the strength than that cured at 60°C and rate of strength development was very high during this curing period. It was also observed that the increase in temperature results develops of higher strength in both cases i.e. lime treated soil and RHA treated soil. It was observed that addition of lime increases the CBR value considerably, in the case of unsoaked and under soaked condition. Efficiency of lime stabilized soil greatly increased the CBR value by the addition of RHA and 12% addition of RHA was found to be optimum for maximum improvement in CBR for all the three lime contents considered for study. After 12 cycles of wetting and drying, the average strength retention lies in the range of 59 to 69% of the original

strength of specimen when samples containing RHA and moist cured for 28 days. The sample with 12 % RHA content retained the highest strength after wetting and drying.

Alhassan, M. (2008) investigated the performance of the different percentage as 2, 4, 6, 8, 10 and 12% of RHA when mixed with lateritic soil. With increase in the RHA content, the MDD reduced and OMC improved. The author also analyzed the change in CBR with RHA content varying from 0 to 12%. CBR values initially lowered down by adding 2% RHA, for unsoaked samples after which the values increased upto its peak at 6% RHA, then again dropped at 8% RHA and was constant upto 12% RHA. In case of soaked samples, it was observed that the CBR was increasing even after the adding 6% RHA. The UCS values increased to maximum with further addition of RHA at between 6-8% RHA after which it dropped.

Brooks, R. M. (2009) used fly ash and rice husk ash to improve the properties of expansive soil and thus making it suitable for construction purpose, which are waste materials. Mix proportions of different percentage of RHA as 0, 3, 6, 9, 12 & 15% and FA as 0, 15, 25 & 30% was admixed with soil for this study. For a curing time of 28 days, the UCS of the soil increased upto 12% of RHA content, after this the value decreased. In case of FA, UCS decreased, after addition of 25% which is the optimum value of FA. Conversely, at any FA content, increase in RHA up to 12% indicated the increase in UCS. At any FA content, addition of RHA up to 12% led to increases in CBR also, further increase in RHA decreased CBR. The CBR value increased when the FA admixed with soil upto 25% with all percentage of RHA after this value decreased. Brooks thus recommended a fly ash content of 25% and RHA content of 12% for strengthening the subgrade soil expansive in nature and fly ash content of 15% blend into RHA was recommended for swell reduction.

Choobbasti, A. J. et al. (2010) investigated the influence of mixing RHA on mechanical and physical characteristics of soil admixed and the reaction between soil and lime. Different soil tests were carried out such as CBR, Atterberg limits, direct shear test and compaction test to analyze the effect of adding RHA in lime and soil. The plasticity index value decreases as the lime percentage increases. As the RHA percentage is increased to 7%, fluctuating trend was observed in the combination of soil and lime mixture. Increasing the percent of lime decreases

the maximum dry density of soil gradually. The increase in internal friction angle parameters and cohesion was observed on adding lime to soil, while adding RHA admixed with lime and soil increased soil internal parameters. As the RHA amount increases, the shear strength of soil-lime increases. From the experimental results, it was concluded that an increase in RHA above 5%, does not lead to a positive impact on shear strength value. The deformability of soil samples decreases resulting in brittle materials on addition of RHA and lime but increases shear strength. The lime and soil combination with 5% RHA gives highest shear strength. The dilation parameter increases with RHA and soil mix with 4% lime, but combination of soil with 6% lime decreases the rate.

Muntohar, A. S. (2011) improved the tensile strength and toughness index by stabilizing clayey soil with lime and RHA mixtures with plastic waste fibers. The fiber of length 20 mm were varied as 0.2% and 0.4% by dry weight of soil. Three sizes of cylindrical specimen's with 50 mm, 70 mm & 150 mm diameter and 100 mm, 140 mm & 300 mm height respectively were tested. The proportion of lime used was 12% of the dry soil mass with lime to RHA ratio as 1:1of the weight of dry soil. The reasonable strengths were obtained for second specimen with 70 mm diameter with fiber lengths of less than 20 mm. Further increase in sample size showed no significant change in tensile strength. Addition of plastic waste fiber upto 0.2% and 0.4% improved tensile strength of the stabilized soil.

Yadu, L. et al. (2011) investigated the potential of RHA to stabilize black cotton (BC) soil. Soil was stabilized using different amounts of RHA, as 3, 6, 9, 11, 13, and 15%. The performance of RHA modified soils were evaluated using different performance tests namely, CBR and UCS. They determined CBR value of unsoaked soil samples, to maximum value of 24% with addition of 9% RHA. Further increase of RHA amount resulted lowering down the CBR value. There was approximately 77% increase in UCS at 9% RHA as compared to black cotton soil. Based on these performance tests, optimum amount of RHA was determined as 9% of RHA for improving the strength characteristics of black cotton soils.

Seco, A. et al. (2011) improved the swelling and mechanical properties by adding industrial wastes and in the stabilization of an expansive soil. Different additives like lime, magnesium

oxide (PC-7), natural gypsum (NG), rice husk fly ash (RHFA), coal fly ash (CFA), coal bottom ash (CBA), steel fly ash (SFA) and aluminatum filler (AF). The results shown in Figure 2.4 recommend the best combination is 2% lime & 1% of PC-7 and another one is 5% RHFA which reduce free swelling of expansive clays.

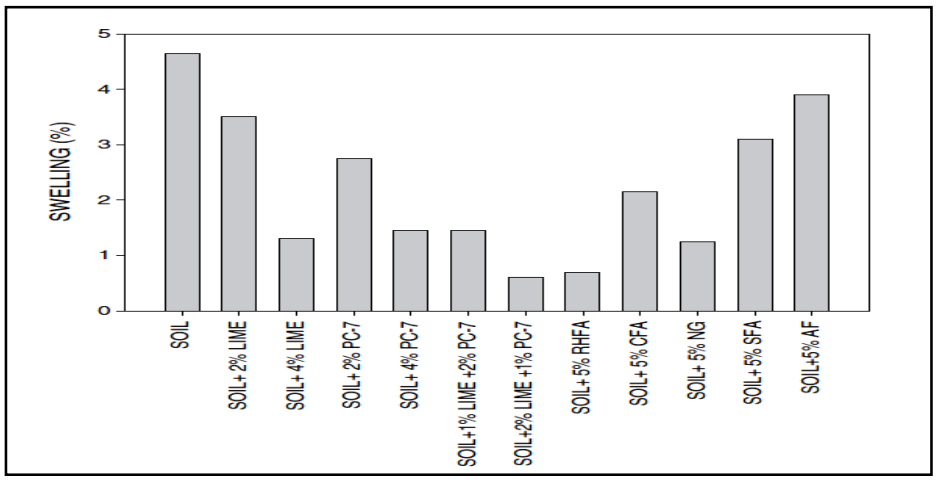

(Source: Seco, A. et al., 2011)

Figure 2.4 Free Swelling Results for the Anti-Expansive Treatment

Figure 2.5 presents the results of unconfined compressive strength for different combinations at varying curing times. Significant improvement was observed for the stabilized mixture at 14 and 28 days with combination of 4% lime and 5% RHFA, which reached 1.572 MPa of UCS. The second highest UCS achieved was 1.269 MPa at combination of 4% PC-7 and 5% RHF.

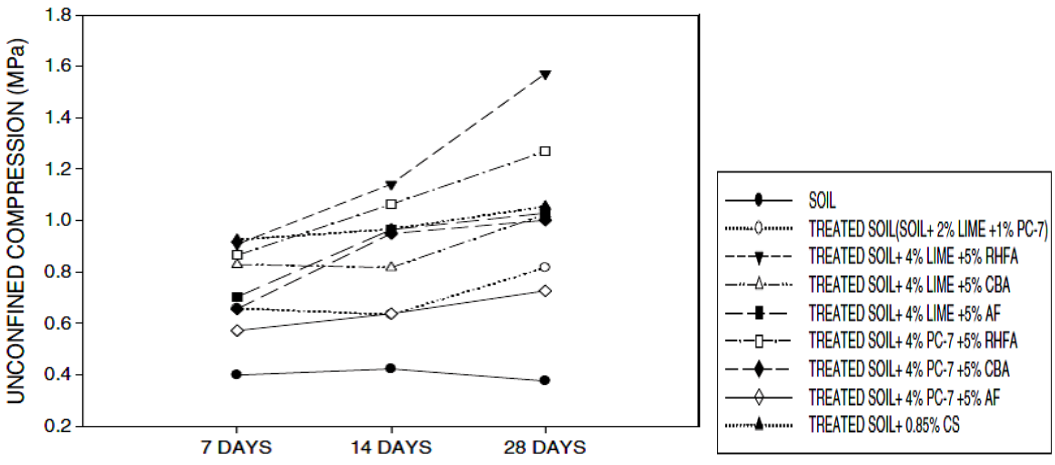

(Source: Seco, A. et al., 2011)

Figure 2.5 Time Evolution of the Compressive Strength Values

Olawale, O. and Oyawale, F. A. (2012) determined the chemical constituents by working on classification of local rice husk. Atomic absorption spectrophotometer (AAS) was used in the process of characterizing the chemical constituents of RHA. The results of analysis for RHA are as given in Table 2.4.

Table 2.4 AAS Results of Raw RHA

Component	Amount (%)
Moisture Content	9.38
Bulk Density	0.72
Ash	11.34
Volatile Matter	6.74
Nitrogen	1.15
Carbon	20.63
Sulphur	1.31

(Source: Olawale, et al., 2012)

Prepared ash specimens were tested at varying conditions and temperatures. Table 2.5 shows the chemical constituents of RHA obtained using standard wet chemical methods with instrumental techniques calcinated at 50-750°C, and at 400°C temperature major changes were observed.

Table 2.5 Chemical Constituents of Raw RHA

Temp (°C)	SiO_2 (%)	Fe_2O_3 (%)	Zn (%)	Mn (%)	CaO (%)	MgO (%)	Na_2O (%)	K_2O (%)	LOI (%)	SSA (m^2/g)
400	97.42	0.37	0.003	0.059	0.20	0.18	0.88	0.88	1.71	150
500	97.38	0.40	0.015	0.034	0.18	0.18	0.90	0.90	0.67	75
600	97.46	0.46	0.003	0.004	0.02	0.26	0.89	0.89	1.33	125
700	97.50	0.41	0.009	0.038	0.03	0.11	0.88	1.01	2.33	216.6
750	97.39	0.39	0.007	0.038	0.03	0.29	0.92	0.92	0.92	100

(Source: Olawale, et al., 2012)

The results showed that maximum silica production was at 700°C and with highest specific surface area. High percentage of K_2O and Na_2O were observed in RHA. The dark colour of the raw rice husk was because of these impurities along with black particles and carbon content of RHA. RHA with low impurity level indicated that it is highly reach in silica.

Behaka, L. and Nunezb, W. P. (2013) used RHA as a stabilizer to increase strength and stiffness of sandy soil with lime. Result indicated that the stabilisation of sandy soils with RHA, the highest UCS values obtained for mixtures with controlled temperature with respect to the residual RHA. Splitting tensile strength values also increased with an improvement in the residual RHA lime content and with the curing period.

2.4 APPLICATION OF BAGASSE ASH

About 1711.087 Mt of sugar cane is produced annually throughout the world and India produce 292.3 Mt in 2010 as shown in Figure 2.6. India has just over 500 sugar mills, of which about 95% of mills are within nine states (Maharashtra & Gujarat in the western region Uttar Pradesh, Bihar, Punjab and Haryana in the northern region; and Andhra Pradesh, Tamil Nadu and Karnataka in the southern region) as shown in Figure 2.7. The Production of sugarcane in past 12 years is as shown in Figure 2.8 with a value of 347.87 Mt in year 2011-12. Sugar mills in India are already using bagasse to fulfill their steam and power necessities making it energy efficient. Out of total bagasse produced, only 20-30% of all bagasse is ustilized in these purposes, and the surplus is currently a “waste”, and which is mostly used as a captive boiler fuel along with its minor use less than 2% in the paper industry, packing etc as a raw material. Advanced cogeneration systems with high pressure boilers and condensing cum extraction turbines are used presently in the sugar mills specially the private ones to produce bagasse ash. In general, sugar factories generate bagasse approximately 30% of sugar cane and produced 2-3% ash of bagasses. Majority of the bagasse ash is available from the regions where expansive soil exits (Figure 1.3), hence can be effectively used to improve soil strength in that region.

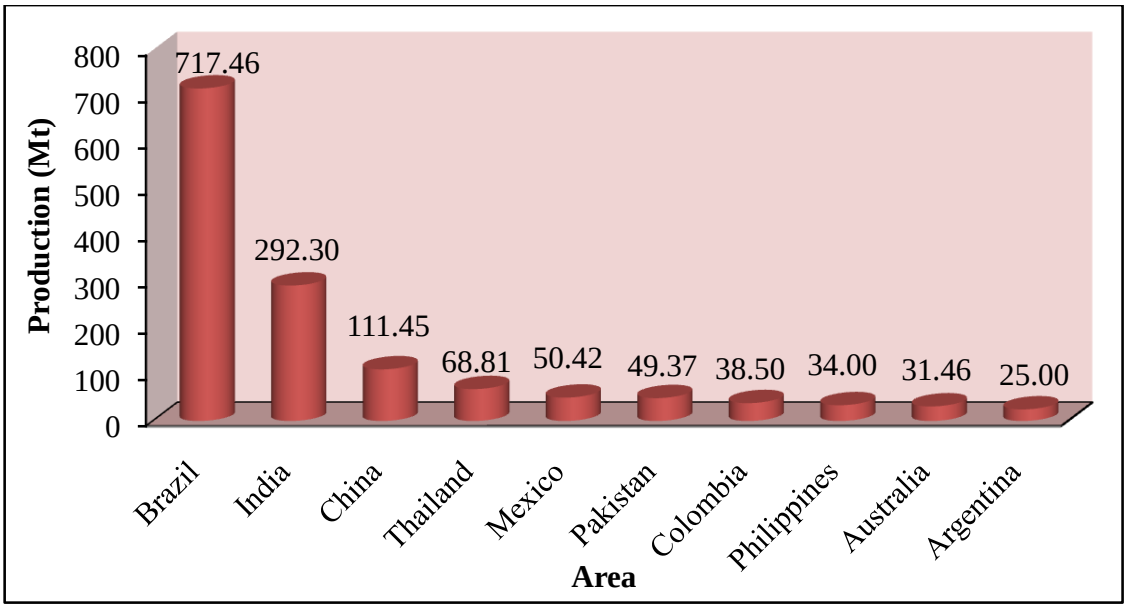

(Source: FAOSTAT, 2012)

Figure 2.6 Ten Highest Sugar Cane Producing Countries for the Year 2010

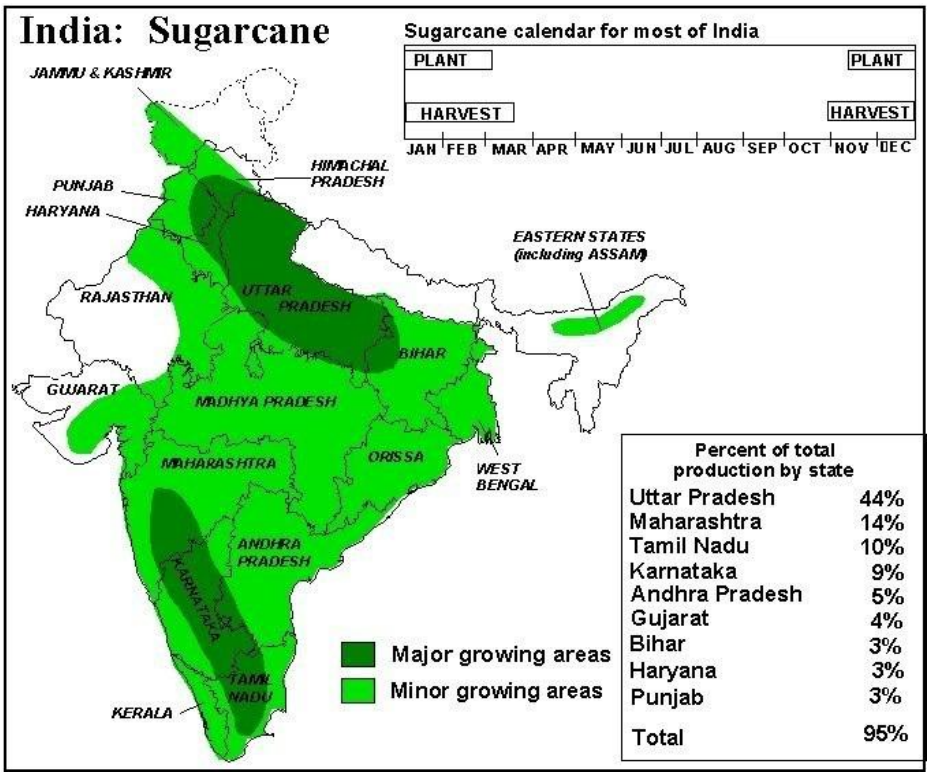

(Source: Bagasse cogeneration global review and potential, 2004)

Figure 2.7 Coverage of Sugarcane in India

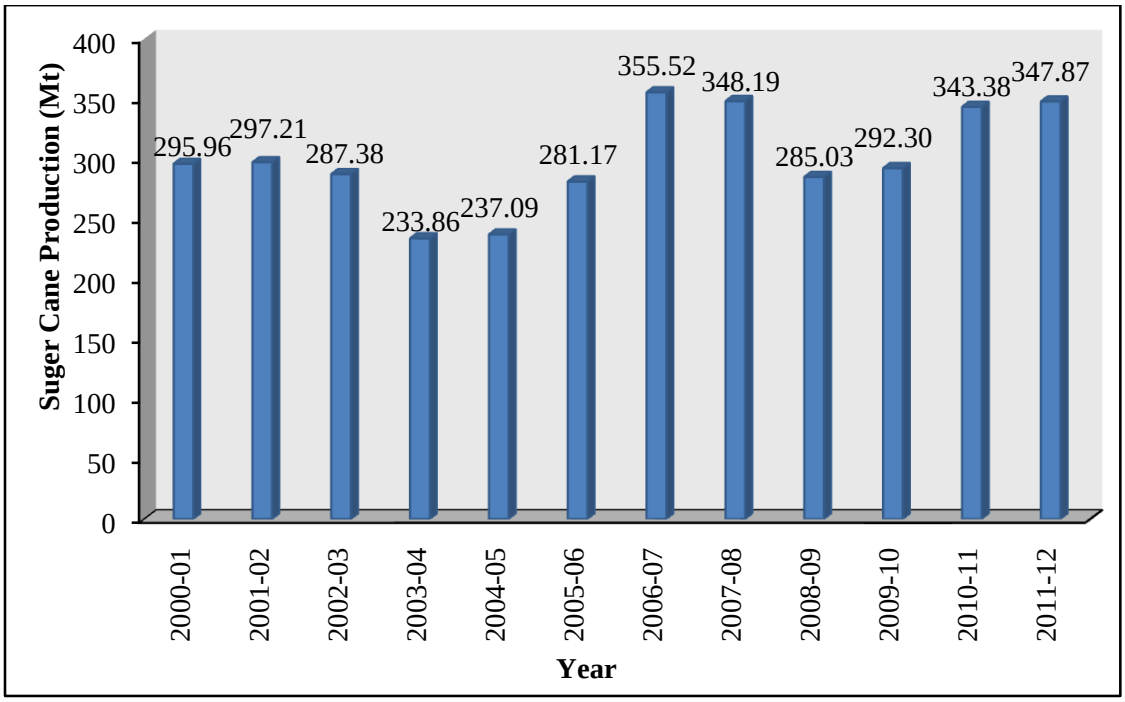

(Source: Indian Institute of Sugarcane Research, 2012)

Figure 2.8 Sugarcane Production in India

Singh, N. B. et al. (2000) studied hydration of bagasse ash (BA) blended with Portland cement and discussed its behaviour. The rate of increase in initial and final setting times was slow up to 20% BA after that it rapidly increased with increase in BA. It was concluded that BA acts as a pozzolanic material based on electrical conductivity value and non-evaporable water content. Free lime values decreases because of pozzolanic reaction which increased with BA content. In controlled condition the compressive strength increased with hydration period but on addition of 10% BA also the values improved with time and were observed always more in case of control. The compressive strength values decreased at 28 days of hydration with further addition of BA beyond 10%. Thus, the acceptable optimum limit was 10% admixing of BA to OPC. The pozzolanic reaction of calcium hydroxide enhanced the acid resistance of the cement mould blended with BA, which is immediately attacked by H_2SO_4 and also decrease the permeability.

Ganesan, K. et al. (2007) replaced to some extent the cement with BA and analyzed the physical and mechanical characteristics of hardened concrete. Mineralogical analyses by X-ray

diffraction of BA showed amorphous silica structure having a broad scattering peak at centre about 22° 2θ, Cu Kα radiation. The crystal-phases like quartz and crystobalite were present in minute quantities as shown in Figure 2.9.

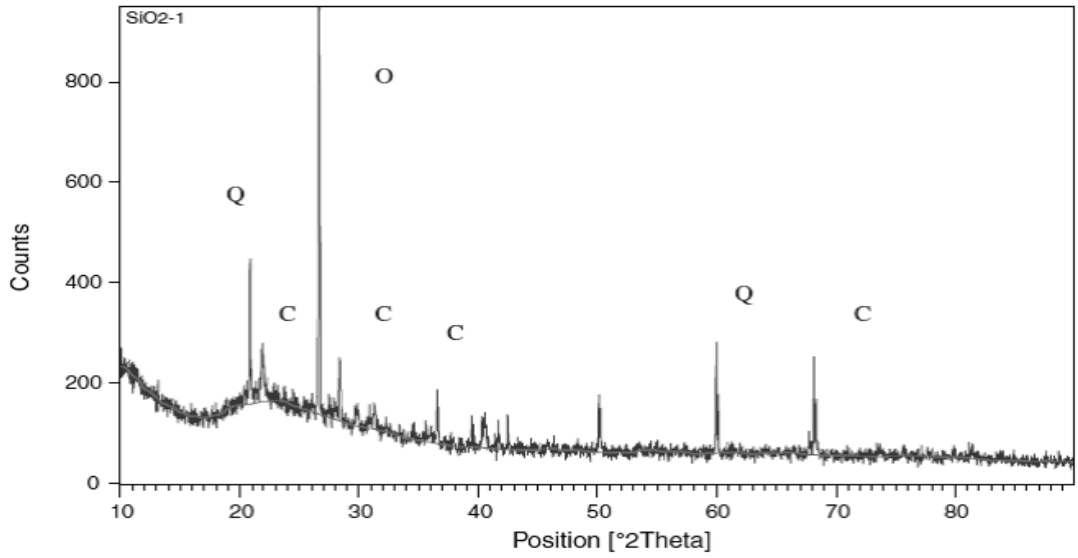

(Source: K. Ganesan et al., 2007)

Figure 2.9 X-Ray Diffraction Analysis of BA

Table 2.6 shows the results of physical properties which indicate that the specific gravity, density and mean particle size of BA were lesser in values than those of OPC and surface area of BA is 3 times greater than OPC.

Table 2.6 Physical Properties of OPC and BA

Materials	Bulk Density (g/cm^3)		Specific Gravity	Fineness Passing 45 µm Sieve	Specific Surface (Blain's) (m^2/kg)	Mean Grain Size (µm)
	Compacted	Loose				
OPC	1.56	1.16	3.1	85	326	22.50
BA	0.59	0.41	1.85	99	943	5.40

(Source: K. Ganesan et al., 2007)

Table 2.7 shows the results of chemical analysis which indicates that BA has 3 times more silica proportion than OPC and also shows presence of substantial amount of Al_2O_3, CaO, and Fe_2O_3.

Table 2.7 Chemical Composition of OPC and BA (%)

Materials	SiO_2	Al_2O_3	Fe_2O_3	CaO	MgO	Na_2O	K_2O	Loss of Ignition
OPC	19.25	5.04	3.16	63.61	4.56	0.08	0.51	3.12
BA	64.15	9.05	5.52	8.14	2.85	0.92	1.35	4.90

(Source: K. Ganesan et al., 2007)

The addition of BA upto 20% in blended concrete increases the compressive strength and splitting tensile strength as compared to control concrete for all curing periods. Further addition of BA decreases the strength relatively to a small value as compared to that of control samples. Rapid chloride permeability test showed that charge passing through concrete samples admixed with BA decreased continuously on increasing BA content up to 25%. It was recommended as 20% of BA replaced to OPC is an optimal blend with no adverse effect on the concrete properties.

Osinubi, K. J. et al. (2009) stabilized lateritic soil with sugar mills bagasse ash, an agricultural and industrial waste product. Locally available bagasse dumped in the outskirts of Jimeta area, Adamawa State in Nigeria was used. The bagasse dried in air burnt in a locally constructed incinerator and material passing through BS No. 200 sieve was used. Table 2.8 shows the results of X-ray fluorescence (XRF) analysis for BA.

Table 2.8 Detectable Oxide Composition of Bagasse Ash

Property	Concentration (% by weight)
CaO	3.23
SiO_2	41.17
Al_2O_3	6.98
Fe_2O_3	2.75
MgO	0.11
K_2O	8.72
SO_3	0.02
TiO_2	1.10
Loss on Ignition	17.57

(Source: Osinubi et al., 2009)

The increase in bagasse ash in soil resulted in decrease of MDD and increase of OMC. UCS test results on solid samples with 2% BA at 7, 14 and 28 days showed an increase in strength

from 366 kN/m^2 to 836.0, 842.0 and 973.0 kN/m^2 respectively. The soil mixed with 2% bagasse ash gave maximum CBR of 16%.

Khobklang, P. et al. (2009) tested the interlocking block prepared from the mixture of lateritic soil and bagasse ash admixed with portland cement. In this mixture bagasse ash content was varied in a range of 0-40% of Portland cement and mixed with river sand, water and lateritic soil. The results showed significant increase in the water absorption of interlocking blocks with increase in bagasse ash content. Addition of 15% of bagasse ash in the interlocking block resulted in satisfactory compressive strengths at 14 days and with 30% of BA resulted in the highest compressive strength at 90 days.

Cordeiro, G.C. et al. (2009) characterized sugar cane bagasse ash (SCBA) to extract materials having optimum pozzolanic action under controlled calcinations conditions. Mechanical test by pozzolanic activity index and chemical analysis by Chapelle methods were used to evaluate the SCBAs reactivity. Bagasse samples were burnt for 3 h at 350°C at rate of 10°C/min in an aired electric oven, and burning was continued by increasing the 100°C temperature at regular interval upto 800°C, for another 3h. LOI decreased with temperature increase as presented in Table 2.9. It was concluded that the calcinations conditions remove the carbon and volatile compounds, at temperatures higher than 600°C. The carbon removal resulted in increase of PAI of the SCBA produced by burning at 400 to 600°C with increasing calcination temperatures. At temperatures more than 600°C the PAI slightly decrease and forms crystalline compounds. So at 600°C temperature ash generated is predominantly amorphous, giving PAI value as 77.0% and LOI value as 5.70%.

Table 2.9 Physical Properties of SCBA Produced Under Different Burning Conditions

Samples	LOI (%)	P_{10} (µm)	P_{10}(µm)	P_{90} (µm)	PAI (%)
SCBA-400	84.5	1.78	12.20	29.78	28
SCBA-500	14.0	1.69	11.27	28.17	73
SCBA-600	5.7	1.23	11.56	29.05	77
SCBA-700	3.0	1.14	12.31	29.14	63
SCBA-800	1.3	0.88	10.10	27.99	69

(Source: Cordeiro, G.C. et al., 2009)

Chusilp, N. et al. (2009) compared effects on compressive strength and sulfate resistance of mortars prepared from partial replacement of ground bagasse ash for Portland cement. The BA at different LOIs as shown in Figure 2.10 was considered.

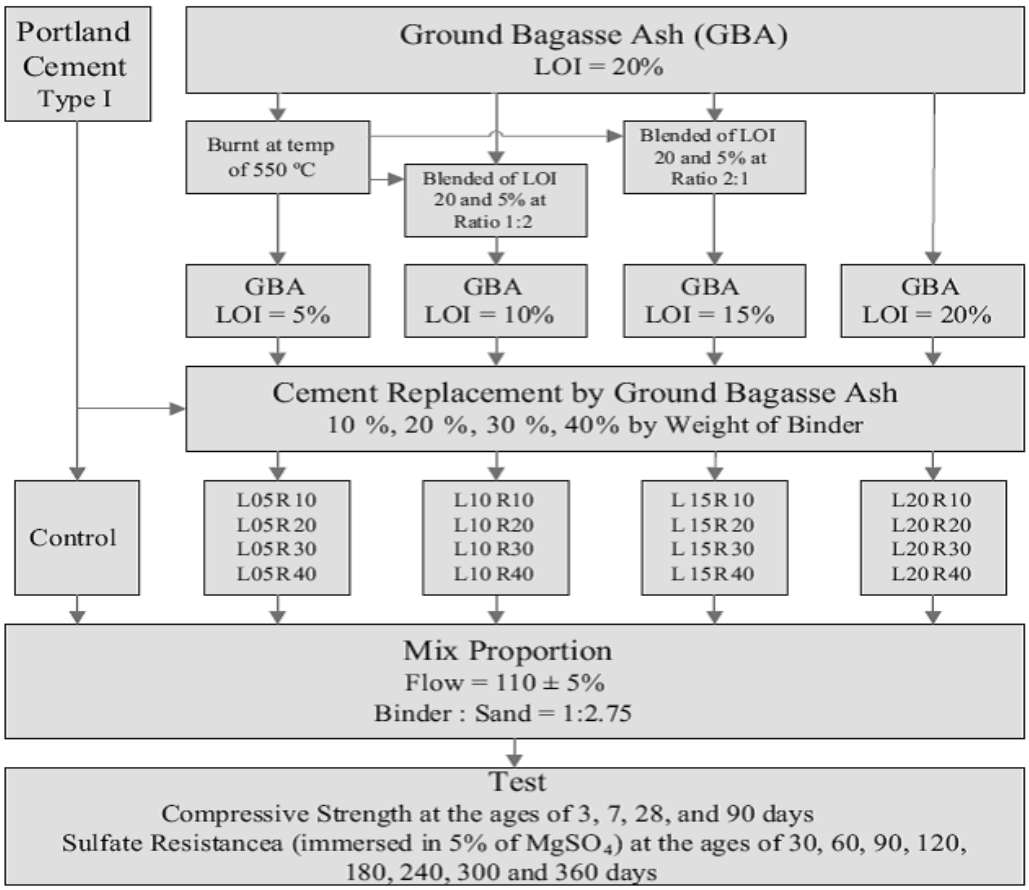

(Source: Chusilp, N. et al., 2009)

Figure 2.10 Flow Chart to Study the Effects of Ground Bagasse Ash on Mortar

The compressive strengths were observed lower for mortars with GBA having greater than 10% LOI than the mortar with GBA having less than 10% LOI. GBA mortars with 10–30% replacement of Portland cement had more or equal compressive strengths compared to the control mortar. GBA was proved to be a good pozzolna and depends on grain size and fineness. Mixing GBA with high or low LOI to 20% by weight of Portland cement type-I, high degree of sulphate resistance can be obtained. A high LOI of a GBA, either because of carbon content or the unignited bagasse, had no undesirable influence on the characteistics of a mortar. It was

summarized that Portland cement in concrete can be partially replaced by GBA with low LOI to have an exceptional pozzolanic material; thereby minimizing the waste disposal and be environment safe.

Osinubi, K. J. et al. (2009) investigated geotechnical properties of lime stabilized black cotton soil admixed with Bagasse Ash (BA). The combination of 2, 4, 6 & 8% of BA and 2, 4, 6 & 8% of lime with soil were used to carry out the tests. It was observed that as the lime content increased, the MDD decreased but bagasse ash improved in the MDD which peaked at a value of 1.40 Mg/m^3 at 2% lime/ 4% bagasse ash content.CBR value changed favorably on inclusion of BA and lime in black cotton soil and found 20% peak value of CBR at 4 % lime with 6% BA.

Srinivasan, R. and Sathiya, K. (2010) analyzed the effect of SCBA in concrete by partial replacement of cement at the ratio of 0, 5, 10, 15 and 25% by weight. After investigation of different tests they obtained that the addition of SCBA in plain concrete increases its strength under compression, tension, young's modulus, and flexure up to 10% of replacement after that strength decreases. The density of concrete decreased with increase in SCBA content, low weight concrete produced in the society with waste materials (SCBA).Partial replacement of cement by SCBA increased workability of fresh concrete, therefore use of super plasticizer is not substantial.

Cordeiro, G. C. et al. (2010) determined the optimum burning conditions of the bagasse ash for maximum pozzolanic activity and replaced 10, 15 and 20% of cement by bagasse ash to study its influence on the properties of high-performance concrete. Pozzolanic activity index, calculated from the compressive strength of 37.81 MPa of bagasse ash at different burning temperatures is presented in Figure 2.11. With respect to investigated performance indicators, the burning temperature of 600°C was most appropriate to produce pozzolana from sugar cane bagasse ash.

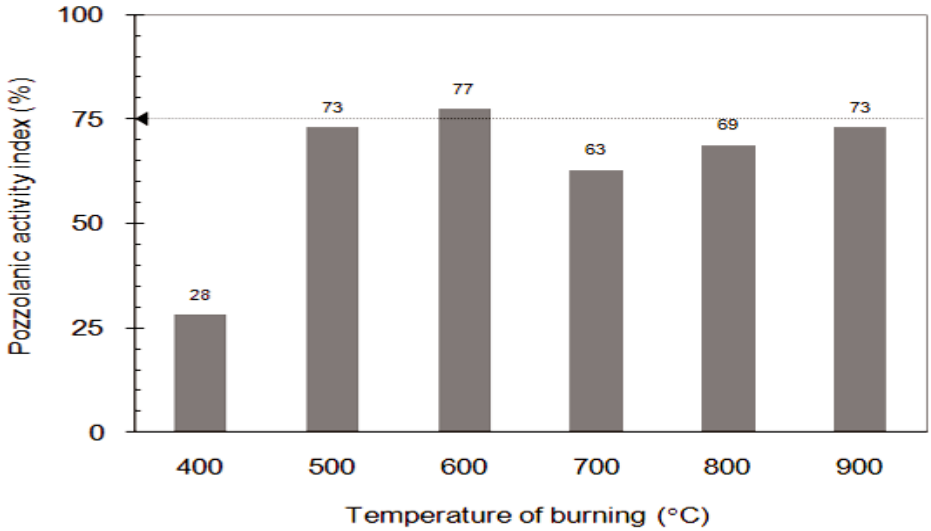

(Source: Cordeiro, G. C. et al., 2010)

Figure 2.11 Pozzolanic Activity Index Values of Sugar Cane Bagasse Ash

From various experimental results they concluded that replacement of cement up to 20% with ultrafine grinded ash is possible to improve the rheological properties, non-reduction of the compressive strength and with "very low" chloride-ion penetration in high performance concrete.

Aigbodion, V. S. et al. (2010) characterized the bagasse ash chemically and physically, to access its feasibility for use in the industry. X-ray diffraction analysis was done for ash samples and X-ray diffraction patterns were developed using siemens D-500 diffractometer using Co-Kc radiation and is presented in Figure 2.12.

XRD analysis revealed that ash contained carbon and silica as the highest percentage of all compunds. Silica appeared in prismatic particles or retained features of epidermal layer have been seen in other bagasse fly ash powders. Figure 2.13 shows the result of the EDAX scan, and as observed in rectangle label A the fibrous ones compose of only C and Si. The SEM result showed that both SiO_2 and carbon have a fine structure. It was concluded that ash is appropriate for refectory and ceramic products such as membrane filters, insulation and structural ceramics due to the existence of oxides and carbon.

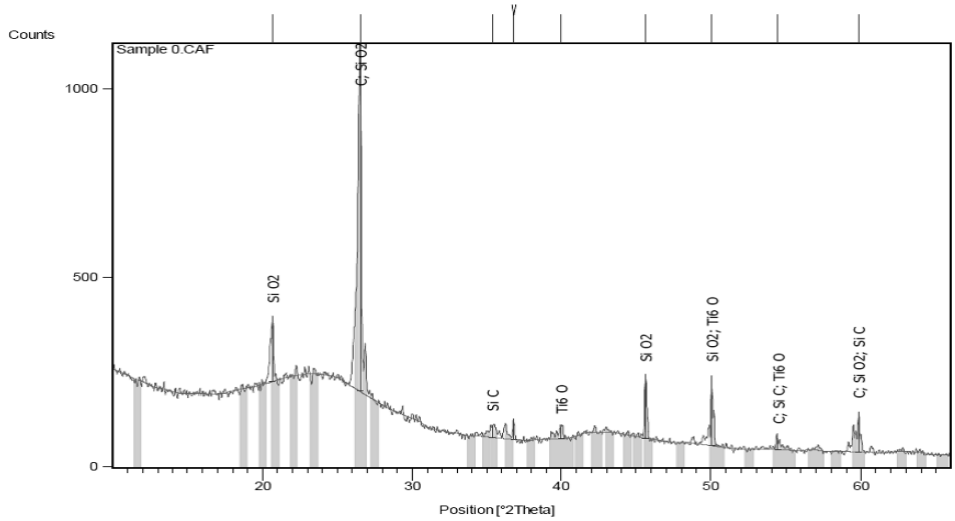

(Source: Aigbodion, V. S. et al., 2010)

Figure 2.12 X-ray Diffraction Pattern of the Bagasse Ash

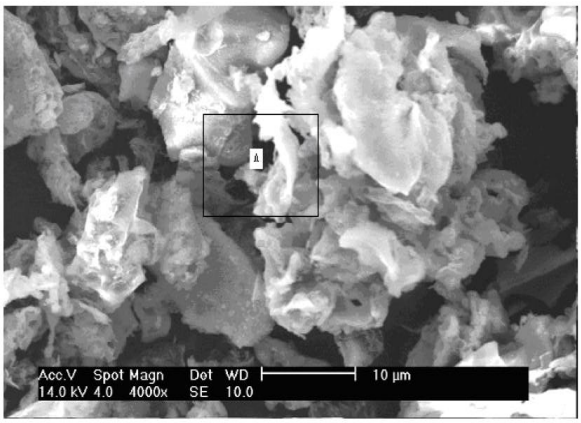

(Source: Aigbodion, V. S. et al., 2010)

Figure 2.13 Structure of the Bagasse Ash as Revealed by SEM/EDAX

2.5 APPLICATION OF RICE STRAW ASH

Rice is a staple food in the diet for much of the world. Production of rice was 696.32 Mt in the world and India stands second largest in the production with 142 Mt as shown in Figure 2.14. Factors like seasons, soil types, and irrigation conditions affect the amount of agricultural residues and it varies from crop to crop. Production of agricultural residues depends on the crop production and proportion of residues produced from main crop, and differs with varieties of

seeds within a crop type. Likewise, the accessibility of agricultural residues has also been altering with time. Some data for various agricultural residues in India are given in Table 2.10.

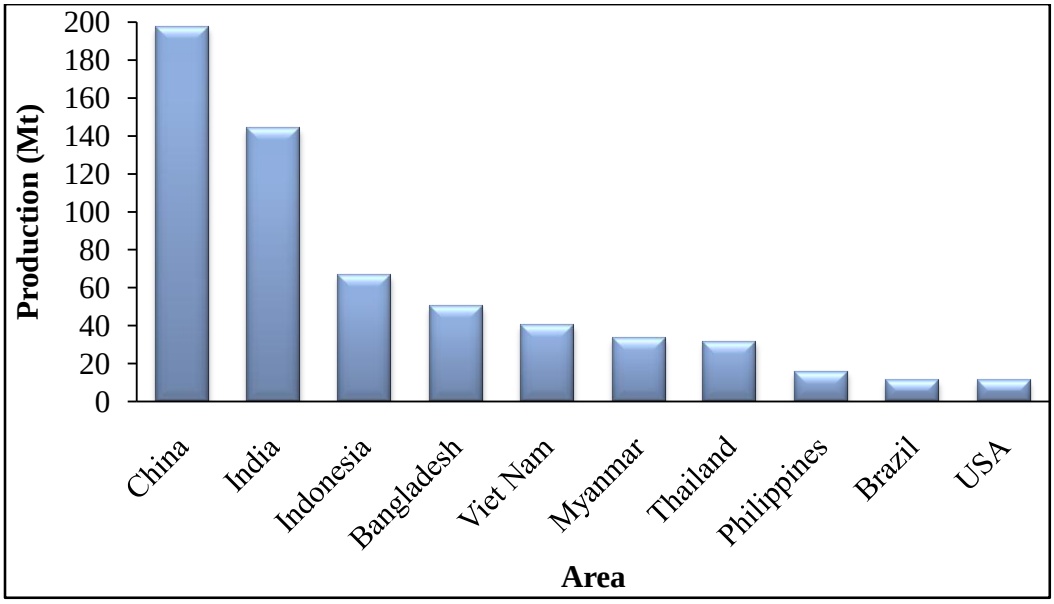

(Source: FAOSTAT, 2012)

Figure 2.14 Ten Highest Producing Countries of Rice for the Year 2010

Table 2.10 Agricultural Crop Residues Production in India

Crop Residue	Production (Mt)	
	1994	**2010**
Rice straw	214.35	284.99
Wheat straw	103.48	159.98
Millet stalks	19.42	17.77
Maize stalks	18.98	29.07
Cassava stalks	0.36	0.40
Cotton stalks	19.39	30.79
Soybeans (straw + pods)	12.87	34.87
Jute stalks	4.58	1.21
Sugar cane tops	68.12	117.97
Cocoa pods	0.01	0.01
Groundnut straw	19.00	23.16
Total	480.56	700.22

(Source: Mandey, S, 2011)

Han, Y. W. and Anderson, A. W. (1974) analyzed the problem of waste rice straw, the dry matter which consisted of cellulose and hemicellulose. The rest is comprised of lignin, nitrogenous compounds, and ash – mostly silica as shown in Table 2.11. There is very little interest at the present time in using straw in fiber board, other building materials or animal feed. The main shortcomings of straw as animal feed are its (a) low digestibility, (b) low protein content, (c) poor palatability, and (d) bulkiness.

Table 2.11 Composition of Rice Straw

Composition	**Percent of dry Matter**
Digestible Energy, mcal/kg	1.9
Crude Protein	4.5
Ether Extract	1.5
Crude Fiber	35.0
Lignin	4.5
Cellulose	34.0
Nitrogen-free Extract	42.0
Total Digestible Nutrient (TDN)	43.0
Ash	16.5
Silica	14.0
Ca	0.19
K	1.2
Mg	0.11
P	0.10
S	0.10

(Source: Han, Y. W. and Anderson, A. W., 1974)

Charaverty, A. and Kaleemullah, S. (1991) analyzed the RSA by Thermo-gravimetric analysis (TGA) to obtain the change in physical and chemical behaviour of rice straw when burnt under controlled conditions in a furnace. TGA showing the burning behaviour of rice straw is shown in Figure 2.15. The percentage mass loss at various stages is shown in Table 2.12.

Table 2.12 Percentage of Mass Loss at Different Stages for Rice Straw

The Temperature Ranges of Different Stages	I	II	III	IVa	IVb
Temperature Ranges (°c)	25-150	150-200	200-315	315-500	500-750
% Mass Loss	10.5	1.0	68.0	7.5	1.5

(Source: Charaverty, A. and Kaleemullah, S., 1991)

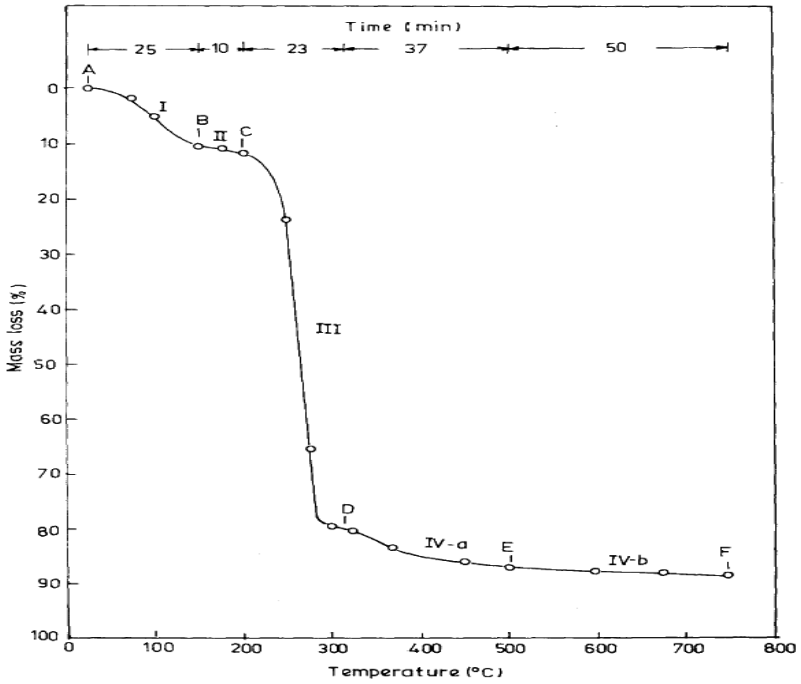

(Source: Charaverty, A. and Kaleemullah, S., 1991)

Figure 2.15 TGA Curve of Rice Straw

It can be observed from the TGA curves that at temperature range 25-150°C moisture is removed from the material in the first stage with a weight loss of 10-10.5%. In the second stage at temperature range 150-200°C very less weight loss of 0.5-1.0% is observed. This stage is defined as the transition stage. In the third stage during the range of 175-325°C maximum weight loss took place with a steep fall in TGA curve. The volatile matter was removed in this stage resulting in weight loss of 60-68%. The weight losses of 7.50-17.75% and 1.50-2.25% were observed at temperature ranges of 315-500°C and 500-750°C respectively in sub stages IVa and IVb. The weight loss was due to combustion of solid (fixed) carbon at slow rate in this stage. The oxidation of fixed carbon takes place at a temperature range of 315 to 325°C

minimum as noted from the table. Thus it can be concluded that silica can be obtained from rice straw after its complete combustion at minimum 325°C or more furnace temperature.

Ranasinghe and Arjurna, P. (1993) reported about the ash and silica content of some of the plants derivatives as shown in Table 2.13. It has been seen that rice straw has 14.65% ash after burning, thus for every 1000 kg of rice straw burnt 146.5 kg ash is produced having about 82% of silica content.

Table 2.13 Ash and Silica Content of Some Plants

Plant	Part of plant	Ash (%)	Silica (%)
Sorghum	Leaf Sheath Epidermis	12.25	88.75
Wheat	Leaf Sheath	10.48	90.56
Corn	Leaf Sheath	12.15	64.32
Bamboo	Nodes(Inner Portion)	1.44	57.40
Bagasse	--------	14.71	73.00
Lantana	Leaf And Stem	11.24	23.38
Sunflower	Leaf And Stem	11.53	25.32
Rice husk	--------	22.15	93.00
Rice straw	--------	14.65	82.00
Bread Fruit Tree	Stem	8.64	81.80

(Source: Ranasinghe and Arjurna, P., 1993)

El-Sayed, M. A. and El-Samni, T. M. (2006) reported the effect of partial replacing of three different types of cement as ordinary Portland cement, high-slag cement and sulphate resistance cement by RSA. They heated RSA at 550°C for one hour to obtain the maximum pozzolanic activity and minimum percentage of carbon and sieved through sieve No. 200 before use. It was absolutely isolated from humidity by packing until use. The specific gravity of ash was found to be 2.25 and the specific surface area was 18,460cm^2/g. Laser diffraction analysis was carried out to determine particle size distribution of RSA as shown in Figure 2.16. Chemical composition of RSA was also analyzed and reported in Table 2.14 .The chemical reactivity of the ash is related to the form of silica and carbon content in the ash.

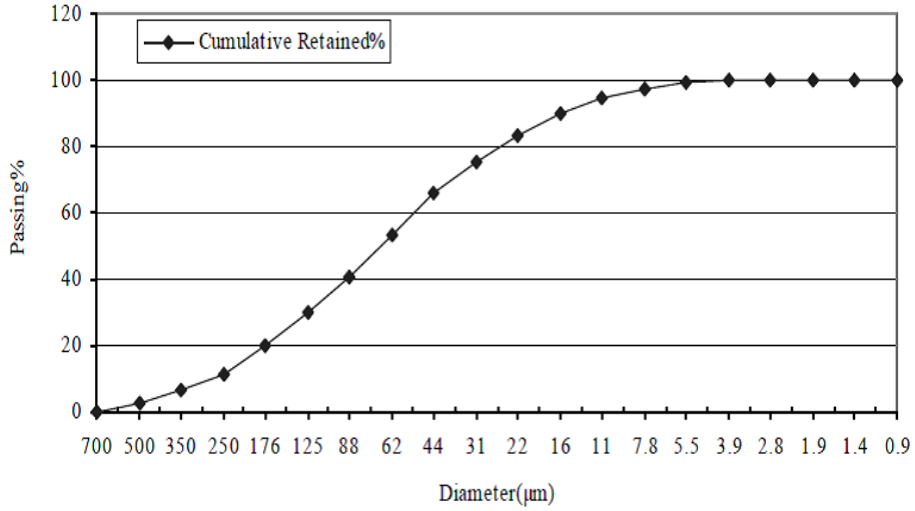

(Source: El-Sayed, M. A. and El-Samni, T. M., 2006)

Figure 2.16 Grain Size Distribution of RSA

Table 2.14 Chemical Composition of RSA

Constituents	**RSA (%)**
Silica Dioxide, SiO_2	65.92
Aluminum Oxide, Al_2O_3	1.78
Ferric Oxide, Fe_2O	3 0.2
Calcium Oxide, CaO	2.4
Magnesium Oxide, MgO	3.11
Sulfur Trioxide, SO_3	0.69
Loss on Ignition	9.71
Silica Activity Index (SAI)	70.3

(Source: El-Sayed, M. A. and El-Samni, T. M., 2006)

Rice straws are a residue produced in significant quantities all over the world. At some places they are efficiently used whereas at other places there are causing pollution and disposal problems. When burnt, the RSA is highly pozzolanic it is possible to use it in lime-pozzolana mixes as an replacement of portland cement replacement. The contents of RSA were 5, 10, 15, 20 and 25% by the weight of cement for experimental tests. For the three types of cements used in this test, the experimental results on cement paste showed an increase in the water demand in the standard consistency test as the ratio of RSA replacement increased. He further mentions

that RSA is a pozzolanic material that satisfies the minimum requirements of ASTM Class N, F and C pozzolana.

Wattanasiriwech, S. et al. (2010) used enzymatic hydrolysis approach to obtain amorphous silica from rice straw. Microbial isolate (T. reesei TISTR 3080) or a microbial community (LDD1) was used, and was found to be most suitable for decaying biomass. Figure 2.17 (a)–(b) shows the structure of rice straw with dense layer of amorphous silica of the thickness between 5 and 10 μm in exterior surface, lignocellulosic layers of collapsed plant cell wall in the interior region. The amorphous silica layer was not affected by the microbial attack even after 72 h of hydrolysis by the LDD1 mixed culture whereas the interior part was significantly "delaminated". Figure 2.19 (c)–(d) presents the change in micro structural of rice straw that was observed after 72 h hydrolysis by LDD1 culture.

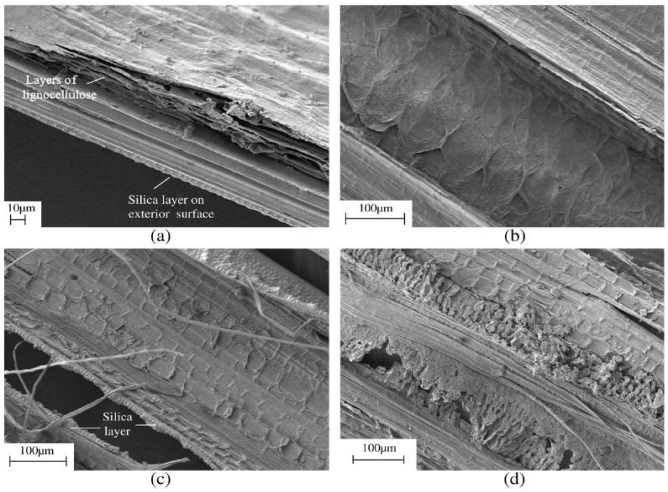

(Source: Wattanasiriwech, S. et al., 2010)

Figure 2.17 Scanning Electron Micrographs of Rice Straw: (A) Cross-Sectional View (B) Interior Surface Before Hydrolysis (C) Rice Straw Residue (D) Degraded Interior Surface after LDD1 Hydrolysis

Figure 2.180 shows TGA curves of natural and hydrolyzed rice straw by Trichoderma reesei TISTR 3080 (T. reeset) and by LDD1 microbial community (LDD1). In the first stage about 185°C of mass loss was observed in the natural rice straw, which was because volatile matters decomposed. In second stage there was mass loss of about 50% since hemicellulose (H) and

cellulose (C) decomposed from 245°C to 340°C. Further 20–30% decrease in weight was observed between 350°C and 480°C due to the decomposition of lignin.

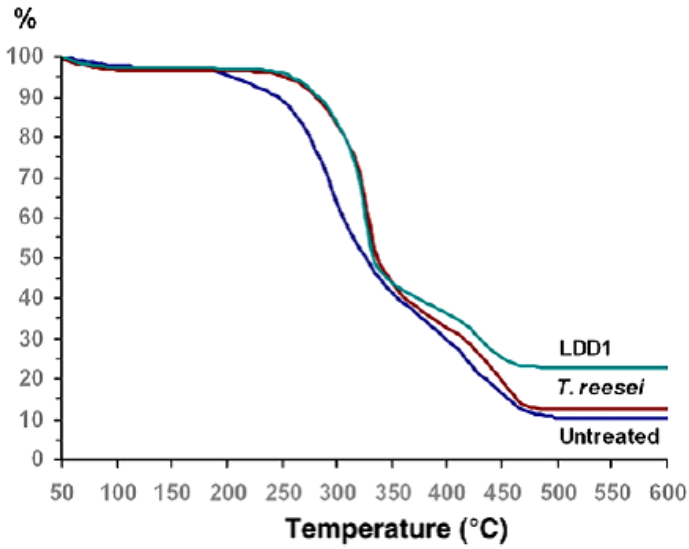

(Source: Wattanasiriwech, S. et al., 2010)

Figure 2.18 TGA Curves of Untreated and Hydrolyzed Rice Straw Samples

Rice straw residues after heat treated at 500°C, produced about two times higher ash content in the LDD1 pre-treated. However, silica was present in the LDD1 and T. Reesei pretreated ash samples with presence of other impurities like manganese and phosphate minerals allied with microbial actions. It was confirmed by XRD analysis of the ash samples that amorphous form of the silica was produced.

2.6 APPLICATION OF FIBER

In general soil has low tensile and shear strength and it varies with type of soils. The tensile and shear strength of soil can be increased by inclusion of fiber reinforcement. Soils deform in compression or shear due to stress and develop tension in another direction. This tension is resisted by fiber-soil frictional interactions thereby preventing the deformation, as the fibers are generally stronger and stiffer than the soil. In past decade the engineering properties of soil have been improved by chemical stabilization of soils. The change of soil index characteristics by admixing stabilizers such as fly ash, lime, cement or combination of these, improve the physical and chemical properties of the soil along with strength of soil. Current trend is to

improve soil properties with different types of fiber as reinforcement. However, there is limited research done on soil stabilization with fiber reinforcement particularly studying the effect on bearing capacity, slope stability, swelling and shrinkage, consolidation settlement, drainage, and as a separation layer. There may be different form (strips, sheets, grids, bars or fibers), textures (rough or smooth) or relative stiffness (high such as steel or low such as fabrics and fibers) of reinforcements. A detail classification system for fiber is given in Figure 2.21. Many researchers have used geosynthetics for soil reinforcement as embankments on steep slopes, soft foundations, backfills of retaining walls and abutments. Geosynthetics is used primarily for filtration, drainage, separation, reinforcement, fluid barrier and protection (Holtz, R. D., 2001). The comprehensive review on the application of various fibers as reinforcement for pavement construction and composite materials is presented in this paper.

Mandal, J. N. & Joshi, A. A. (1996) conducted model tests to study the stability of embankment of soft soil for short period by using various types of reinforcements. Four combinations were used as unreinforced, reinforced with cotton, reinforced with jute and reinforced with combination of jute and bamboo mat for testes of three embankment cases as slope 1:1& H/D=0.50, slope 1:1 & H/D=1.00 and slope 1:1 & HID = 2.00. The vertical settlements and horizontal displacements of points at the contact surface between fill and foundation were measured during the test and it was observed that, as the strength of reinforcement increases, the settlement reduces. This can be endorsed by the observation that the addition of the bamboo mat to the jute reduces the settlement.

Puppala, A. J. and Musenda, C. (2000) investigated the influence of randomly distributed polypropylene fiber reinforcement to study the swelling, shrinkage characteristics and strength properties of the stabilized expansive clayey soils. Two expansive soils from Irving & San Antonio, two fiber types of nominal lengths 25-mm & 50-mm and four fiber dosages (0, 0.3, 0.6, and 0.9% by dry weight of soil) were used for the testing. The UCS value of Irving clay samples treated with both fibers reached at their peak strengths at 0.3 percent for 25 mm and 0.6 percent for 50 mm fiber dosage levels. Similar results were obtained for San Antonio clay samples. The increase in the fiber reinforcement of both types (25-mm & 50-mm length)

decreased volumetric shrinkage strains, increased the free vertical swell strains and reduced the swell pressures of the expansive clays.

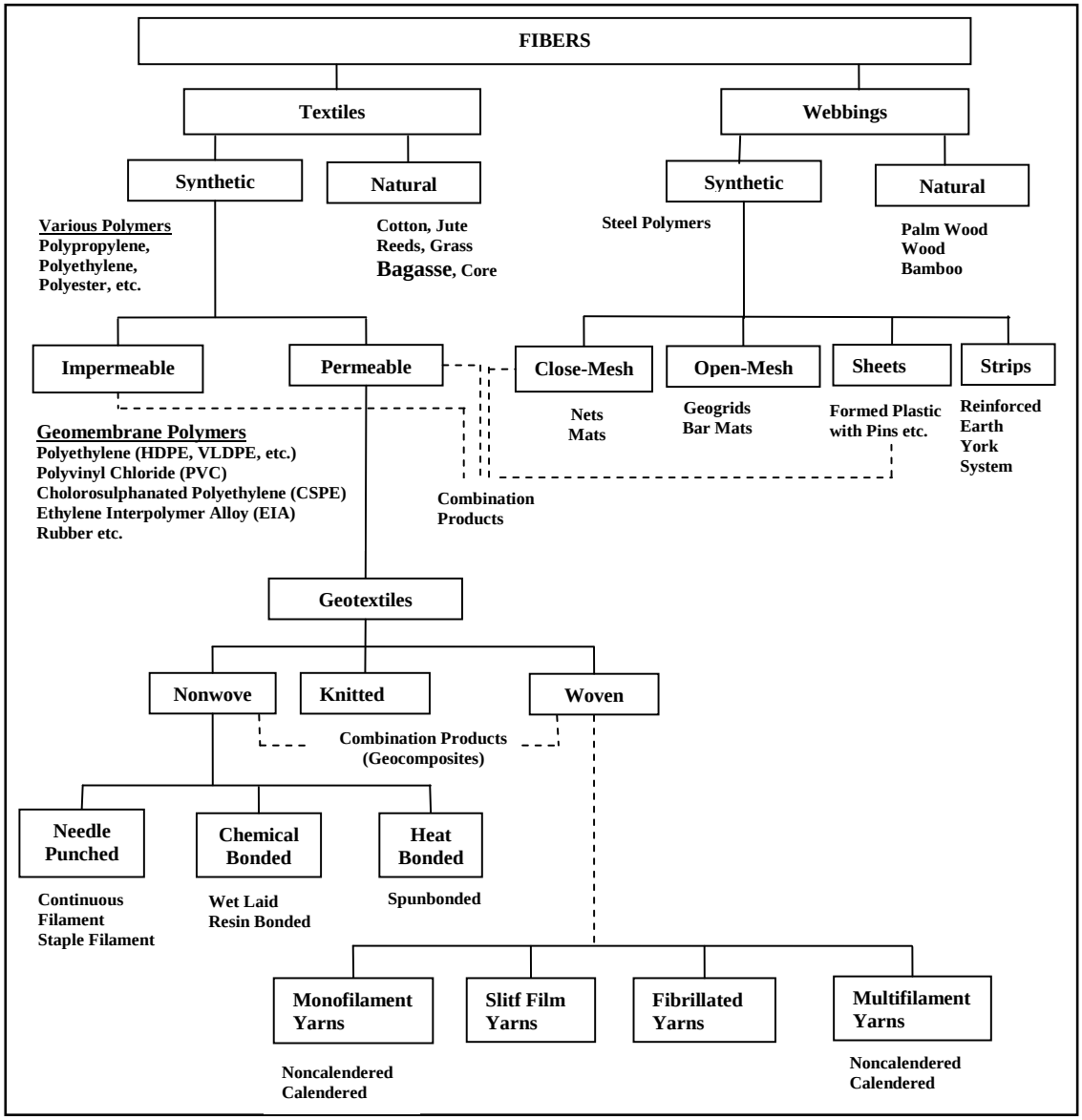

(Source: Holtz R. D., 2001)

Figure 2.19 Classification of Fibers

Consoli, N. C. et al. (2003) used chopped polypropylene fibers-reinforced in sandy soil and determined load–settlement response by plate load tests. Trixial test was also conducted on soil admixed with 0.5% of fiber at four different confining pressure 20, 60, 100, and 200 kN/m2 to

determine stress–strain behavior of soil with or without reinforced in saturated drained condition. Hardening behaviour was observed up to the end of the tests at axial strains larger than 20%, whereas un-reinforced soil showed an almost perfectly plastic behaviour at higher strain. Fiber reinforcement can be potentially used in shallow foundations, embankments on top of soft soils, and earthworks suffering from excessive deformation; since fiber addition shows soil improvement behaviour. The admixing of polypropylene fibers increases the friction angle from 30 to 31° and cohesion from 23 to 122 kN/m^2 as observed from triaxial test data.

Gosavi, M. et al. (2004) used strips cut from woven fabrics and glass fibers as reinforcing material to improve the strength and stability properties in soft soil subgrade. The woven fabrics with 25 & 50 and glass fiber with 250 & 500 aspect ratio were mixed in proportion of 1, 2 and 3% by weight of soil for experimental work. The results showed that OMC values increased and the values of MDD decreased with the increase in woven fabrics and glass fibers content upto 2% in black cotton soil. With the addition of up to 2% of each fiber, the cohesion increases and angle of internal friction (φ) value decreases in black cotton soil, there after the trends was reversed on further increase of reinforcement. Black cotton soil's CBR value also showed an increase up to 2% addition of each fiber in the soil and beyond that rate of increase was very less.

Ravi Shankar, A. U. and Suresha, S. N. (2006) stabilized the Shedi subgrade soil with geogrid by placing it at different locations from top of subgrade. Inclusion of a single layer of geogrid at a depth of 0.5a reduced elastic modulus and modulus of subgrade reaction values to 60 and 40 per cent respectively. On placing of two layers of geogrid in the subgrade at a spacing of 0.5a and 0.75a, elastic modulus and modulus of subgrade reaction values reduced to 36 and 12 per cent respectively (where 'a' is diameter of loading plate).

Pateriy, I. K. and Patil, K. A. (2006) studied on polypropylene fibers which used in flexible pavement and reported that, on addition of 2% polypropylene fibers with aspect ratio of 40, the soaked CBR value can be improved up to 75% in comparison with the unreinforced soil. The crust thickness is reduced by 75 to 100 mm for different ESAL applications.

Marandi, M. et al. (2008) reported the influence of palm fiber admixed with soil with 0.5% and 1.0% by weight of soil. The results showed that the MDD decreases and OMC increases with increase in palm fiber. CBR test was performed on soil admixed with fiber inclusion of 0.25%, 0.50%, 0.75%, 1.00% and 1.50%, for fiber lengths of 20 mm and 40 mm and for wet and saturated condition. Results showed that CBR values increased with increases in fiber content this trend was more increased with increase in fiber length. But in case of saturated soil CBR values decreased. A noteworthy result was that the sample failures were controlled by sliding failure strength instead of the rupture failure strength. Reinforced soil using palm fibers as the primary reinforcement are beneficial engineering materials.

Chandra, S. et al. (2008) investigated the use of polypropylene fiber having aspect ratios of 50, 84, and 100 as a reinforcement in three different types of subgrade soils. The fibers were admixed with these three types of soil in different percentages of 0.75, 1.5, 2.25, and 3 by dry weight of soil. CBR value of reinforced soils increased with the increased of both fiber content and aspect ratio but mixing was extremely difficult beyond the fiber content of 1.5%. The optimum fiber content was found to be as 1.5% fiber content and an aspect ratio of 100 for Soils A & B, and with an aspect ratio of 84 for Soil C. The following linear equations were developed for CBR of soil and correlated with fiber content (FC) and aspect ratio (AR).

For Soil A

$$CBR=-2.286+0.0388\ (AR)+ 1.17\ (FC) \quad ....(1)$$

For soil B

$$CBR= -0.353+0.0354\ (AR)+1.27(FC) \quad ....(2)$$

For soil C

$$CBR=9.147+0.0492\ (AR)+1.35(FC) \quad ....(3)$$

The failure stress and corresponding strain improved with increase in all types of soils admixed with fiber content. They also used mechanistic-empirical design approach to evaluate the benefits of reinforcing the subgrade soils. By finite-element modeling authors concluded that the thickness of the subbase reduces by 38.52, 26.23, and 16.67%, respectively for reinforced soils A, B, and C with constant thickness of base& DBM and also improved pavement service life.

Justiz-Smith, N. G. et al. (2008) designed and manufactured the composite material using three natural cellulosic fibers viz. bagasse from sugar cane, banana trunk from banana plant and coconut coir from the coconut husk. Various tests like ash and carbon content, moisture content, tensile strength, water absorption, were performed on these samples as shown in Table 2.15. Ash content of fiber after combustion showed the carbon content of each fiber as carbon content increases with increase in ash content. Table 2.16 shows the results of the chemical analyses. The lignin content in coconut coir fiber is accountable for the firmness of the fibers resulting in higher molecular weight and 3-dimensional polymer structure and higher tensile strengths are achieved for composite materials due to presence of the cellulose content. Table 2.17 shows the outcomes of the metal element analyses. Based on these results natural cellulosic fibers can be used in interior and structural works.

Table 2.15 Physical Properties of Cellulosic Fibers

Fiber	Moisture content (wt.%)	Ash content (wt.%)	Carbon content (wt.%)	Water absorption (wt.%)	Tensile strength (MPa)
Banana	85.6	8.3	50.9	40	142.9
Coconut	27.1	5.1	51.5	169	138.7
Bagasse	52.2	4.5	53.0	235	29.6

(Source: Justiz-Smith, N. G. et al. 2008)

Table 2.16 Chemical Properties of Natural Cellulosic Fibers

Fiber	Lignin (wt.%)	Cellulose (wt.%)	Hemicellulose (wt.%)
Banana	9.00	43.46	38.54
Coconut coir	59.40	32.65	7.95
Bagasse	13.00	30.27	56.73

(Source: Justiz-Smith, N. G. et al. 2008)

Table 2.17 Metal Elements Present In Natural Cellulosic Fibers (Wt.%)

Fiber	Al^{3+}	Ca^{+}	Mg^{+}	Na^{+}	Si^{+4}
Banana	0.14	5.72	1.77	0.28	1.41
Coconut coir	0.03	2.44	0.76	2.53	2.56
Bagasse	3.89	3.87	1.32	0.97	27.0

(Source: Justiz-Smith, N. G. et al. 2008)

Prasad, D.S.V. et al. (2009) concluded based on the results of CBR tests that for moorum and fly ash materials reinforced with waste plastics in different proportion, the optimum percentages were equal to 0.30% for moorum and 0.40% for fly ash. CBR test results on moorum and fly ash mix reinforced with waste tyre rubber in different proportions, showed that 5.0% for moorum subbase and 6.0% for fly ash is optimum combination.

Basu, G. et al. (2009) developed Jute–HDPE (high density polyethylene) woven geotextiles for construction of unpaved roads having medium traffic-volume in form of separation layer and reinforcing material and compared with the conventional synthetic geotextile prepared from HDPE slit-film. They compared cost of 100% HDPE, jute–HDPE blended, and 100% jute geotextiles. The cost of Jute–HDPE woven geotextiles is lower than 100% jute geotextiles but more than 100% HDPE fabrics of same type. The blended geotextiles were used for construction of an unpaved lateritic road and the results of the field trial showed that even after 18 months no rutting was observed. However without the geotextile 5–35 mm deep ruts were observed for remaining portion of road. CBR value improved 67% after eleven months and 73% after eighteen months of construction done using jute admixed synthetic geotextile as compared to the road portions without geotextiles.

Prasad, D. S. V. et al. (2010) studied on different reinforcement materials in the gravel subbase courses laid on expansive soil subgrades. They used geogrid reinforced subbase, bitumen coated chicken mesh (BCCM) reinforced sub base, bitumen coated bamboo mesh (BCBM) reinforced subbase, waste plastics (WP) reinforced subbase, waste tyre rubber (WTR) reinforced subbase separately between two compacted layers of gravel subbase course, as shown in Figure 2.20.

Cyclic Plate load tests were performed on various test stretches having different reinforcement materials to evaluate its performance under different tyre pressures varying from 500-1000 kPa. The load carrying capacity increased substantially for subbase with reinforced geogrid at all the deformation levels which exhibits high load carrying capacity followed by BCCM, BCBM, WP and WTR stretches.

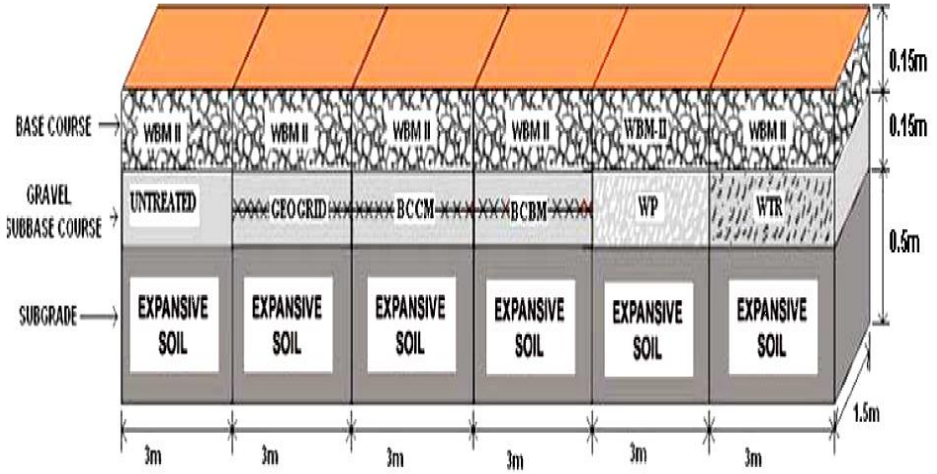

(Source: Prasad D.S.V. et al., 2010)

Figure 2.20 Preparation of Test Stretches

Punith, V. S. and Veeraragavan, A. (2011) investigated the feasibility of using reclaimed polyethylene (PE) fibers produced from low-density polyethylene (LDPE) tote bags obtained from domestic waste as an admixture in OGFC. The test results revealed that tensile strength, resistance to permanent deformation, fatigue-induced damage, and moisture susceptibility were improved on admixing reclaimed in OGFC mixtures as compared to the mix without fibers.

Singh, H. P. et al. (2011) used randomly distributed discrete natural coir fiber as fiber reinforcement with soil. 0.25%, 0.5%, 0.75% and 1% of coir fibers by dry weight of soil with random lengths were admixed for shear strength parameters, stiffness modulus and the CBR. Results showed that cohesion and angle of friction increase as the fiber content increases and their values were 110% and 88% respectively at 1% fiber over the untreated soil. Stiffness modulus of coir- fiber reinforced soil (CFRS) was higher than the stiffness of plain soil at every strain level. Stiffness modulus increased with increase in fiber content upto the highest fiber content. The variation of stiffness was found to be similar in all the cases. It was observed that CBR value of soil admixed with fiber increases as the fiber content increases up to highest fiber content at 1%. The increase in CBR value was 185% at 1% fiber content with respect to untreated soil.

Rao et al. (2009) demonstrated the used of polyster fiber waste as a reinforcing material in concrete for road construction. Itwas observed from the experimental resutls that the addition of fibers improved the compressive strenght of the concrete. Maheshwari, K. V. et al. (2011) stated that increase in bearing capacity of highly compressible clayey soil with the inclusion of polyester fibers. The soil bearing capacity (SBC) and safe bearing pressure (SBP) improve with increase in fiber content up to 0.5% and then decrease with further addition of fibers. The SBC and SBP are maximum at 0.5% fiber content having 25 mm depth of fiber reinforced soil (B/4). Thus though the soil is affected to a significant depth of 2 to 2.5 times the width of footing, there is no need to put the fiber reinforced soil throughout this depth.

Malekzadeh, M. and Bilsel, H. (2012) conducted experimental program to study of the effect of polypropylene fiber on mechanical behaviour of expansive soils. The experimental program of compaction, unconfined compression, tensile strength and one dimensional swell tests was carried out on clay sample admixed with 0% to 1% polypropylene fiber. Compaction test result showed that OMC does not show much change, whereas maximum dry density reduces by addition of polypropylene fiber. Unconfined compressive strength and cohesion increased with increasing fiber content and the highest values attend for samples with 1% fiber inclusion. Split tensile strength results showed that the tensile strength increasing with fiber additions upto 1%. The ratios of unconfined compressive strength to split tensile strength indicated that fiber reinforcement is more effective in improving tensile strength than the compressive strength. They also studied on influence of polypropylene fiber on swell characteristics, that one-dimensional swell decreases considerably with 1% fiber addition.

2.7 APPLICATION OF CONSTRUCTION AND DEMOLITION WASTE

Construction and demolition (C&D) debris is a component of the waste material produced during construction, renovation, or demolition of structures like buildings of all types (both residential and non-residential), roads and bridges. It is considered to be a non-hazardous waste material. Municipal solid waste (MSW), sludge from wastewater and water treatment plants, non-hazardous wastes from industrial processes, spent automobiles, oil and gas wastes, mining wastes, agricultural wastes, and trees and brush are examples of other non-hazardous waste materials as shown in Figure 2.21.

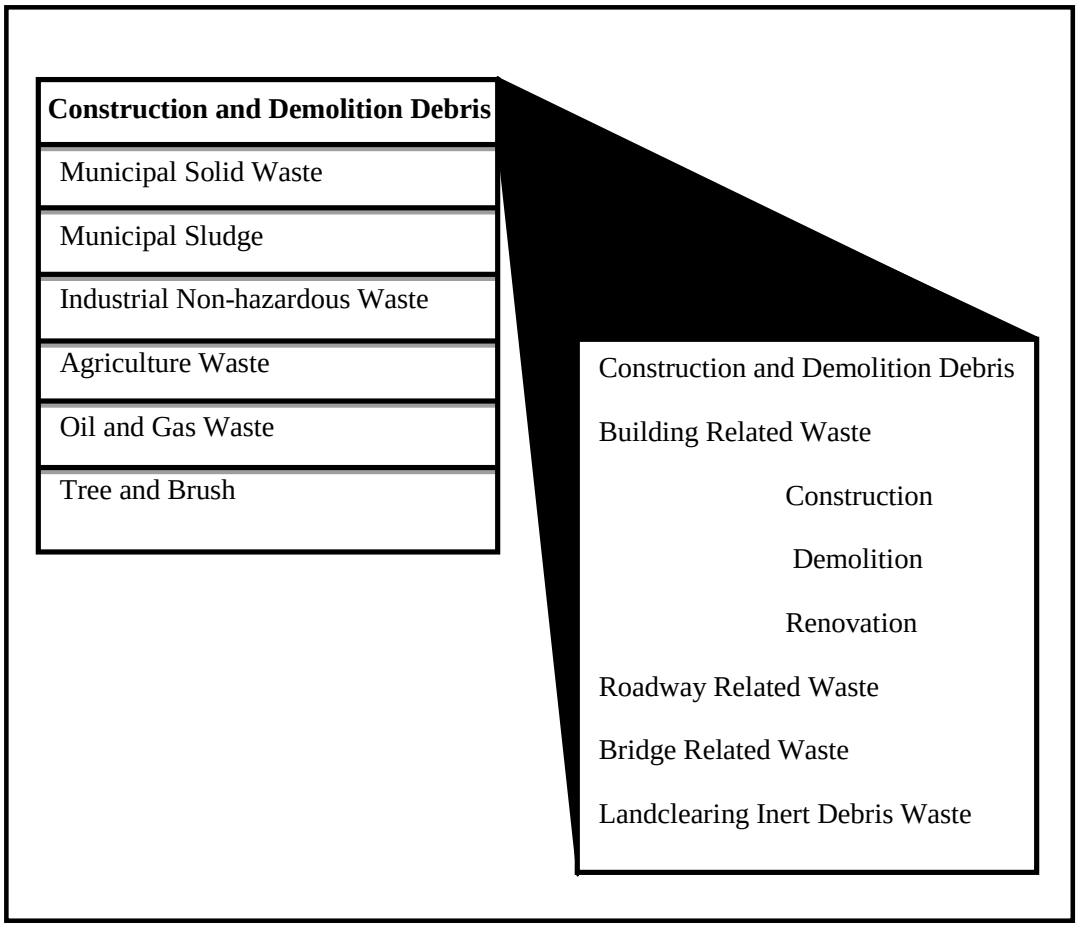

(Source: Franklin associates, 1998)

Figure 2.21 C& D Debris in Perspective

More than billions of tons of construction and demolition building waste are generated every year globally. All countries face a severe social and environmental problem due to its disposal. The recycling and reuse of this waste thus has a prime importance.

The use of different building material types makes the generated waste more complex but generally it may constitute of following materials:

Major components

- Cement concrete
- Stone (granite, sand stone, marble, etc.)
- Cement plaster
- Timber/wood

- Bricks
- Rubble
- Steel (from RCC, roofing support, railings of staircase, door/window frames, etc.)

Minor components

- Conduits (iron, plastic)
- Panels (wooden, laminated)
- Electrical fixtures (copper/aluminium wiring, wire insulation, plastic switches, etc)
- Pipes (GI, iron, plastic)
- Others (glazed tiles, glass panes)

India generates solid wastes from construction industries about 14.5 Mt yearly as shown in Figure 1.4, which include bitumen wasted sand, concrete, masonry, bricks, gravel, etc. C&D waste composition in India is shown in Figure 2.22. However, a part of this waste is used in building materials after recycling and portion of recycled materials varies from 25% in old buildings to as high as 75% in new buildings. In India nearly 50% of Construction & Demolition waste is being re-used and recycled, while the remainder is mostly landfilled. In India it is common practice for large C&D projects to pile waste in the road, resulting in traffic congestion. C&D wastes from individual households are dumped into nearby municipal bins and waste storage depots due to which the waste becomes heavy, and its quality degrades for treatments such as composting or energy recovery. India's construction industry is extremely labour demanding and has accounted for about 50% of the country's capital outlay in successive.

Bairagi, N. K. et al. (1990) stressed on the importance of conserving natural resources and conservation of environment during any development. The most suitable method of mix design for recycled aggregate concrete (RAC) has been identified from conventional methods that are available for mix design. An influencing parameter was identified and an empirical relation was recommended to modify the affecting parameter. The desired and designed target strength can be obtained for RAC without attempting any trial mixes due to the new mix design parameters. As per the new design procedure, about 10% more cement was required which is considered quite satisfactory and sensible in view of the inferior quality of recycled aggregate.

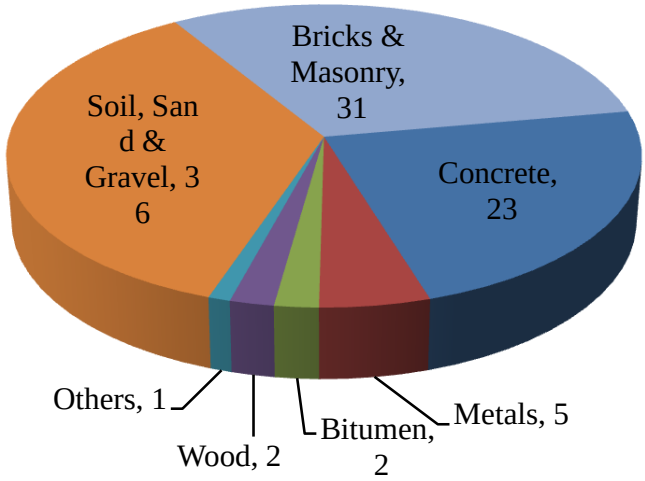

(Source: Department of Urban Development)

Figure 2.22 C&D Waste Composition (in %)

Zaharieva, R. H. et al. (2003) recommended the use of building recycled waste to decrease the environmental pollution by reusing the dumped waste and reduce use of natural aggregates sources. The need of building waste management strategies in the country was discussed. It was suggested to use selective recycling and recycling by a mobile plant on site. The waste produced has good mechanical properties as it homogenous without impurities. Hence recycled aggregates can be used for various purposes, including manufacturing of concrete. The transportation cost can be saved by disposing, recycling and reusing the waste at the nearby places and also these recycled aggregates will be cheaper than conventional aggregates. When the stocks are cleared the mobile plant can be shifted to new place.

Petkovic, G. et al. (2004) have set the criteria for use of recycled materials on the basis of suggested procedure for typical road scenarios. The threshold values for material input were calculated for different combinations of material and scenario which were within acceptable limits of environmental impact. This calculation is iterative in nature and results in a set of values defining the satisfactory composition of a recycled material or the leaching properties. For selected recycled materials used in road construction, environmental quality guidelines have been defined by Norwegian roads recycled materials R&D program.

Shen, D. H. and Du, J. C. (2004) preformed experimental work for assessment of building materials recycling on hot mix asphalt permanent deformation. The performance of hot mix asphalt with Reclaimed building materials (RBM) in Taiwan resulted in more absorption of asphalt cement aggregate. Deformation resistance was increased due to internal friction. The mixtures with 100% RBM and coarse RBM plus fine CS performs better than that with river crushed stone aggregate. The instability of the deformation depth of 50% RBM plus 50% CS is not capable for use. The analysis of variance of permanent deformation test revealed that the aggregate types have noteworthy effect on any test temperatures and type of binders used. The permanent deformation performance does not show any changes on use of asphalt cement either AC-10 or AC-20.

Shrivastava, S. and Chini, A. (2009) identified that, due to growth in construction, it is expected that C&D waste production in India will increase. If proper measures are not taken to reduce the C&D waste it will lead to disturb the environment. It will be hazardous to mankind. C&D waste minimization and handling are necessary in view of limited landfill space and increasing quantum of demolition waste otherwise there may be issues related to handling the waste and finding space for land filling. This will cause an extra burden on solid waste management plans, which are already looking for new ways to fight with the growth in municipal solid waste due to increase in urban population and developments in the country. Government policies and laws should be reformed to motivate and make C&D waste management mandatory for all types of construction activities. It would be desirable to have more accurate and detailed data such as C&D waste generation and the way it is managed in India.

Blengini, G. A. (2009) achieved a definite combination of actual and recycled raw material which was environmentally, socially and economically feasible for mankind development. It can be confirmed with such approaches, that the natural raw materials and energy resources are over used. Also it is clear from the yearly data for construction and demolition waste production (0.70 ton per capita) as compared to yearly building aggregate requirement in Italy (6.0–11.0 ton per capita), that the Italian requirement for potential contribution of recycled aggregates ranges from 6% to 9%. More stress should be given on the combined use of

recycled and natural aggregates for the construction industry rather than comparing which one of them is used more.

Dongxing, X. et al. (2010) concluded that more water is required for cement treated mix granulate (CTMG) than for normal cement treated crushed aggregates for good workability; as recycled materials are porous in nature. Linear increase in UCS and ITS was observed with increase in ratio of cement and curing time, while it increases exponentially with the dry density or the degree of compaction, in log scale. The economic and efficient way of getting good strength is by improving the compaction rather than modifying the cement content. The predictive models with parameters like cement content, degree of compaction and curing time have been developed for CTMG for the mix containing 65% crushed masonry and 35% crushed concrete (by mass).

Soutsos, M. N. et al. (2011) replaced 60% for the coarse fraction, i.e. 6 mm, and 20% for the fine fraction, i.e. 5 mm-to-dust levels for recycled concrete aggregate (RCA). Whereas for recycle masonry aggregate (RMA) the replacement was 20% for the coarse fraction, i.e. 6 mm, and 20% for the fine fraction, i.e. 5 mm-to-dust. The compressive strength of blocks was not changed with partial replacement for both the coarse and fine fractions. Since RMA has shown a greater detrimental effect on strength, RCA may contaminate in presence of RMA. Use of RCA in masonry was recommended to a limit of 10% only due to above reason.

Leite, F. C. et al. (2011) conducted geotechnical characterization by conducting bearing capacity and repeated load triaxial tests on recycled construction and demolition waste (RCDW) samples. The physical properties of the RCDW aggregate were affected by its composition and compaction level. The grain-size distribution was changed and the percentage of cubic grains increased during the compaction resulting in partial crushing and breaking of RCDW aggregates. The bearing capacity, resilient modulus and resistance to permanent deformation were improved due to these physical changes in RCDW aggregates. The use of RCDW aggregate in coarse base and sub-base layer for low-volume roads was recommended.

Xuan, D. X. L. et al. (2011) reported that decreasing the masonry content as well as increasing the cement content and the degree of compaction can enhance the unconfined compressive strength and the elastic modulus of cement treated mix granulates with recycled masonry and concrete. The cement content and the RMA content play an equally important role for influencing the ratio of UCS to E. Obtaining a high ratio value, one has to adjust the masonry content and the cement content. Increasing the degree of compaction is an economical method to enhance the strength, but it is not an efficient method to enhance the admissible elastic strain and improve the flexural rigidity of the CTB layer. The higher this ratio and the better the structural behaviour of the cement treated mix granulates with recycled masonry and concrete base layer. Optimizing the mixture composition of cement treated mix granulates with recycled masonry and concrete should not only consider its material properties, but also the stresses, strain and deformation to which the material is used pavement layer.

Vegas, I. et al. (2011) selected mixed recycled aggregates formed from the treatment of mixed rubble to determine the mineralogical, chemical and physical characteristics, for its use in unpaved road structural layers. The combined presence of concrete and ceramic materials resulted in pozzolanic reactions there by increasing the bearing capacity of the compacted mixed recycled aggregate. The chemical characteristics resulted that total sulphur compound content, soluble salt contents and gypsum content can be regulated with reference to the water soluble sulphates test, given the strong correlation existing between those parameters. It was recommended that the granular material containing mixed recycled aggregates with ceramic material contents below 35%, organic matter contents below 0.8% and water soluble sulphate contents below 0.4% is suitable for use in unpaved pavement sections.

2.8 CYCLIC TRIAXIAL TEST

Flexible pavement structure consists of top asphalt layer laid over base and/or sub-base compacted over a appropriate subgrade soil. Soil subgrade is considered to be important structural element of pavement structure, because the failure of subgrade due to poor bearing capacity will result in rutting on the upper granular base and subbase layers resulting in progressive fatigue cracking of top asphalt layers. The in service pavement is subjected to number of cyclic loads and the soil strength under these loading depends on a various factors

like number of cycles, frequency of loading and the magnitude of the cyclic stress (Seed, H. B. and Chan, C. K., 1966). Resilient and permanent deformations occur in subgrade when subjected to cyclic loading. The stiffness characteristics of the material affect these deformations and hence it should be relatively high to prevent the fatigue cracking of top layer. The gradual accumulation of permanent deformations during each loading cycle, results in deterioration of the structure due to excessive rutting. Thus, subgrade soil should be of sufficient bearing capacity capable of buildup of permanent deformations during the service life of pavement and result in a steady and basically resilient response to avoid early failure.

Pavements layers are subjected to a combination of resilient strains that recover after each load cycle and permanent strains, which build up with every load cycle. The resilient and permanent strains can occur at small stresses also. The stress-strain correlation is given by a non-linear curve, in form of a hysteresis loop and is not retraced on the elimination of stresses. The values for the permanent and resilient strains per load cycle can be obtained from this hysteretic loop as shown in Figure 2.23.

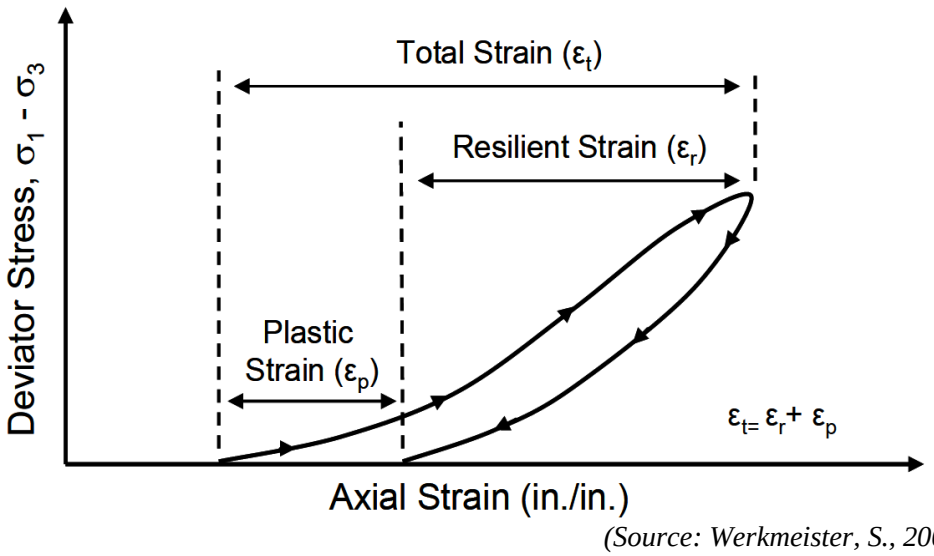

(Source: Werkmeister, S., 2003)

Figure 2.23 Hysteresis Loop for Viscous-Elastic Permanent Behaviour

Nunes, M. C. M. and Dawson, A. R. (1997) studied on alternative materials for pavement construction under repeated loading which were by-products of the U.K. power generation,

mining, and mineral industries. Stress/strain results of tests performed on unbound slate waste are presented and development of permanent deformations in repeated-load triaxial tests is shown in Figure 2.24. It is assumed in this plot that the permanent deformation rate reduces with the number of load cycles that is often the case for low stress levels. This behavior is the case for the first few thousand cycles but depending on stress level permanent deformation rate may decrease, remain constant, or increase and quickly fail with increasing load cycles.

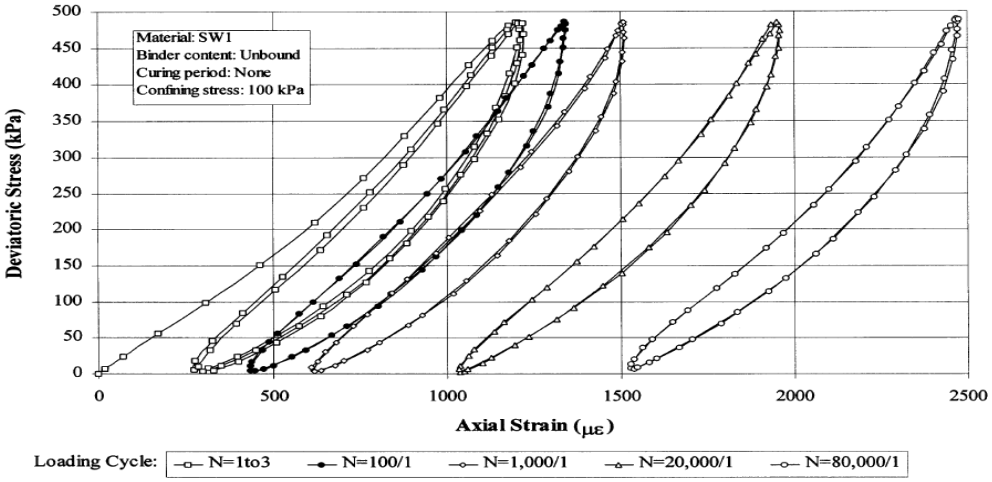

(Source: Nunes, M. C. M. and Dawson, A. R.,1997)

Figure 2.24 Developments of Permanent Deformations in Repeated-Load Triaxial Tests

Muhanna, A. S. et al. (1999) considered the different variables that can influence the resilient modulus of fine-grained subgrade soils. They used two different types of soils to study the effects of specimen end condition, repeated load sequence, rest period, number of load applications, effects of grouting and effects of the impact and kneading compaction methods on the resilient modulus. It was concluded that the number of load applications, the rest period, and the load sequence do not have any significant effect on the measured M_R. Confining pressure in the range of 0 to 69 kPa had less than a 5 percent effect on the measured M_R and grouting the soil specimen to the pedestal and the end caps of the triaxial cell did not cause any significant change. Only Soaked specimens recognized a decrease in resilient modulus in the range of 15 to 25 percent.

Unnikrishnan, N., et al. (2002), studied the properties of reinforced clay soils by triaxial compression tests done under cyclic and static loading conditions. The behaviour of specimens

reinforced with woven geotextile and micro-grid tested under 100 kPa cyclic load intensity are compared and is shown in Figure 2.25 that grid type reinforcement is more efficient even under cyclic loading. After some loading cycles the strain in these specimens remains constant with the load repetitions thus the curves for reinforced samples with sandwich layers becomes vertical; it indicates that the increase in the permanent strain under load repetition in these specimens is insignificant.

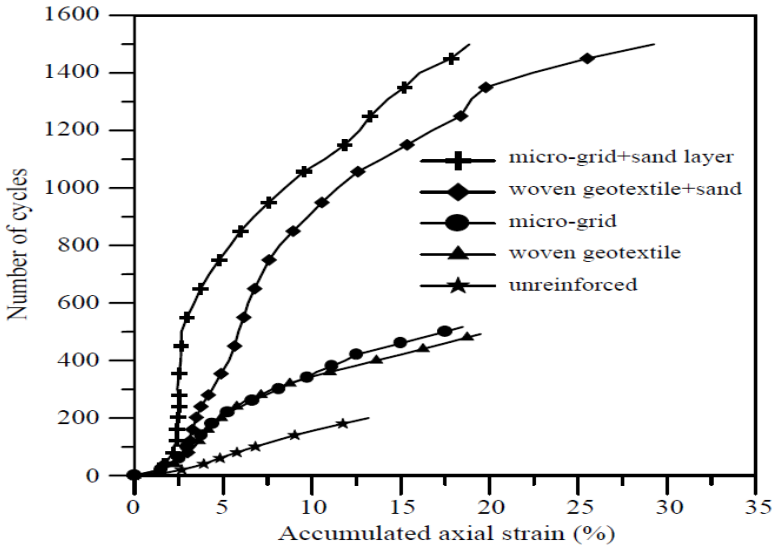

(Source: Unnikrishnan, N., Rajagopal, K. and Krishnaswamy, N.R., 2002)

Figure 2.25 Number of Cycles vs. Accumulated Axial Strain for Reinforced Clay (110 Kpa Confining Pressure)

Puppala, A, J. et al. (2003) used three chemical additives as sulfate resistant cement, low-calcium fly-ash mixed with sulfate resistant cement, and ground granulated blast furnace slag (GGBFS) to determine repeated load triaxial tests on clayey soil to assess the effectiveness of these three stabilizers in enhancing resilient modulus (M_R) properties of the soil. To understand the effects of σ_3 and σ_d on M_R response of control and treated soils and effects of stabilizers on M_R properties authors selected five deviatoric pressures under the three confining pressure. An increase in σ_d resulted in a reduction of M_R for control, cement, and GGBFS treated soils as shown in Table 2.18. These strain-softening trends of cement, cement–fly-ash, and GGBFS-treated soils can be attributed to increased load-induced damage taking place in treated soils at higher σ_d.

Table 2.18 Average M_R Values of Control and Treated Soils

σ_3 (kPa)	σ_d (kPa)	Control Soil		Cement (8%) Treated Soil		Fly Ash (15%) + Cement (5%) Treated Soil		GGBFS (20%) Treated Soil	
		M_R (MPa)	CV (%)	M_R (MPa)	CV (%)	M_R (MPa)	CV (%)	M_R (MPa)	CV (%)
14	12	89.5	20.6	902.4	3.3	366.4	15.4	519.9	12.4
14	25	78.7	24.8	970.3	2.9	340.9	0.4	359.2	31.1
14	37	78.7	17.9	689.0	4.1	387.0	0.6	296.3	4.9
14	50	77.7	10.6	655.5	25.1	415.2	1.2	285.7	10.4
14	62	76.9	10.0	596.2	21.8	439.5	0.4	297.7	13.1
28	12	89.0	21.2	812.1	7.8	6.6.3	2.9	421.2	17.1
28	25	89.1	17.7	914.3	24.4	481.6	7.4	410.2	17.1
28	37	88.0	11.0	830.1	27.2	498.8	11.8	323.5	10.4
28	50	86.9	5.6	630.6	13.2	501.1	1.4	325.9	11.4
28	62	84.5	5.8	625.8	8.7	496.7	1.7	331.2	8.7
42	12	112.8	11.2	1164.0	3.3	660.8	1.6	898.9	0.2
42	25	110.0	9.5	896.7	0.6	714.7	16.6	455.2	10.4
42	37	103.0	13.3	880.7	9.7	505.1	0.4	397.2	6.7
42	50	94.2	12.8	739.6	12.2	518.3	1.1	383.4	0.2
42	62	90.9	9.5	656.3	16.5	546.2	4.7	367.4	5.2

(Source: Puppala, A, et al., 2003)

Figure 2.26 shows that the cylindrical element will deform in both the axial and radial direction with each stress pulse. The elastic deformation recovers after each load cycle. However, there is a small permanent deformation applied to the element during each load cycle. The amount and rate of permanent deformation accumulation is dependent on material properties, the stress level, and loading history. The accumulating non-recoverable deformation from each of the stress applications is the permanent deformation (Arnold, 2004).

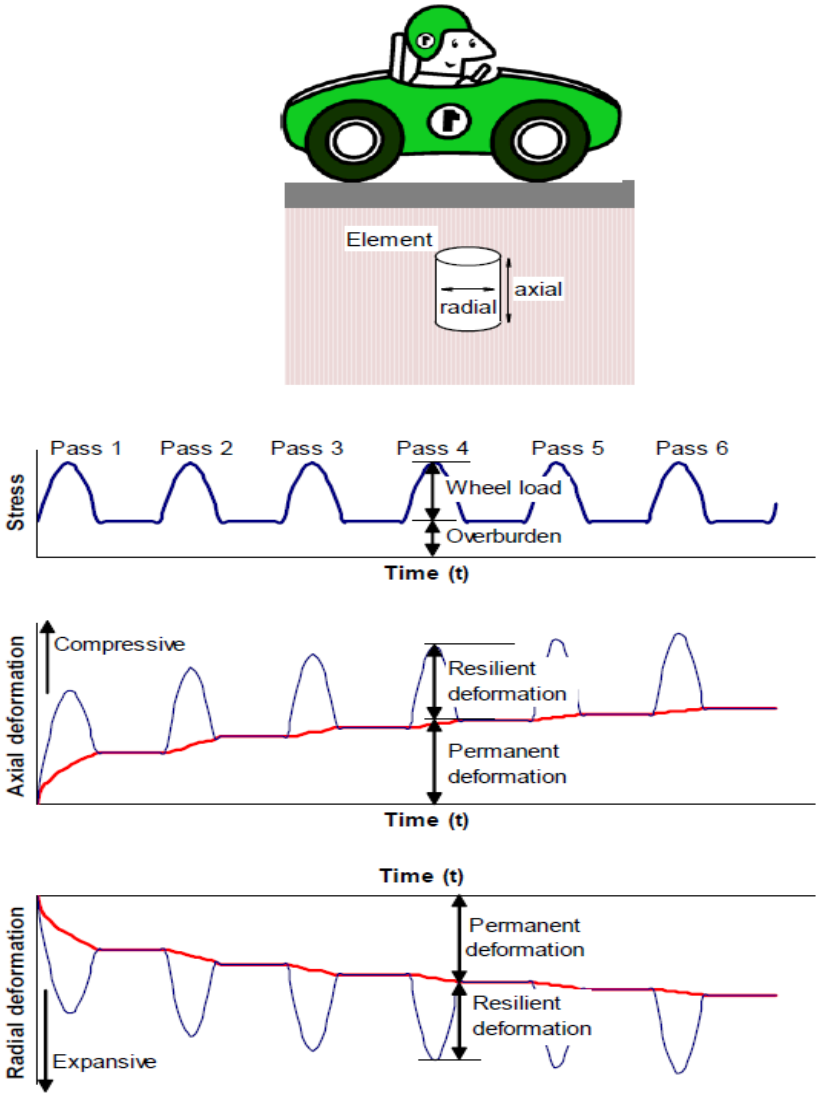

(Source: Arnold, G. K. 2004)

Figure 2.26 Loading in Pavements under Traffic

2.9 SUMMARY

This chapter presents the comprehensive literature review of different types of waste materials as FA, RHA, BA, RSA, FDCS and BF. The total production, physical properties, chemical properties, and other engineering properties of these stabilizers have been summarized briefly. The utilization of these waste materials for pavement construction, civil infrastructure construction and others are described. The variations in engineering properties in expansive soil with addition of different additives are also presented.

CHAPTER 3

EXPERIMENTAL PROGRAME

3.1 GENERAL

The influence of different waste materials on the geotechnical characteristics of soil were investigated by conducting various laboratory tests. This chapter entails test procedure adopted in the laboratory to perform various tests so as to achieve the objectives cited in Chapter 2. Various combinations of soil-waste materials mixtures considered in present study are presented in Figure 3.1. The detailed methodology adopted for the experimental work program in the present study is as shown in Figure 3.2.

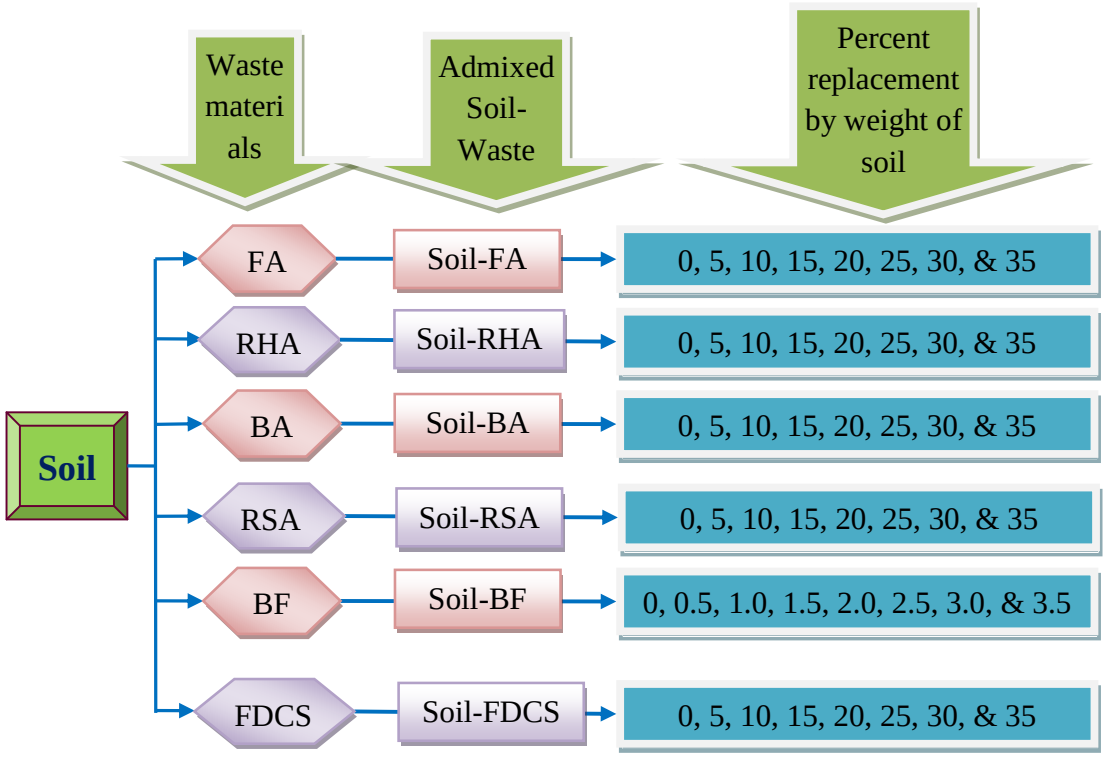

Figure 3.1 Soil–Waste Materials Mixtures Testing Plan

PROCUREMENT OF MATERIALS

Fly Ash (FA), Bagasse Ash (BA), Rice Straw Ash (RSA), Rice Husk Ash (RHA), Bagasse fiber (BF), Fines obtained from demolished concrete slab (FDCS) and Soil

LABORATORY INVESTIGATION

Studies Conducted on Selected Materials

- **Clayey Soil**
  - PI, Specific gravity
  - Grain Size Distribution
  - Proctor test
  - CBR
  - Free Swelling Index
  - Permeability
  - UCS
- **FA, BA, RSA and RHA**
  - Thermo gravimetric analysis
  - Scanning Electron Microscopy (SEM)
  - Lime reactivity
  - Grain size distribution
  - PI, Specific gravity
- **Bagasse Fiber (BF)**
  - Specific gravity
  - SEM
- **Fines of demolished concrete slabs (FDCS)** (Material Passing 1.18 mm IS)
  - Lime reactivity
  - Specific gravity
  - Particle size
  - SEM

Tests on Admixed Soil Samples

- Atterbergs Limit Test
- Proctor Test
- Permeability
- Swelling index
- CBR Test
- Unconfined Compression Test
- Split Tensile Test
- Static Triaxial Test
- Repeated Triaxial Test
- Plate Load Test
- SEM
- Model Tank Test

ANALYSIS OF RESULTS

- Comparison of laboratory results between clayey soils, fly ash stabilized soil and soil treated with other waste materials.
- Analysis of strength parameters for soil samples with or without waste materials.
- Analysis of performance related test parameters under repeated loading condition
- Development of regression model between various strength parameters for selected soil samples
- Microstructural analysis for stabilized and unstabilized soil samples to understand strength development.
- Simulating model tank test result using KENPAVE software
- Evaluation of construction cost for modified soil subgrade

Figure 3.2 Methodology of the Study

Soil is a complex and heterogeneous material substance formed over long period of time due to various geological wastes and other material processes. There are various types of soils which differ in physical and chemical composition like sand, silt, clay, loam, peat etc. In the endeavor of infrastructure development, soil is an indispensable ingredient and knowledge of its properties determine its suitability for a particular purpose. Hence initially an attempt was made to characterise afore mentioned waste materials including natural expansive soil. Various tests on soil can be broadly categorized into two types: classification tests and test to determine engineering properties. Classification tests provide information about the general soil characteristics as well as the mechanical properties like practical size distribution, strength, permeability etc. Whereas, in the case of test to determine engineering properties usefulness and suitability of soil for construction is evaluated. Waste materials or stabilizers FA, RHA, RSA, BA, RSA, BF and FDCS are used in the present study, as stabilizers.

3.2 ATTERBERG LIMITS TEST

Atterberg limits play an important role in soil identification and classification. Liquid limit (LL), Plastic limit (PL), and Plasticity index (PI), indicate some of the geotechnical problems such as swell potential and workability. One of the important and principle aims of this study was to evaluate the changes in liquid limits, plastic limits and plasticity index with addition of different wastes materials (stabilizers) to the natural soils. To achieve this objective, Atterberg limits test (including PL, LL, and PI) was conducted on material passing 0.0425 mm IS sieve size for both natural soils and different wastes-soil mixtures, according to IS: 2720 (Part 5). Description of soil based on its PI is presented in Table 3.1 for ready reference.

Table 3.1 Description of Soil Based on its PI

PI	Description
0	Nonplastic
1-5	Slightly plastic
5-10	Low plasticity
10-20	Medium plasticity
20-40	High plasticity
>40	Very high plasticity

(Source: Burmister, D. M., *1949)*

3.3 SHRINKAGE LIMIT TEST

Shrinkage is the opposite to swelling of soil. Soil swells with increase in moisture content and will shrink with decrease in moisture content. Soil shrinkage can cause serious distress to a pavement/structure. The mechanism is the same as the expansion, but in the opposite direction. When wetter than the shrinkage limit (SL), the soil is fully saturated, but when drier, the soil becomes unsaturated. The soil changes to a lighter color at the SL due to the water receding within the pores. In fact, the volume continues to decrease on drying beyond the SL as soil is dried below the plastic limit it shrinks and gets brittle until finally all the particles are in contact and the soil can shrink no further. This point is called the shrinkage limit. The soil still has moisture within it but if any of this moisture is lost by further drying, air has to enter the soil to replace it. SL test was conducted as per IS: 2720 (Part 6). The purpose of conducting SL was to evaluate the shrinkage effect on admixing of stabilizer to natural expansive soil.

3.4 FREE SWELL INDEX TEST

Free swell index (FSI) test is commonly used for identifying expansive clays and to predict the swelling potential. Test was conducted in accordance with IS: 2720 (Part 40). Free swell of soil helps to identify the potential of a soil to swell which might need further detailed investigation regarding swelling and swelling pressures under different field conditions. Material passing 0.045 mm IS sieve size was taken in two glass graduated cylinders each of 100 ml capacity, one filled with kerosene oil and other with distilled water up to the 100 ml mark. After removal of entrapped air the soils in both the cylinders were allowed to settle for 24 hours as shown in Figure 3.3. The final volume of soils in each of the cylinders was noted. The level of the soil in the distilled water cylinder was read as the free swell level. The FSI (%) of the soil was calculated as given below using Equation 3.1.

$$\text{Free swell index} = \frac{V_d - V_k}{V_k} \times 100 \qquad (3.1)$$

Where, V_d = the volume of soil specimen read from the graduated cylinder containing distilled water, and V_k = the volume of soil specimen read from the graduated cylinder containing kerosene.

Figure 3.3 Laboratory Setup for Determination of Free Swell Index

According to ministry of road transport and highways (MoRT&H) specification, free swelling index should not be more than 50 percent for road construction. The potential of swelling of soil samples after admixing waste material are noted and their results are compared.

3.5 MODIFIED PROCTOR TEST

The geotechnical properties of soil (such as CBR, compressive strength, permeability, cohesion etc.) are dependent on the moisture content and density at which the soil is compacted. Generally, a high level of compaction of soil enhances the geotechnical parameters of the soil, so that achieving the desired degree of relative compaction necessary to meet specified or desired properties of soil is very important (Nicholson, P. et al., 1994). The aim of the proctor test was to determine the optimum moisture contents (OMC) and maximum dry density (MDD) of both natural soil and treated stabilized soil-

mixtures. In order to obtain these parameters, heavy compaction test was employed in accordance with IS: 2720 (Part 8). Figure 3.4 shows the proctor test conducted in the laboratory.

Figure 3.4 Standard Proctor Test in Laboratory

3.6 CALIFORNIA BEARING RATIO TEST

It is in essence a simple penetration test developed to evaluate the strength of road subgrade. It basically determines the resistance of the subgrade, to deformation under the load from vehicle wheels. Higher the California bearing ratio (CBR) reading shows stronger the subgrade and lesser would be the thickness of pavement, hence considerable cost saving is made. Conversely low CBR reading indicates the subgrade is weak and hence more thickness of pavement has to be provided so as to spread the wheel load over a greater area of the weak subgrade in order that the weak subgrade material is not deformed, causing the road pavement to fail.

Compacted CBR mould with or without stabilizers were kept at 90% relative humidity prior to water soaking. CBR moulds were prepared for each mix so that three moulds each

are available for the test at 3, 7, 14, 28, 56 and 128 days after expose to 90% relative humidity and 96 hours water soaking respectively.

The CBR test was conducted in accordance with IS: 2720 (Part 16). The samples of natural soil and admixed soil were compacted by statically Compaction. The mass of the wet soil at the required moisture content to give the desired density when occupying the standard specimen volume of 2250 cm^3 in the mould of height 127.3 mm and diameter 150 mm were calculated. A batch of soil was thoroughly mixed with water to give the required water content. The correct mass of the moist soils was placed in the mould and static compaction obtained by pressing the displacer disc as shown in Figure 3.5. Weights to produce a surcharge equal to the weight of base material and pavement to the nearest 2.5 kg was placed on the compact soil specimen. These admixed soil samples were kept in humidity chamber for 7, 14, 28, 56 and 128 days separately.

Figure 3.5 Static Compaction of CBR Specimen

3.6.1 Test for Swelling

After the expiry of 3, 7, 14, 28, 56 and 128 days humidity curing, the whole mould and weights were immersed in a tank of water allowing free access of water to the top and bottom of the specimen. The tripod for the expansion measuring device was mounted on

the edge of the mould and the initial dial gauge reading (d_i) was recorded. This set-up was kept undisturbed for 96 hours. The readings of CBR swelling were taken at 1, 2, 4, 8, and 12 hours and thereafter at an interval of 12 hours upto 96 hours. At the end of the soaking period, the final dial gauge reading (d_f) was noted. A constant water level was maintained in the tank through-out the period of test. The laboratory setup for the same is as shown in Figure 3.6. The expansion ratio (ER) based on tests conducted was calculated using Equation 3.2.

$$\text{Expansion Ratio (\%)} = \frac{d_f - d_i}{h} \times 100 \qquad (3.2)$$

Where, d_f =final dial gauge reading (mm),

d_i =initial dial gauge reading (mm), and

h =initial height of the specimen (mm).

The expansion ratio is used to qualitatively identify the potential expansiveness of the soil.

Figure 3.6 Laboratory Setup for Determination of Expansion Ratio

3.6.2 Penetration Test

The samples prepared with or without stabilizers were subjected to CBR testing machine after having proper requisite number of days of curing. The mould containing the specimen, base plate with surcharge was placed on the lower plate of the testing machine as shown in Figure 3.7. The cylindrical plunger of 50 mm diameter was seated under a load of 4 kg so that full contact is established between the surface of the specimen and the plunger. Load was applied to the plunger into the soil at the rate of 1.25 mm per minute and reading of the load was taken at penetrations of 0.5, 1.0, 1.5, 2.0, 2.5, 4.0, 5.0, 7.5, 10.0 and 12.5 mm. The maximum load corresponding to its penetration was recorded to determine the CBR values by following Equation 3.3.

$$\text{CBR Value}\,(\%) = \frac{\text{Unit load carried by the soil at defined penetration value}}{\text{Standard unit load carried at the same penetration value}} \times 100 \qquad (3.3)$$

Figure 3.7 Laboratory Setup for Determination of CBR

Standard loads at specified penetrations for determination of CBR value are given in Table 3.2.

Table 3.2 Standard Loads at Specified Penetrations

Penetration depth (mm)	Total standard load (Kgf)
2.5	1370
5.0	2055
7.5	2630
10.0	3180
12.5	3600

The general relationship between CBR values and the quality of the subgrade soils used in pavement applications is given in Table 3.3.

Table 3.3 CBR Values Corresponding to Quality of Subgrade

CBR - values	Quality of sub-grade
0 – 3 %	Very Poor
3 – 7 %	Poor to Fair
7 – 20 %	Fair
20 – 50 %	Good
> 50 %	Excellent

(Source: Bowles, J., 1992)

3.7 UNCONFINED COMPRESSIVE STRENGTH TEST

UCS test is the main test recommended for the determination of the required amount of additive to be used in the stabilization of soil. The unconfined compression test is a quick and relatively inexpensive mean to obtain undrained shear strength of cohesive soils. In this test, the confining pressure σ_3 is kept zero. This test is commonly used in practice because of its simplicity. In most cases, undrained strength results from an unconfined compression test are conservative. The maximum stress measured at failure (σ_1 max.) is equal to unconfined compression strength (q_u). The undrained shear strength result from UCS test is half of the unconfined compression strength as shown in Figure 3.8. For conducting the UCS test, cylindrical specimens of size 50 mm diameter and 100 mm length were prepared at optimum moisture content and maximum dry density. Figure 3.9 (a & b) shows the

arrangements made for UCS test. Test samples were prepared under static compaction and compacted specimens were placed in polyethylene bag immediately after compaction to maintain the required moisture content and then cured for 7, 14, 28, 56 and 128 days to protect the samples from the free moisture by maintaining a temperature of 23.0 ± 1.7°C and a relative humidity of not less than 96% for moist curing specimens as specified in ASTM D1632-07. After proper curing, unconfined compression load was applied at strain rate of 1.25 mm/min. The test was conducted in accordance with IS: 2720 (Part 10). Figure 3.10 shows UCS test in progress.

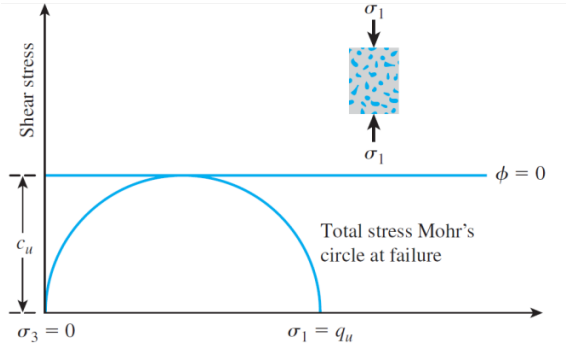

Figure 3.8 Unconfined Compression Test

(a) Static Compaction

(b) Compacted Specimens Kept in Polyethylene Bag

Figure 3.9 UCS Test Arrangements

Figure 3.10 UCS Test in Progress

The general relationship between unconfined compressive strength and the quality of the sub-grade soils used in pavement applications is presented in Table 3.4.

Table 3.4 General Relationship of Consistency and Unconfined Compression Strength

Consistency	kN/m^2
Very soft	0–25
Soft	25–50
Medium	50–100
Stiff	100–200
Very stiff	200–400
Hard	400

(Source: Das, B. M., 2010)

3.8 HYDRAULIC CONDUCTIVITY TEST

Any given mass of soil consists of solid particles of various sizes with interconnected void spaces. The continuous void spaces in a soil permit water to flow from a point of high energy to a point of low energy. Permeability is defined as the property of a soil that allows the seepage of fluids through its interconnected void spaces. In order to obtain a fundamental relation for the quantity of seepage through a soil mass under a given condition by Darcy's law. Darcy's Law states that under steady conditions of flow through beds of sands of various thicknesses and under various pressures, the rate of flow is always

proportional to the hydraulic gradient. This principle has been found to be generally valid for the flow of water in soils, except at high velocities when turbulence occurs. Darcy's law is expressed mathematically as

$$\upsilon = ki \tag{3.4}$$

$$q = \upsilon A = kiA = k\frac{\Delta h}{L}A \tag{3.5}$$

Where, q is the total rate of flow through the cross-sectional area A, and k is the so called coefficient of permeability.

The proportionality constant (k) is referred to as the hydraulic conductivity, which describes the ability of a porous material to allow the passage of a fluid, and is not a fundamental property of soil, but depends upon a number of factors. Particle size distribution has a significant effect on the material's permeability, in which the smaller the particles, the smaller the voids between them, and therefore the permeability decreases. On the other hand, particle shape and texture influences permeability. Irregular shape and rough surface texture tend to reduce the flow rate of water through the soil. Different techniques are available to determine soil hydraulic conductivity (k). The degree of permeability is determined by applying a hydraulic pressure difference across a soil sample, which is fully saturated and measuring the consequent rate of flow of water (Head, K. H., 1992).

The permeability test was conducted as per IS: 2720 (Part 17). For the present study falling head permeability test is done. Oven dry soil and other additives were taken to compact in permeameter mould having a capacity of 1000 ml, with an internal diameter of 100 mm and internal effective height of 127.3 mm. The compaction was done at optimum moisture content and its maximum dry density. The mould with the specimen inside was assembled to the drainage base and cap having porous discs. The assembled mould with specimen was kept for full saturation. The fully saturated specimen was connected to falling head test arrangement. Top inlet was connected to stand-pipe and the bottom outlet was opened and the time interval required for the water level to fall from a known initial head to a known

final head as measured above the centre of the outlet was recorded as shown in Figure 3.11. The permeability is then calculated using the Equation 3.6.

$$k = 2.3\frac{aL}{A\Delta t}\log_{10}\frac{h_1}{h_2} \quad (3.6)$$

Where,

k = coefficient of permeability (cm/sec), from falling head test

a = cross-sectional area of reservoir (cm^2)

L = length of specimen (cm)

A = cross- sectional area of specimen (cm^2)

h_1, h_2 = water levels (cm), and

Δt = time required for water falling from h_1 to h_2 (sec)

Figure 3.11 Laboratory Setup for Determination of Permeability

3.9 TRIAXIAL TEST

Unconsolidated undrained (UU) triaxial tests are most commonly used for specimen of earth-fill materials which are compacted in laboratory under specified condition of optimum moisture content and maximum dry density. While other triaxial type, i.e., consolidated drained (CD) or consolidated undrained (CU) will produce more meaningful strength parameters, the UU test carried out in the present study was intended as a ranking test. It was planned to perform the CD test, but during the course of the testing program it was observed that saturation of clayey soil became very difficult and takes more time to achieve complete saturation. As a large number of specimens have to be tested, it was decided to conduct UU tests on natural and treated stabilized specimens in accordance with IS: 2720 (Part 11). All triaxial tests were conducted at a constant axial strain of 1.25 mm/min under UU condition to simulate the behavior of soils subjected to quick loading immediately after construction. The cylindrical test samples were prepared of dimension 100 mm height and 50 mm diameter. The cell was assembled with the loading ram and specimen then water was injected to the cell and the pressure rose to the desired value as shown in Figure 3.12. Three different confining stresses such as 100, 150 and 200 kPa were applied on specimens to obtain peak deviator stress. The range of confining stresses was chosen to obtain more well defined and accurate plots of Mohr envelopes to obtain shear strength parameters, cohesion (c) and angle of internal friction (φ) of the natural and treated stabilized specimens.

3.10 SPLIT TENSILE STRENGTH TEST

Normally, compressive strength testing is used for evaluating strength of stabilized soils and there are fewer studies concerning their tensile strength. Tensile strength is a very important geotechnical parameter to predict the cracking behavior of pavements, earth dams, and earth structures using stabilized soils (Baghdadi, Z. A. et al., 1995). Knowledge of the tensile strength is needed in the study of stability of earth dams, highways, and airfield pavements. Tensile stresses are set up due to movement of traffic on pavement, shrinkage of soils, seasonal variation in temperature and alternate wetting and drying of soils, etc.

Figure 3.12 Test Setup for Triaxial Test

Various tests and modifications have been developed and used for evaluating tensile strength of soils and stabilized soils. For conducting the split tensile test, cylindrical specimens of size 50 mm diameter and 100 mm length were prepared at optimum moisture content and maximum dry density in the same way as in case of unconfined compression tests. The specimens were placed horizontally as shown in Figure 3.13 between the bearing blocks of the compression testing machine as per ASTM D3967–08. All tests were conducted at a constant axial strain at 1.25 mm/min after 7, 14, 28, 56 and 128 days curing periods to obtain failure load. The split tensile strength (STS) is obtained by the following Equation 3.7.

$$\text{Split tensile strength } (\sigma_t) = \frac{2P}{\pi LD} \tag{3.7}$$

Where, P=Failure load; L= Length of specimen; and D=Diameter of the specimen.

Figure 3.13 Test Setup for Split Tensile Strength Test

3.11 CYCLIC TRIAXIAL TEST

The strength of soil under cyclic loading depends on a number of factors such as the number of cycles, frequency of loading and the magnitude of the cyclic stress (Seed, H.B. and Chan, C. K., 1966). In particular, the global response of subgrade results in resilient and permanent deformations when subjected to repeated loading. Resilient deformations are related to the stiffness characteristics of the material that should be sufficiently high in order to avoid the fatigue cracking of top layer. On the other hand, the gradual accumulation of permanent deformations, although they are very small during each loading cycle, could lead to deteriorate the structure due to excessive rutting. Therefore, sufficient bearing capacity pavement subgrade should experience accumulation of permanent deformations that during its service life will eventually cease resulting in a stable and basically resilient response in order to avoid premature failure.

A review of these issues (Brown, S. F., 1996 and 2004) described how observations from repeated load triaxial testing had demonstrated the existence of a threshold deviator stress level, below which the magnitude of accumulated plastic shear strain is quite small. The same phenomenon is apparent in the theoretical concept of shakedown, derived from structural engineering and first applied to pavements (Sharp, R.W. and Booker, J. R., 1984). In this context, the main aim of this test is focused on a better understanding of the permanent deformation behaviour under repeated loading on natural and treated stabilized specimens.

A repeated load triaxial apparatus, consisting essentially of a main cyclic load device and a removable pressure chamber, allowed a constant confining pressure and a cyclic axial load to be applied on the specimen through the test. During the test, two LVDTs measured the axial deformations at the top of the specimens and load cell measured the cyclic load on specimen. Load and deformation data were then stored by a proper data acquisition system. All tests were performed in undrained conditions. Cyclic triaxial strength tests were conducted under undrained conditions to simulate essentially undrained field conditions during moving traffic. The cyclic loading generally causes an increase in the pore-water pressure in the specimen, resulting in a decrease in the effective stress and an increase in the cyclic axial deformation of the specimen.

Repeated triaxial test were conducted on sample of size 100 mm diameter and 200 mm height in conventional triaxial cell by static compaction at OMC as shown in Figure 3.14. The frequency of load application in all tested were kept 70 cycle per minute; this was fixed based on traffic density (Kumar, P. and Singh, S. P., 2008). The loads were applied upto 10,000 cycles and behavior of various parameters such as resilient strain, permanent strain and resilient strain was observed at different cycles by computerized dataloger system as shown in Figure 3.15. In the present study, the cyclic triaxial tests were conducted as per ASTM D5311-11 on natural and treated stabilized specimens. Stress-strength ratio in this study is called deviator stress levels (DSL) and can be defined as the ratio of the σ_d of repeated load triaxial test to the soil strength obtained from undrained triaxial (σ_s). Three levels of σ_3 (50, 100 and 150 kPa) at 0.50 DSL and 0.80 DSL were

applied. The average response of total resilient strain (ε_r) under each deviator stress (σ_d) for the last five cycles of the testing phase were measured to determine the resilient modulus (M_R) by using following Equation 3.8.

$$M_R = \frac{\sigma_d}{\varepsilon_r} \tag{3.8}$$

Figure 3.14 Specimen for Repeated Triaxial Test

Figure 3.15 Test Setup for Repeated Triaxial Test

3.12 PLATE LOAD TEST

Plate load test method covers for determination of ultimate bearing capacity of soil in place which assumes that a soil stratum is reasonably uniform. The load test included in the standard is also used to find modulus subgrade reaction useful in the design of pavements. Data from the tests are applicable for the design of both flexible and rigid pavements. In plate bearing test, a compressive stress is applied to the soil or pavement layer through rigid plates relatively large size and the deflections are measured for various stress values.

Plate load tests were conducted in excavated test pits of size 1500 mm × 1500 mm × 1500 mm by using 300 mm in diameter and 25 mm thick rigid circular steel plates. The setup shown in Figure 3.16 for conducting the plate load test was established in accordance with IS: 1888. The load was applied through a system comprising a hydraulic jack, a reaction beam, a loading platform, and a calibrated proving ring. Three dial gauges with divisions of 0.01 and 50 mm travel were used for settlement measurement. Measurements were made directly on the plate, as well as on the top of the treated layer adjacent to the plate. Settlements on the top of the plate were taken at three points, separated 120° from each other. The gauges were fixed to a reference beam and supported on external rods. A seating load of 0.07 kg/cm^2 was applied and released before starting the load test. For each load increment, measurement of settlements was made.

Figure 3.16 Test Setup for Plate Load Test

3.12.1 Modulus of Subgrade Reaction

Modulus of subgrade reaction (K) is ratio of load per unit area of horizontal surface of a mass of soil to corresponding settlement of the surface. It is determined as the slope of the secant drawn between the point corresponding to zero settlement and the point of 1.25 mm settlement, of a load-settlement curve obtained from a plate load test on a soil using a 75 cm diameter or smaller loading plate with corrections for size of plate used.

$$K= \frac{p}{0.125} \ MPa/cm^2 \tag{3.9}$$

Where, P = load intensity corresponding to settlement of plate of 1.25 mm.

For this study 30 cm diameter loading plate was used to determine the K value. After that K values was corrected by following formula.

$$K = K_1 \frac{a_1}{a} \tag{3.10}$$

Where, K_1 is modulus of subgrade reaction of smaller plate of radius a_1 and K is modulus of subgrade reaction of standard plate of radius a.

3.12.2 Ultimate Bearing Capacity

The load was applied in equal increments of not more than one-tenth of the estimated ultimate bearing capacity (Consoli, N. C. et al., 1998 and 2003). The 'time settlement' curve is plotted at each load stage and load is increased till the curve indicates that the settlement has exceeded 70 to 80 percent of the probable ultimate settlement at that stage (Consoli, N. C. et al., 2009 and Ker, R. K. et al., 2012). Load - settlement curves was plotted with the data obtained from the plate load tests in laboratory. If obtained curves are not well defining the yield point, then the ultimate bearing capacity are found from the tangent intersection of the two straight portions of the load-settlement curve at the initial straight portion and the steeper straight portion at the end. From the corrected load settlement curves no difficulty was experienced in arriving at the ultimate bearing capacity in case of curves D and B as the failure is well defined as shown in Figure 3.17. But in the case of Curves A and C where yield point is not well defined settlements were plotted as

abscissa against corresponding load intensities as ordinate, which give two straight lines, the inter-section of which will be considered as yield value of soil.

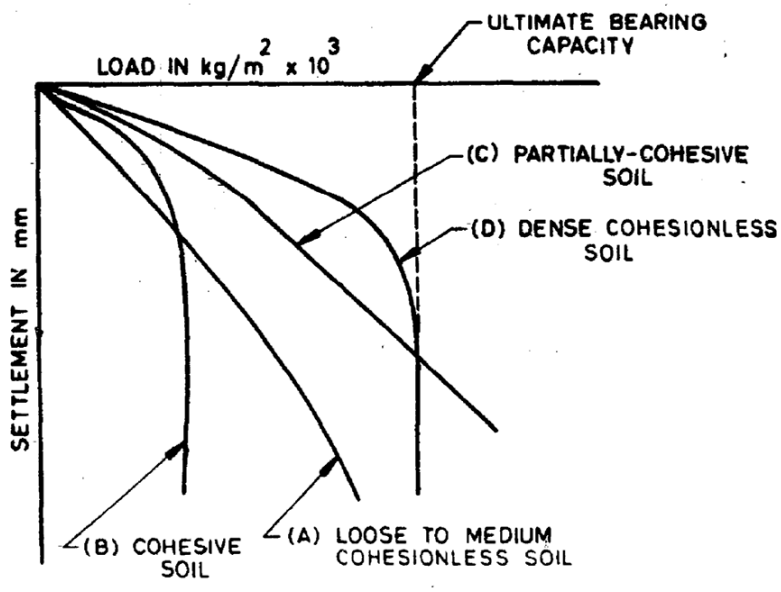

(Source: IS : 1888 – 1982)

Figure 3.17 Load Settlement Curves

3.13 MODEL TANK TEST

The present study mainly emphasized on strengthening of natural weak soil (expansive soil). An attempt was made to improve the engineering properties of locally found expansive soil by incorporating silica rich waste materials.

The process of improving locally available weak soil by admixing some suitable additives or stabilizers is called chemical soil stabilization. In the present study silica rich waste materials like FA, BA, RHA, RSA and FDCS were employed for soil stabilization. In order to characterise subgrade material tests have to conducted to understand their behavioural properties to be able to determine how the material would perform in the actual field environment particularly when any additives or stabilizers are incorporated in subgrade soil with a motive to improve soil engineering properties. To observe the subgrade layer performance as well as layers overlain above subgrade layer, a steel model tank shown in Figure 3.19 is chosen. Figure 3.18 shows the pavement structure used for this research

work, and was constructed with and without a stabilized subgrade of 300 mm compacted layer inside the steel model tank. The subgrade layer with optimum moisture content was compacted to achieve at least 98% degree of compaction. Subsequently, 100 mm thick granular sub base (GSB), 110 mm wet mix macadam (WMM), 50 mm compacted layer of dense graded bituminous macadam (DBM) and 40 mm bituminous concrete (BC) have been overlain on top of 300 mm compacted subgrade layer.

The compaction was achieved by using dynamic compacter for all the layers. Also to simplify the compaction process, a line of measurements were made on the side of tank to ensure the required calculated mass of material was compacted for necessary height as shown in Figure 3.19 (a) using the density calculated through experimentation.

The degree of compaction of these layers were monitored by using non destructive density meter as shown in Figure 3.19 (c). For GSB layer construction, grading III conforming to MoRT&H section 400 was employed and 98% degree of compaction was ensured with the help of non distractive test (NDT) density meter. Just on top of GSB layer, 110 mm WMM compacted layer was provided by ensuring 98% of degree of compaction with respect to the laboratory dry density.

For DBM layer construction, grading 2 conforming to MoRT&H was chosen. Bituminous mix was prepared with VG 30 bitumen and Marshall density of compacted bituminous Marshall mould worked out for the corresponding optimum binder content (OBC) was noted. This Marshall density was used as referral density to compare the degree of compaction achieved in the tank. Similarly, 40 mm BC layer conforming to MoRT&H section 509 was compacted on the top most surface of the tank. The degree of compaction maintained for both DBM and BC are 98% with respected to laboratory Marshall density. In order to simulate the contact area a 300 mm diameter plate (Huang, Y. H., 2004) of 25 mm thickness was used to transfer the load plunger to pavement surface.

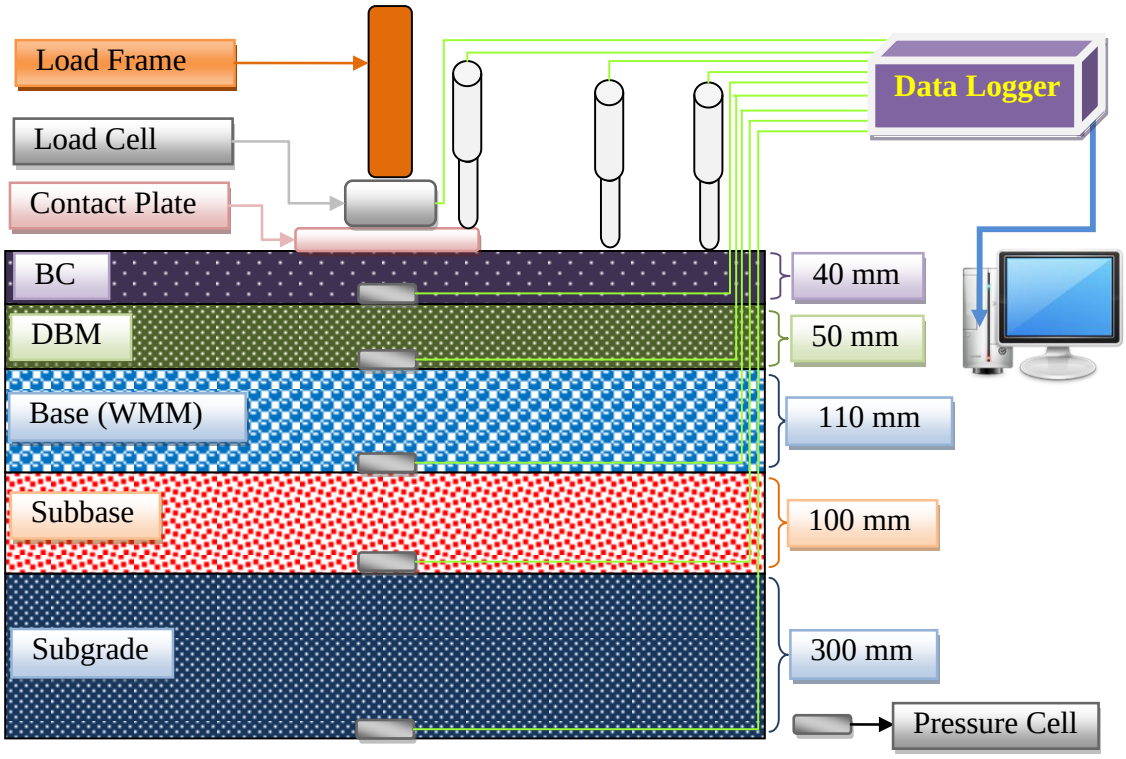

Figure 3.18 Locations of Load Cell and Pressure Cells in Pavement Structure

The main motive behind this task was to measure the vertical deflection and vertical stresses of the compacted pavement structure. Hence to draw the deformation characteristic of pavement, total three linear variable differential transformers (LVDT) were placed as one on top of plate and two LVDTs on surface of pavement. To measure the vertical stress of different pavements layers, total five pressure cells were placed on every compacted layer. Embedment of cell on every compacted layer is clearly depicted in Figure 3.17. In the very beginning one pressure cell was placed in the middle of bottom tank prior to subgrade material was spread. Ones subgrade layer is compacted to required density, another load cell was placed on top of compacted subgrade surface i.e. at the interface of subgrade top and bottom of GSB layer. In the same manner, pressure cell were placed at the interface of GSB layer top and bottom of WMM layer, WMM top & DBM bottom and DBM top and BC bottom. Lastly one load cell is placed on the top of 300 mm diameter plate so as to record the magnitude of load experience by top of pavement system.

(a) Load cell placed at top of subgrade (b) Load cell at interface of sub base and WMM

(c) Determine the degree of compaction (d) Load cell at interface of WMM and DBM

(e) Compaction of DBM by dynamic loading (f) Checking degree of compaction of DBM

Figure 3.19 Preparation of Model Tank in Laboratory

All the pressure cells, load cell and LVDTs were connected to data logger system and the same was attached to computer to obtain all the data in each cycle. The complete set up is

shown in Figure 3.20. The frequency of load applications was set as 70 cycles per minute to keep impact ranges from 5 % to 10 % on pavement, which simulates the actual traffic condition. The frequency corresponds to 4200 repetitions per hour.

Figure 3.20 Test Setup for Model Tank Test

3.14 SUMMARY

This chapter presents the detailed methodology adopted for this study. Various combinations of soil and additives like RHA, RSA, BA, RSA, BF and FDCS used for the study are described. Detailed test procedures adopted for testing the geotechnical properties of soil with and without additive are described. Laboratory investigations done for this study include various tests like Atterberg limits, free swell index, Proctor test, California bearing ratio, expansion ratio, hydraulic conductivity, unconfined compressive strength, split tensile strength, triaxial, cyclic triaxial, plate load test and model tank test. All tests were performed as per IS and ASTM standards.

CHAPTER 4

MATERIAL CHARACTERIZATION

4.1 GENERAL

This Chapter presents the details of sources and basic properties of all materials like soil, FA, RHA, RSA, BA, BF and FDCS collected for experimental study to achieve the objectives defined in Chapter 1. The soil and waste materials utilized in the present study were collected from different sources as shown in Figure 4.1. The details of their locations are given in Table 4.1. Physical & chemical and other impotent parameters of these materials are studied. Figure 4.2 shows the different waste materials used in the present study.

Table 4.1 Location of Procured Materials

Material	Procured Location (District Name)
Soil	Dhanpura (Haridwar)
FA	NTPC Dadri (Gautambudhnagar)
RHA	Roorkee (Haridwar)
RSA	Roorkee (Haridwar)
BA	Eakbal Pur and Deoband (Haridwar)
BF	Eakbal Pur and Deoband (Haridwar)
FDCS	Bhagwan Pur (Haridwar)

4.2 SOIL

4.2.1 Physical and Chemical Analysis

American Association of State Highway and Transportation Officials (AASHTO) and Unified Soil Classification System (USCS) were referred while classifying the soil group. These classification systems are based on the consistency limit and the particle-size analysis of soil. Table 4.2 presents the physical properties of natural soil and soil groups classified by both AASHTO and USCD. Grain size analysis and consistency limit tests were conducted in accordance with IS: 2720 (Part 4) and IS: 2720 (Part 5) respectively. Fine grained soil analysis was done by sedimentation technique using hydrometer. Specific gravity and Shrinkage limit

tests were conducted for natural expansion of soil as per IS: 2720 (Part 3) and IS: 2720 (Part 6) respectively.

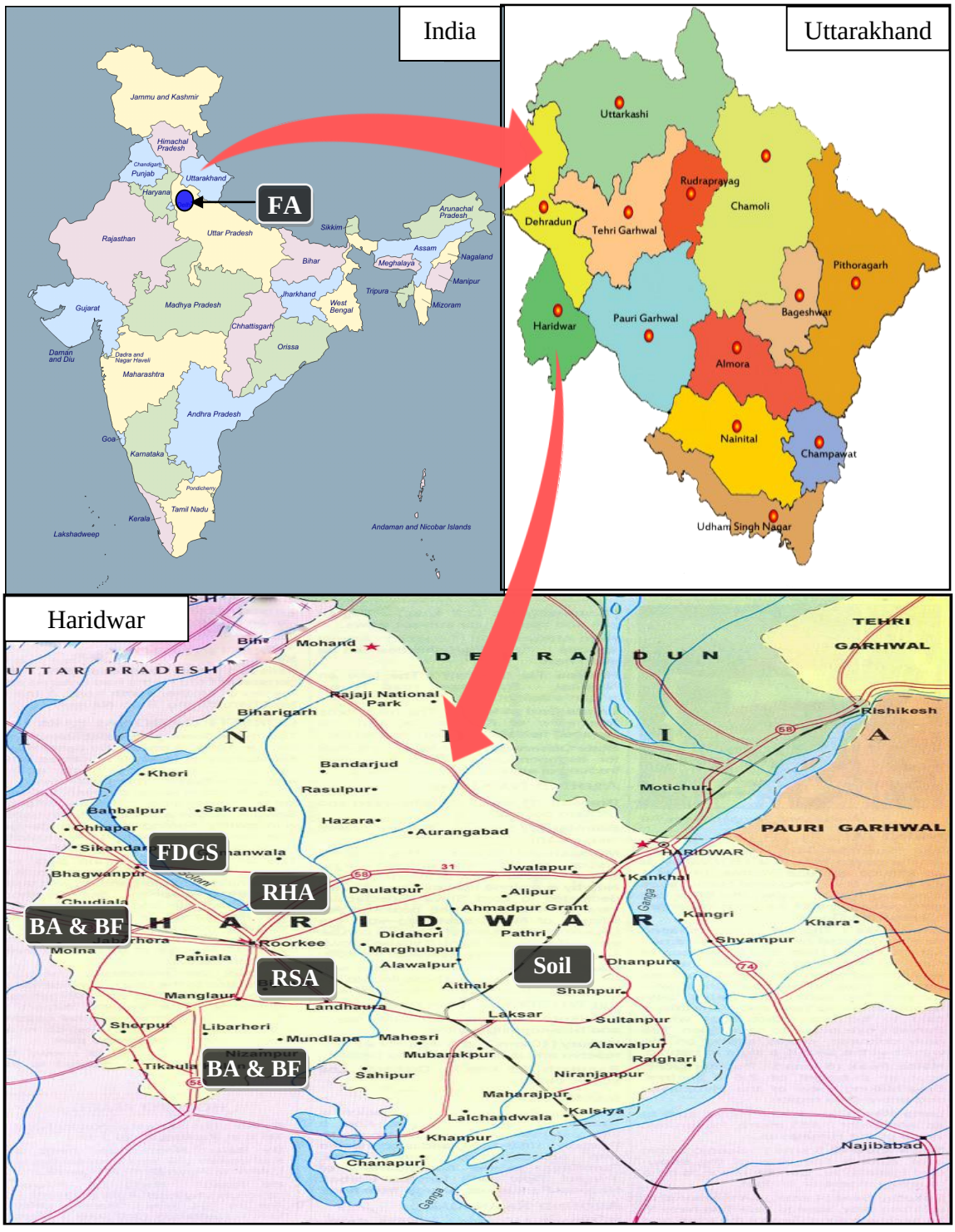

Figure 4.1 Location Map of Waste Materials and Soil

(a) Fly ash

(b) Rice husk ash

(c) Rice straw ash

(d) Bagasse ash

(e) Bagasse fiber

(f) Fines obtained from demolished concrete slab

Figure 4.2 Waste Materials Used for the Present Study

Table 4.2 Physical Properties of Natural Soil

Property	Value
Specific gravity	2.74
Liquid limit (%)	46
Plastic limit (%)	21
Fineness by sieving	
Sand particles (%)	5.5
Silt particles (%)	50
Clay particles (%)	44.5
Shrinkage limit (%)	16
Plasticity index (PI)	25
Unified soil classification	CL
AASHTO soil classification	A-7-6
Type of Soil	Clay of medium compressibility

As may be seen, natural soil passes more than 50 percent from 0.075 mm IS sieve size and its liquid limit and plasticity index were found to be 46 percent and 25 percent respectively. Hence this soil belongs to CL group according to the unified soil classification system. Similarly, according to AASHTO soil classification system, this particular soil is being classified as A-7-6 soil group because particles finer then than 0.075 mm is more is more than 35 percent and values of liquid limit and plasticity index are more than 40 percent and 16 percent respectively. In addition to this information, it is very pertinent to assess shrinkage potential of the soil as shrinkage limit is useful in area where soils undergo large volume of changes when going to wet and dry cycles. The present soil's shrinkage limit was found to be 16 percent indicating degree of expansion is medium "marginal".

Table 4.3 shows the chemical composition of natural expansive soil. The present soil is comparable very close to bentonite which is also known as commercial clay. The approximate content of SiO_2, Al_2O_3, Fe_2O_3, CaO & MgO are 67.60%, 20.38%, 4.41%, 2.51% and 2.43% respectively for bentonite. This clearly infers that the present soil has potential to swelling. Figure 4.3 shows the grain size distribution of natural expansive soil.

Table 4.3 Chemical Composition of Natural Soil

Chemical Element	Value (%)
SiO_2	48.2
Al_2O_3	13.70
Fe_2O_3	6.17
CaO	12.21
MgO	2.03
K_2O	2.15
MnO	0.075
SO_3	5.11
LOI	5

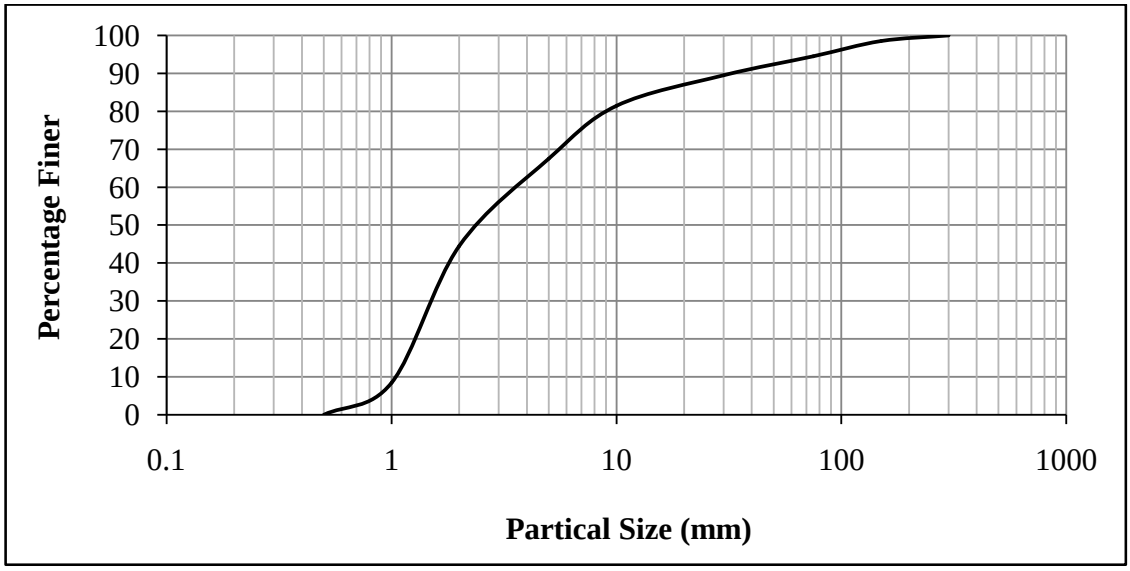

Figure 4.3 Grain Size Distribution for Natural Soil

4.2.2 Geotechnical Properties

4.2.2.1 Compaction

In order to ascertain the maximum dry density and optimum moisture content of natural soil, standard proctor test was conducted in accordance with IS: 2720 (Part- 8). Figure 4.4 depicts the relationship between MDD and OMC of the soil sample. The maximum dry density of 1.71 g/cm^3 and the optimum moisture content of 17% are read from the Figure.

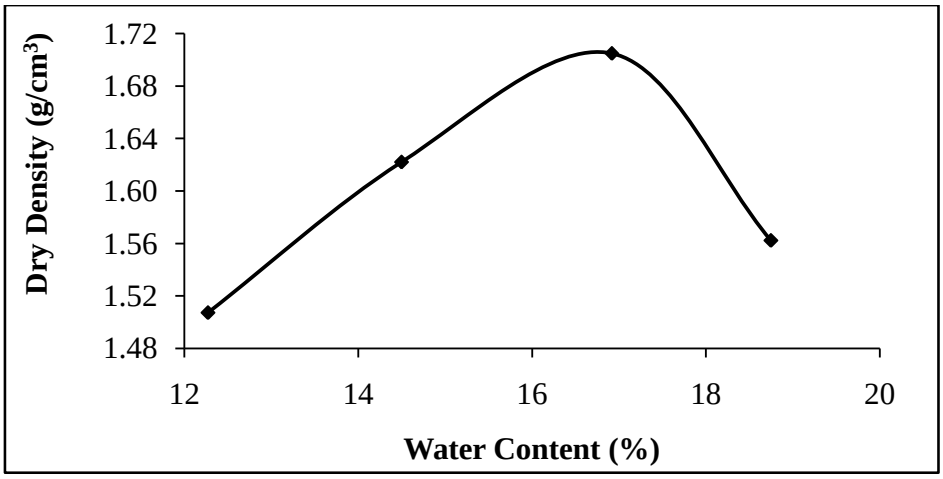

Figure 4.4 Compaction Characteristic Curve of Soil

4.2.2.2 California bearing ratio

Effort was also made to determine soaked CBR value of natural soil so as to get the idea of its load bearing capacity. Three CBR moulds were prepared at its OMC and kept for water soaking for 96 hours. The samples were tested in accordance with IS: 2027 (Part 16). Figure 4.5 depicts the graphical plot between penetrations in mm versus load sustained by the specimen in kN. From this analysis, it was found that soaked CBR value of natural soil at 2.5 mm and 5 mm penetration are 1.86 and 1.82 respectively. Since the CBR value of natural soil is less than 2 percent, it can not be classified as a good subgarde soil (IRC 37: 2001). Such kind of soil demands some treatment prior to use in the road construction (Bowles, 1992).

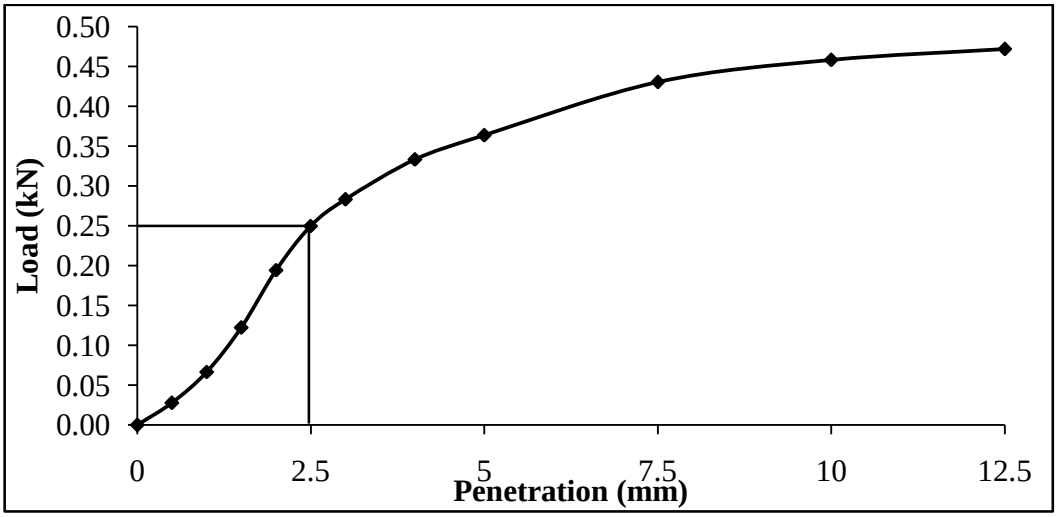

Figure 4.5 Load Penetration Curve of Soil

4.3 FLY ASH

4.3.1 Thermo Gravimetric Analysis

Fly ash samples were subjected to thermo gravimetric analysis (TGA) in a dry air atmosphere at heating rates 10°C/min. Samples weighing 80 mg were heated at preselected heating rates from ambient temperature to 850°C in a Mettler thermal analyzer. The continuous records of weight loss and temperature were obtained and analyzed using a Mettler thermal analysis software system to determine the weight loss with increase in temperature. The TGA curve in Figure 4.6 shows that the mass loss for fly ash even after heating at a high temperature of 650°C is only about 1.7% which infers that the chosen fly ash is free from solid (fixed) carbon. This analysis clearly suggested that the present fly ash obtained from thermal power plant is readily usable without prior treatment for road construction.

4.3.2 Physical and Chemical Analysis

The physical and chemical properties of fly ash depends on the type and source of coal used, method and degree of coal preparation, cleaning and pulverization, type and operation of power generation unit, ash collection, handling and storage methods etc. hence it is very pertinent together the detail of fly ash particularly physical and chemical properties of fly ash. Considering the necessity of the tests, physical and chemical properties of fly ash was got conducted and the same is being presented in Table 4.4 and Table 4.5 respectively.

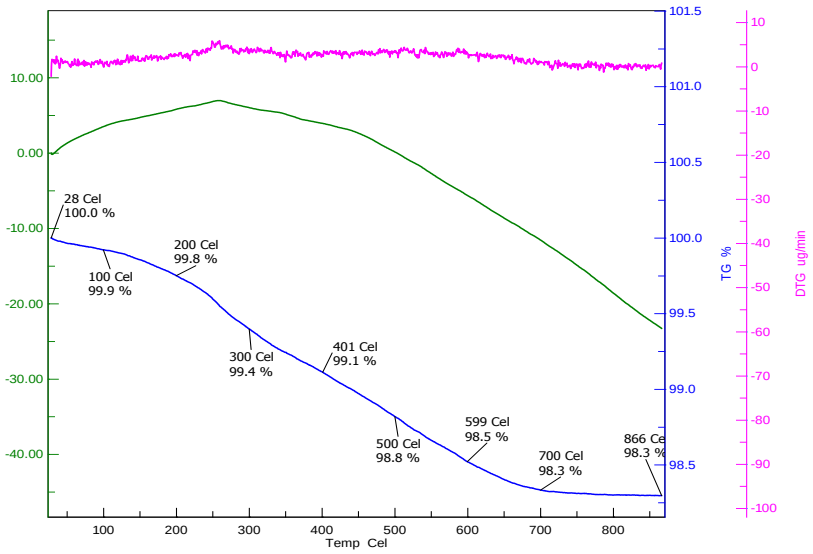

Figure 4.6 TGA Curve for Fly Ash

Table 4.4 Physical Properties of Fly Ash

Property	Value
Specific gravity (G)	2.24
Liquid limit (%)	47
Plastic limit (%)	Non-plastic
Fineness by sieving	
Finer fraction sand's particle size (%)	25.5
Finer fraction Silt particles size (%)	74.0
Finer fraction Clay particles size (%)	5.5
Optimum moisture content (%)	25
Maximum dry density (g/cm^3)	1.4
Lime reactivity (kg/cm^2)	34

Table 4.5 Chemical Properties of Fly Ash

Property	Value (%)
SiO_2	51.78
Fe_2O_3	7.31
Al_2O_3	24.92
CaO	8.77
MgO	0.68
N_2O	0.28
K_2O	1.44
Loss on Ignition	3

Figure 4.7 shows the grain size distribution of fly ash in its as received state without any treatment. From the distribution curve, it is learnt that finer fraction is predominantly present and of uniform graded material as smooth 'S' graded curve is observed from the graphical plot.

4.3.3 SEM Study

The approximate analysis of the fly ash sample was made. As expected, it contains enormous amount of ash and is amorphous in nature, evident from SEM images Figure 4.8 (a) & (b).

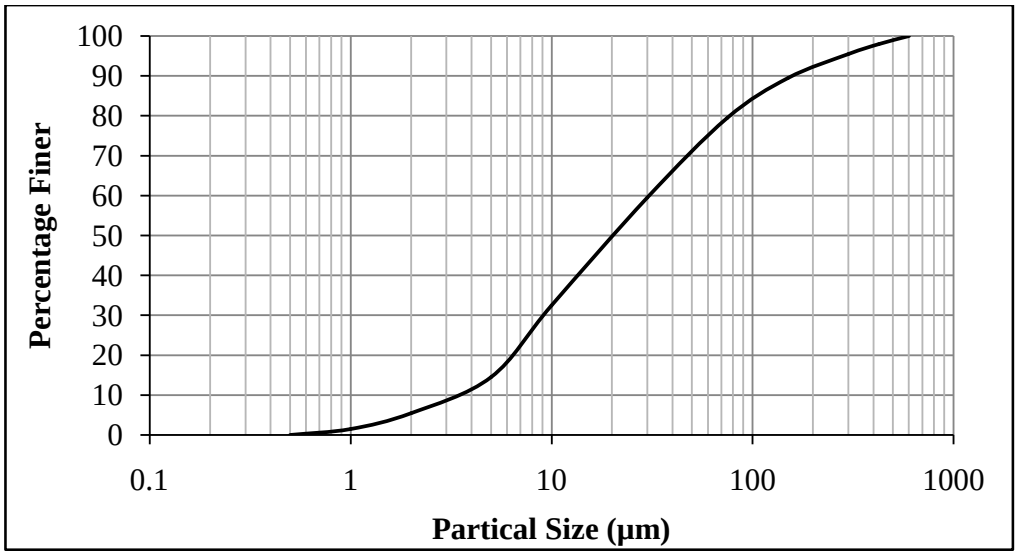

Figure 4.7 Grain Size Distribution for Fly Ash

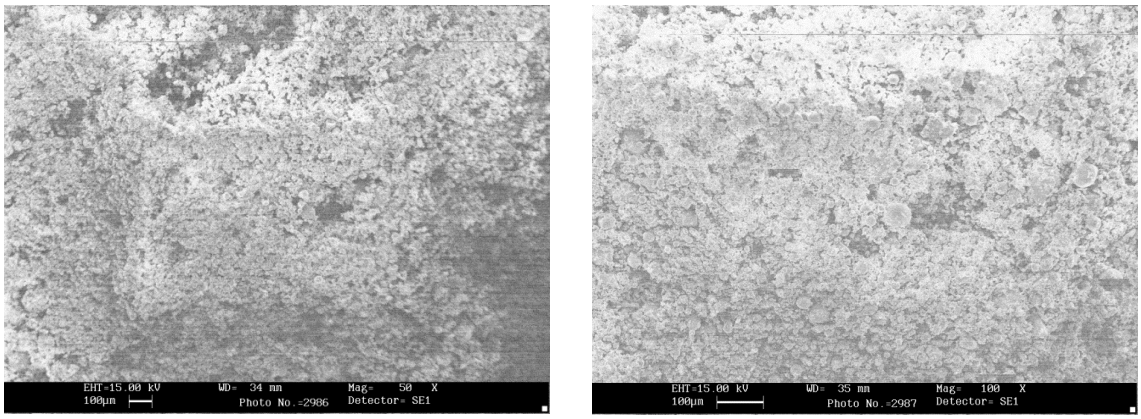

(a) **(b)**

Figure 4.8 SEM Images of Fly Ash (a) 50x (b) 100x

4.4 RICE HUSK ASH

4.4.1 Thermo Gravimetric Analysis

In order to assess the change in physical properties of rice husk ash sample under temperature effect, TGA was performed. Rice husk ash sample was subjected to TGA in a dry air atmosphere at heating rates 10°C/min. Samples weighing 80 mg were heated at preselected heating rates from ambient temperature to 850°C in a Mettler thermal analyzer. The TGA curve in Figure 4.9 indicates about 1.5% of mass loss for rice husk ash after heating at a temperature

of 600°C and at higher temperatures the mass loss is almost negligible. This analysis infers that rice husk ash can be used in road construction without further heating to remove carbon.

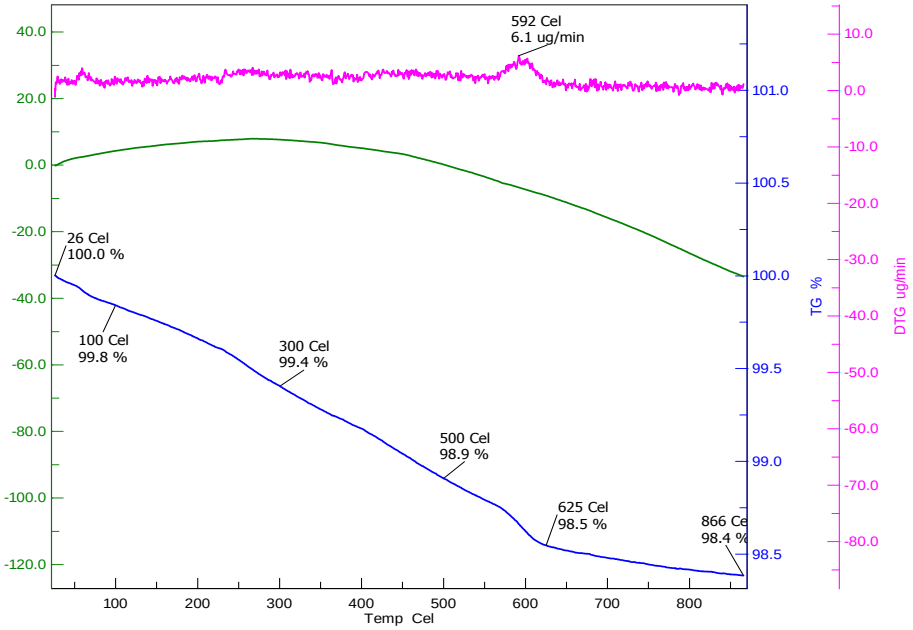

Figure 4.9 TGA Curve for Rice Husk Ash

4.4.2 Physical and Chemical Analysis

Rice husk is unusually high in ash compared to other biomass fuels. Generally, the ash is 87-97% silica highly porous in nature. Suitability of rice husk ash depends on the chemical composition of ash, predominantly silica content in it. There are various factors which influence rice husk ash properties such as incinerating condition, rate of heating, burning technique, crop variety and even fertilizer used. The rice husk ash used in this present investigation showed about 72.24% SiO_2, 5.4% Al_2O_3, 4.12% CaO and trace quantities of Fe_2O_3 and MgO. Finesses of material can be noticed from grain size distribution curve shown in Figure 4.9. The pattern of curve developed is very similar to that of fly ash material. Rice husk ash was obtained from paddy mill. It was fine grained, siliceous in nature, light weight and grey in color. The physical and chemical properties are given in Table 4.6 and Table 4.7 respectively.

Table 4.6 Physical Properties of Rice Husk Ash

Property	Value
Specific gravity	1.86
Liquid limit (%)	78
Plastic limit (%)	Non-plastic
Optimum moisture content (%)	45
Maximum dry density (g/cm^3)	1.60
Fineness by sieving	
Finer fraction sand's particle size (%)	27.0
Finer fraction Silt particles size (%)	67.5
Finer fraction Clay particles size (%)	5.5
Lime reactivity (kg/cm^2)	34

Table 4.7 Chemical Properties of Rice Husk Ash

Constituent	Value (%)
SiO_2	72.24
Al_2O_3	5.4
Fe_2O_3	2.1
CaO	4.12
MgO	1.7
Ignition Loss	8.2

Figure 4.10 shows the grain size distribution of collected rice husk ash without extra heating. The curve depicts that the rice husk ash contains uniformly graded particles with almost same size.

4.4.3 SEM Study

The morphology of silica extracted from rice husk ash is shown in Figure 4.11 (a) & (b), with magnification of 100 & 500 levels respectively. Different shapes of silica particles; globular and rectangular shapes were distinctly noticed from the SEM images. Also, a few silica deposits along the skeleton of rice husk are also seen.

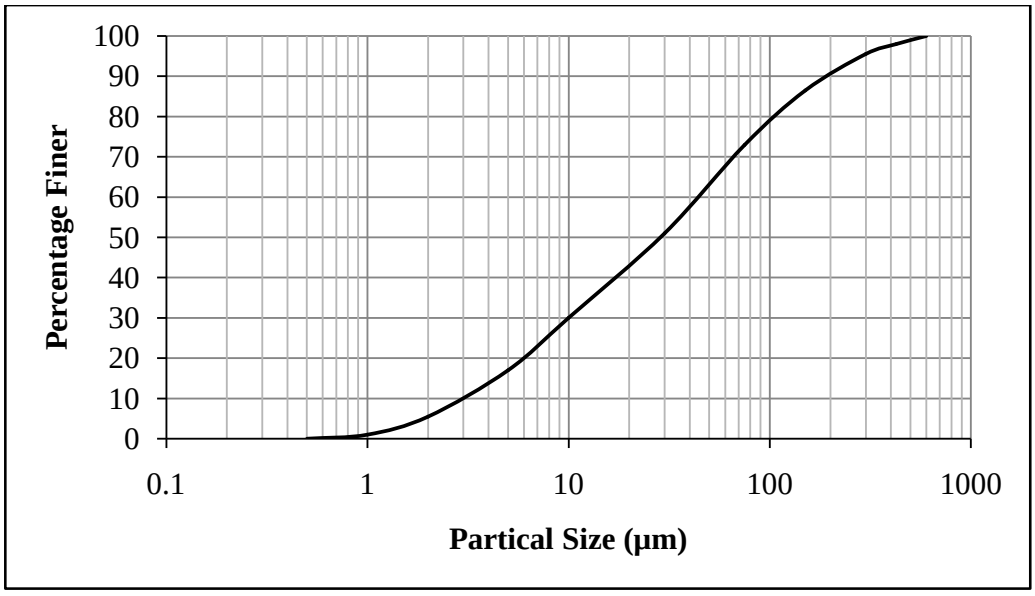

Figure 4.10 Grain Size Distribution for Rice Husk Ash

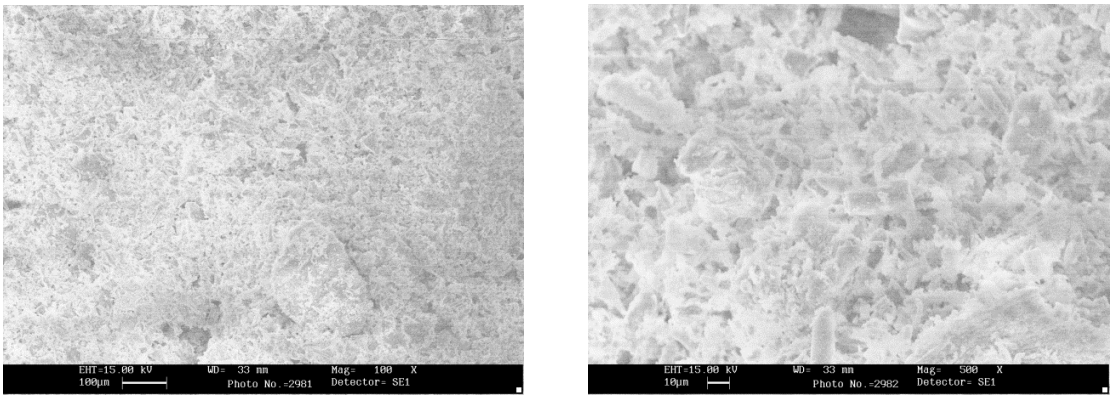

(a) **(b)**

Figure 4.11 SEM Images of Rice Husk Ash (a) 100x (b) 500x

4.5 BAGASSE ASH

4.5.1 Thermo Gravimetric Analysis

Baggase ash was collected from sugar mill located near Roorkee city of India. As this ash was obtained directly from sugar mill, they are not that reactive because they are burnt under uncontrolled conditions. Therefore, an attempt was made to have thermo gravimetric analysis using a mettler thermal analyzer so as to find out the appropriate burning temperature. The bagasse ash produced at the plant was about 2-2.5% of the bagasse used in boiler. Figure 4.12

presents the TGA curve for the bagasse ash. The bagasse ash samples were subjected to TGA in a dry air atmosphere at heating rates: 10°C/min. Samples weighing 80 mg were heated at preselected heating rates from ambient temperature to 850°C in a Mettler thermal analyzer. The continuous records of weight loss and temperature were obtained and analyzed using a Mettler thermal analysis software system to determine the weight loss with increase in temperature.

The TGA curve shows that in the first stage at the temperature range of 0-250°C the mass loss was hardly 0.8-1%. The major part of the mass loss took place in the second stage, in the range 250-550°C indicating a steep fall in the TGA curve. The mass loss of 10% in this stage was due to the removal of volatile matter. In the third stage the mass loss was only 0.4% at temperature above 550°C. This finding clearly implies that the chosen ashes contained minor quantity of carbon.

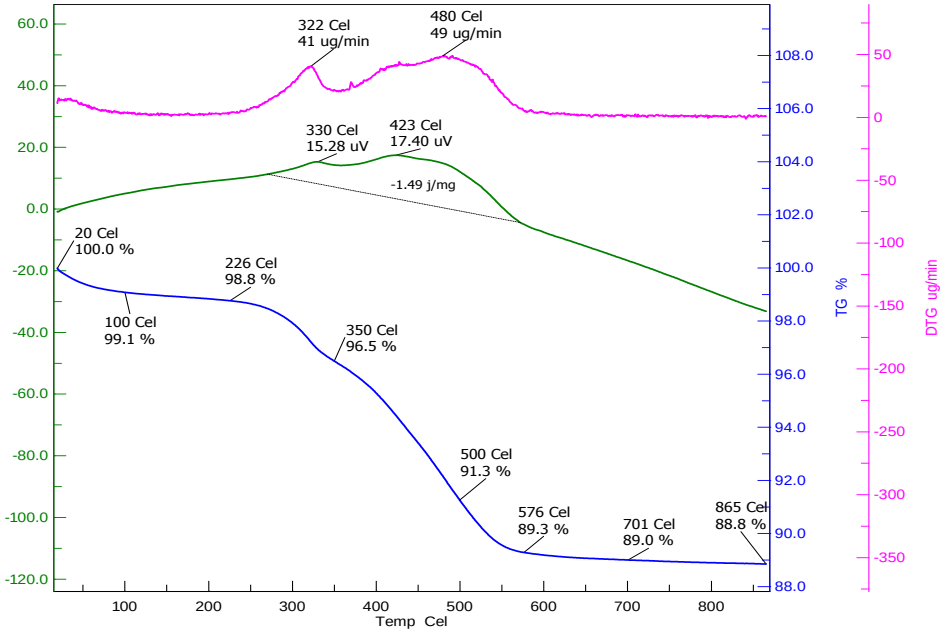

Figure 4.12 TGA Curve for Bagasse Ash

4.5.2 Physical and Chemical Analysis

The bagasse ash collected from sugar mill was was taken for physical and chemical properties studies. Tables 4.8 and 4.9, indicate that BA is silicious material and non-plastic in nature.

Also, BA possessed substantial amount of lime reactivity comparable to fly ash and rice husk ash.

Table 4.8 Physical Properties of Bagasse Ash

Physical Property	Value
Specific gravity	2.38
Liquid limit (%)	32
Plastic limit (%)	Non-plastic
Optimum moisture content (%)	26
Maximum dry density (g/cm^3)	1.5
Fineness by sieving	
Finer fraction sand's particle size (%)	16.9
Finer fraction Silt particles size (%)	77.3
Finer fraction Clay particles size (%)	5.8
Lime reactivity (kg/cm^2)	22

Table 4.9 Chemical Properties of Bagasse Ash

Chemical Composition	Value (%)
SiO_2	65.27
Al_2O_3	4.74
Fe_2O_3	3.11
CaO	11.16
MgO	1.27
Na_2O	1.89
K_2O	5.26
Loss on Ignition	2.11

Figure 4.13 shows that BA particles are well graded and fine enough.

4.5.3 SEM Study

Scanning electron microscope images of bagasse ash are shown in Figure 4.14 (a) & (b). The particles of baggase ash revealed an irregular shape. A few granular structures are also observed and they are amorphous in nature.

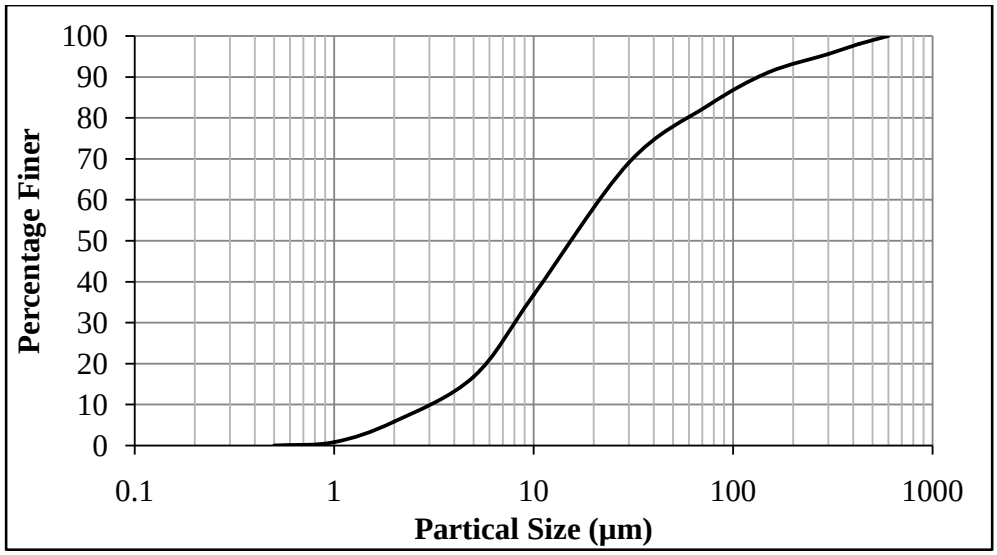

Figure 4.13 Grain Size Distribution for Bagasse Ash

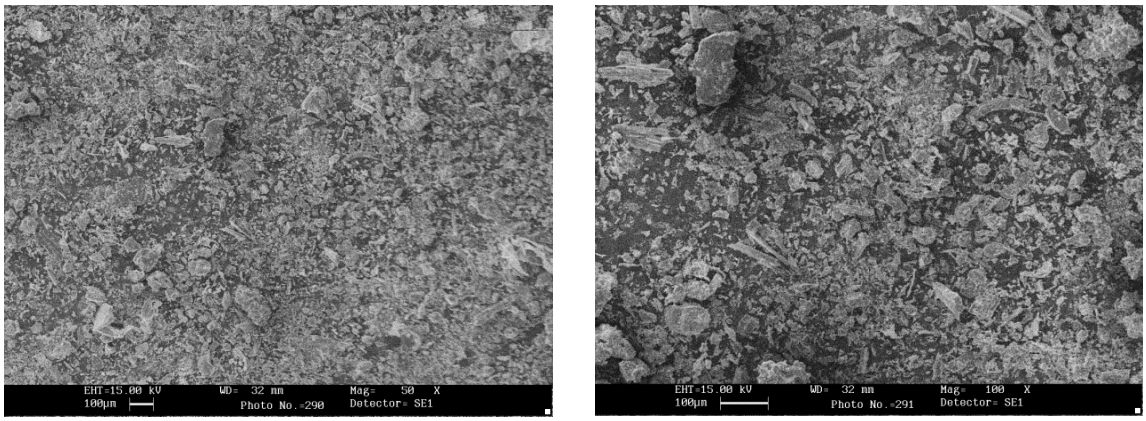

(a) **(b)**

Figure 4.14 SEM Images of Bagasse Ash (a) 50x (b) 100x

4.6 RICE STRAW ASH

4.6.1 Thermo Gravimetric Analysis

Figure 4.15 presents the TGA curve of RSA. Samples weighing 80 mg were heated at preselected heating rates from ambient temperature to 850°C in a Mettler thermal analyzer at heating rates, 10°C/min in a dry air atmosphere. The continuous records of weight loss and temperature were obtained and analyzed using a Mettler thermal analysis software system to determine the weight loss with increase in temperature.

The curve shows that the mass loss was about 3.6% in the first stage when sample was heated between 0-200°C. This loss increased to 7.6% in the second stage heating temperature between 200-500°C. Finally, this loss goes upto 12.1 % when sample was heated to a temperature of 866°C.

4.6.2 Physical and Chemical Analysis

Rice straw ash used in the present study was processed from agricultural field near Roorkee city, India. Collected rice straw ash was light grey in color. The physical and chemical properties of RSA tested in laboratory are presented in Tables 4.10 and 4.11 respectively.

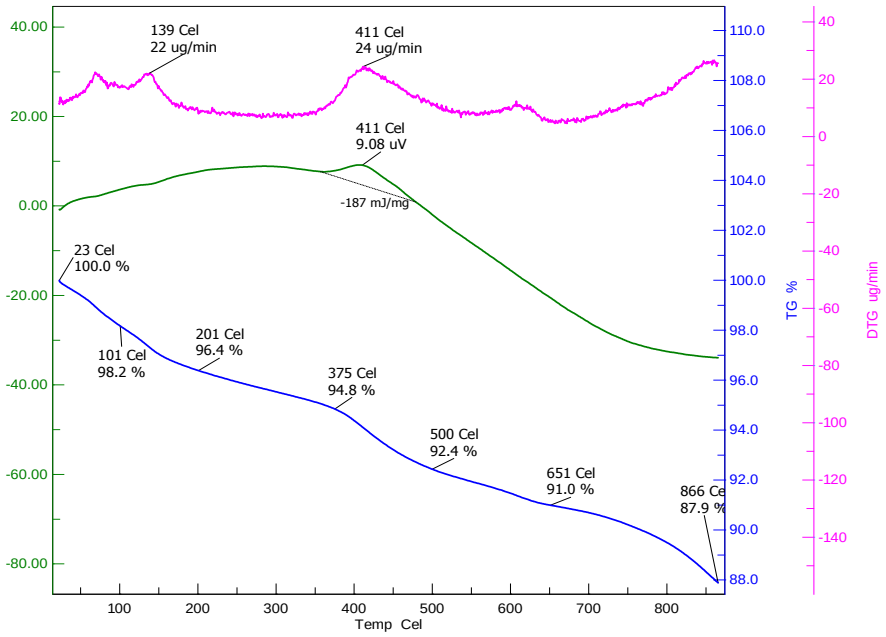

Figure 4.15 TGA Curve for Rice Straw Ash

Rice straw ahs showed usually high water absorption and has substantial amount of lime reactivity at par with rice husk ash, fly ash and baggasse ash, etc. Rice straw is a siliceous material and Fe_2O_3 is prominently present in it. Fe_2O_3 is the most natural state of iron oxide where it is combined with the maximum amount of oxygen. Higher amounts of Fe_2O_3 exhibit would considerably increase fluidity. Figure 4.16 shows the grain size distribution of rice straw

ash. The curve represents the rice straw ash contains uniform graded particles with little fine particles.

Table 4.10 Physical Properties of Rice Straw Ash

Property	Value
Specific gravity	1.81
Liquid Limit	72
Plastic Limit	Non-plastic
Optimum moisture content (%)	41
Maximum dry density (g/cm^3)	1.30
Fineness by sieving	
Finer fraction sand's particle size (%)	30.8
Finer fraction Silt particles size (%)	64.4
Finer fraction Clay particles size (%)	4.8
Lime Reactivity (kg/cm^2)	28

Table 4.11 Chemical Properties of Rice Straw Ash

Constituents	% by Weight
Ignition loss	9.4
SiO_2	62.75
Al_2O_3	2.4
Fe_2O_3	24.18
CaO	2.76
MgO	5.12

4.6.3 SEM Study

The SEM images revealed that rice straw ash particles seemingly to be more porous in nature as shown in Figure 4.17. Besides, few acicular structures are also noticed.

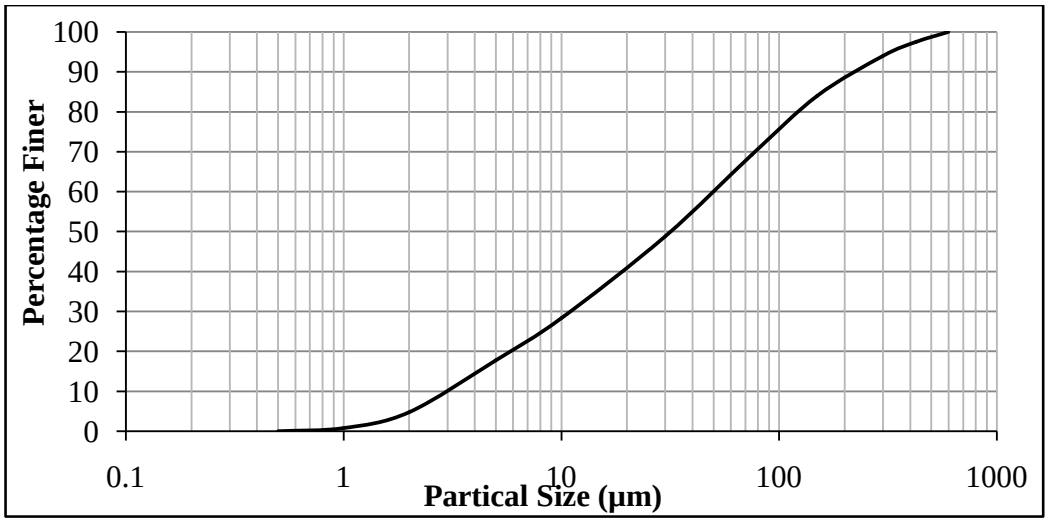

Figure 4.16 Grain Size Distribution of Rice Straw Ash

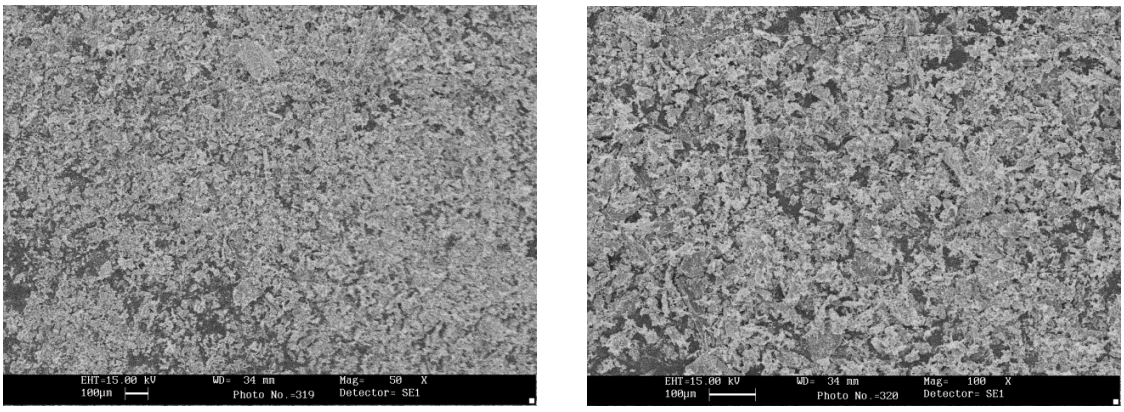

(a) **(b)**

Figure 4.17 SEM Images of Rice Straw Ash (a) 50x (b) 100x

4.7 FINES OBTAINED FROM DEMOLISHED CONCRETE SLAB

4.7.1 Physical and Chemical Analysis

In the present study, an attempt was also made to incorporate FDCS as soil stabilizer. Demolished concrete slabs were collected from sabzi mandi of Roorkee, India. Initially, demolished concrete slabs were hand broken into smaller pieces then fed into mini jaw crusher. The end product was collected and sieved through various standards IS sieve sizes. Material passing 1.18 mm IS sieve size was collected for further investigation in the laboratory. Table 4.12 and 1.13 presents the physical and chemical properties of FDCS respectively. As may be

seen from Table 4.12, FDCS showed significant amount of lime reactivity which is even far greater than that of fly ash, rice husk ash, rice straw ash and bagasse ash. This strongly infers that FDCS would be an effective soil stabilizer. This is why FDCS has been considered in the present research work.

Table 4.12 Physical Properties of Fines obtained from demolished concrete slab

Property	Value
Specific gravity	1.92
Liquid Limit (%)	14
Plastic Limit (%)	Non-plastic
Optimum moisture content (%)	9
Maximum dry density (g/cm^3)	1.62
Fineness by sieving	
Finer fraction sand's particle size (%)	37.0
Finer fraction Silt particles size (%)	58.3
Finer fraction Clay particles size (%)	4.7
Lime Reactivity (kg/cm^2)	41

Table 4.13 Chemical Properties of Fines obtained from demolished concrete slab

Chemical Composition	Value (%)
SiO_2	36.14
Al_2O_3	4.84
Fe_2O_3	4.07
CaO	41.89
MgO	1.15
K_2O	1.52
Loss on Ignition	4.5

4.7.2 SEM Study

Figure 4.18 (a) & (b) presents the scanning electron microscope image of FDCS which indicates the formation of mineral crystal (as a product of pozzolanic reaction at long-term) within the pore spaces.

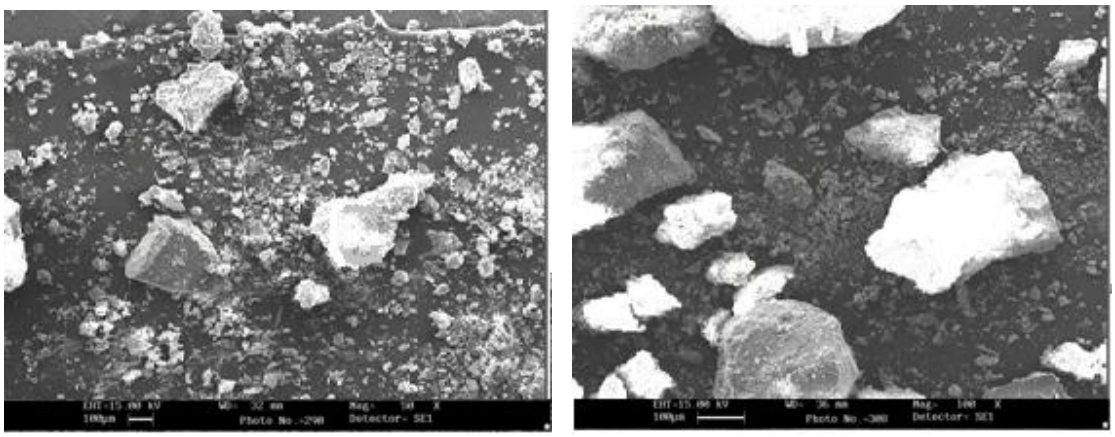

(a) **(b)**

Figure 4.18 SEM Image of FDCS (a) 50x (b) 100x

4.8 BAGASSE FIBER

4.8.1 Physical and Chemical Analysis

The bagasse fiber used in the present study was collected from sugar mill. The collected sugarcane bagasse was dried in oven at 50°C for 24 hrs to remove moisture content. Bagasse is generally gray-yellow in color. The main chemical constituents of bagasse used are cellulose, hemicellulose and lignin. Hemicellulose and cellulose are present in the form of hollow cellulose in bagasse which contributes to about 70 % of the total chemical constituents present in bagasse. Another important chemical constituent present in bagasse is lignin. Lignin acts as a binder for the cellulose fibers and also behaves as an energy storage system. It is bulky and quite non uniform in particle size. Length of collected BF varies from 10 mm to 50 mm. Table 4.14 present the physical properties of BF.

Table 4.14 Physical Properties of Bagasse Fiber

Property	Value
Specific Gravity	0.76
Length	10 to 50 mm
Diameter	1to 3 mm
Water Absorption	24 %

4.8.2 SEM Study

Figure 4.19 (a) & (b) presents the scanning electron microscope image of bagasse fiber which indicates that raw bagasse is very hard.

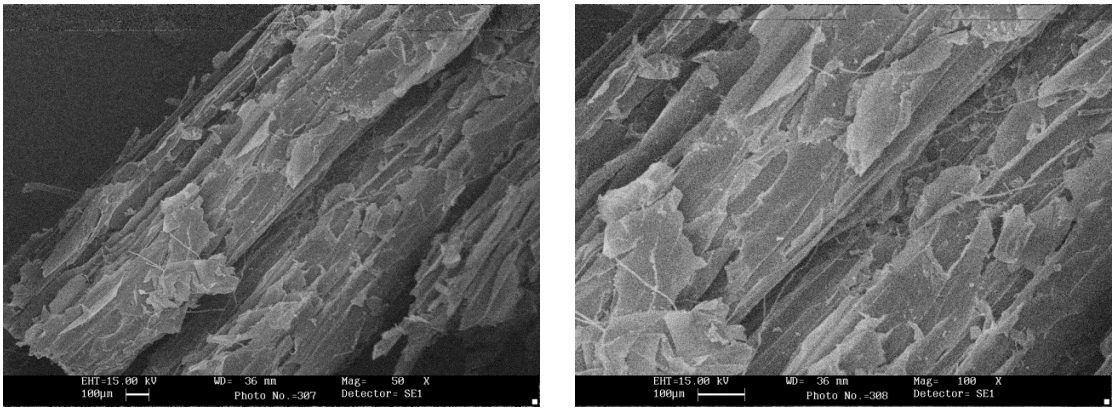

(a) **(b)**

Figure 4.19 SEM Image of Bagasse Fiber (a) 50x (b) 100x

4.9 SUMMARY

Sources and location image of all materials is presented in this chapter. This chapter also covers the TGA analysis, physical and chemical properties, grain size distributions and SEM study of soil and different waste materials.

CHAPTER 5

RESULTS AND DISCUSSION

5.1 GENERAL

This chapter entails the test results of experimental work conducted in the laboratory. Silica rich waste materials like fly ash (FA), rice husk ash (RHA), bagasse ash (BA), rice straw ash (RSA) and fines obtained from demolished concrete slabs (FDCS) were used as low cost soil stabilizers in the present study. In addition, effort was also made to investigate the potential of bagasse fiber (BF) as low cost soil stabilizer to judge it suitability for road construction. The effect of these stabilizers on engineering properties of expansive natural soil was studied. The effect on performance related tests like plasticity, free swelling index (FSI), compaction, California bearing ratio (CBR), expansion ratio, hydraulic conductivity, unconfined compressive strength (UCS), split tensile strength (STS), triaxial, cyclic triaxial, plate load and ultimate strength of natural expansive soil and admixed soils were studied. Attempt was also made to establish relationship between these parameters. For clarity of the investigations, discussion of test results and analyses are presented separately for each of these stabilizers.

5.2 SOIL-FLY ASH MIXTURES

5.2.1 Atterberg limits

Figure 5.1 illustrates the plasticity index (PI) of expansive soil and admixed soils. This plot clearly depicts that admixing of fly ash leads to reduction in plasticity index. The plasticity index of the admixed soils decreased as the fly ash content increased. About 32%, 40%, 56%, 72%, 80%, 84% and 88% reductions were observed when 5%, 10%, 15%, 20%, 25%, 30% and 35% respectively of FA were admixed with natural expansive soil. This analysis clearly showed that reduction in plasticity index is more pronounced at higher fly ash content. This finding is in agreement with Shafique, S B. et al. (2010). The reduction in plasticity index is attributed to the presence of different cations in fly ash which facilitates increase of flocculation of clay particles and consequently reduced soil dispersion and thus plasticity index of fly ash admixed soil reduces (Tishmack, J. K. et al. 2001).

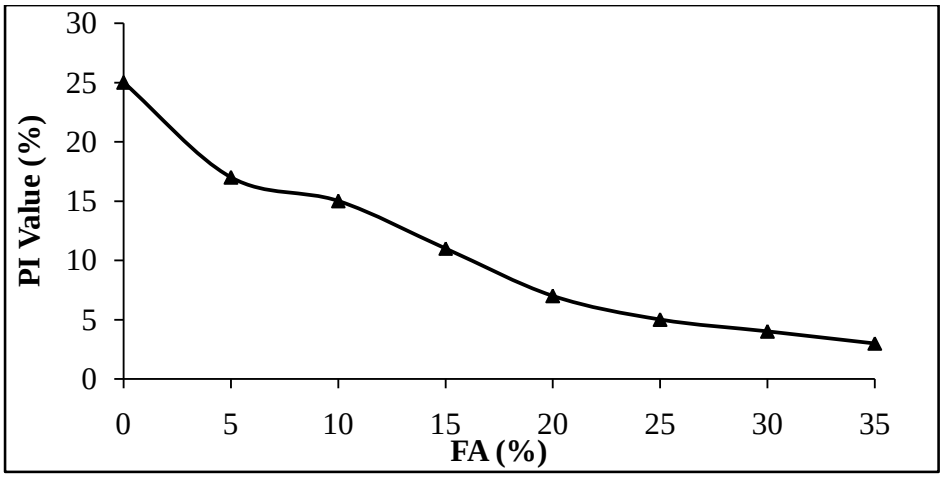

Figure 5.1 Atterberg Limits of Soil-FA Mixtures

It is also observed that, addition of FA to an expansive natural soil increase the shrinkage limit remarkably as depicted in Figure 5.2. The term shrinkage limit (SL); expressed as water content, is typically assumed to represent the amount of water required to fill the voids of clayey soil at its minimum void ratio obtained by oven drying. An addition of FA 5%, 10%, 15%, 20%, 25%, 30% and 35% resulted in an increase of the shrinkage limit (SL) to 20.1%, 35.6%, 51.4%, 62.3%, 77.9%, 85.5% and 96.3% respectively. The trend of increase of SL maintained linear relationship with FA content approximately. However, this increase is slackened after 25% FA content. This phenomenon is mainly attributed to the flocculation of clay particles caused by the free lime present in the FA resulting in the reduction of friction between the particles. Similarly, another possible reason for having higher shrinkage limits on admixing of stabilizers is due to the substitution to finer particles of clayey soil by relatively coarser FA particles.

5.2.2 Free Swelling Index

Figure 5.3 shows the laboratory test results of free swelling test for the soil admixed with various content of fly ash. Test was conducted in accordance with IS: 2720 (Part-40). Free swelling index is the ratio of the amount of swell to the original thickness of the specimen and it is expressed in percentage. The test results indicate that addition of fly ash reduces swelling potential of natural expansive soils. Soils with high swelling potential exhibits high swell pressure. The magnitude of free swelling index decreases from 45% to 13.8% as the FA content

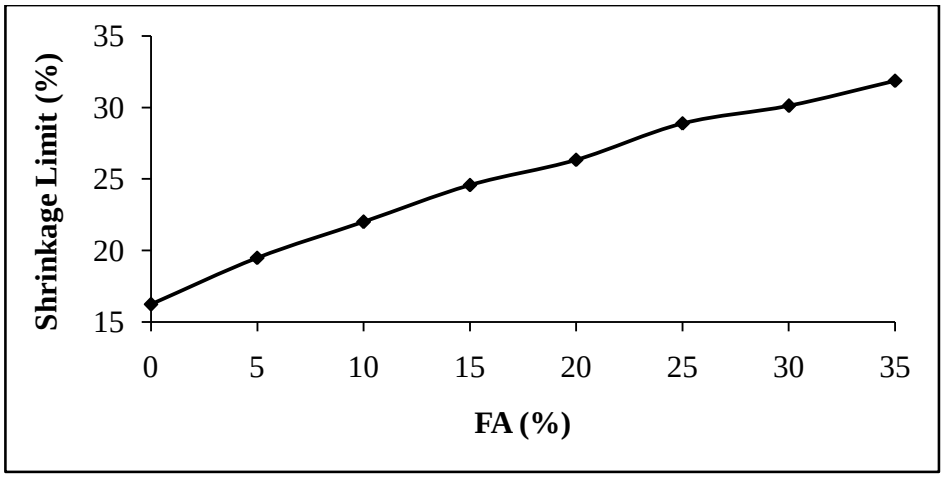

Figure 5.2 Shrinkage Limit of Soil-FA Mixtures

increases from 0% to 35%. When compared to expansive soil, percent reductions of free swelling index are 8.2%, 21.8%, 29.1%, 42.1%, 53.7%, 60.5% & 69.3% respectively for 5%, 10%, 15%, 20%, 25%, 30% & 35% of FA inclusion levels. The finding is in agreement with PhaniKumar, B. R. et al. (2004) and Prabakar, J. et al. (2004). As it can be seen from Figure 5.3, swelling index decreased more than 50% when 20% FA was admixed with natural expansive soil. The reduction in magnitude of free swell may be attributed to the slower rate of water uptake by soil particles due to FA particle obstruction. Furthermore, FA particles replaced expansive soil particles which absorbed appreciable amount of water and thus increase its volume. The reduction in swelling potential of expansive soil on admixing of FA is due to non-expansive characteristics of FA and particle shape and size of FA. Present study strongly suggested that swelling behavior of the expansive soil can be effectively controlled by inclusion of FA. FA inclusion level shall be decided depending upon the severity of swelling potential of expansive soil and requirements of other strength parameters.

5.2.3 Proctor Test

As shown in Figure 5.4 the OMC of soil-FA mixture increases with increase in percentage content of FA. The percentages increase in OMC are 5.9%, 11.8%, 15.3%, 20.0%, 24.7%, 28.2% and 41.2% on admixing of FA @ 5%, 10%, 15%, 20%, 25%, 30% and 35% respectively. The increase of OMC was approximately linear with FA content upto 10%, after which the rate of increase of OMC was slightly sluggish upto 20% and again considerable

increase in OMC was observed at 25% FA inclusion level and thence starts declining. The increase in OMC on admixing of FA could be mainly due to increasing demand for water by soil-FA mixtures for hydration reaction.

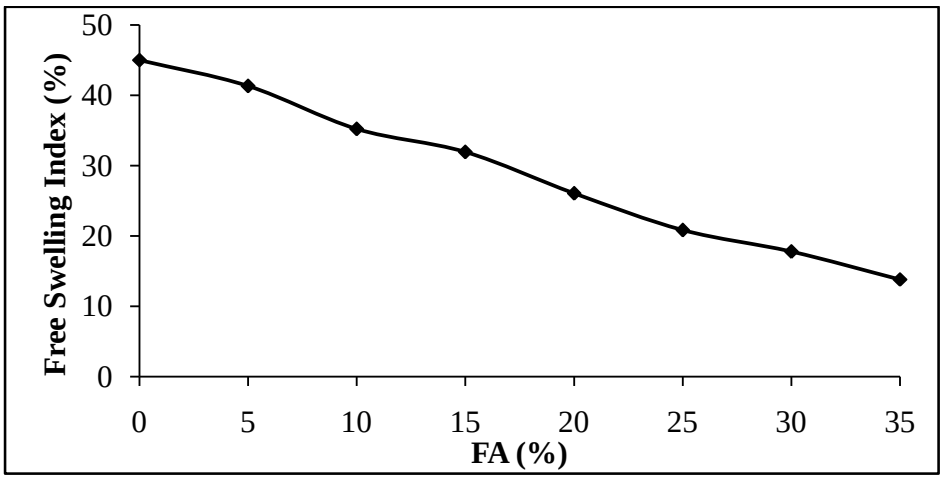

Figure 5.3 Free Swelling Index of Soil-FA Mixtures

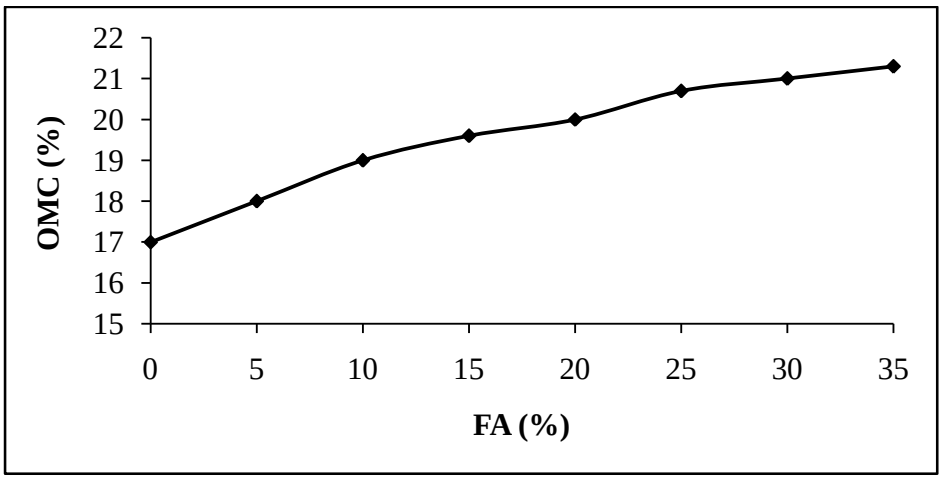

Figure 5.4 OMC of Soil-FA Mixtures

Admixing of fly ash to natural expansive soil obviously affected the compaction characteristics primarily due to alteration of gradation of soil mixture. The maximum dry density of FA admixed soils decreased with increase in the percentage of FA as depicted in Figure 5.5. The present finding is in agreement with Senol, A. et al. (2006); Kolias, S. (2005); Kumar, A. et al. (2007) and Prabakar, J. et al. (2004). Nearly about one percent maximum dry density reduction

is observed on admixing of FA upto 15% by weight of dry soil. Similarly, about 1.4% reduction in maximum dry density is observed on admixing of FA upto 25%. This reduction further goes up to 1.8% when 35% FA is admixed with expansive soil. 100% FA mixture produced 12.24% lower maximum dry density in comparison to expansive soil. Typical of such mixtures, the maximum dry density decreased with higher fly ash content since the fly ash is of low specific gravity (Osinubi, K. J. et al. 2006).

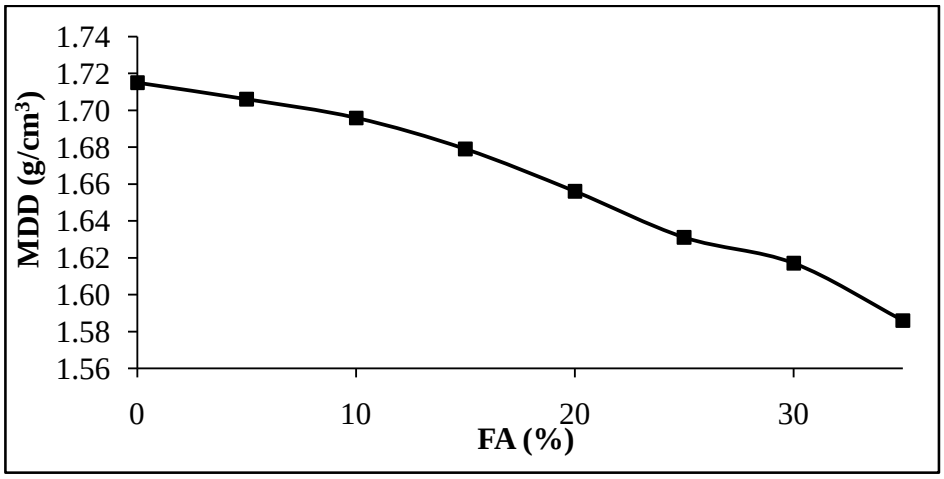

Figure 5.5 MDD of Soil-FA Mixtures

5.2.4 California Bearing Ratio

The trend of increase of CBR values monitored over a curing period for 3, 7, 14, 28, 56 and 128 days for soil-FA mixtures prepared at optimum moisture content is presented in Figure 5.6. Figure 5.6 clearly illustrates that inclusion of FA improves CBR value of expansive soil considerably. Senol, A. et al. (2006) and Prabakar, J. et al. (2004) have also revealed that admixing of FA to natural soil produced higher CBR value as compared to that of natural soil. Irrespective of days of curing period, maximum CBR value was observed for soil mixture containing FA 25% followed by 30%, 35%, 20%, 15%, 10%, 5% and 0% FA respectively. Sharper rate of improvement of CBR value was maintained upto 25% FA content for all considered FA admixed soils except at 15% FA inclusion level because of which the graph appears slightly wavy. Such typical pattern may be due to the distribution of fly ash in soils was not uniform. But it is quite evident from the present analysis that the rate of CBR value improvement starts declining after 25% FA inclusion level irrespective of curing time.

However, these values are much higher than CBR value of expansive soil. The percentage increase of CBR value after admixing FA @ 5%, 10%, 15%, 20%, 25%, 30% and 35% are 61.3%, 120.4%, 168.8%, 233.3%, 319.4%, 287.1% and 265.3% respectively with respect to expansive soil. It has also been found that relative humidity curing imparts considerable role in improving CBR value irrespective of types of additives used. Maximum CBR value was read at 25% FA inclusion level and the rate of increase of CBR values were 2.6%, 6.4%, 9.0%, 12.8% & 15.4% respectively for 7, 14, 28, 56 & 128 days relative humidity curing with respect to 3 days. This analysis strongly suggests appreciable improvement of CBR values with curing time and hence, prolong relative humidity curing is suggested for FA admixed soils to draw pozzolanic reaction benefits. CBR value improvement on admixing of FA is mainly attributed to the frictional resistance offered by the FA and cementitious products formed. Horpibulsuk, S. et al. (2010) had also stated that at the initial stage of stabilization, the volume of small pores (smaller than 0.1micron) considerably decreases while the volume of large pores (larger than 0.1 micron) increases with increasing FA. The increase in volume of the large pores is induced by the unhydrated grains. After 7 days of curing, the large pore volume and total pore volume decrease while the volume of the small pores increase. This is because of the growth of the cementitious products that fill the large pores.

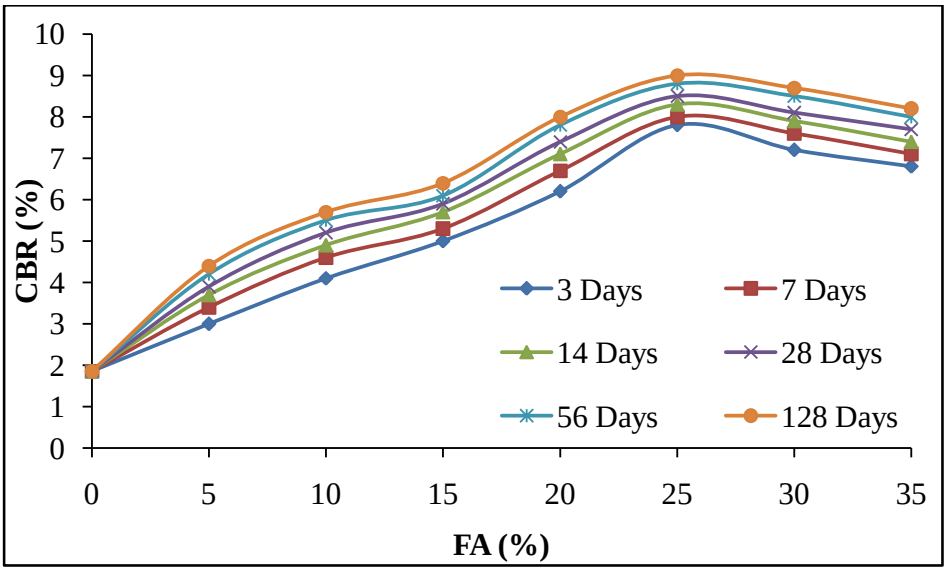

Figure 5.6 CBR of Soil-FA Mixtures

5.2.5 Expansion Ratio

Because of special geological engineering characteristics of expansive soil, cute slopes and embankments of expansive soils are bound to damag and slide. Highway construction in expansive soils is a great challenge for highway engineers, therefore, it is a high time for researchers, engineers and builders to venture out cost effective measures to overcome such challenges. Keeping this constraint in mind, effort has been made to ascertain swelling potential of soil mixture by incorporating FA in varying dosages so as to examine expansion ratio. Figure 5.7 presents the expansion ratio measured in the laboratory FA admixed soils. Expansion ratio for expansive soil is found to be 32%. Whereas after incorporating FA @ 5%, 10%, 15%, 20%, 25%, 30%, and 35%, these expansion ratios considerably reduced to 12.5%, 22.5%, 30.0%, 35%, 40%, 47.5% and 52.5% respectively. This again confirmed the suitability of FA for control of swelling potential of expansive soil.

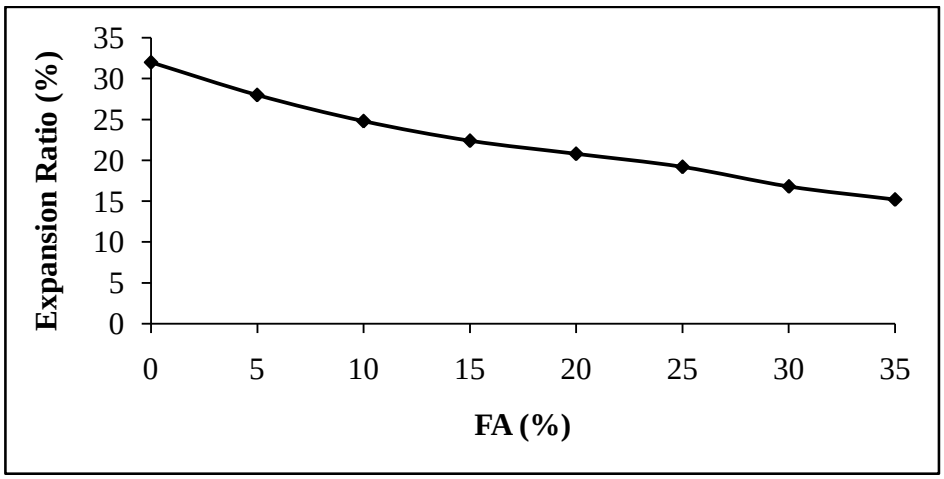

Figure 5.7 Expansion Ratio of Soil-FA Mixtures

5.2.6 Hydraulic Conductivity Test

The variations of hydraulic conductivity of soil with the addition of FA at their respective maximum dry density and optimum moisture content for curing period of 7 days is presented in Figure 5.8. Permeability of expansive soil is found to be 3.3×10^{-7} cm/sec. Incorporation of FA to expansive soil led to decrease in permeability. Significant decrease in permeability was observed upto FA 20%, after which the rate of decrease becomes sluggish. The permeability decrease is in the order of 17.13%, 26.61%, 38.84%, 57.19%, 60.24%, 66.36% & 69.42% after

admixing FA @ 5%, 10%, 15%, 20%, 25%, 30% & 35% respectively. This decrease was as a result of the formation of cementitious compounds by calcium and silica and/or alumina contributed from both soil and FA, which fills the soil voids thereby obstructing the flow of water. The finding of this study is in agreement with Osinubi, K. J. (1998).

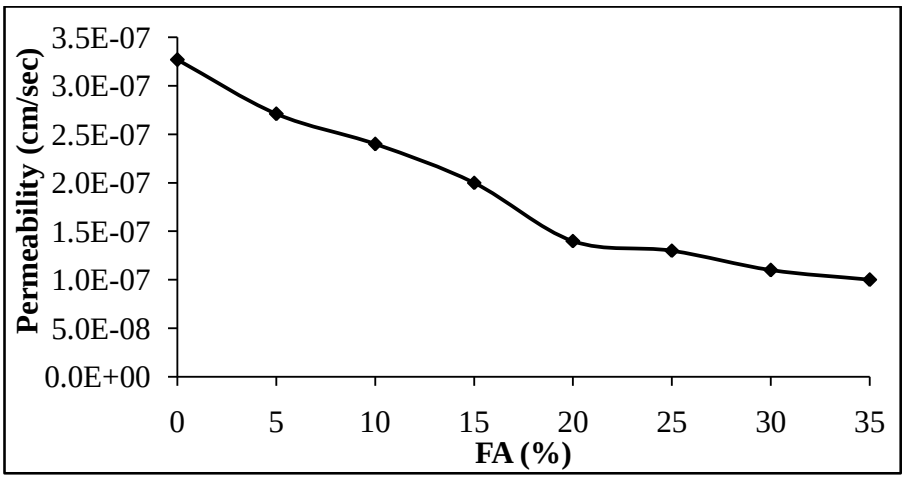

Figure 5.8 Permeability of Soil-FA Mixtures

5.2.7 Unconfined Compressive Strength

Unconfined compressive strength (UCS) of FA admixed soils including expansive soil were ascertained by plotting values of UCS against FA contents as depicted in Figure 5.9. One can easily read in the Figure 5.9 that UCS value increased with higher fly ash content. About 15.84%, 27.97%, 36.87%, 43.76%, 47.33%, 49.96% & 31.58% increments in UCS were observed when FA was incorporated to an expansive soil @ 5%, 10%, 15%, 20%, 25%, 30% & 35% respectively at 7 days curing. Whereas for 14 days, 28 days, 56 days and 128 days cured samples, these values further increased to 21.97%, 35.44%, 43.08%, 48.04%, 51.26%, 52.77% & 35.99%; 27.78%, 39.90%, 48.80%, 51.32%, 55.24%, 56.56% & 43.35% ; 31.30%, 45.77%, 51.99%, 54.84%, 58.76%, 60.07% & 52.04% ; 33.56%, 48.11%, 54.34%, 57.19%, 59.94%, 62.42% & 53.22% respectively. From present analysis, it is very pertinent to note here that curing period plays a vital role in the improvement of UCS particularly for FA admixed soil samples. The rate of UCS improvement is very rapid and cohesive upto 15% FA content and thereafter the increment rate becomes sluggish up to 25% FA content irrespective of curing period. But highest UCS was offered by 30% FA admixed soil samples irrespective of days of

curing. However, it is very interesting to note that further addition of FA beyond 30% led to reduction in UCS and this value is even less than that of 15% FA admixed soil sample. Several mechanisms are responsible for strength development in soil stabilized with FA. The main generator of UCS in FA admixed soils is the formation of cementitious products under pozzolanic reaction and additional strength is mobilized by granular packing in the matrix formed with FA acting as filler (Consoli et al., 2001). On other hand, the decrease in the UCS value beyond 30% FA inclusion level may be due to extra FA that could not be mobilized for the chemical reaction which consequently occupies spaces within the sample. This ultimately reduced bond between the soil and FA particles and hence, UCS reduced. In another study conducted by Shafique, S. B. et al. (2010), they have also reported that admixing of 20% FA to soft soil and expansive soil could increase UCS from 210 to 800 kPa and 180 to 560 kPa respectively.

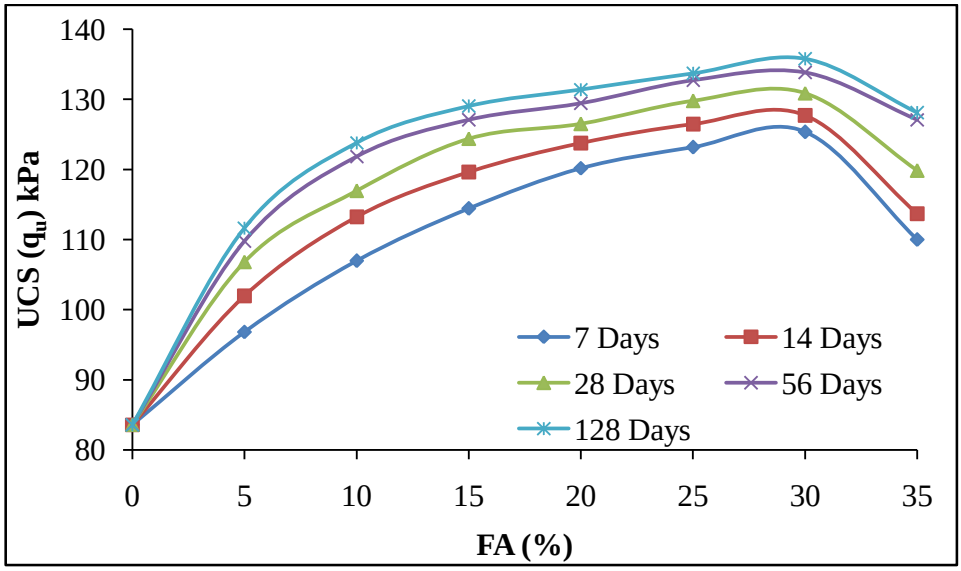

Figure 5.9 UCS of Soil-FA Mixtures

5.2.8 Split Tensile Strength Test

Inclusion of FA to expansive soil enhances split tensile strength as presented in Figure 5.10. The increase of split tensile strength is significant upto 30% FA inclusion level. However, this increase is sluggish between 10% and 25% FA inclusion level but highest STS was observed at 30% FA inclusion level irrespective of curing time. Inclusion of FA beyond 30% reduces STS

considerably and these values are almost at par with 5% FA admixed soil samples. Percentage reduction of STS is higher in comparison to UCS under same working condition for FA admixed soil samples irrespective of days of curing. This strongly suggested that FA admixed samples yield better compressive strength than tensile strength. Prolong curing showed significant impact in the development of tensile strength and the probable reason for the same is due to the formations of cementitious products which facilitate to bridge the inter-soil particle pores better and hence improved the interfacial zones of soil particles.

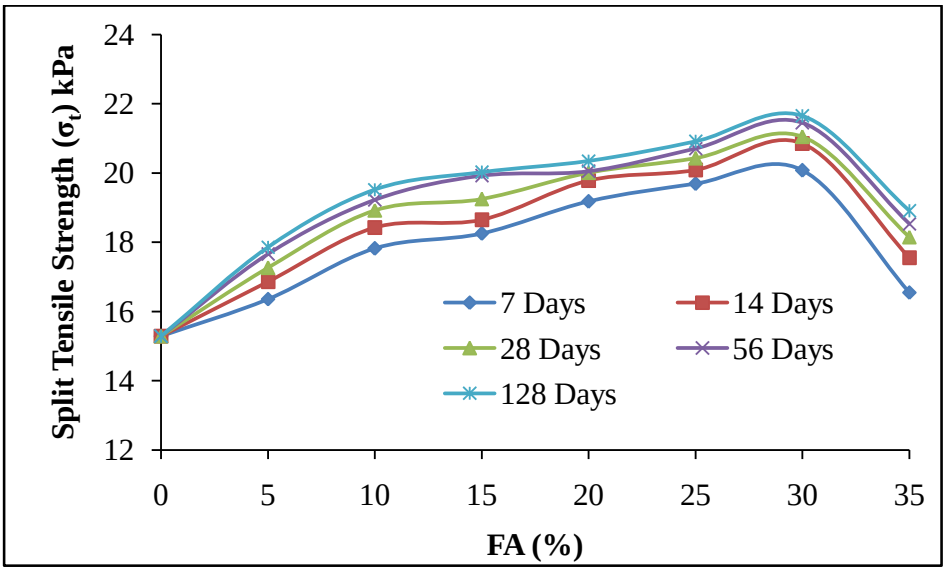

Figure 5.10 Split Tensile Strength of Soil-FA Mixtures

5.2.9 Ratio of Split Tensile to Unconfined Compressive Strength

The relative relationship and mobilization between the tensile strength and compressive strength could be discussed by plotting the tensile/compressive strength ratio (σ_t/q_u) versus curing time. Figure 5.11 depicts the influence of FA content on the ratio of split tensile strength and unconfined compressive strength. The results show that unconfined compressive strength and split tensile strengths are closely related. It can be observed that the ratio of split tensile strength and unconfined compressive strength decreased with increase in FA content, indicating that FA is more efficient when soil was subjected to compression rather than to tension.

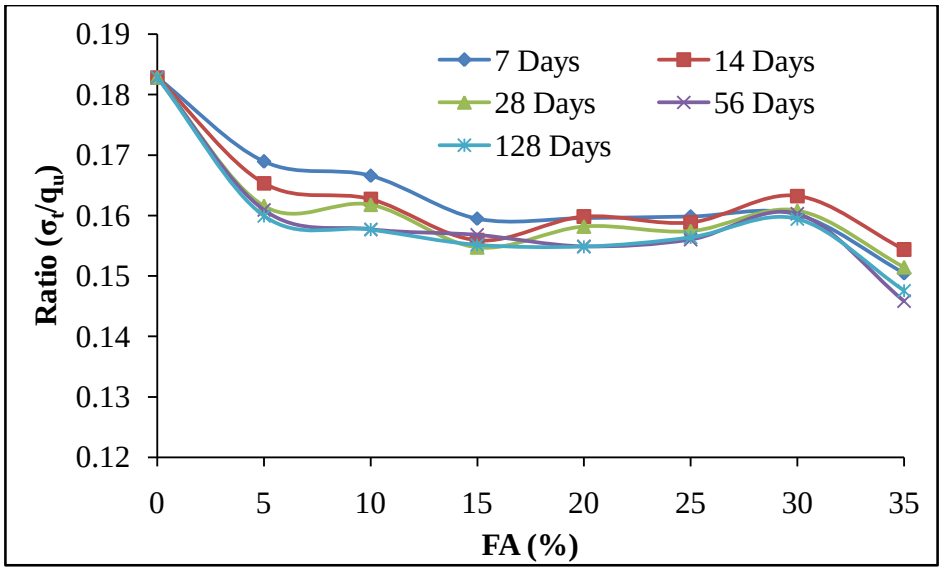

Figure 5.11 σ_t/q_u Ratio of Soil Admixed with FA

5.2.10 Triaxial Test

Three different confining stresses such as 100, 150 and 200 kPa were applied on specimens to obtain peak deviator stress as presented in Table 5.1. The range of confining stresses were chosen to obtain more well defined and accurate plots of Mohr envelopes to obtain shear strength parameters cohesion (c) and angle of internal friction (φ) of the soils mixed with FA. The variation of c and φ with admixing FA are evaluated and results are as shown in Figures 5.12 & 5.13 respectively.

Admixing of FA shows positive influence on deviator stress (Table 5.1). Higher deviator stresses were observed for higher FA content irrespective of confining pressure applied and days of curing. However, beyond 30%FA content, the deviator stress starts declining gradually. Admixing of FA causes increase in cohesion and internal friction angle. Increase in cohesion is more pronounced upto 10% FA content. The cohesion of soil ranges from 28 to 43 kPa and from 28 to 49.98 kPa at 7 and 128 days of curing respectively for FA contents between 0 & 30%. Improvement on cohesion due to addition of FA becomes sluggish beyond 10% FA content. However, these cohesions are much higher than that of expansive soil. Marked reduction in cohesion is observed beyond 30% FA content (Fig 5.12). As in the case of cohesion, similar trend of improvement is observed for internal friction angle. The rate of improvement of internal friction angle is rapid upto 5% FA, after which the rate of

improvement is slightly sluggish and this trend maintained upto 30% FA but beyond 30% FA content, angle of internal friction reduces significantly as it can be seen from Figure 5.13. As may be seen from the Table 5.1, higher deviator stresses are observed for higher confining pressures irrespective of days of curing. Improvements on cohesion and internal friction angle on admixing of FA may be due to the increase of *c* of the soil upon the action of its ultra fineness and self –hardening effect or self cementitious characteristics of fly ash. Improvement on internal friction angle due to admixing of FA may be due to the fact that the internal friction angle of the fly ash is more than that of expansive soil.

Table 5.1 Deviator Stress for FA Admixed Soil at Different Confining Pressure

% FA	Confining Pressure (kPa)	Deviator Stress (kPa)				
		7 Days	14 Days	28 Days	56 Days	128 Days
0	100	207.34	213.19	204.83	209.01	196.47
	150	279.91	287.81	276.52	282.17	265.24
	200	342.11	351.77	337.97	344.87	324.18
5	100	242.11	252.88	262.81	267.85	273.58
	150	319.59	331.28	341.65	345.53	350.19
	200	399.48	414.73	428.38	433.92	440.47
10	100	264.27	277.43	284.22	293.70	299.67
	150	346.19	360.66	366.65	375.94	380.58
	200	428.11	446.66	454.76	466.99	473.47
15	100	279.20	289.48	298.57	307.52	310.98
	150	362.96	373.43	382.17	390.55	398.05
	200	452.31	466.07	477.72	488.96	493.67
20	100	295.66	301.99	311.22	319.75	325.91
	150	387.32	398.63	410.81	415.67	423.68
	200	478.97	489.23	501.06	511.60	518.19
25	100	305.48	312.35	320.59	326.53	335.62
	150	391.02	402.93	410.35	421.22	422.89
	200	491.82	502.89	513.74	520.15	530.28
30	100	312.18	319.95	327.22	337.25	343.55
	150	399.58	406.34	412.30	421.57	427.72
	200	502.60	513.52	521.92	532.86	540.41
35	100	271.71	279.70	287.04	296.18	300.38
	150	350.51	358.01	368.85	373.63	389.00
	200	437.46	447.51	458.12	469.44	476.11

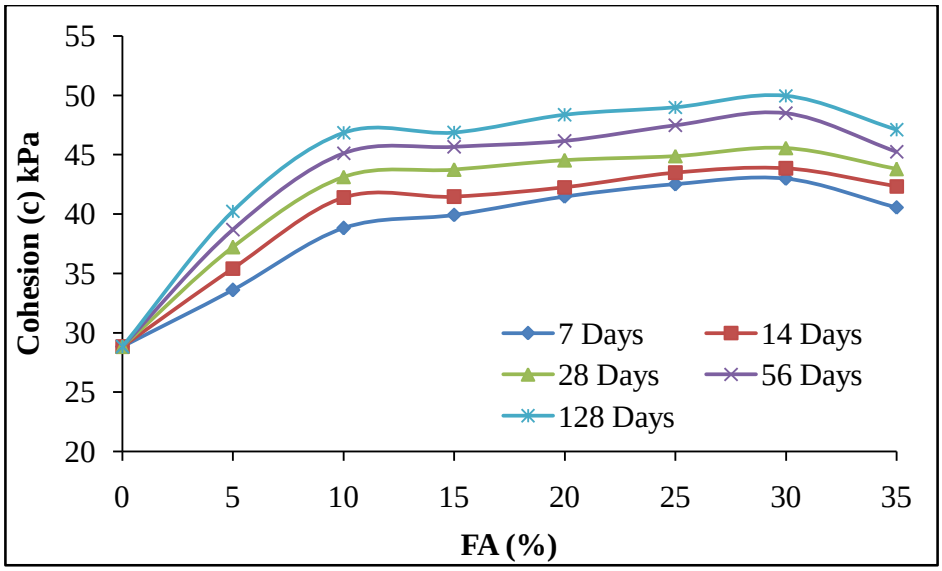

Figure 5.12 Cohesion of Soil-FA Mixtures

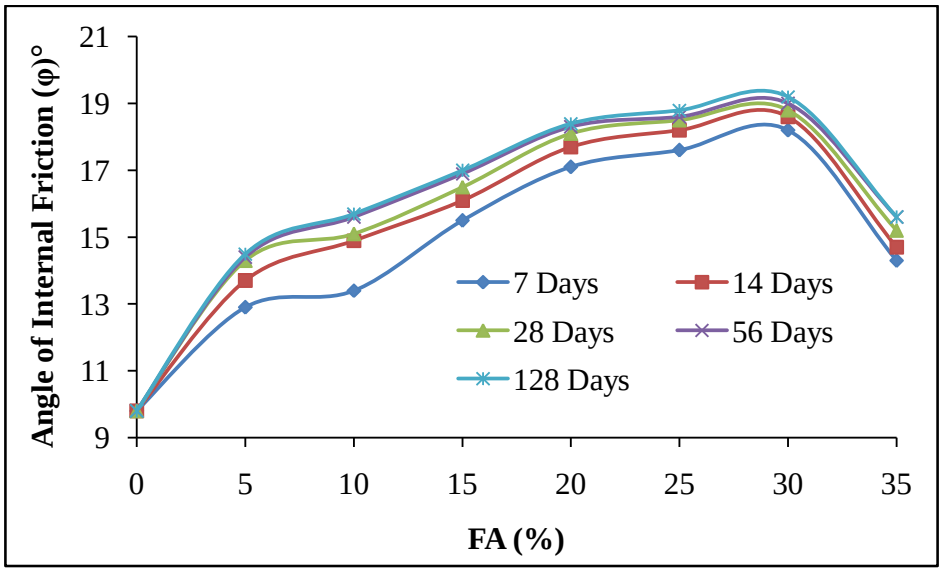

Figure 5.13 Angle of Internal Friction of Soil-FA Mixtures

5.2.11 Cyclic Triaxial Test

The effects of various percent of FA and loading cycles on the permanent deformations of expansive soil and FA admixed soils were studied. The effects of deviator stress level (DSL) ratios and confining pressure with number of loading cycles on the permanent deformations were studied for all FA admixed soils. Three confining pressures such as 100, 150 & 200 kPa

and two DSL such as 0.5 DSL and 0.8 DSL were chosen for determining permanent strain upto 10000 cycles under constant axial loading. Graphical plot was established between vertical percent permanent strain as ordinate and number of cycles as abscissa. Graphical plots have been drawn for each of this deviator stresses (i.e. 0.5 DSL and 0.8 DSL) at three pre-determined confining pressures (100 kPa, 150 kPa & 150 kPa) and they are shown in Figures 5.14 & 5.15.

5.2.11.1 Effect of load cycle

Rapid increase in deformation of the expansive soil and FA admixed soils were observed during the initial approximate hundred cycles of loading and the strain rate was high during this stage in all cases as shown in Figure 5.14 & 5.15. After few hundred cycles of loading, the increase in deformations was progressively increased upto 2000 cycles thereafter deformation almost stabilized for FA admixed soils. But deformation was still taking place for expansive soil. For FA admixed soils, the matrix behaves almost elastically under the applied load. The maximum permanent strain of 6.15% was observed for expansive soil when 0.8 DSL and 100 kPa confining pressure were applied. Consequently, the minimum permanent strain of 2.21% was measured for 30% FA inclusion level by having 0.5 DSL at 200 kPa for 10000 cycles.

5.2.11.2 Effect of confining pressure

Effort was also made to study the permanent deformation characteristics of expansive soil and FA admixed soils at pre-determining three different confining pressures. Figures 5.14 (a, b & c) and 5.15 (a, b, & c) depict permanent deformation at three confining pressure 100, 150 and 200 kPa respectively. From the present study, the minimum permanent deformation observed after 10000 cycles at 100 kPa, 150 kPa and 200 kPa confining pressure are 4.3%, 3.8% & 3.4% respectively at 0.5 DSL. Whereas, the permanent deformation for 0.8 DSL under the same working condition are 6.1%, 5.3% & 4.5% respectively. This analysis suggested that permanent deformation decreases with increase in confining pressure irrespective of types of samples. However, least permanent deformation was recorded for 30% FA inclusion level.

5.2.11.3 Effect of deviator stress level

The permanent strain values measured at 0.5 DSL for expansive soil and FA admixed soils are illustrated in Figure 5.14. To appreciate better the effect of σ_d the permanent strain recorded at 0.8 DSL is also presented in Figure 5.15. These different plots have been drawn considering all the three different confining pressures. Decrease of σ_d value signifies improvement in permanent strain. Based on the investigation, the least value of σ_d was observed for 30% FA admixed soils (2.21%) for 0.5 DSL at 200 confining pressure. Whereas for 0.8 DSL, 2.94% was observed. This again confirmed that least permanent deformation is offered by 30% FA inclusion level.

For analysis of resilient modulus (M_R) results, set of six tests was conducted on both expansive and FA admixed soils. Tests were conducted at two pre-determined deviator stress level, i.e., 0.5 DSL & 0.8 DSL. Similarly, three confining pressure of 100 kPa 150 kPa and 200 kPa were chosen for the test. Throughout the test, the aforementioned DSL rates and confining pressures were maintained. The main objective of this study was to understand the effects of confining pressure and DSL on expansive soil and FA admixed soils.

Figure 5.16 explains that increase in confining pressure resulted enhancements of M_R of all cases but these value diminish at higher DSL value. M_R values increase with increase in FA content irrespective of DSL and confining pressure. The maximum M_R values observed were 110 MPa & 69 MPa at 0.5 & 0.8 DSL respectively for a constant 200 kPa confining pressure when no admixing was done. But these values increased to 171 & 107 MPa respectively after admixing of 30% FA. Improvement in resilient modulus of expansive soil on admixing of fly ash may be due to the pozzalanic activity and self-cementitious characteristics of fly ash.

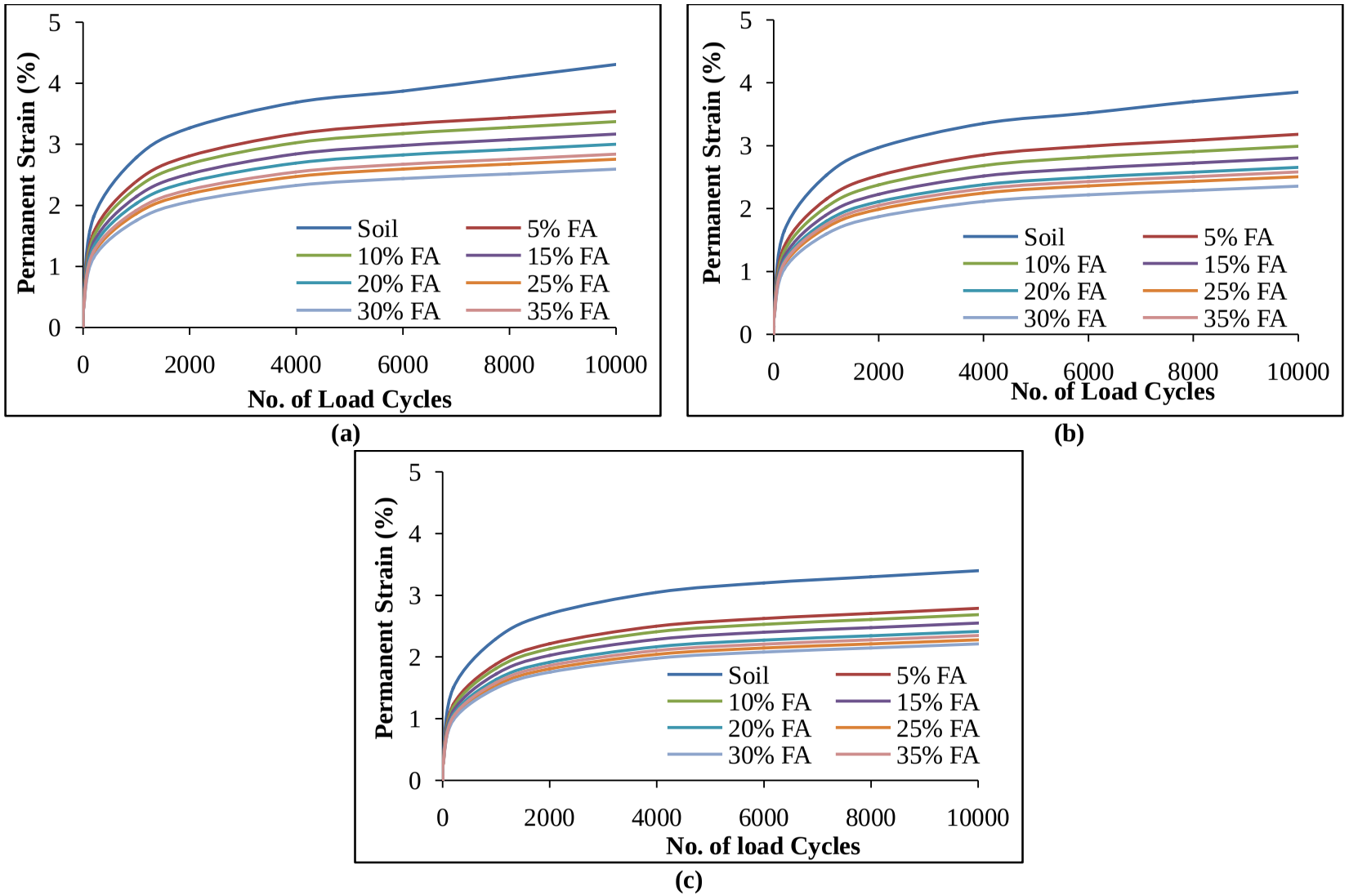

Figure 5.14 Permanent Strain of Soil-FA Mixtures at 0.5 DSL (a) at 100 kPa CP (b) at 150 kPa CP (c) at 200 kPa CP

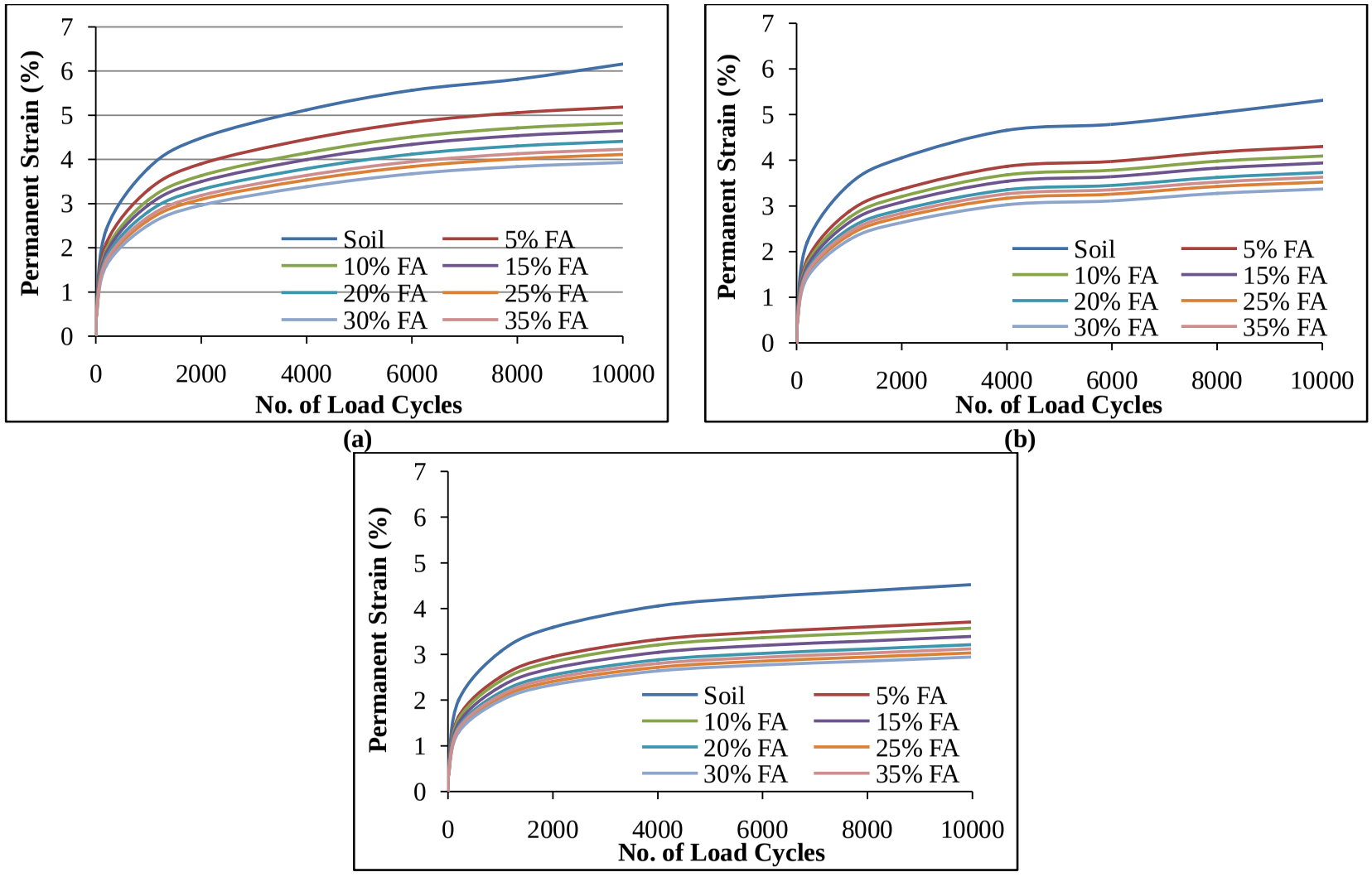

Figure 5.15 Permanent Strain of Soil-FA Mixtures at 0.8 DSL (a) at 100 kPa CP (b) at 150 kPa CP (c) at 200 kPa CP

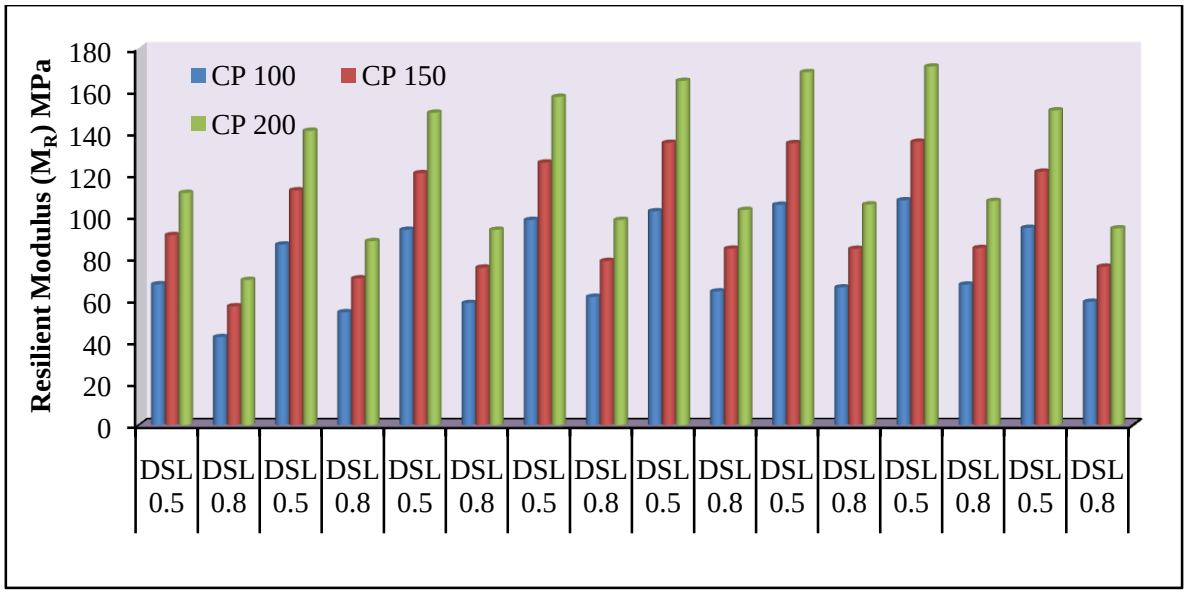

Figure 5.16 Resilient Modulus of Soil-FA Mixtures

5.2.12 Plate Load Test

The influence of FA in improving the modulus of subgrade reaction (k) of mixtures was evaluated by comparing the measured k-values for the natural expansive soil and soil-FA mixtures. Inclusion of FA to expansive soil considerably improved k-value as presented in Figure 5.17. The modulus of subgrade reaction of expansive soil was found to be 17 MPa/m. The rate of improvement of k-value is significant upto 25% FA inclusion level beyond which k-value starts declining. If FA was admixed with expansive soils @ 5%, 10%, 15%, 20%, 25%, 30% & 35%, the percentage increase of k-values were 92.11%, 135.46%, 154.51%, 186.53%, 203.49%, 197.89% & 191.65% respectively with respect to expansive soils.

Efforts have also been made to obtain load-settlement curves using laboratory data accrued from the plate load tests. As definite yield point could not be obtained from the derived curves, the ultimate bearing capacity for expansive soil and FA admixed soils were worked out by extending tangents from the two straight portions of the load-settlement curve one at the initial straight portion and another tangent at the steeper straight portion at the end.

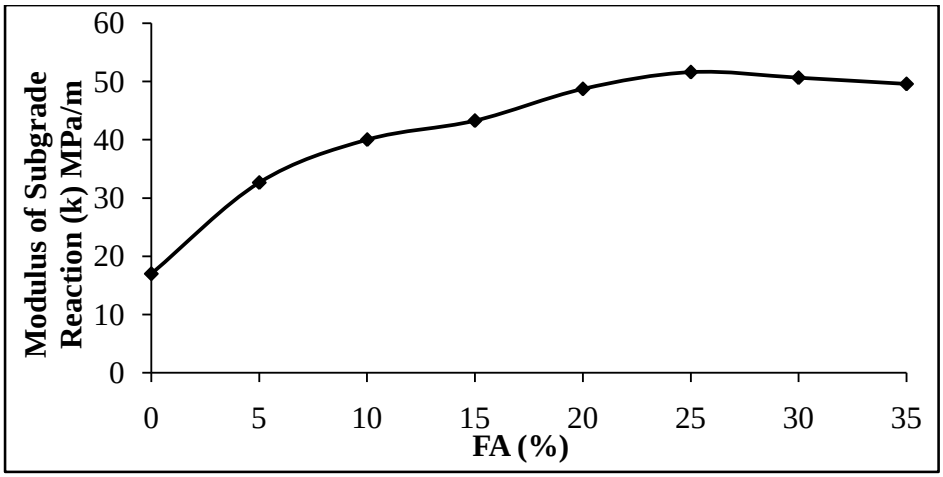

Figure 5.17 Modulus of Subgrade Reaction of Soil-FA Mixtures

Figure 5.18 shows the ultimate bearing capacity of soils with or without FA. 198 kPa ultimate bearing capacity was noted for natural expansive soil. This bearing capacity improves significantly on admixing of FA and better improvement in bearing capacity was noted for higher FA inclusion level. The percentage improvement of bearing capacity are 21.2%, 29.8%, 36.4%, 42.4%, 45.5%, 48.0% & 33.8% on admixing of FA @ 5%, 10%, 15%, 20%, 25%, 30% & 35% respectively. It was also found that admixing of FA beyond 30% led to reduction in bearing capacity substantially. Based on the above analysis, the optimal inclusion level of FA is 30% if expansive soil is to be stabilized.

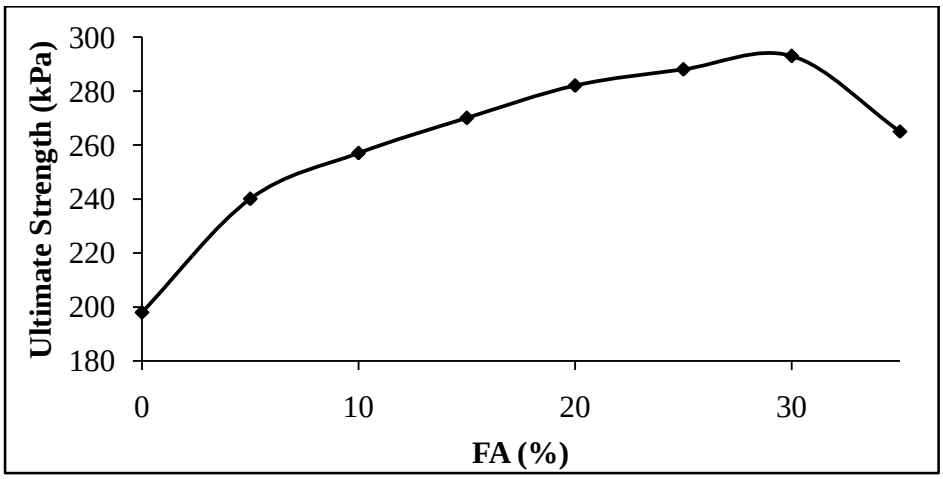

Figure 5.18 Ultimate Strength of Soil-FA Mixtures

5.2.13 Microstructural Investigation

Fly ash is classified as hydraulic binders. As the fly ash used in the present investigation is conforming to IS: 3812, the same can be included in the category of hydraulic binder. This means fly ash can be reactive in presence of moisture. As a result of which pozzolanic reaction can occur when it comes in contact with water. Using SEM technique, morphological properties of soil-FA mixtures were studied. From Figure 5.19 (a) to (d), as expected, upon stabilization, formations of Calcium Silicate Hydrate (C-S-H) gel along with Portlandite [Ca (OH_2)] were observed in all the soil-FA mixtures. As can be seen from Figure 5.19 (b), ettringite was formed using fly ash spheres as nucleation site. In addition to this compound formation, better degree of agglomeration of FA and soil particles are also distinctly noticed for 25% FA and 35% FA [Figure 5.19 (b) & (d)] resulting in an increased strength. Also from the present SEM image analysis, presence of enormous quantities of amorphous compounds are also confirmed.

5.2.14 Correlation between Different Strength Parameters

5.2.14.1 Relation between CBR, % FA & Curing Days

The correlation between CBR, % FA and curing days (D) was established using multiple linear regression analysis (MLRA). Test results obtained at 7, 14, 28 & 56 days of curing were considered for the analysis. The developed relation is given in Eqn. (5.1), with $R^2 = 0.849$. High values of R^2 show close proximity to predicted values with experimental data. The validation of the developed relation was done using laboratory CBR values obtained at 128 days of curing. CBR results obtained through predicted equation [CBR (P)] and CBR results accrued from the laboratory [CBR (L)] were compared as shown in Figure 5.20. The equation has high values of R^2 suggesting closeness of predicted values the experimental data.

$$CBR = 2.559+0.172\%FA+0.0144D \quad (5.1)$$

Where, CBR = California bearing ratio, % FA = percentage fly ash, D = number of curing days.

This predictive equation will facilitate prediction of CBR values at any given days from 3 to 128 days for a known FA content in expansive soil.

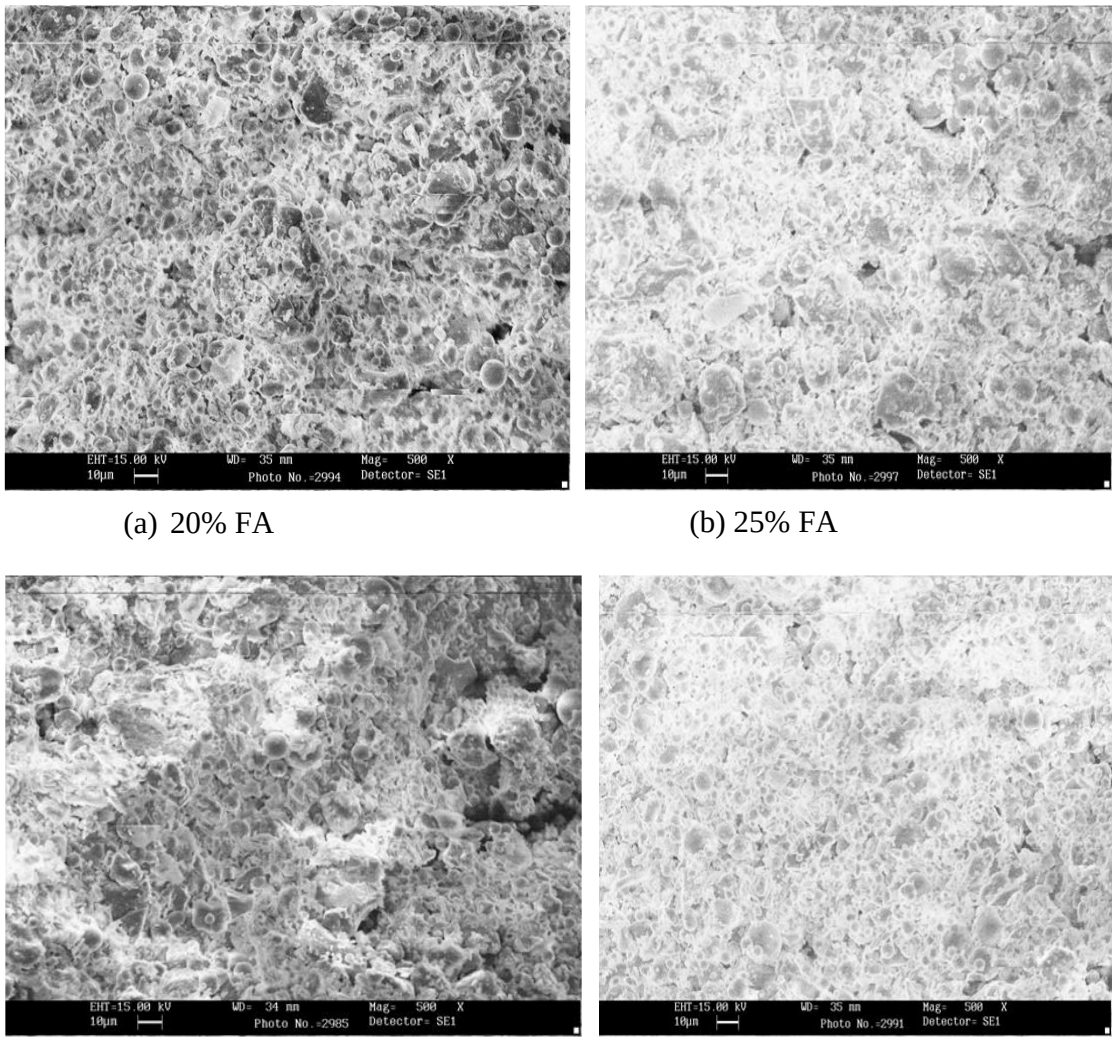

(a) 20% FA (b) 25% FA

(c) 30% FA (d) 35% FA

Figure 5.19 SEM Images of Soil-FA mixtures captured at 500 X magnification

5.2.14.2 Relation between UCS, CBR, % FA & Curing Days

In a very similar manner, as in the case of CBR, %FA and curing days relationship; UCS values obtained from the laboratory for FA admixed soil samples cured for 7, 14, 28, 56 & 128 days were considered for establishing general equation to compute predicted UCS value. The relationship developed between UCS as dependent variable and other parameters as independent variable is given in Eqn. (5.2), with R^2= 0.964. UCS test results of 128 days were used for validation of the predicted equation. Predicted UCS [UCS (P)] values and laboratory

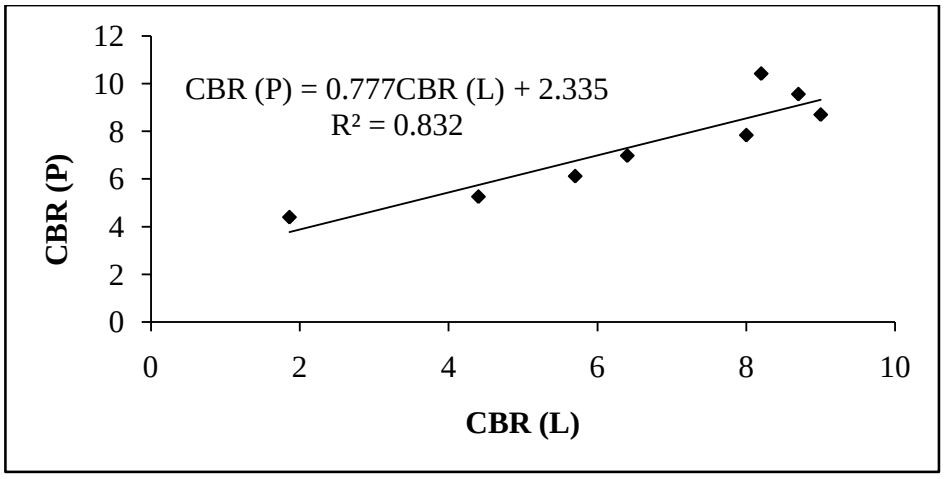

Figure 5.20 Validation of CBR Results

UCS [UCS (L)] values were compared as shown in Figure 5.21. As this equation showed high values of R^2, predicted UCS values have close proximity with experimental data.

$$UCS = 67.8233 - 0.73\%FA+0.05D+9.88CBR \quad (5.2)$$

where, UCS = Unconfined compressive strength (kPa)

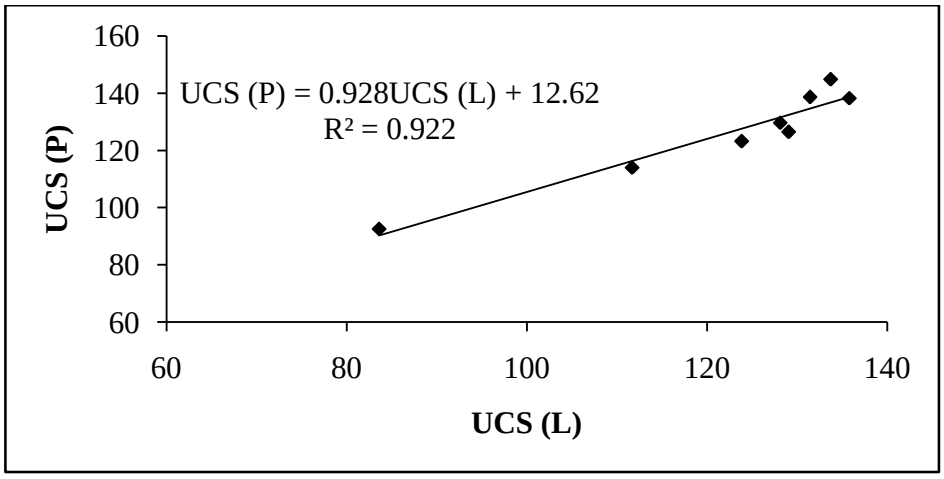

Figure 5.21 Validation of UCS Results for Soil-FA Mixtures

5.2.14.3 Relation between STS & UCS

Relationship has been established between split tensile strength and unconfined compressive strength of FA admixed soil samples from the data of present study. Various models like linear,

exponential, polynomial, power and logarithmic were tested, but polynomial relation as shown in Figure 5.22 was best fitted with R^2 = 0.937. Further, the proposed equation was validated using ST laboratory results accrued after 128 days of curing as presented in Figure 5.23

The predicted STS [STS (P)] values and laboratory STS [STS (L)] values were compared and showed excellent relationship as high R^2 values exhibit between them.

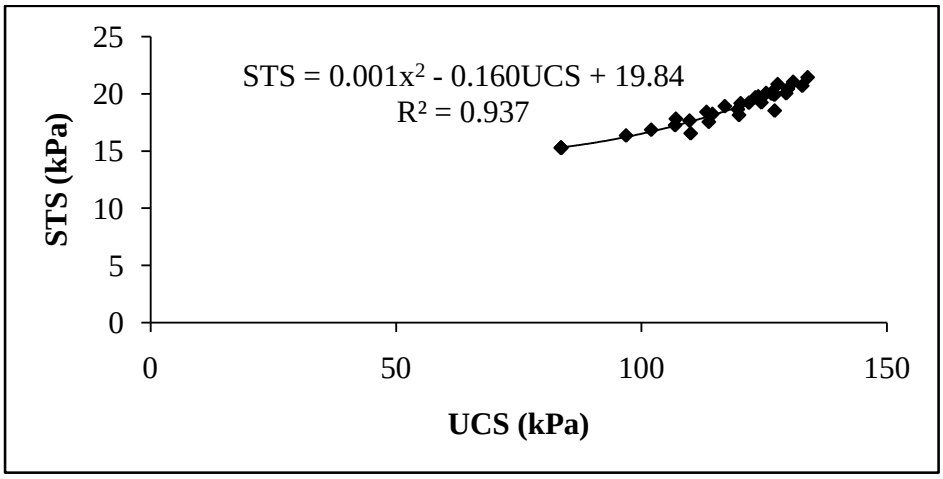

Figure 5.22 Relationship between STS & UCS for Soil-FA Mixtures

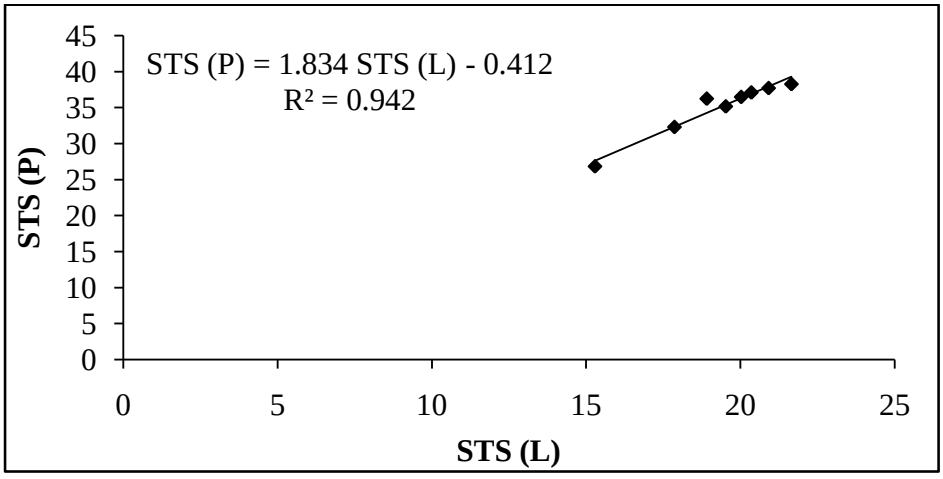

Figure 5.23 Validation of STS Results for Soil-FA Mixtures

5.2.14.4 Relation between M_R & CBR

The cyclic triaxial tests were conducted as per ASTM D5311-11 on natural expansive soil and FA admixed soils. Tests were conducted after the expiry of 28 days curing period. Three levels of σ_3 (50, 100 and 150 kPa) at 0.50 DSL and 0.80 DSL were applied during the test. The main intention behind this effort was to establish correlation between M_R & CBR using regression analysis for each three levels of σ_3 0.50 DSL and 0.80 DSL respectively. Mathematical analysis of data shows good relationship between M_R & CBR described by a power series as presented in Figure 5.24 (a to f).

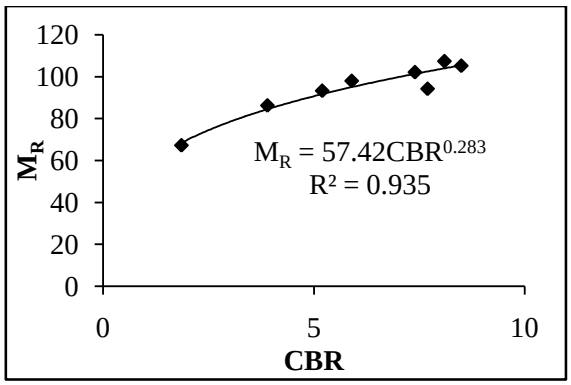

(a) CP 100; DSL 0.5

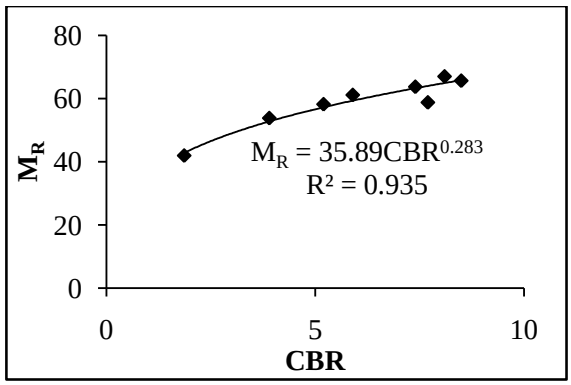

(b) CP 100; DSL 0.8

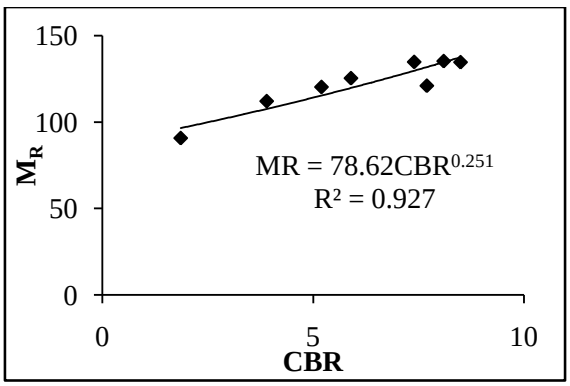

(c) CP 150; DSL 0.5

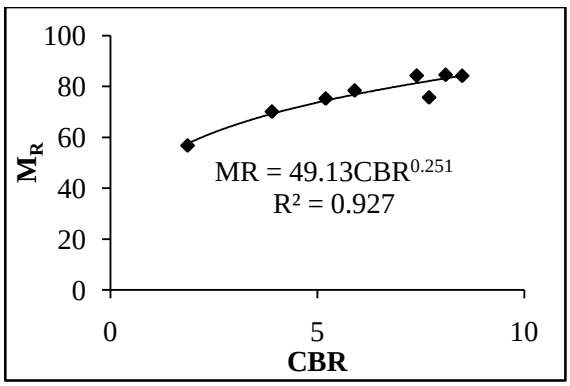

(d) CP 150; DSL 0.8

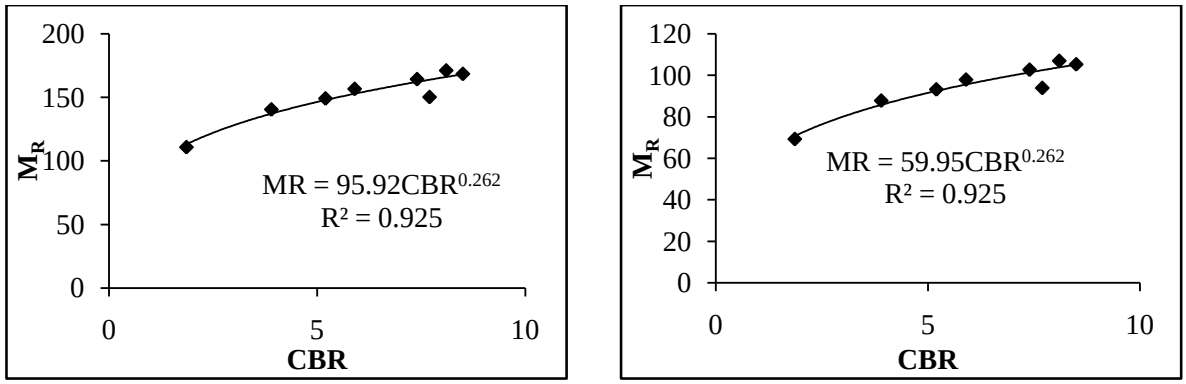

(e) CP 200; DSL 0.5 (f) CP 200; DSL 0.8

Figure 5.24 Relation between M_R & CBR for Soil-FA Mixtures

5.3 SOIL-RICE HUSK ASH

5.3.1 Atterbergs Limit Test

Figure 5.25 presents the plasticity index (PI) of expansive soil and RHA admixed soils. Admixing of RHA reduced plasticity index of expansive soil. This finding is in agreement with Yadu, L. et al. (2011) and Muntohar, A. S. (2002). The percentage reduction in PI of expansive soil on admixing of RHA @ 5%, 10%, 15%, 20%, 25%, 30% and 35% are 16%, 28%, 40%, 56%, 64%, 80% and 84% respectively. Higher reduction in PI was observed for higher percentage inclusion of RHA. However, percentage reduction in PI is apparently higher for FA admixed soil samples in comparison to RHA admixed soil samples. In overall, about 1.4 times higher percentage reduction in PI was noted for FA admixed soils when compared to RHA admixed soils irrespective of RHA inclusion levels. This analysis strongly suggested that FA showed better efficacy over RHA to control plasticity index of expansive soil. Laboratory results revealed that the reduction in plasticity of RHA admixed soil is as a result of increase in liquid limit and plastic limit. However, the rate of increase of plastic limit is higher than liquid limit. As a result of which plasticity index decreases. Reduction in the plasticity index indicates an improvement in soil engineering properties.

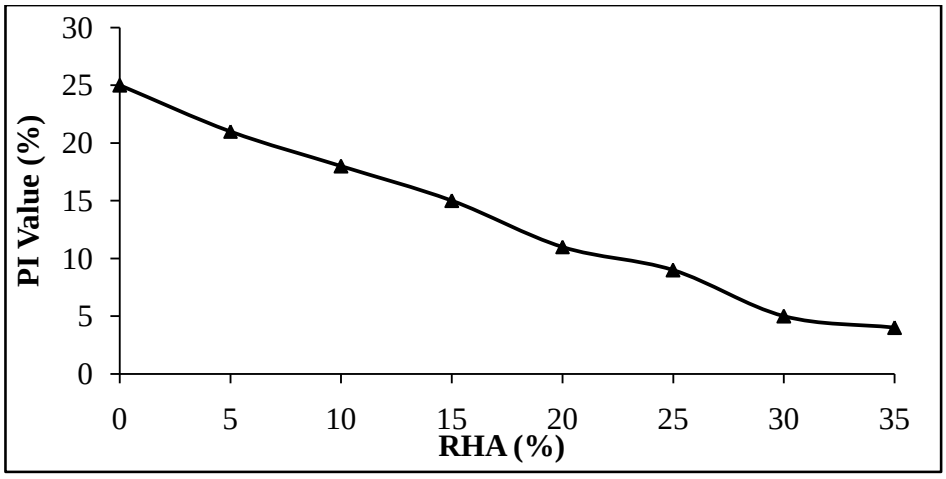

Figure 5.25 Atterbergs Limit of Soil-RHA Mixtures

Figure 5.26 shows the variation of shrinkage limits of expansive soil and RHA admixed soils. Shrinkage limit increased for higher inclusion levels. The percentage increase of shrinkage limit on admixing of RHA @ 5%, 10%, 15%, 20%, 25%, 30% and 35% resulted in an increase of the shrinkage limit to 26.0 %, 40.7%, 59.5%, 73.4%, 88.8%, 99.6% and 103.4% respectively with respect to expansive soil. Substantial increment in shrinkage limit was observed upto 30% RHA inclusion level beyond which, the same starts decreasing gradually. Based on this analysis, it is pertinent to note here that inclusion of RHA produced nearly 1.1 times higher percentage shrinkage limit than FA admixed soils. Analysis results inference that rice husk ash could be a good alternative additives to fly ash for controlling shrinkage potential of expansive soils.

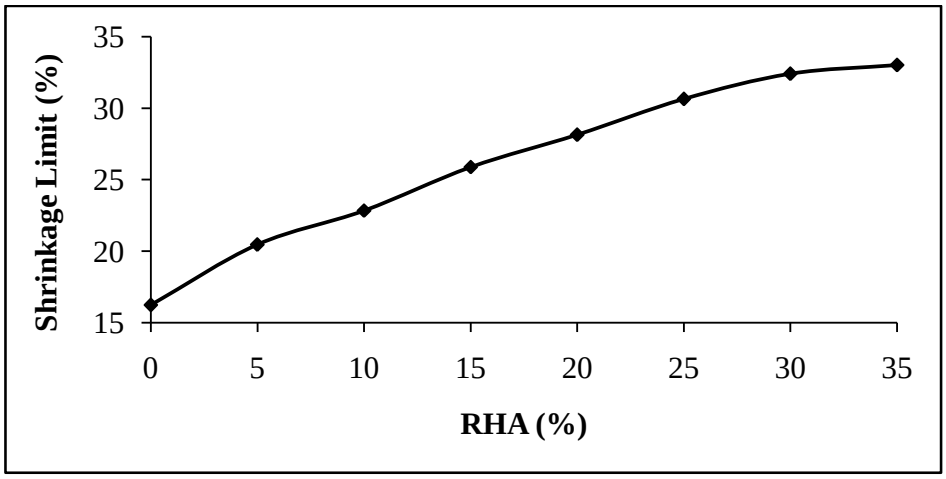

Figure 5.26 Shrinkage Limit of Soil-RHA Mixtures

5.3.2 Free Swelling Index

Figure 5.27 presents the free swelling index of RHA admixed soils and expansive soil. Free swelling index decreases with increase in RHA substitution levels. When compared to expansive soil, percent reductions of free swelling indices on admixing of RHA @ 5%, 10%, 15%, 20%, 25%, 30% and 35% respectively are in the order of 13.04%, 29.08%, 39.74%, 53.70%, 60.51%, 67.21% & 75.81%. Percentage reduction in swelling index on admixing RHA showed about 1.2 times higher than FA admixed soil irrespective of substitution levels. This analysis clearly suggested that RHA could be a better additive to admixed with expansive soil to control swelling potential of expansive soil in lieu of fly ash.

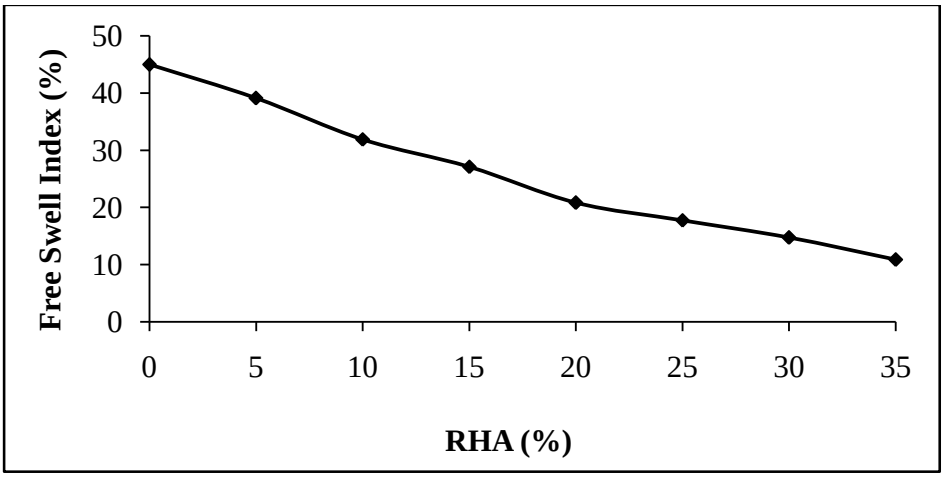

Figure 5.27 Free Swelling Index of Soil-RHA Mixtures

5.3.3 Proctor Test

Figure 5.28 explains the increasing trend of OMC for expansive soil when percentage content of RHA increases. This increase was relatively gradual upto 20% RHA inclusion level. But from 25% inclusion level onwards upto 35%, very sharp rate of increase in OMC was observed. This effect may be due to presence of appropriate quantity of RHA to reconfigure the whole matrix system physically as well as chemically. The percentages increase in OMC on admixing of RHA @ 5%, 10%, 15%, 20%, 25%, 30% and 35% are 17.6, 41.2%, 52.9%, 70.6%, 100%, 129.4%, 147% and 341.2% respectively with respect to expansive soil. OMC analysis revealed that RHA admixed soils produced 1.6 times higher percentage increase than that of FA admixed soils with no regards to RHA inclusion levels. This high water demand is

attributed to cellular structure of RHA which exhibits large surface area caused by the presence of coarse microstructural shape like cubes of cellular beehives as revealed by SEM images.

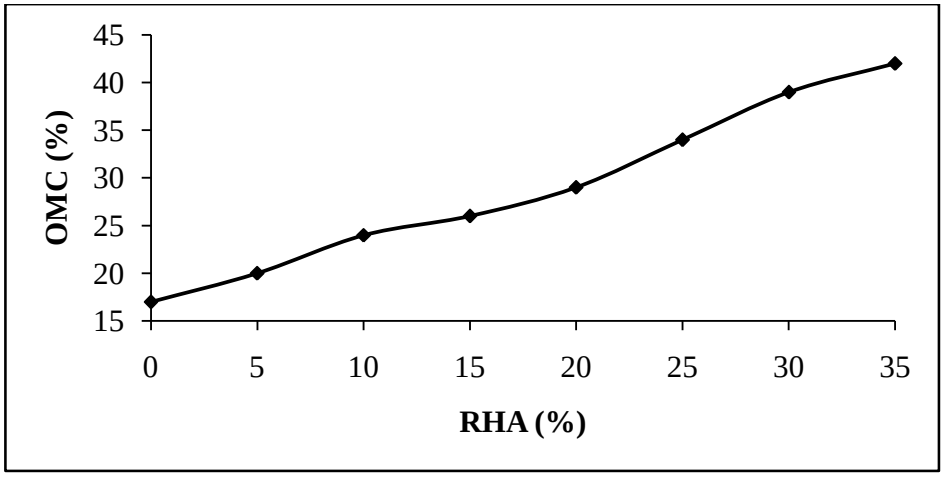

Figure 5.28 OMC of Soil-RHA Mixtures

Addition of RHA to expansive soil decreased dry density considerably as shown in Figure 5.29. The trend of decrease in dry density on admixing RHA is very similar to that of FA admixed soils (Figure 5.5). However, percentage reduction in dry density of expansive soil due to admixing of RHA is about 4.0% in over all irrespective of inclusion levels. Whereas, the percentage reduction in dry density for 100% RHA admixed soil was 28.9% with respect to expansive soil. The decrease in dry density may be due to partially admixing of lower specific gravity (1.86) material (RHA) into the soil mass having higher specific gravity (2.74). This finding is in agreement with Osinubi & Katte (1997) and Ola (1975).

5.3.4 California Bearing Ratio Test

Inclusion of RHA improves CBR value of expansive soil considerably irrespective of RHA inclusion levels as shown in Figure 5.30. The percentages increase of CBR value due to admixing of RHA @ 5%, 10%, 15%, 20%, 25%, 30% and 35% are 144.1%, 258.6%, 351.6%, 455.4%, 499.5%, 454.3% & 418.3% respectively with respect to expansive soil. This analysis clearly suggests that admixing RHA to expansive soil improves CBR value better than FA admixed soils and this increase is about two folds of that FA admixed soils. The improvement of soil strength in CBR is the function of soil-RHA interlocking phenomena. Another good

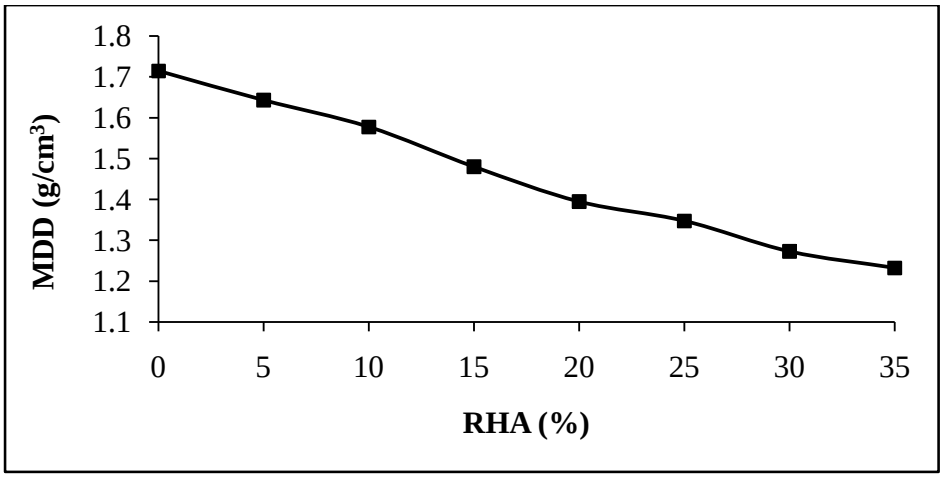

Figure 5.29 MDD of Soil-RHA Mixtures

reason is that due to presence of substantial amount of SiO_2 and adequate quantity of CaO in RHA which enables to initiate pozzolanic reaction better. Maximum CBR value was offered by 25% RHA inclusion level with no regards to curing time. Beyond 25% inclusion level, no appreciable improvement was observed. Hence, analyses of results have done only for 25% RHA inclusion level. It was also observed that substantial improvement in CBR values were recorded with respect to curing time particularly relative humidity. These increases were about 8.4%, 12.9%, 16.6%, 19.3% & 21.1% respectively for 7, 14, 28, 56 & 128 days curing period with respect to 3 day's CBR values. The gradual decrease of CBR value beyond 25% RHA inclusion level may be due to surplus RHA present around the soil particles and hence could not be activated in the chemical reaction, which occupies spaces within the sample thereby reduced bond between the soil particles and RHA. This finding is in agreement with Brooks, (2009) and Chioobbasti et al. (2010).

5.3.5 Expansion Ratio

Figure 5.31 presented the expansion ratio measured in the laboratory for soil-RHA mixtures. Expansion ratio for natural expansive soil was found to be 32%. Whereas after incorporation of RHA @ 5%, 10%, 15%, 20%, 25%, 30%, and 35%, these expansion ratios considerably reduced by 20%, 30.0 %, 35.0%, 42.5%, 47.5%, 57.5% and 60.0% respectively. On average, about 1.3 times better efficiency is show n by RHA over FA with respect to percentage of reduction of ER of expansive soil.

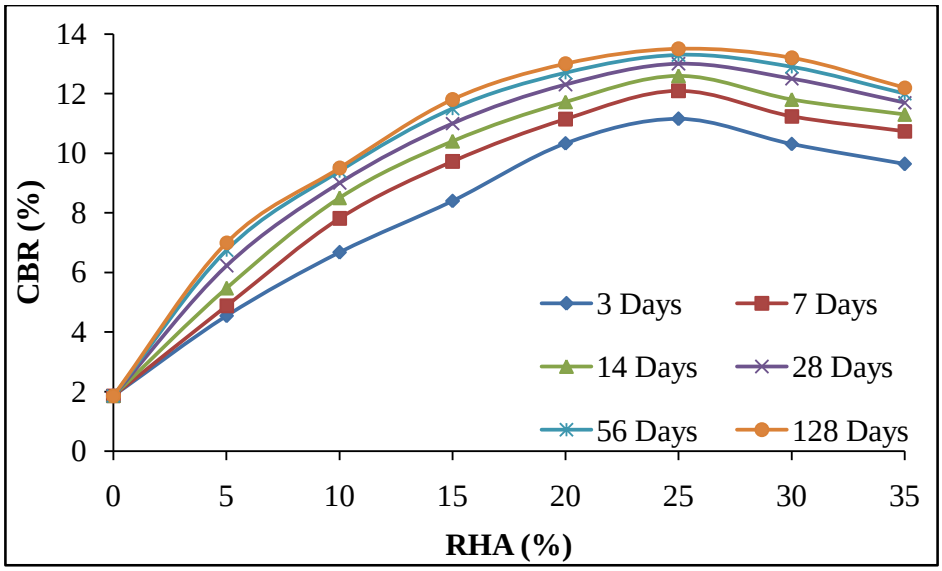

Figure 5.30 CBR of Soil-RHA Mixtures

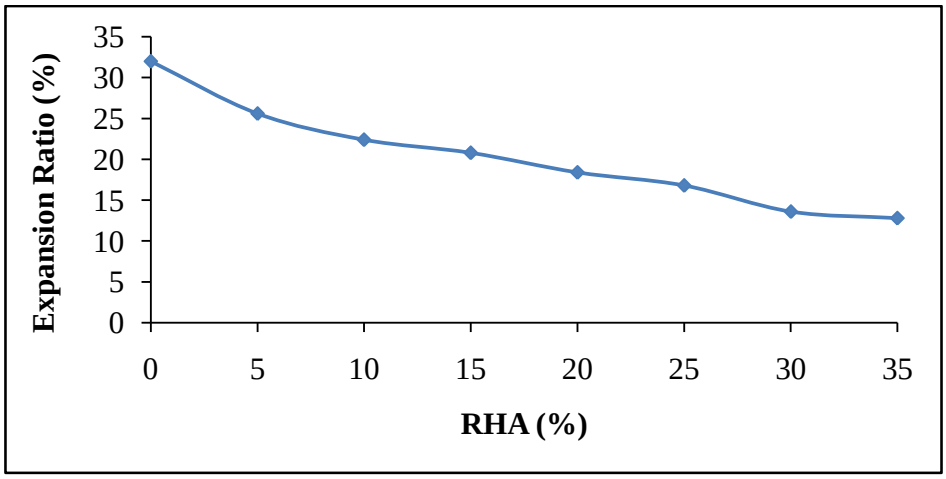

Figure 5.31 Expansion Ratio of Soil-RHA Mixtures

5.3.6 Hydraulic Conductivity

The effects of RHA addition on the permeability of the mixtures cured for a period of 7 days is shown in Figure 5.32. Inclusion of RHA reduces permeability considerably as can be seen from the plot shown below. The decrease in permeability is more for higher RHA inclusion levels. This decrease is more pronounced for 20% RHA inclusion level. Beyond this inclusion level, the drop in permeability is very gradual. In regard of permeability, RHA seems to be more effective than FA as the percentages decrease in coefficient of permeability is higher for RHA

admixed soils. These decreases are about 29.50%, 44.11%, 52.43%, 65.92%, 67.76%, 73.81% & 78.26% on admixing of RHA @ 5%, 10%, 15%, 20%, 25%, 30% & 35% respectively. The decrease in permeability was as a result of the formation of cementitious compounds by calcium and silica and/or alumina from both the soil and RHA, which fills the soil voids thereby obstructing the flow of water. These effects may be due to the partial dissociation of the calcium hydroxide in samples. The calcium ions combined with the reactive silica or alumina, or both, which obstructed flow through the soil voids (Osinubi 1998).

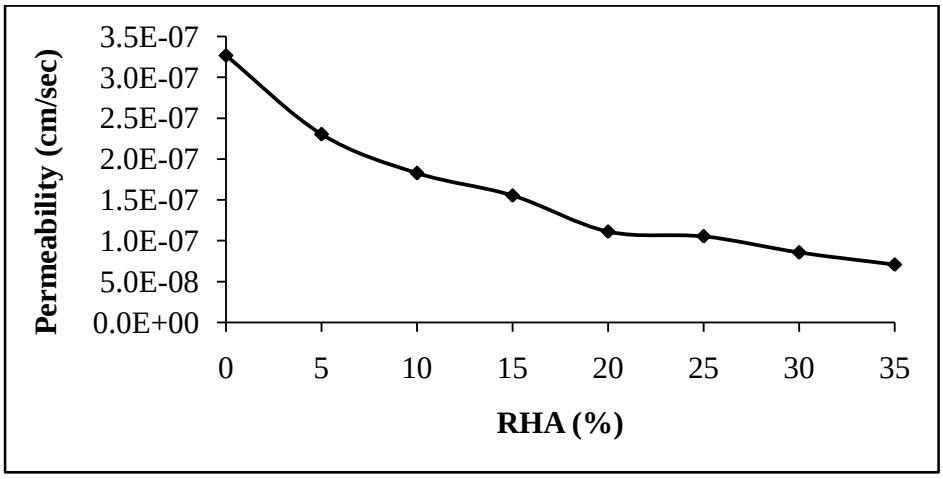

Figure 5.32 Permeability of Soil-RHA Mixtures

5.3.7 Unconfined Compressive Strength

UCS value was remarkably improved by admixing of RHA with expansive soil as shown in Figure 5.33. One can easily read in the Figure 5.33 that UCS values increased with higher RHA content. However, inclusion of RHA beyond 25% inclusion level, UCS drops significantly. This finding is in agreement with Pal (2012) and Yadu (2011). About 36.36%, 51.31%, 62.66%, 70.39%, 73.37%, 69.23% & 41.70% increment in UCS were observed when RHA was incorporated to expansive soil @ 5%, 10%, 15%, 20%, 25%, 30% & 35% respectively at 7 days curing. Whereas for 14 days, 28 days, 56 days and 128 days cured samples, these values further increased to 48.87%, 66.14%, 79.36%, 86.54%, 88.45%, 80.53% & 57.11%; 52.98%, 72.19%, 84.74%, 94.16%, 97.73%, 88.97% & 64.34 %; 62.36%, 80.40%, 91.78%, 100.73%, 103.59%, 99.53% & 83.10% and 67.05%, 86.26%, 96.47%, 104.25%, 107.11%, 102.58% & 93.66% respectively.

On average, RHA to FA ratio for curing period of 7, 14, 28, 56 and 128 days are 1.59, 1.70, 1.64, 1.67 and 1.70 respectively. This apparently indicates that present RHA has better potential for improving compressive strength of admixed soil in comparison to FA.

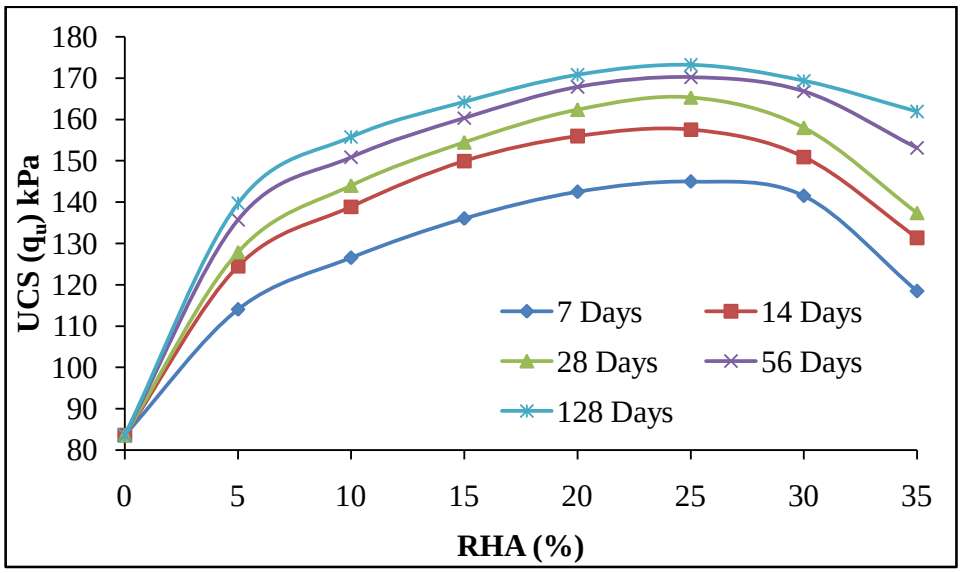

Figure 5.33 UCS of Soil-RHA Mixtures

5.3.8 Split Tensile Strength Test

Admixing of RHA to expansive soil enhances split tensile strength as presented in Figure 5.34. The increase of split tensile strength is significant upto 25% RHA inclusion level. However, sharper increase in tensile strength was noted at 15% RHA inclusion level. Beyond this level, improvement in tensile strength is almost stabilized to a large extent beyond 25% inclusion level, thence tensile strength considerably reduced. Inclusion of RHA improves STS to about 49.7%, 51.6%, 54.2%, 57.0% & 59.2% at the curing periods of 7, 14, 28, 56 and 128 days respectively. Percentage reduction in STS is more in comparison to UCS under same working condition for RHA admixed soils irrespective of days of curing. This strongly suggested that RHA admixed soils yield better compressive strength than tensile strength. Prolong curing showed significant impact in the development of tensile strength and the probable reason for the same is due to the formations of cementitious products with time, hence, inter-soil particle pores are filled up and thus the total pore volume decreases thereby improve the interfacial zone of soil particles.

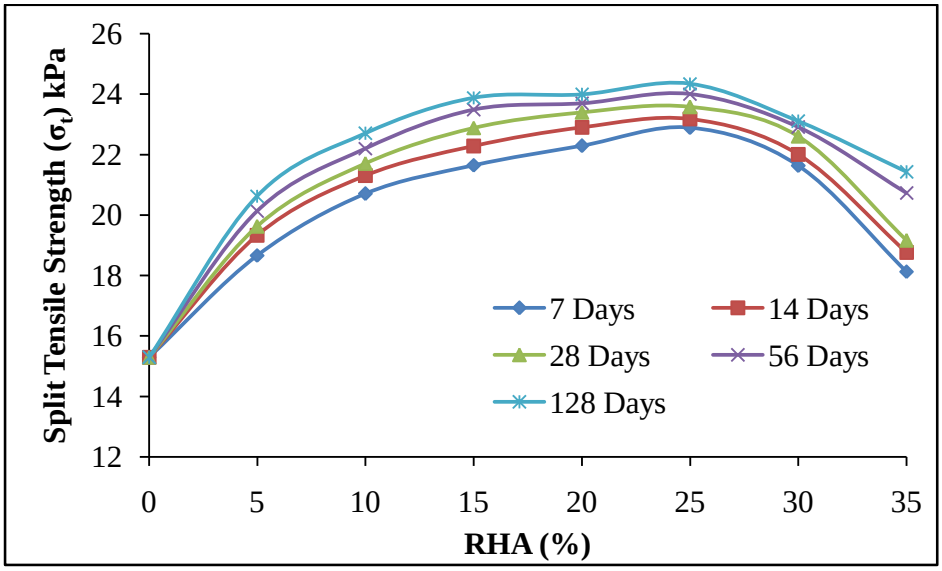

Figure 5.34 Split Tensile Strength of Soil-RHA Mixtures

5.3.9 Ratio of Split Tensile to Unconfined Compressive Strength Test

Effort was made to establish relative relationship and mobilization between the tensile strength and compressive strength. This could be discussed by plotting the tensile/compressive strength ratio (σ_t/q_u) versus curing time. Figure 5.35 presents the influence of RHA content on the ratio of split tensile strength and unconfined compressive strength. The results show that unconfined compressive strength and split tensile strengths are closely related. It can be observed that the ratio of split tensile strength and unconfined compressive strength decreased with increase in RHA content, indicating that RHA is more efficient when soil was subjected to compression rather than to tension.

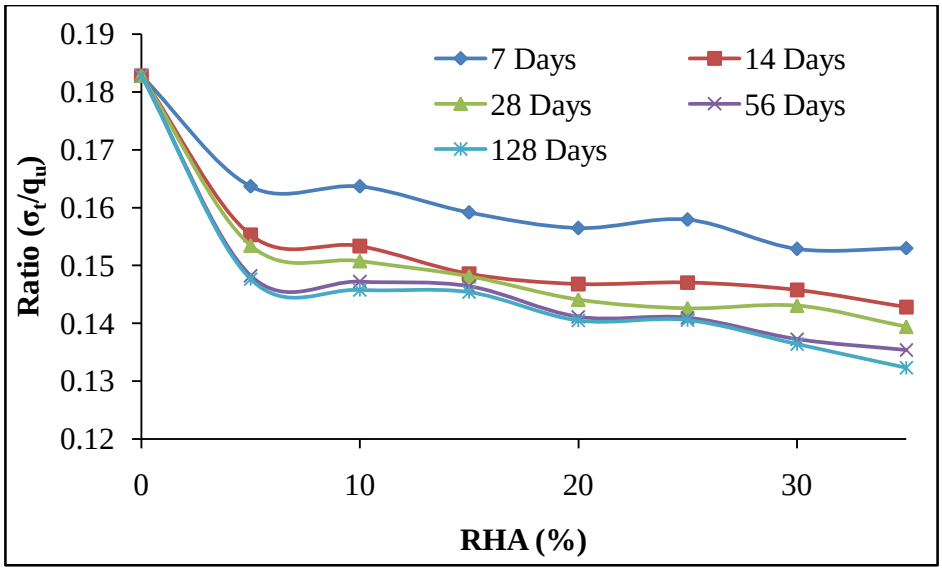

Figure 5.35 σ_t/q_u Ratio of Soil-RHA Mixtures

5.3.10 Triaxial Test

Three different confining stresses such as 100, 150 and 200 kPa were applied on specimens to obtain peak deviator stress as presented in Table 5.2. The range of confining stresses was chosen to obtain well defined and accurate plots of Mohr envelopes to obtain shear strength parameters; cohesion (c) and angle of internal friction (φ) of the soils mixed with RHA. The variation of c and φ with admixing RHA were evaluated and results are shown in Figures 5.36 & 5.37 respectively.

Inclusion of RHA shows positive influence on deviator stress (Table 5.2). Higher deviator stresses are observed for higher RHA content irrespective of confining pressure applied and days of curing. However, beyond 25 % RHA content, the deviator stress starts declining gradually. Inclusion of RHA causes increase in cohesion and internal friction angle. Increase in cohesion is more pronounced upto 10% FA content. The cohesion of soil ranges from 28 to 46.12kPa and from 28 to 55.75 kPa at 7 & 128 days of curing respectively, for RHA contents between 0 & 25%. Improvement on cohesion due to inclusion of RHA found to be retarded beyond 10% RHA inclusion level. However, these cohesions are much higher than that of expansive soil. Marked reduction in cohesion is observed beyond 25% RHA content (Fig 5.36). As in the case of cohesion, similar trend of improvement is observed for internal friction

angle. The rate of improvement of internal friction angle is rapid upto 5% RHA, after which the rate of improvement is slightly sluggish and this trend maintained upto 30% RHA but beyond 30% RHA content, angle of internal friction reduces significantly as it can be seen from Figure 5.37. As may be seen from the Table 5.2, higher deviator stresses are observed for higher confining pressures irrespective of days of curing. Improvements on cohesion and internal friction angle on admixing of RHA may be due to pozzolanic activity and also may be due to the fact that internal friction angle of RHA is more than that of expansive soil.

Table 5.2 Deviator Stress for RHA Admixed Soil at Different Confining Pressure

% RHA	Confining Pressure (kPa)	Deviator Stress (kPa)				
		7 Days	14 Days	28 Days	56 Days	128 Days
0	100	205.34	206.19	204.83	205.01	204.47
	150	275.91	277.81	276.52	278.17	276.24
	200	337.11	339.77	337.97	338.87	339.18
5	100	285.02	308.67	314.63	331.21	342.18
	150	376.22	404.35	409.02	427.27	437.99
	200	470.28	506.21	512.84	536.57	550.91
10	100	312.45	340.31	349.81	363.48	376.85
	150	409.31	442.41	451.26	465.25	478.60
	200	506.17	547.90	559.70	577.93	595.43
15	100	331.82	362.89	370.69	388.02	395.87
	150	431.36	468.13	474.48	492.78	506.71
	200	537.55	584.25	593.10	616.95	628.44
20	100	350.44	380.52	399.33	414.52	423.50
	150	459.08	502.29	527.12	538.88	550.55
	200	567.72	616.45	642.93	663.24	673.36
25	100	359.46	389.16	408.31	418.72	434.62
	150	460.11	502.02	522.64	540.15	547.62
	200	578.73	626.55	654.32	667.03	686.70
30	100	352.29	378.09	394.98	420.38	428.50
	150	450.93	480.18	497.67	525.48	533.48
	200	567.18	606.84	629.99	664.20	674.03
35	100	292.61	323.13	329.06	356.69	379.68
	150	377.46	413.61	422.84	449.96	491.68
	200	471.10	517.01	525.17	565.35	601.79

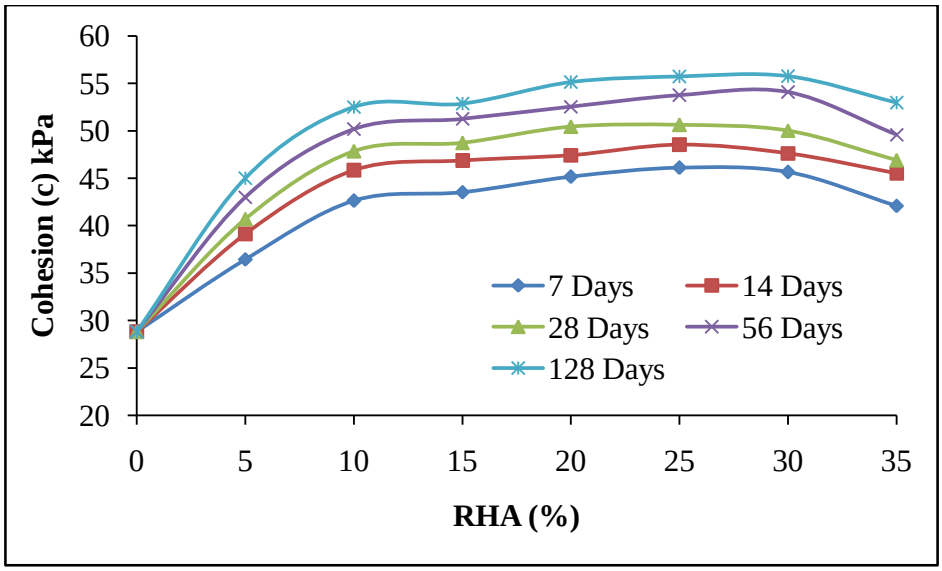

Figure 5.36 Cohesion of Soil Admixed with RHA

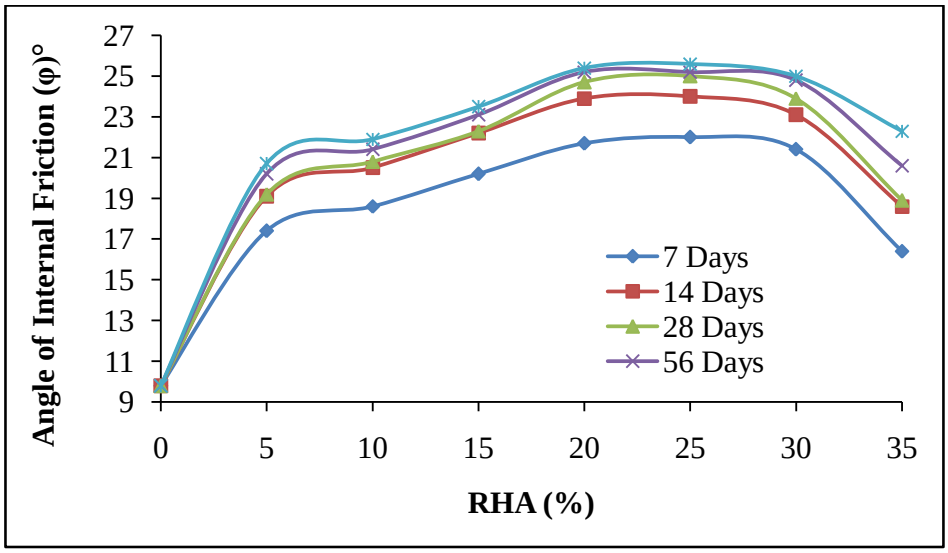

Figure 5.37 Angle of Internal Friction of Soil-RHA Mixtures

5.3.11 Cyclic Triaxial Test

The effects of various percent of RHA and loading cycles on the permanent deformations of the expansive soil and RHA admixed soil were studied. The effects of DSL ratios and confining pressure with number of loading cycles on the permanent deformations were evaluated for all combinations of admixed soils. Three confining pressures as 100, 150 & 200 kPa and two DSL as 0.5 and 0.8 were chosen for determination of permanent strain upto 10000 cycles under

constant axial loading. The test results plotted for vertical percent permanent strain as ordinate and number of cycles as abscissa is shown in Figures 5.38 & 5.39 at 0.5DSL and 0.8 DSL respectively.

5.3.11.1 Effect of load cycle

Figures 5.38 [(a) to (c)] show that rapid increase in deformation of the RHA admixed soils and expansive soils were observed during the initial approximate hundred cycles of loading and the strain rate was high during this stage in all cases. After few hundred cycles of loading, the increase in deformations was progressively increased upto 2000 cycles thereafter deformation almost stabilized for admixed soils. Whereas, for expansive soil, the permanent deformation continued to take place. But for admixed soils, the matrix behaves almost elastically under the applied load. The maximum permanent strain of 6.15 % was observed for expansive soil when 0.8 DSL and 100 kPa confining pressure were applied. Consequently, the minimum permanent strain of 2.04% was measured for 25% RHA inclusion level by having 0.5 DSL for 200 kPa confining pressure for 10000 cycles.

5.3.11.2 Effect of confining pressure

Permanent deformations for expansive soil and RHA admixed soils were also dependent on confining pressure. Figures 5.38 [(a) to (c)] and 5.38 [(a) to (c)] showed permanent deformation at three confining pressure 100, 150 and 200 kPa respectively. From the present study, the minimum permanent deformation observed after 10000 cycles at 100 kPa, 150 kPa and 200 kPa confining pressure are 2.4%, 2.3% & 2.04% respectively at 0.5 DSL. Whereas, the permanent deformation for 0.8 DSL under the same working condition are 3.8%, 3.3% & 2.7% respectively. Results indicate that permanent deformation decreases with increase in confining pressure irrespective of types of soils. However, least permanent deformation was recorded for 30% RHA inclusion level.

5.3.11.3 Effect of deviator stress level

The permanent strain values measured at 0.5 DSL for expansive soil and RHA admixed soils are illustrated in Figure 5.38. To appreciate better the effect of σ_d the permanent strain recorded at 0.8 DSL is also presented in Figure 5.39. These different plots have been established

considering all the three different confining pressures. Decrease of σ_d value signifies improvement in permanent strain. Based on the investigation, the least value of σ_d was observed for 25% RHA admixed soils (2.04%) for 0.5 DSL at 200 confining pressure. Whereas for 0.8 DSL, 2.70% was observed. This again confirmed that least permanent deformation is offered by 25% RHA inclusion level.

For analysis of resilient modulus (M_R) results, set of six tests was conducted on both expansive and RHA admixed soils. Tests were conducted at two pre-determined deviator stress level i.e. 0.5 DSL & 0.8DSL. Similarly, three confining pressure of 100kPa 150 kPa and 200 kPa were chosen for the test. Throughout the test, the aforementioned DSL rates and confining pressures were maintained. The main objective of this study was to understand the effects of confining pressure and DSL on expansive soil and FA admixed soils.

Figure 5.40 explains that increase in confining pressure resulted enhancements of M_R of all cases but these value diminish at higher DSL value. M_R values increase with increase in RHA content irrespective DSL and confining pressure. The maximum M_R values observed were 110 MPa & 69 MPa at 0.5 & 0.8 DSL respectively for a constant 200 kPa confining pressure when no admixing was done. But these values increases to 214 & 134 MPa respectively after admixing of 25% RHA. This effect may be attributed to a stiffer soil skeleton structure of RHA admixed soils caused by increased confinement and pozzolanic reactions, which result in a closer bonding of soil particles.

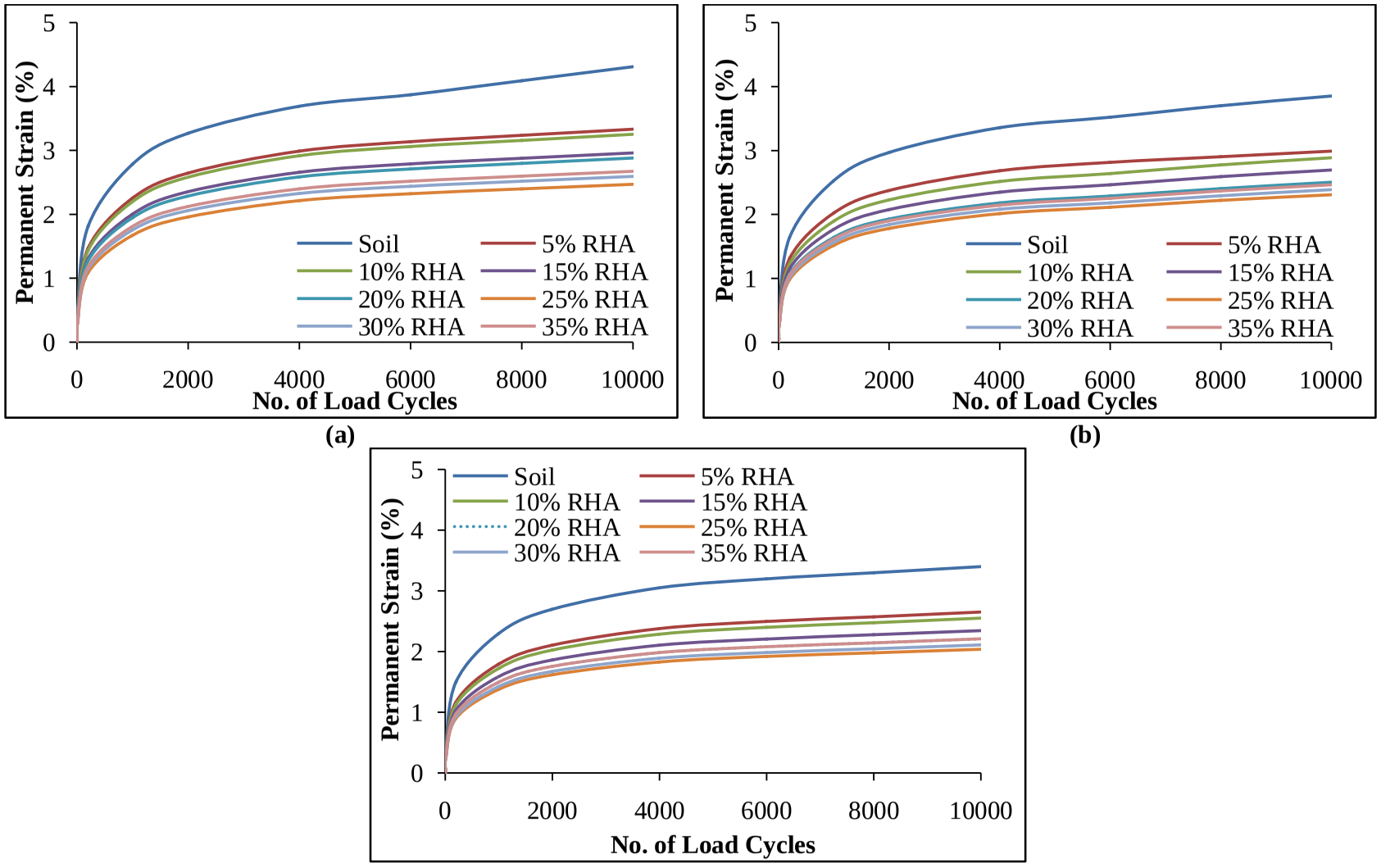

Figure 5.38 Permanent Strain of Soil-RHA Mixtures at 0.5 DSL (a) at 100 kPa CP (b) at 150 kPa CP (c) at 200 kPa CP

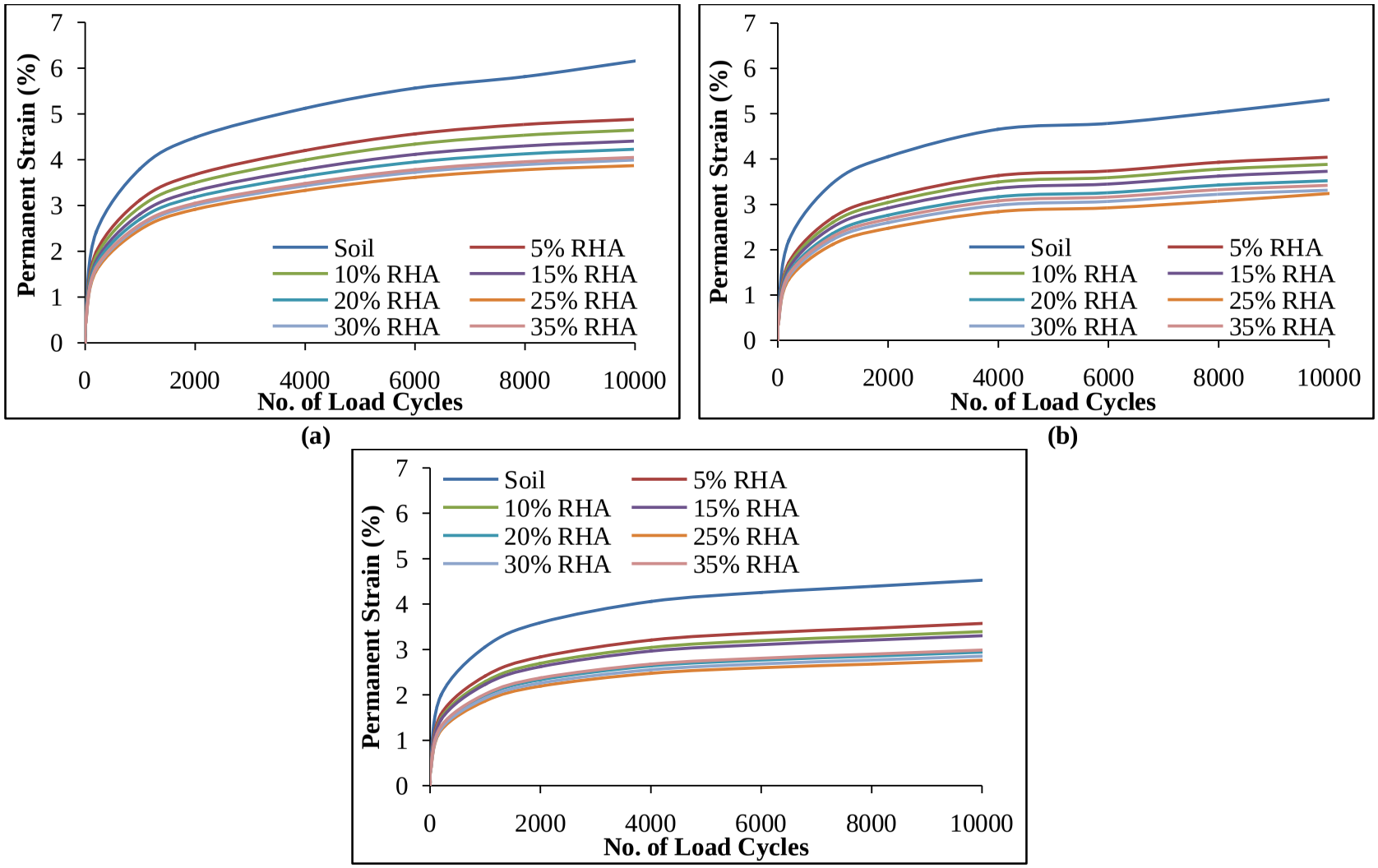

Figure 5.39 Permanent Strain of Soil-RHA Mixtures at 0.8 DSL (a) at 100 kPa CP (b) at 150 kPa CP (c) at 200 kPa CP

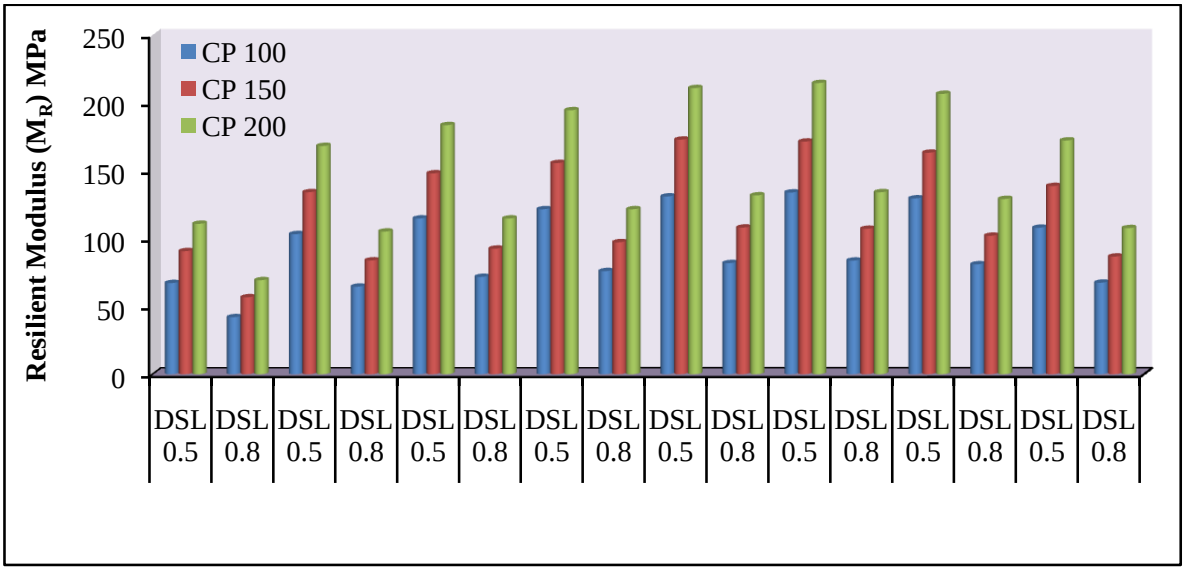

Figure 5.40 Resilient Modulus of Soil-RHA Mixtures

5.3.12 Plate Load Test

From the laboratory study, modulus of subgrade reaction (k-value) of expansive soil was found to be 17 MPa/m. The results obtained from the laboratory study are presented in Figure 5.41. Inclusion of RHA to expansive soil considerably improved k-value upto 15%. The k-value recorded at 15% inclusion level was 55.52 MPa/m. Maximum k-value recorded was 57 MPa/m at 25% RHA inclusion level. As far as k-value improvement is concerned, appreciable improvement was noted upto 15% RHA inclusion level. Beyond 15% inclusion level, the increase of k-value almost stabilized.

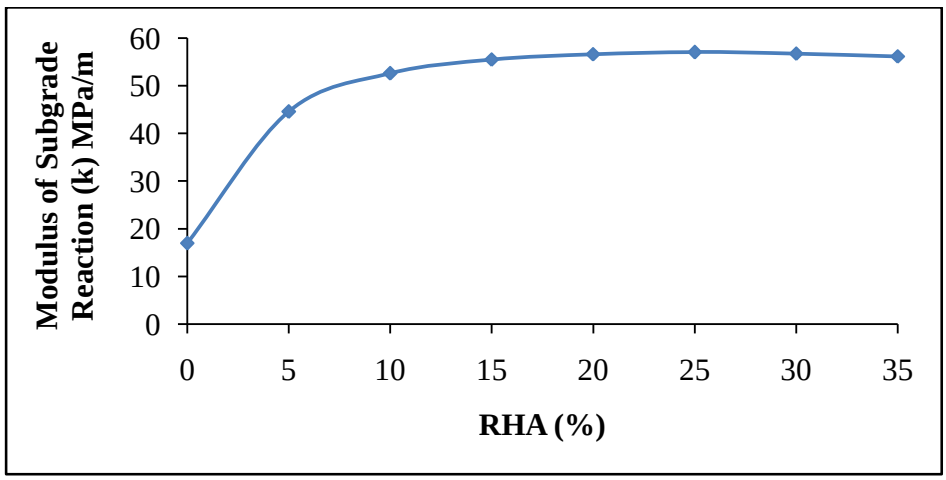

Figure 5.41 Modulus of Subgrade Reaction of Soil-RHA Mixtures

Efforts have also been made to obtain load-settlement curves using laboratory data accrued from the plate load tests. As definite yield point could not be obtained from the derived curves, the ultimate bearing capacity for untreated soil and soil-FA mixtures were worked out by extending tangents from the two straight portions of the load-settlement curve one at the initial straight portion and another tangent at the steeper straight portion at the end.

The ultimate bearing capacity of expansive soil and RHA admixed soils is presented in Figure 5.42. Marked improvement in bearing capacity was observed on admixing of RHA. Better improvement in bearing capacity was recorded for higher RHA inclusion levels. The percentage increase of bearing capacity on admixing of RHA @ 5%, 10%, 15%, 20%, 25%, 30% & 35% are 28.3%, 36.4%, 43.9%, 48.0%, 55.6%, 49.5% & 43.4% respectively at 7 days with respect to expansive soil. This improvement is more pronounced upto 25% RHA inclusion level. Beyond this level, the rate of improvement in bearing capacity decreased considerably. This clearly advocates that maximum possible inclusion level to elevate ultimate bearing capacity of expansive soil shall be 25%, if RHA is intended to use.

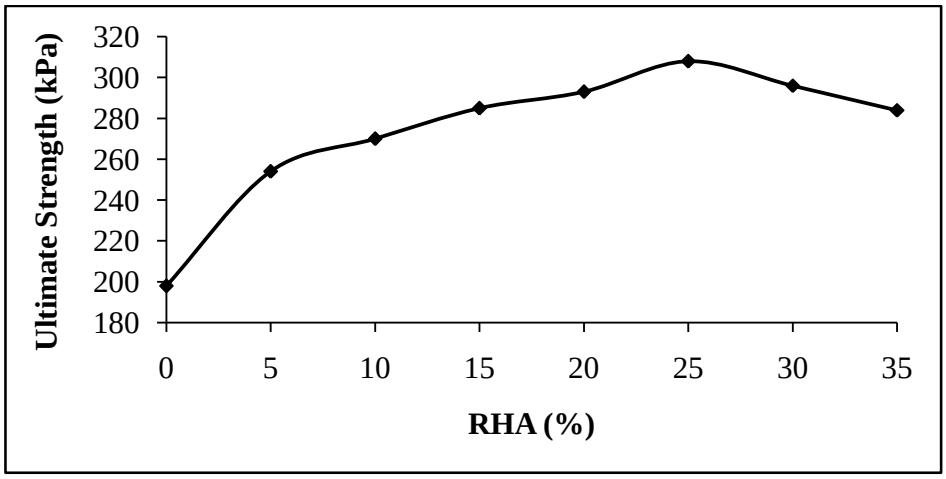

Figure 5.42 Ultimate Strength of Soil Admixed with RHA

5.3.13 Microstructural Investigation

As it can be seen from Figure 5.43 (a to d), cellular structure of RHA could be clearly seen. RHA exhibits large surface area and this is mainly caused by coarse microstructural shape like cubes of cellular beehives [Mahmud et al. (1997); Zhang & Malhotra (1996)]. The cellular

shape of RHA could increase water absorption capacity. As expected, better densification of RHA is observed for 25% & 30% RHA admixed soil samples [Figures 5.43 (b) & (c)] resulting in an increased strength. Also few unavoidable amorphous compounds are also visible in all the SEM images.

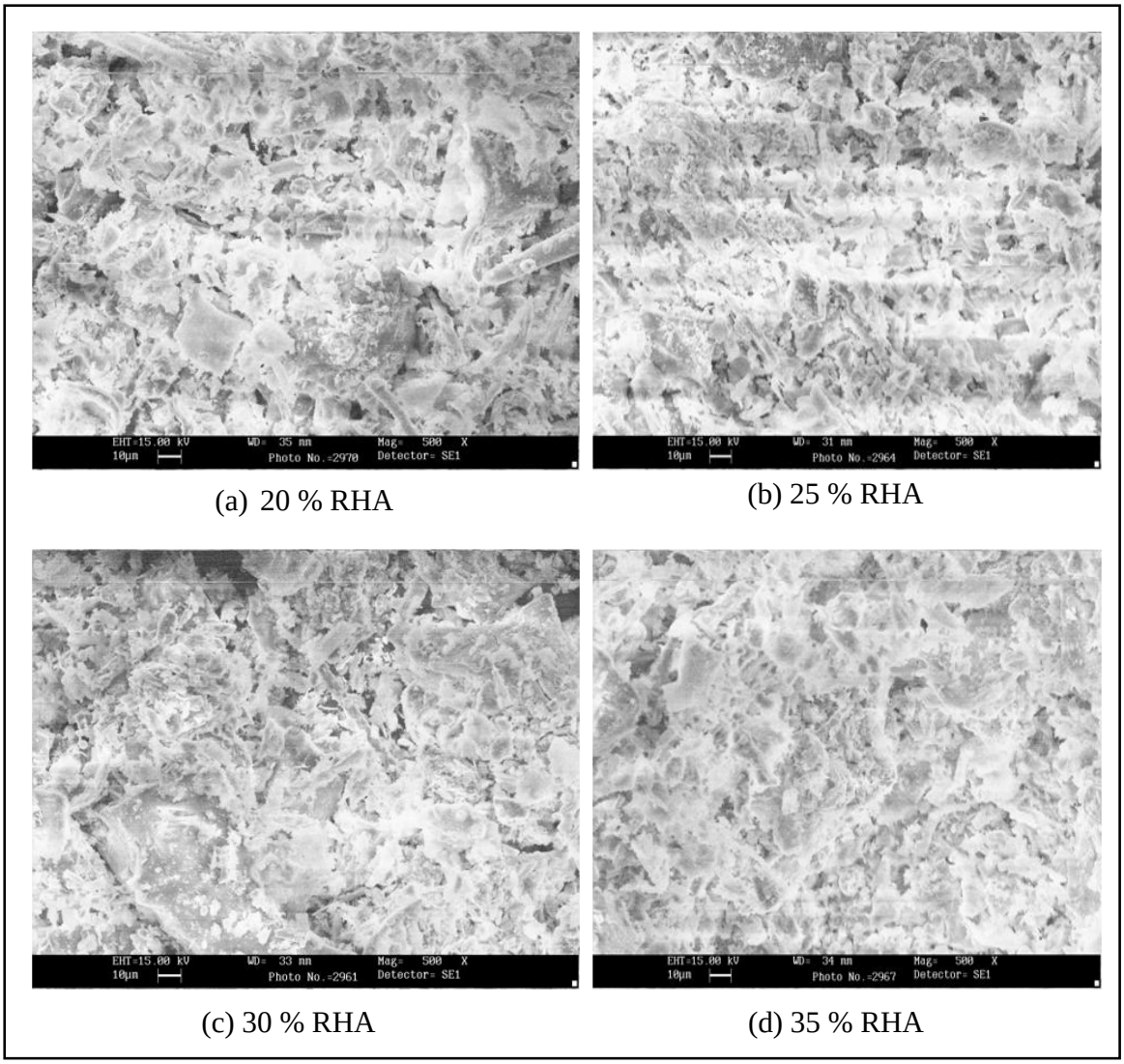

(a) 20 % RHA (b) 25 % RHA

(c) 30 % RHA (d) 35 % RHA

Figure 5.43 SEM Images of Soil-FA Mixtures captured at 500 X magnification

5.3.14 Correlation between Different Strength Parameters

5.3.14.1 Relation between CBR, % RHA & Curing Days

The correlation between CBR, % RHA and curing days (D) was established using multiple linear regression analysis (MLRA). Test results obtained at 7, 14, 28 & 56 days of curing were

considered for the analysis. The developed relation is given in Eqn. (5.3), with R^2 = 0.739. Acceptable values of R^2 show close proximity to predicted values with experimental data. The validation of the developed relation was done using laboratory CBR values obtained at 128 days of curing. CBR results obtained through predicted equation [CBR (P)] and CBR results accrued from the laboratory [CBR (L)] were compared as shown in Figure 5.44. The equation has acceptable values of R^2 suggesting closeness of predicted values with the experimental data.

$$CBR = 4.072 + 0.266\%RHA + 0.025D \quad (5.3)$$

where, CBR = California bearing ratio, % RHA = percentage rice husk ash, D = number of curing days.

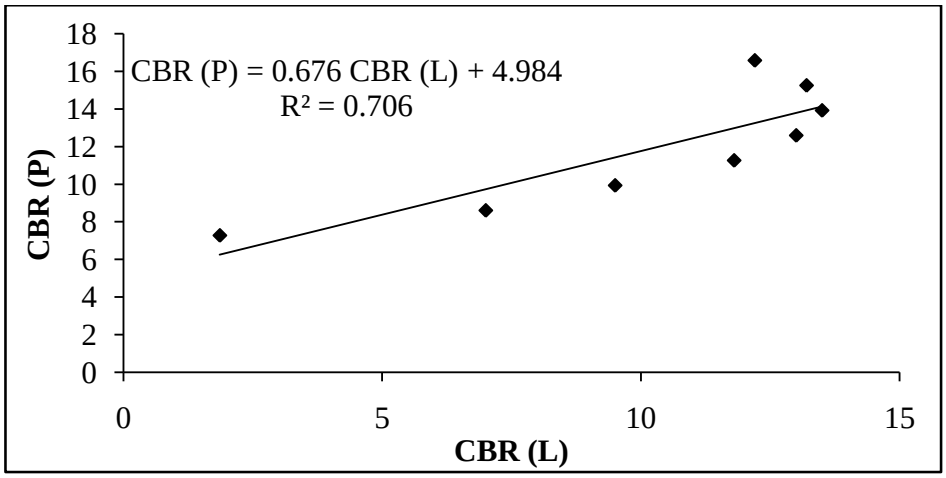

Figure 5.44 Validation of CBR Results

5.3.14.2 Relation between UCS, CBR, % RHA & Curing Days

The relationship developed between UCS as dependent variable and other parameters as independent variable is given in Eqn. (5.4), with R^2= 0.965. UCS test results of 128 days were used for validation of the predicted equation. Predicted UCS [UCS (P)] values and laboratory UCS [UCS (L)] values were compared as shown in Figure 5.45. As this equation showed high values of R^2, predicted UCS values have close proximity with experimental data.

$$UCS = 65.07 - 1.18\%RHA + 0.16D + 9.51CBR \quad (5.4)$$

where, UCS = Unconfined compressive strength (kPa)

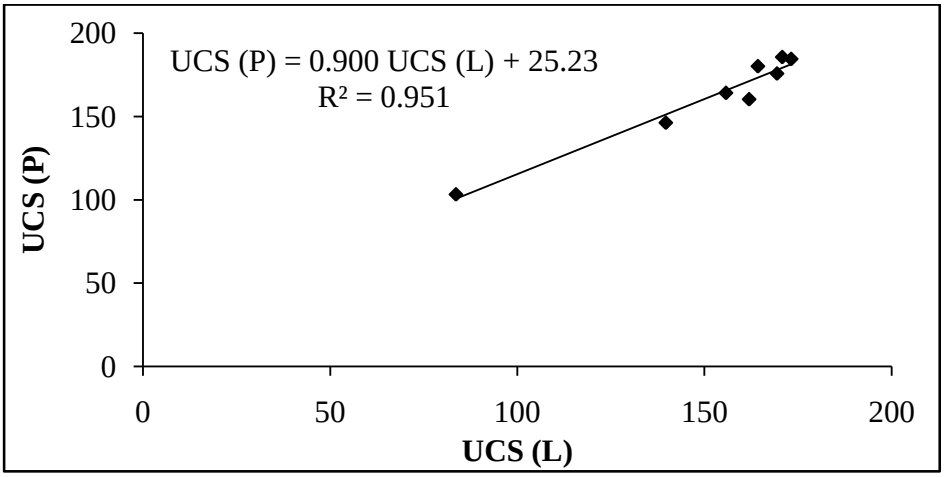

Figure 5.45 Validation Results for UCS for Soil-RHA Mixtures

5.3.14.3 Relation between STS & UCS

Relationship has been established between split tensile strength and unconfined compressive strength of FA admixed soil samples from the data of present study. Various models like linear, exponential, polynomial, power and logarithmic were tested, but polynomial relation as shown in Figure 5.46 was best fitted with R^2 = 0.937. Further, the proposed equation was validated using STS laboratory results accrued after 128 days of curing as presented in Figure 5.47. The predicted STS [STS (P)] values and laboratory STS [STS (L)] values were compared and showed excellent relationship as high R^2 values exhibit between them.

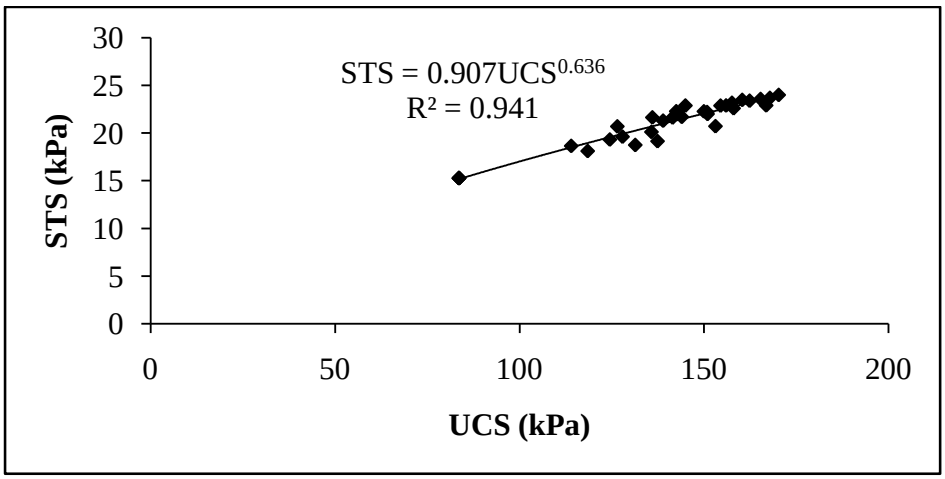

Figure 5.46 Relationship between STS & UCS for Soil-RHA Mixtures

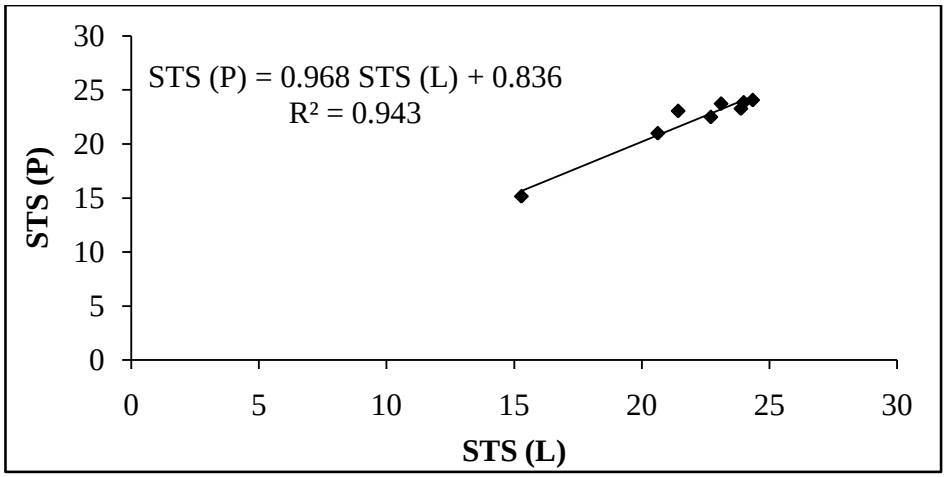

Figure 5.47 Validation of STS Results for Soil-RHA Mixtures

5.3.14.4 Relation between M_R & CBR

The cyclic triaxial tests were conducted as per ASTM D5311-11 on natural expansive soil and RHA admixed soil samples. Tests were conducted after the expiry of 28 days curing period. Three levels of σ_3 (50, 100 and 150 kPa) at 0.50 DSL and 0.80 DSL were applied during the test. The main intention behind this effort was to establish correlation between M_R & CBR using regression analysis for each three levels of σ_3 0.50 DSL and 0.80 DSL respectively. Mathematical analysis of data shows good relationship between M_R & CBR described by a power series as presented in Figure 5.48 (a to f).

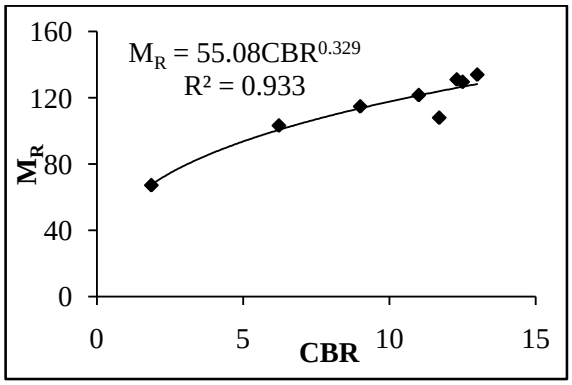

(a) CP 100, DSL 0.5

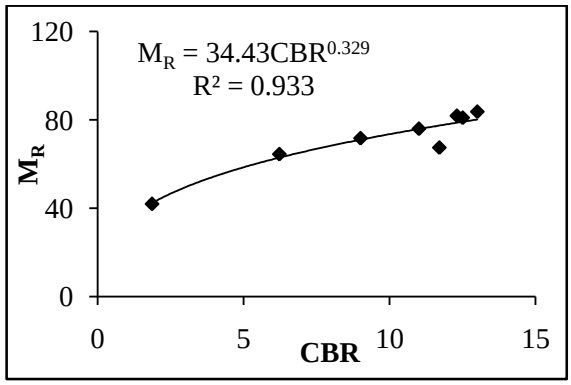

(b) CP 100, DSL 0.8

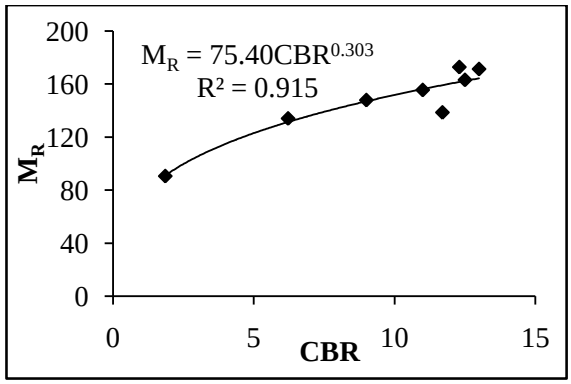

(c) CP 150, DSL 0.5

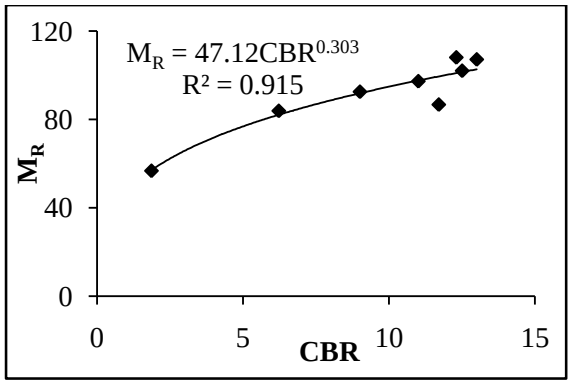

(d) CP 150, DSL 0.8

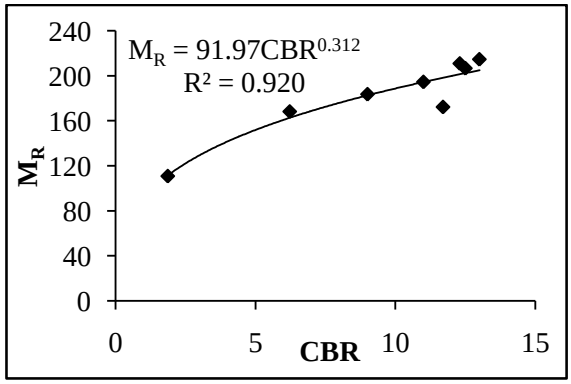

(e) CP 200, DSL 0.5

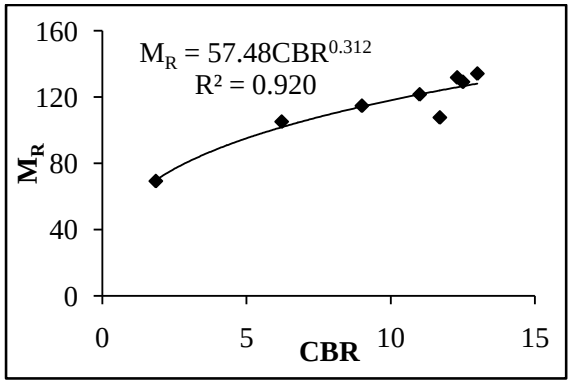

(f) CP 200, DSL 0.8

Figure 5.48 Relation between M_R & CBR for Soil-RHA Mixtures

5.4 SOIL-BAGASSE ASH

5.4.1 Atterberg Limits Test

Plasticity index (PI) of soil admixed with different percentages of BA is presented in Figure 5.49. BA stabilization decreased plasticity index of expansive soil. Plasticity index of expansive soil was found to be 25. This PI reduced to 17, 14, 12, 8, 6, 4 and 3 on admixing of BA @ 5%, 10%, 15%, 20%, 25%, 30% and 35% respectively. In that way, percentage reduction in PI due to admixing of BA @ 10%, 15%, 20%, 25%, 30% and 35% are 32%, 44%, 52%, 68%, 76%, 84% and 88% respectively. The trend of decrease of PI due to admixing of BA is showed very cohesive and gradual. The effect of BA addition on PI is very similar to

that of FA. Closeness of PI values of FA admixed soils and BA soils are attributed to the presence of approximately same chemical compositions.

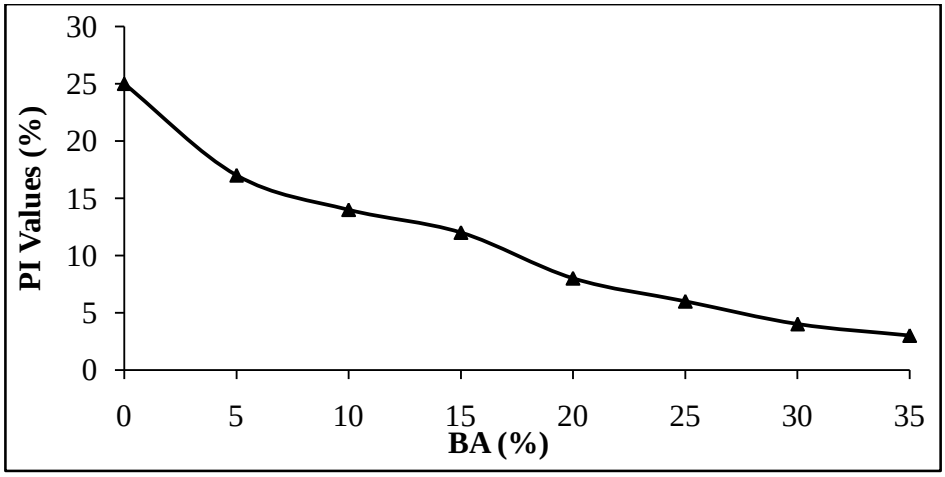

Figure 5.49 Plasticity Index of Soil-BA Mixtures

Shrinkage limit increased considerably by increasing BA content in expansive soil as presented in Figure 5.50. Inclusion of BA @ 5%, 10%, 15%, 20%, 25%, 30% and 35% resulted in an increase of the shrinkage limit to 13.7 %, 24.0%, 34.5%, 50.1%, 61.8 %, 70.2% and 79.4% respectively. The percentage increase of SL on admixing of BA is slightly less as compared to FA. Increase in shrinkage limit on admixing of BA is mainly due to the reduction of friction between soil particles.

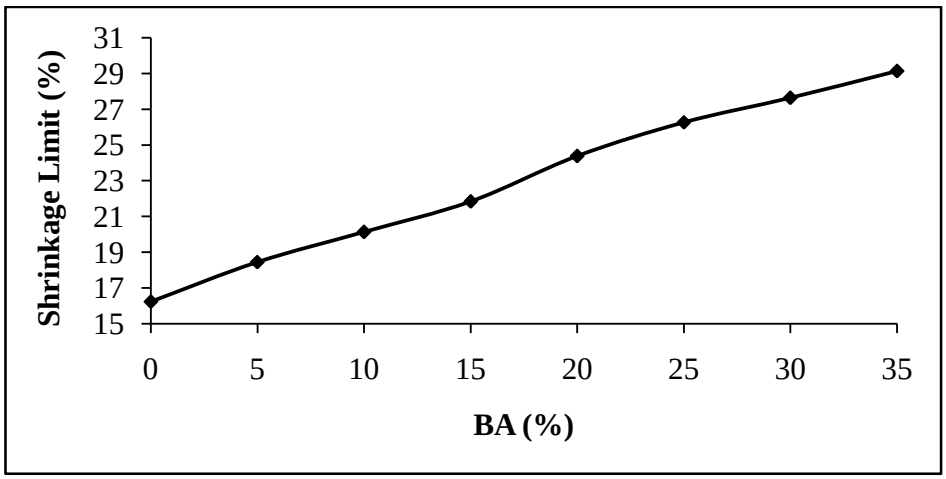

Figure 5.50 Shrinkage Limit of Soil-BA Mixtures

5.4.2 Free Swell Indexing (FSI)

It can be clearly seen from the Figure 5.51 that addition of BA upto 35%, decreases free swelling index of expansive soil considerably. The decrease in FSI is higher for higher inclusion levels. When compared to expansive soil, percent reduction of FSI are 10.13%, 25.55%, 35.55%, 48.15%, 57.76%, 64.48% & 73.01% on admixing of BA @ 5%, 10%, 15%, 20%, 25%, 30% and 35% respectively. It is pertinent to note here that BA admixing could control 1.1 times better swelling potential of expansive soil over FA.

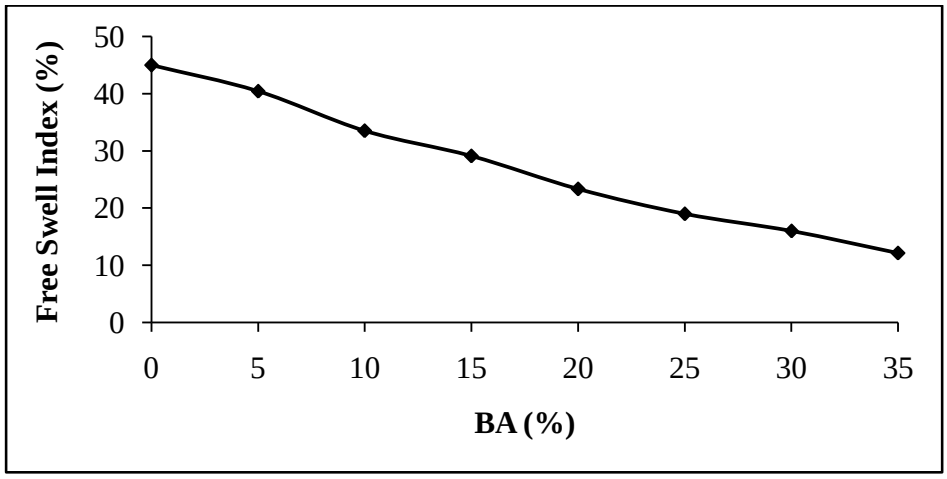

Figure 5.51 Free Swelling Index of Soil-BA Mixtures

5.4.3 Proctor Test

The effects of BA addition on the OMC of the soil mixtures are shown in Figure 5.52. As expected, the OMC increases with BA content of the mixtures irrespective of inclusion levels. About 2.4%, 11.8%, 17.6%, 23.5%, 35.3%, 44.1%, 50.0% and 164.7% increments were observed when BA was admixed to expansive soil @ 5%, 10%, 15%, 20%, 25%, 30% and 35% respectively. Inclusion levels upto 20%, the increase in OMC was slightly lesser in comparison to FA admixed soil mixtures, but beyond 25% BA inclusion level, there was substantial increment in OMC. Higher OMC on admixing FA may be due to its ultra fine characteristics which exhibits larger surface area in comparison to BA. This phenomenon was mainly due to hydration effect and the affinity for more moisture during chemical reaction process.

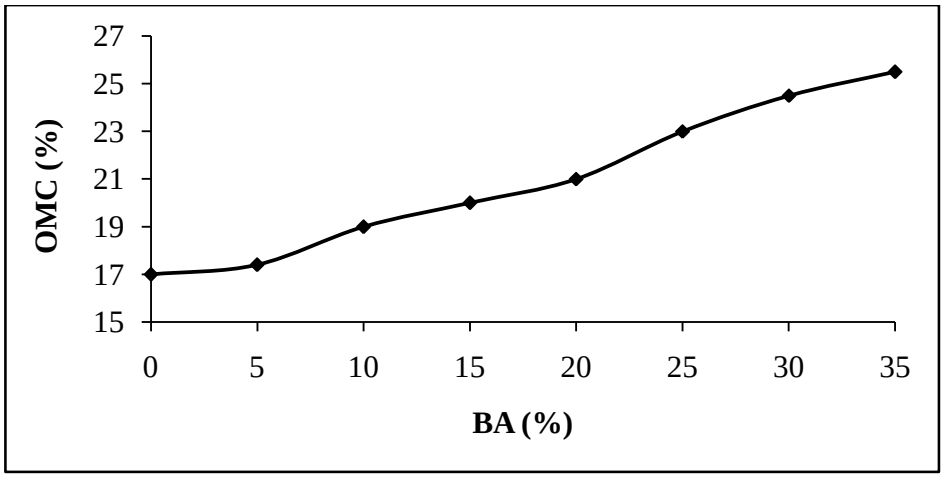

Figure 5.52 OMC of Soil-BA Mixtures

The trend of decrease of dry density for soil-BA mixtures prepared at optimum moisture content is presented in Figure 5.53. The plot clearly illustrates that inclusion of BA decreased the dry density to about 2.5% with respect to expansive soil irrespective of inclusion levels. Decrease in dry density may be due to the flocculation/aggregation and the formation of cementitious products.

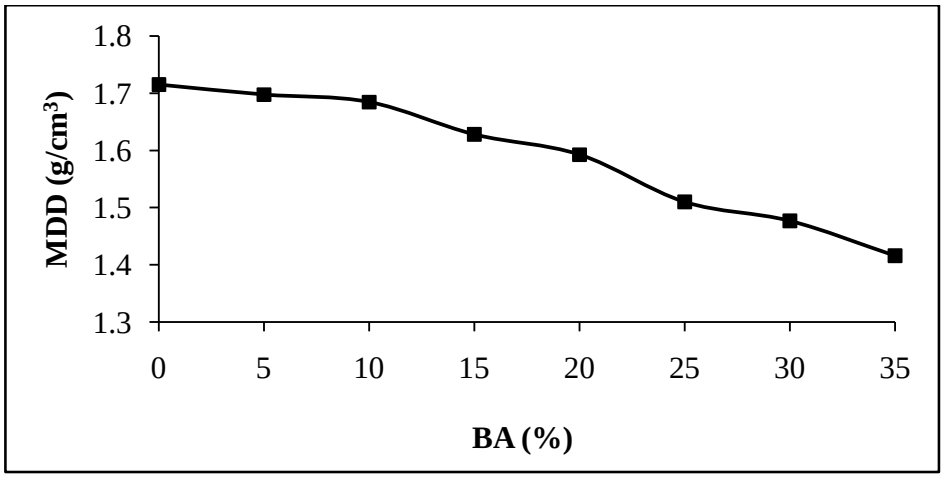

Figure 5.53 MDD of Soil-BA Mixtures

5.4.4 California Bearing Ratio Test

The effect of addition of BA on CBR value for a period of 3, 7, 14, 28, 56 and 128 days curing are shown in Figure 5.54. As it was expected, addition of BA increases CBR value remarkably.

The CBR is increased non-linearly with the increase in BA content in soil. The percentage increase of CBR value after admixing BA @ 5%, 10%, 1 %, 20%, 25%, 30% and 35% are 100.0%, 175.8%, 215.6%, 239.8%, 244.1%, 203.8% & 175.8% respectively with respect to expansive soils. The improvement of CBR is significant upto 15% BA inclusion level beyond which, no appreciable increase was observed. The improvement in CBR value stabilized to a large extent beyond 25% inclusion level irrespective of curing days.

It is also learnt from the laboratory test results that there is an increase in CBR value as the relative humidity curing time increases. The increases are about 8.4%, 15.6%, 21.9%, 26.6% & 29.7%, respectively for 7, 14, 28, 56 & 128 days with respect to 3 days curing for 25% BA inclusion level. Maximum CBR value was offered by the soil samples kept in humidity condition continuously for 7 days prior to soaking. This has inference that to draw maximum strength benefit of BA admixed soils, interns of CBR value of expansive soil, the test specimen preferably be subjected to relative humidity curing for at least 7 days prior soaking. CBR value improvement on admixing BA may be due to very fine particles of BA and self –hardening effect related to the presence of free lime.

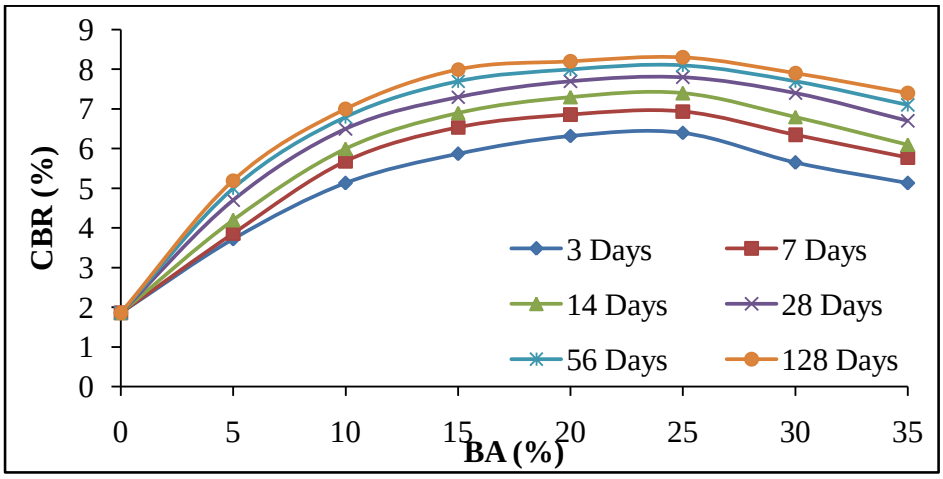

Figure 5.54 CBR of Soil-BA Mixtures

5.4.5 Expansion Ratio

The effects of BA on expansion ratio of the mixtures are shown in Figure 5.55. The pattern of plot conotates decrease of expansion ratio on admixing of BA. Reduction in expansion ratio is

higher for higher BA inclusion level. The trend of decrease in expansion ratio is very similar to that of FA admixed soils. The percentage reduction in expansion ratio after admixing BA @ 5%, 10%, 15%, 20%, 25%, 30%, and 35% are 17.5%, 27.5%, 32.5%, 37.5%, 45.0%, 53.8% and 58.8% respectively. Analysis results inference that BA could be a suitable alternative additive to control swelling potential of expansive soil.

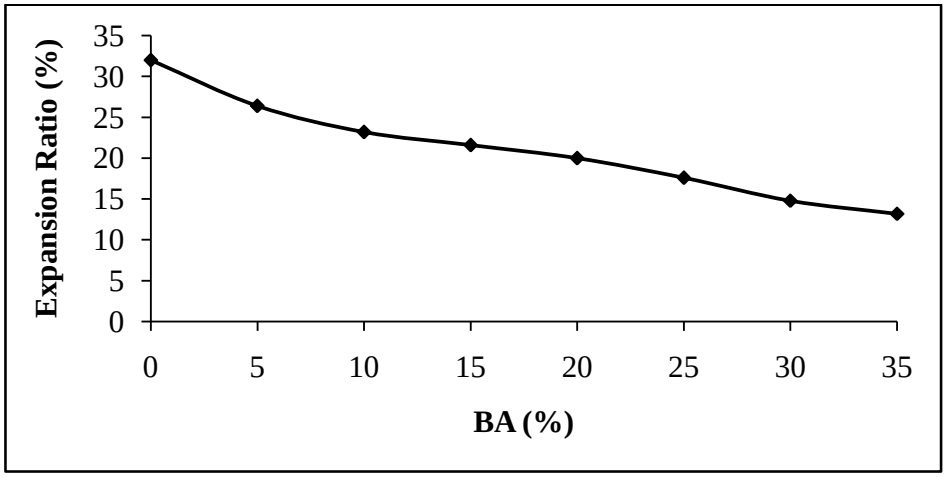

Figure 5.55 Expansion Ratio of Soil-B Mixtures

5.4.6 Hydraulic Conductivity Test

Considerable decrease in coefficient of permeability was observed from Figure 5.56. Permeability of expansive soil was found to be 3.3×10^{-7} cm/sec. Rate of reduction in permeability of expansive soil on admixing BA is very cohesive and gradual. Higher reduction in permeability is observed for higher BA inclusion levels. The percentage of permeability decreases after admixing BA @ 5%, 10%, 15%, 20%, 25%, 30% & 35% are 17.79%, 31.99%, 42.24%, 54.95%, 62.64%, 68.89% & 70.96%respectively. This effect is attributed to densely packed granular structures due to the partial dissociation of the calcium hydroxide in samples and better densification of the matrix as revealed from SEM images. Also, the calcium ions combined with the reactive silica or alumina, or both, which obstructed flow through the soil voids (Osinubi, 1998). Another possible reason of having small value of permeability on admixing of BA is due to the formation of cementitious compounds by calcium oxide and silica and/or alumina from both the soil and BA, which fills the soil voids thereby obstructing the flow of water.

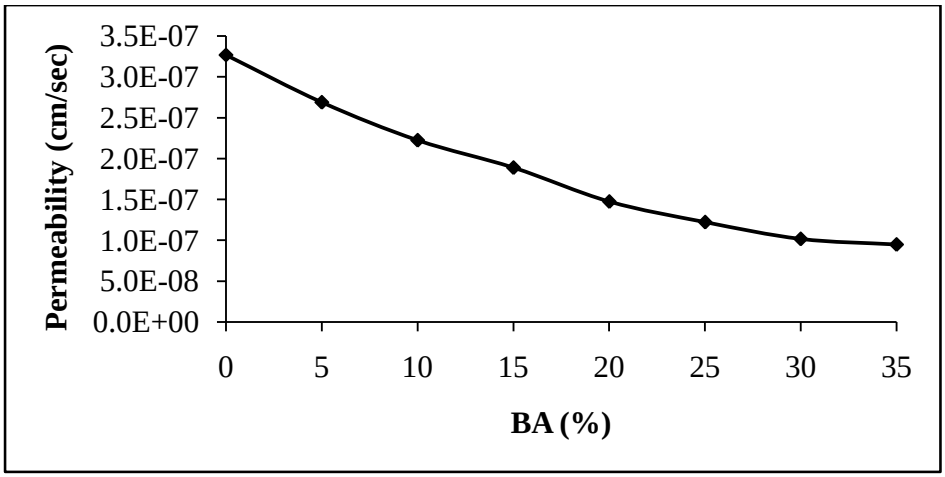

Figure 5.56 Permeability of Soil-BA Mixtures

5.4.7 Unconfined Compressive Strength

Inclusion of BA to expansive soil substantially increased UCS irrespective of days of curing. The rate of increase of UCS at 5% BA inclusion level showed sharp increase. The rate of increase of UCS continued upto 25% BA inclusion level. Beyond 25% BA inclusion level, UCS starts decreasing considerably. Considering the overall UCS development, the percentage increase of UCS on admixing BA @ 5%, 10%, 15%, 20 %, 25%, 30 % & 35% are 29.09%, 44.06%, 55.51%, 63.22%, 66.14%, 62.10% & 36.31% respectively at 7 days curing with respect to expansive soil. Whereas for 14 days, 28 days, 56 days and 128 days cured samples, these values further increased to 39.90%, 57.11%, 70.39%, 77.57%, 79.39%, 73.38% & 49.89%; 45.78%, 65.01%, 77.57%, 87.04%, 88.82%, 81.78% & 57.11%; 52.82%, 74.40%, 84.61%, 94.08%, 97.03%, 91.16% & 73.53% ; and 58.85%, 79.09%, 90.85%, 98.77%, 101.72%, 95.03% & 79.40% respectively. This analysis gives evidence that appreciable compressive strength could be achieved with prolongs curing.

5.4.8 Split Tensile Strength Test

Marked improvement in split tensile strength was observed on admixing of BA as depicted in Figure 5.58. Maximum tensile strength was observed at 25% BA inclusion level. Beyond this level, tensile strength decreases considerably. Therefore, 25% inclusion level is considered to be the optimal dosage at which maximum tensile strength can be achieved. At optimum inclusion level, about 41.9%, 47.8 %, 52.3 %, 54.9 % & 56.2 % improvements on split-tensile

strength were observed at 7, 14, 28, 56 and 128 days of curing respectively with respect to expansive soil.

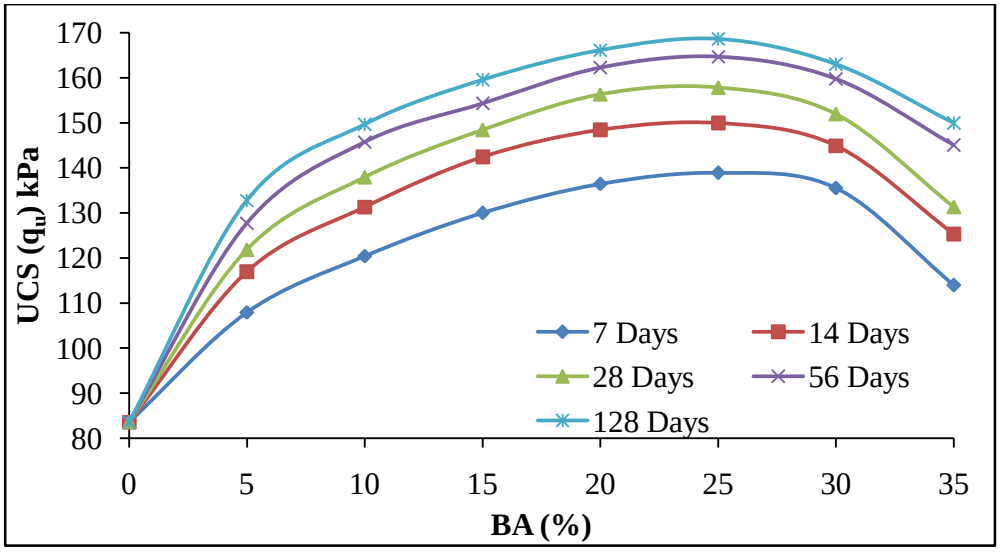

Figure 5.57 UCS of Soil-BA Mixtures

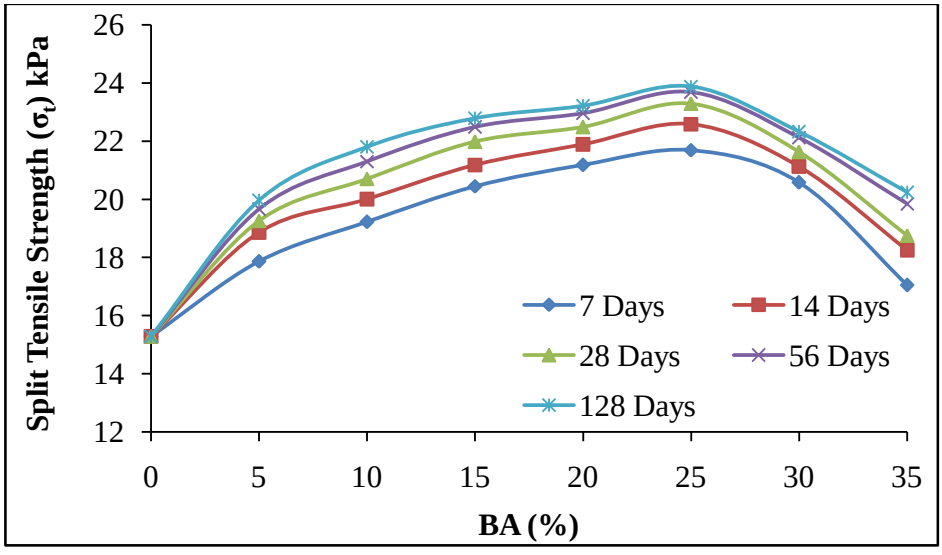

Figure 5.58 Split Tensile Strength of Soil-BA Mixtures

5.4.9 Ratio of Split Tensile to Unconfined Compressive Strength Test

The relative relationship and mobilization between the tensile strength and compressive strength could be discussed by plotting the tensile/compressive strength ratio (σ_t/q_u) versus

curing time. Figure 5.59 shows the influence of BA content on the ratio of split tensile strength and unconfined compressive strength. The results show that unconfined compressive strength and split tensile strengths are closely related. It can be observed that the ratio of split tensile strength and unconfined compressive strength decreased with increase in BA content, indicating that BA is more efficient when soil was subjected to compression rather than to tension.

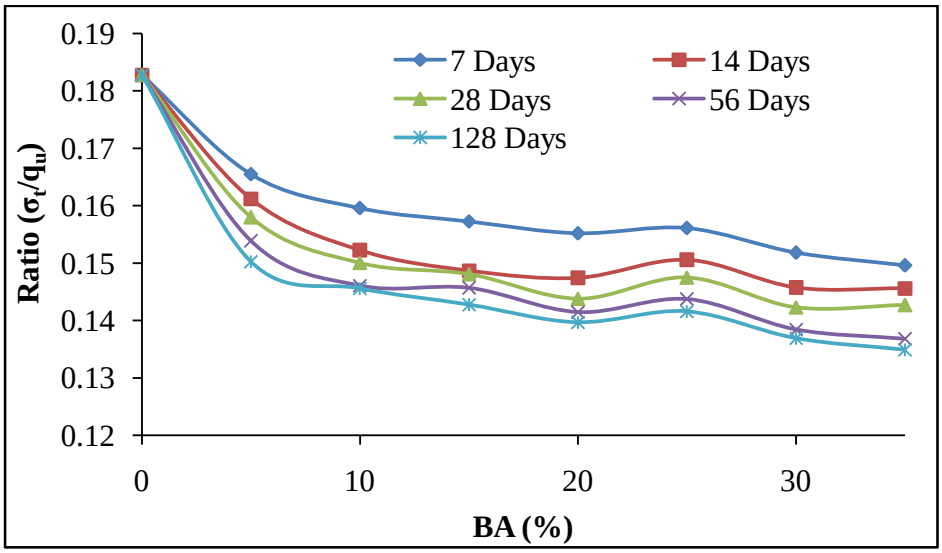

Figure 5.59 σ_t/q_u Ratio of Soil-BA Mixtures

5.4.10 Triaxial Test

Three different confining stresses such as 100, 150 and 200 kPa were applied on specimens to obtain peak deviator stress as shown in Table 5.3. The range of confining stresses was chosen to obtain more well defined and accurate plots of Mohr envelopes to obtain shear strength parameters cohesion (c) and angle of internal friction (φ) of the soils mixed with BA. The variation of c and φ with admixing BA are evaluated and results are shown in Figures 5.60 & 5.61 respectively.

Table 5.3 shows deviator stress of soil admixing of BA after 7, 14, 28, 56 & 128 days curing period at three different confining pressures. Higher deviator stresses are observed for higher BA content irrespective of confining pressure applied and days of curing. However, beyond 25% BA content, the deviator stress starts declining gradually. Admixing of BA causes

increase in cohesion and internal friction angle. Increase in cohesion is more pronounced upto 10% BA content. The cohesion of soil ranges from 28 to 45.15 kPa and from 28.5 to 52.9 kPa at 7 days and 128 days curing respectively, for BA contents between 0 & 25 %. Improvement on cohesion due to addition of BA becomes sluggish beyond 10%. However, these cohesions are much higher than that of expansive soil. Marked reduction in cohesion is observed beyond 25% BA content. As in the case of cohesion, similar trend of improvement is observed for internal friction angle too. The rate of improvement of internal friction angle is rapid for 5% BA inclusion level and beyond this level the rate of improvement is very gradual. In overall, these internal friction angles are higher than that of expansive soil irrespective days of curing (Figure 5.61). This effect may be attributed to the increase in cohesion of the soil upon the pozzolanic action of very fine BA.

Table 5.3 Deviator Stress for BA Admixed Soil at Different Confining Pressure

% BA	Confining Pressure (kPa)	Deviator Stress (kPa)				
		7 Days	14 Days	28 Days	56 Days	128 Days
0	100	205.34	206.19	204.83	205.01	204.47
	150	275.91	277.81	276.52	278.17	276.24
	200	337.11	339.77	337.97	338.87	339.18
5	100	269.82	290.07	299.82	311.74	325.38
	150	356.16	379.99	389.77	402.15	416.49
	200	445.20	475.72	488.71	505.02	523.87
10	100	297.48	321.82	335.24	351.39	362.34
	150	389.70	418.36	432.46	449.77	460.17
	200	481.92	518.13	536.38	558.70	572.49
15	100	317.23	344.75	356.29	373.50	384.53
	150	412.40	444.72	456.05	474.35	492.20
	200	513.92	555.04	570.07	593.87	610.45
20	100	335.69	362.23	384.68	400.78	412.13
	150	439.75	478.14	507.78	521.01	535.77
	200	543.81	586.81	619.33	641.24	655.28
25	100	344.48	370.45	389.92	405.23	423.31
	150	440.93	477.88	499.10	522.75	533.37
	200	554.61	596.43	624.85	645.53	668.83
30	100	337.45	363.12	379.93	402.74	412.53

	150	431.94	461.16	478.71	503.43	513.60
	200	543.30	582.81	605.99	636.33	648.91
	100	281.49	308.27	314.59	338.04	351.72
35	150	363.13	394.59	404.25	426.44	455.48
	200	453.21	493.24	502.09	535.80	557.47

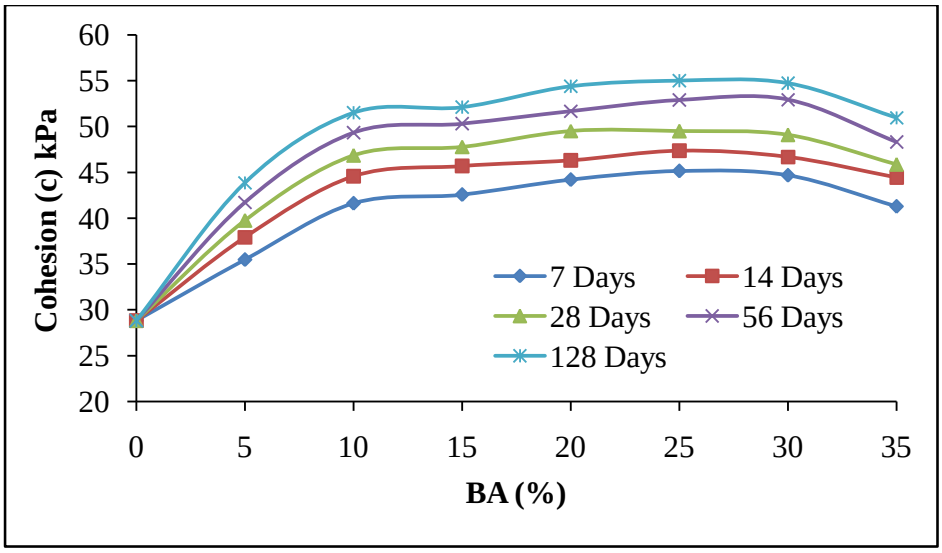

Figure 5.60 Cohesion of Soil-BA Mixtures

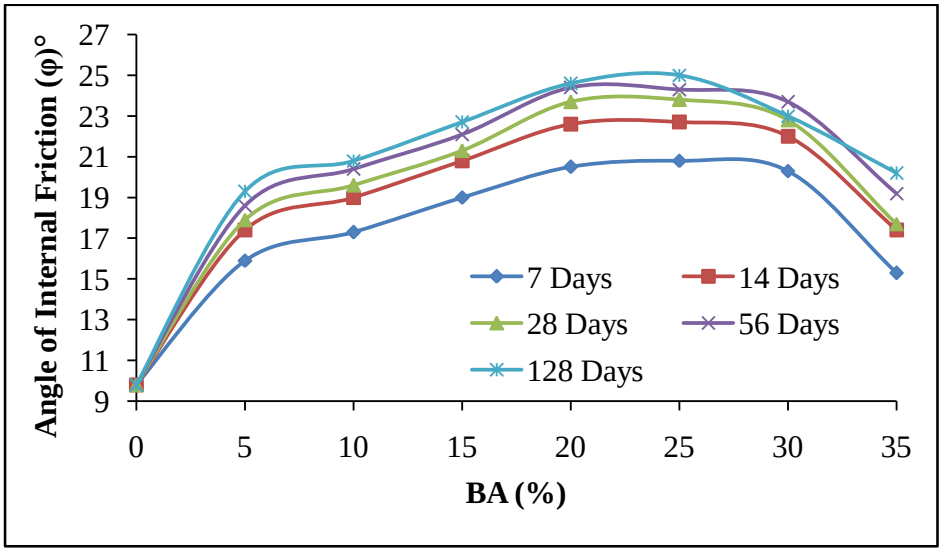

Figure 5.61 Angle of Internal Friction of Soil-BA Mixtures

5.4.11 Cyclic Triaxial Test

The effects of various percent of BA and loading cycles on the permanent deformations were studied. The effects of DSL ratios and confining pressure with number of loading cycles on the permanent deformations were studied for all BA admixed soils. Three confining pressures such as 100, 150 & 200 kPa and two DSL such as 0.5 DSL and 0.8 DSL were chosen for determining permanent strain upto 10000 cycles under constant axial loading. Graphical plot was established between vertical percent permanent strain as ordinate and number of cycles as abscissa. Two different graphical plots have been drawn for each of this deviator stresses (i.e. 0.5 DSL and 0.8 DSL) at three pre-determined confining pressures (100 kPa, 150 kPa & 150 kPa). They are shown in Figures 5.62 and 5.63.

5.4.11.1 Effect of load cycle

Figures 5.62 & 5.63 show that rapid increase in deformation of the expansive soil and BA admixed soils were observed during the initial approximate hundred cycles of loading and the strain rate was high during this stage in all cases. After few hundred cycles of loading, the increase in deformations was progressively upto 2000 cycles thereafter deformation almost stabilized for admixed soils. But deformation was still taking place for expansive soil. For BA admixed soils, the matrix behaves almost elastically under the applied load. The maximum permanent strain of 6.15% was observed for expansive soils when 0.8 DSL and 100 kPa confining pressure were applied. Consequently, the minimum permanent strain of 2.1% was observed for 25% BA inclusion level by having 0.5 DSL for 200 kPa for 10000 cycles.

5.4.11.2 Effect of confining pressure

Figures 5.14 (a, b & c) and 5.15 (a, b, & c) depict permanent deformation at three confining pressure 100, 150 and 200 kPa respectively. From the present study, the minimum permanent deformation observed after 10000 cycles at 100 kPa, 150 kPa and 200 kPa confining pressure are 2.4% at 30% BA and 2.2% & 2.1% at 25% BA at 0.5 DSL Whereas, the permanent deformation for 0.8 DSL under the same working condition are 3.9%, 3.3% & 2.8% respectively. This analysis suggested that permanent deformation decreases with increase in confining pressure irrespective of types of samples. However, least permanent deformation was recorded for 25% BA inclusion level.

5.4.11.3 Effect of deviator stress level

The permanent strain values measured at 0.5 DSL for expansive soil and BA admixed soils are illustrated in Figure 5.62. To appreciate better the effect of σ_d the permanent strain recorded at 0.8 DSL is also presented in Figure 5.63. These different plots have been drawn considering all the three different confining pressures. Decrease of σ_d value signifies improvement in permanent strain. Based on the investigation, the least value of σ_d was observed for 30% BA admixed soils (2.1%) for 0.5 DSL at 200 confining pressure. Whereas for 0.8 DSL, 2.80% was observed. This again confirmed that least permanent deformation is offered by 25% BA inclusion level.

In the analysis of resilient modulus (M_R) results, a set of six tests was conducted on both untreated and treated soils. All M_R tests conducted at two DSL of 0.5 & 0.8 maintaining three different confining pressures of 100, 150 & 200 kPa are presented in Figure 5.16. The main motive behind analyzing M_R test results in the present study was to draw information with respect to effects of confining pressure and DSL on soil-FA mixtures.

Figure 5.64 reveals that an increase in confining pressure resulted enhancements of M_R of all cases but these value diminish at higher DSL value. M_R values increase with increase in BA content at every DSL and along with confining pressure. The maximum M_R value was observed 110 MPa & 69 MPa at 0.5 & 0.8 DSL respectively at 200 kPa confining pressure of soil and it achieves maximum value 205 & 128 MPa after admixing of 25% BA. This M_R increase can be attributed to a stiffer soil skeleton structure of treated soils caused by increased confinement and pozzolanic reactions, which result in a closer bonding of soil particles.

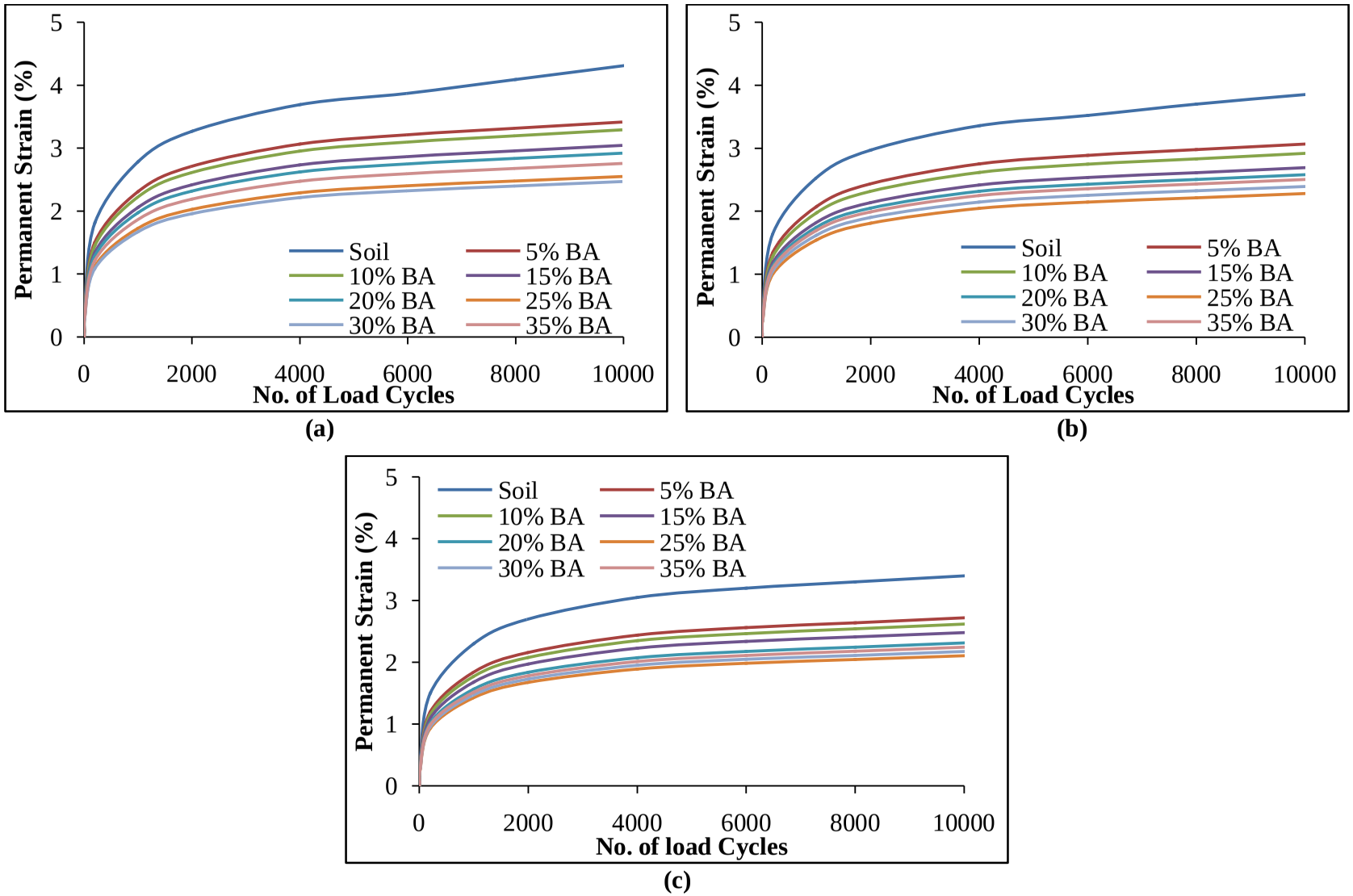

Figure 5.62 Permanent Strain of Soil Admixed with BA at 0.5 DSL (a) at 100 kPa CP (b) at 150 kPa CP (c) at 200 kPa CP

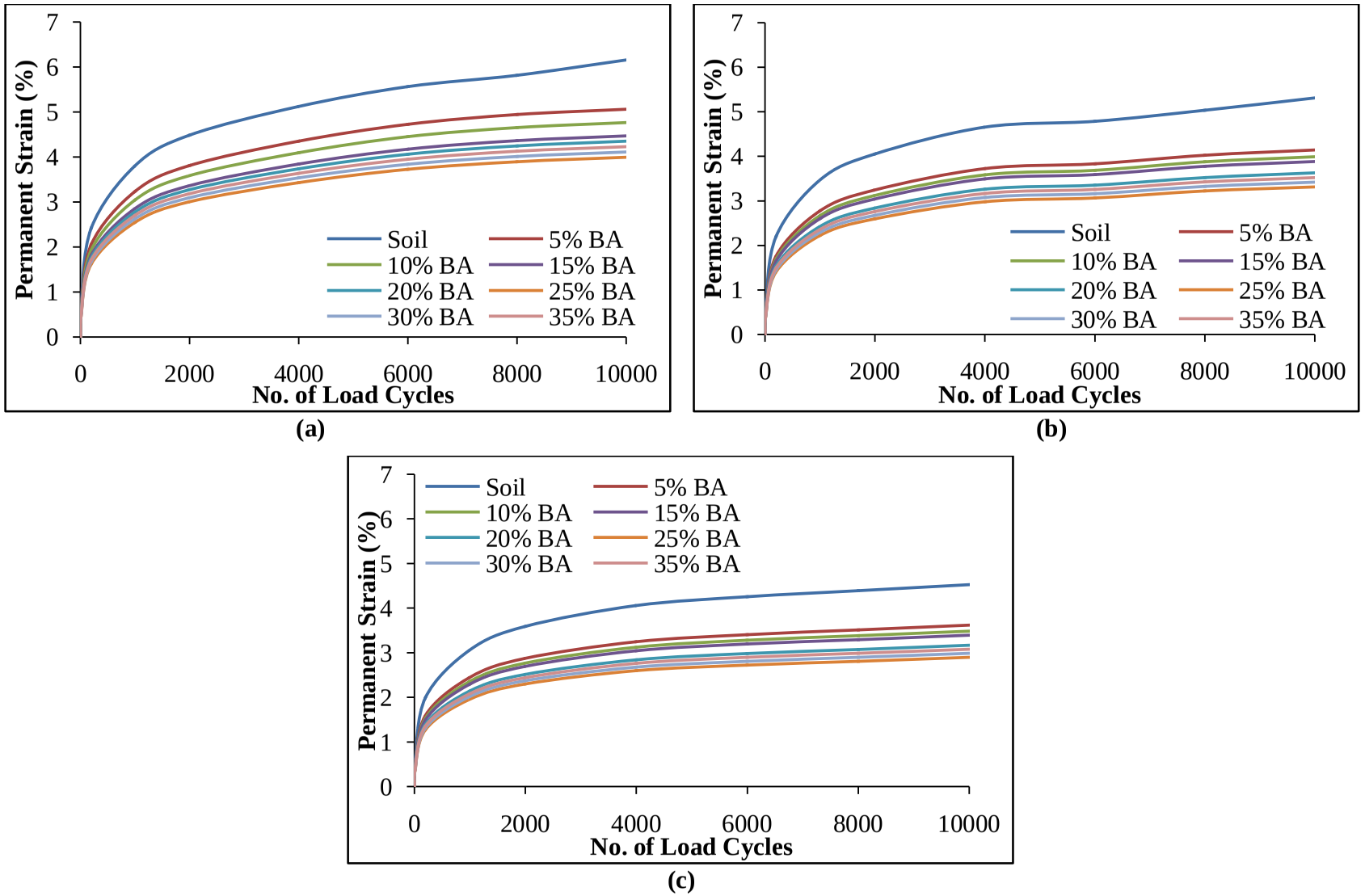

Figure 5.63 Permanent Strain of Soil Admixed with BA at 0.8 DSL (a) at 100 kPa CP (b) at 150 kPa CP (c) at 200 kPa CP

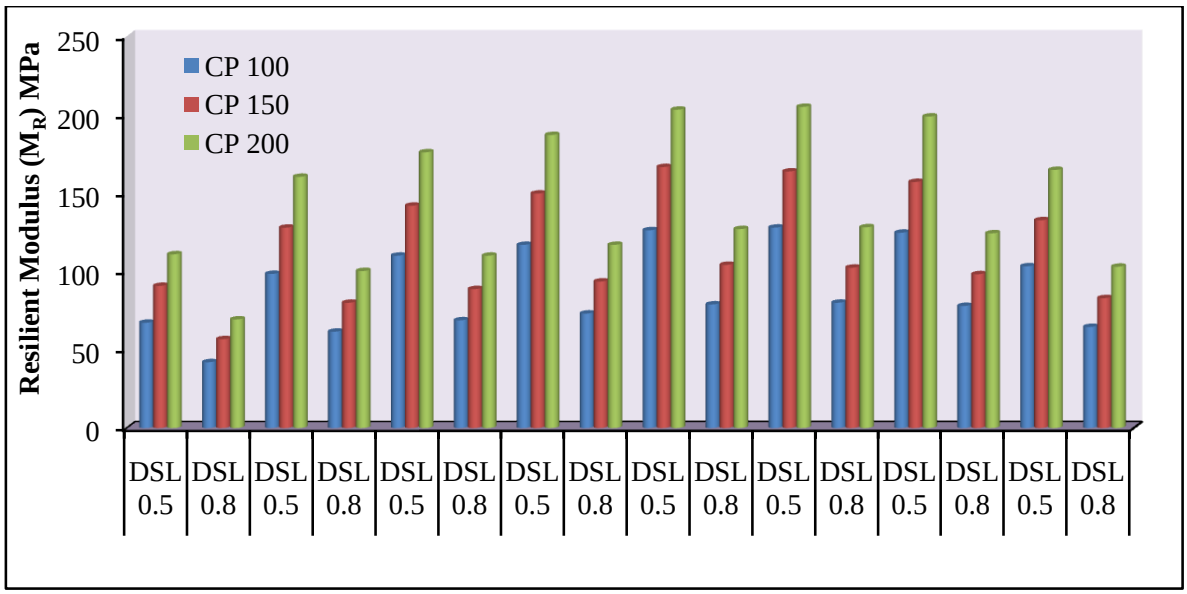

Figure 5.64 Resilient Modulus of Soil-BA Mixtures

5.4.12 Plate Load Test

The result of modulus of subgrade reaction (k) is shown in Figure 5.65. Admixing of BA to expansive soil considerably improved modulus of subgrade reaction and this increased value was 48 MPa/m for 15 % of BA content. It is also observed that the modulus of subgrade reaction is increased by increasing BA content upto 15%, beyond this level; it starts stabilizing upto 25% and thence decreases.

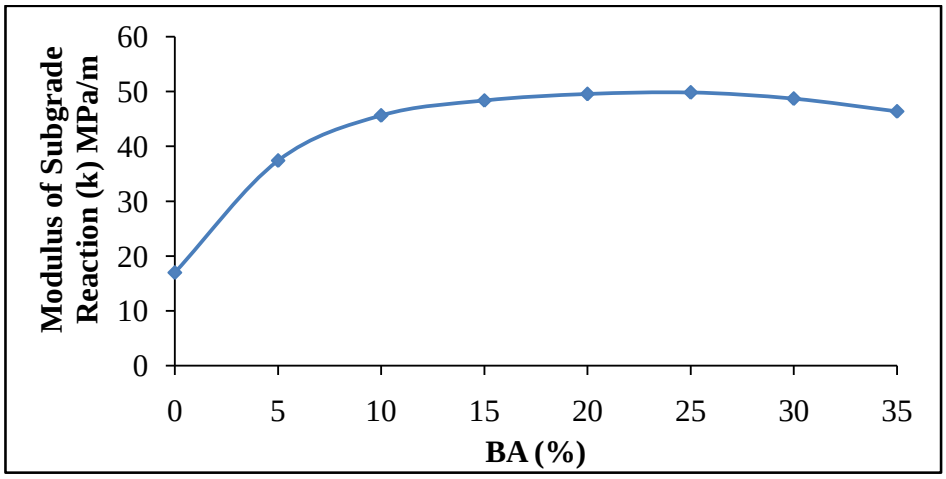

Figure 5.65 Modulus of Subgrade Reaction of Soil-BA Mixtures

Efforts have also been made to obtain load-settlement curves using laboratory data accrued from the plate load tests. As definite yield point could not be obtained from the derived curves, the ultimate bearing capacity for untreated soil and soil-BA mixtures were worked out by extending tangents from the two straight portions of the load-settlement curve one at the initial straight portion and another tangent at the steeper straight portion at the end.

Figure 5.66 shows the ultimate bearing capacity of soils with or without BA. 198 kPa ultimate bearing capacity was noted for natural expansive soil. This capacity improves significantly on admixing of BA and better improvement in bearing capacity was noted for higher BA inclusion level. The percentage improvement of bearing capacity are 23.7%, 32.3%, 40.4%, 45.5%, 51.5%, 46.5% & 31.3% on admixing of BA @ 5%, 10%, 15%, 20%, 25%, 30% & 35% respectively.

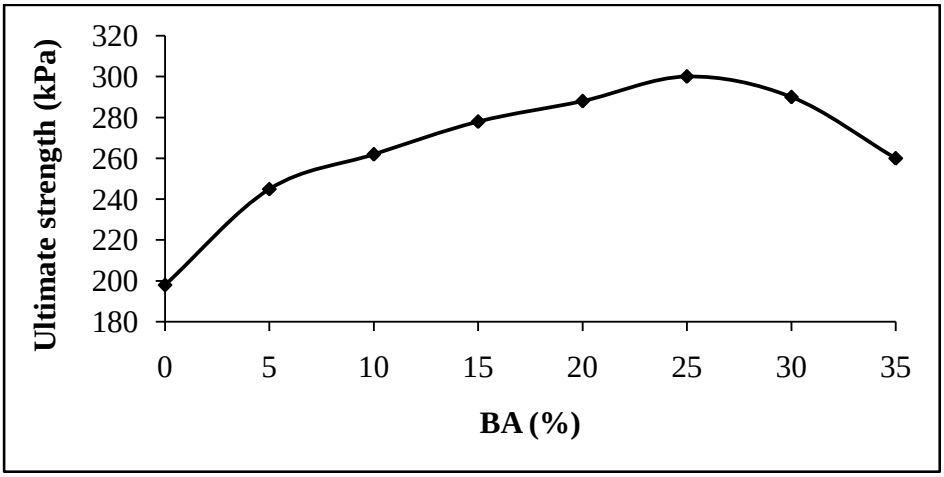

Figure 5.66 Ultimate Strength of Soil Admixed with BA

5.4.13 Microstructural Investigation

The microstructure of BA was investigated by using Scanning Electron Microscope (SEM). The images from Scanning Electron Microscope shown in Figures 5.67 (a to d) demonstrated that bagasse fibers are uniformly distributed over the soil matrix. Presences of abundant granular structures of BA are also distinctly visible from the ground mass. Most of these granular BA are densely packed structures and better densification of the same is in the order of 25% BA, 30%BA, 35% BA and 20% BA respectively. The chemical compositions shown in

Table 4.9 in Chapter 4, reveal that BA can be assigned as class N pozzolan as prescribed by ASTMC 618. BA particles with various sizes and geometry like prismatic, spherical and fibrous were recognized. The result of SEM suggests that prismatic particles consist mainly of silica. The spherical ones might contain Si, Fe, Mg, Al and some other alkalies.

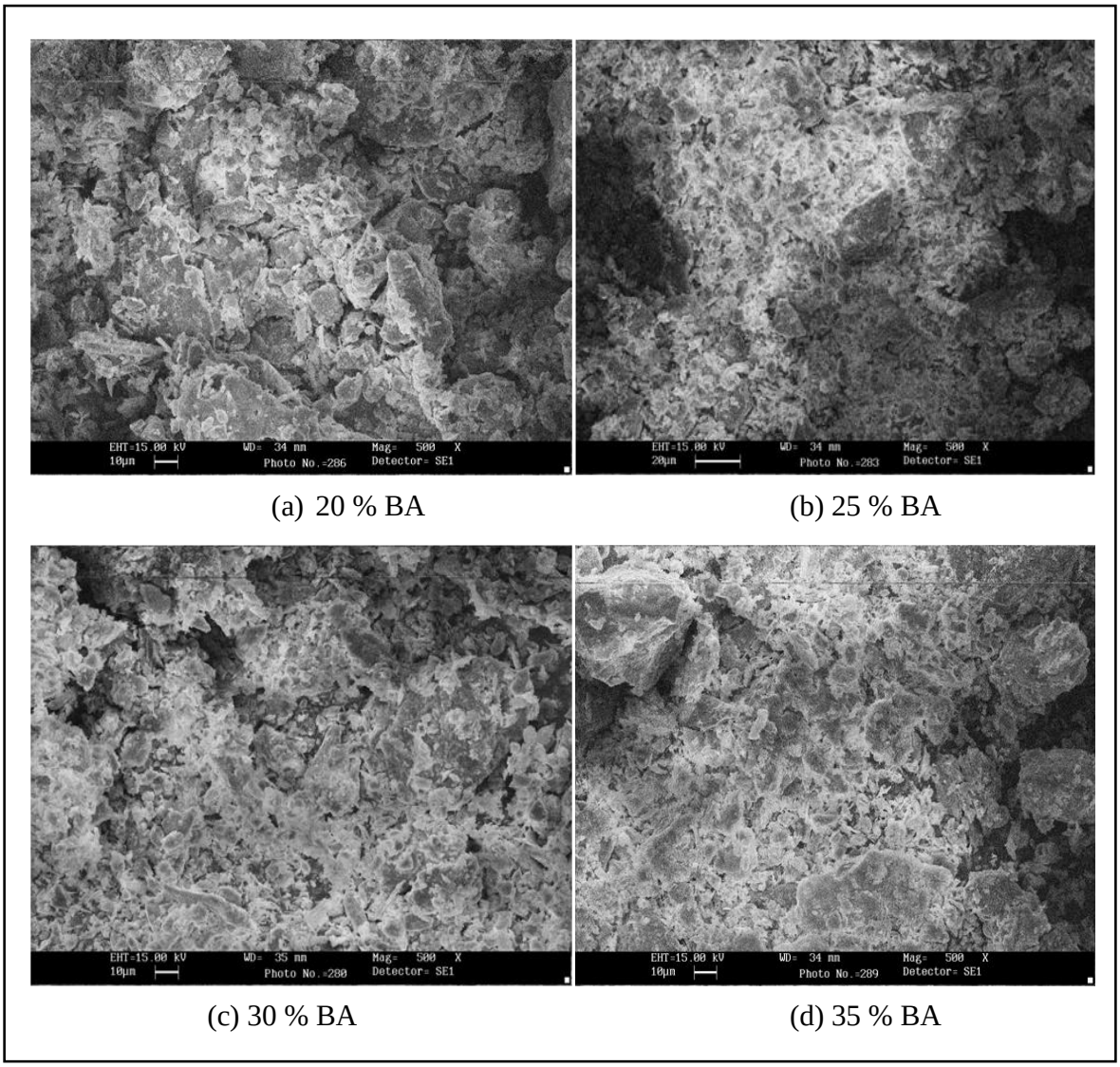

(a) 20 % BA (b) 25 % BA

(c) 30 % BA (d) 35 % BA

Figure 5.67 SEM Images of Soil-BA mixtures captured at 500 X magnification

5.4.14 Correlation between Different Strength Parameters

5.4.14.1 Relation between CBR, % BA & Curing Days

The correlation between CBR, % BA and curing days (D) was established using multiple linear regression analysis (MLRA). Test results obtained at 7, 14, 28 & 56 days of curing were considered for the analysis. The developed relation is given in Eqn. (5.5), with $R^2 = 0.553$. The R^2 value is apparently low; however, their close proximity to predicted values with experimental data needs to be validated. The validation of the developed relation was done using laboratory CBR values obtained at 128 days of curing. CBR results obtained through predicted equation [CBR (P)] and CBR results accrued from the laboratory [CBR (L)] were compared as shown in Figure 5.68. The equation has high values of R^2 suggesting closeness of predicted values the experimental data.

$$CBR = 3.45+0.117\%BA +0.02D \quad (5.5)$$

where, CBR = California bearing ratio, % BA = percentage bagasse ash, D = number of curing days.

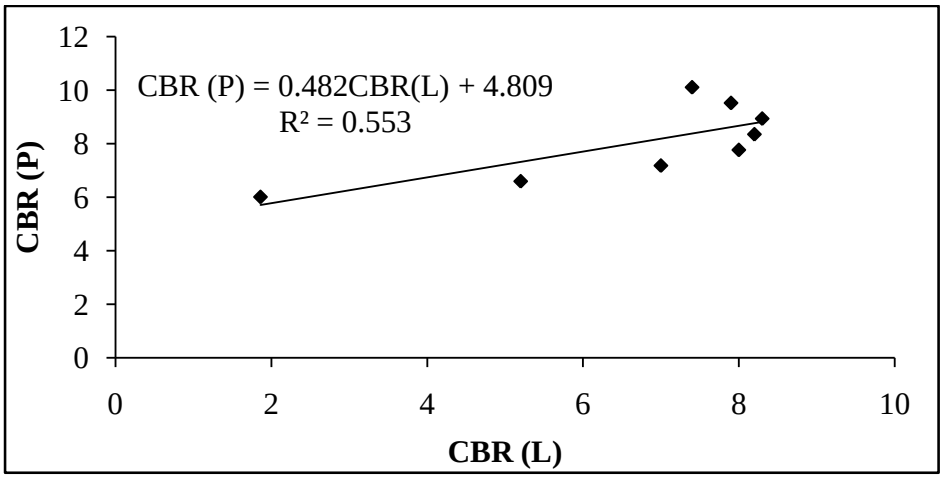

Figure 5.68 Validation of CBR Results for Soil-BA Mixtures

5.4.14.2 Relation between UCS, CBR, % BA & Curing Days

The relationship developed between UCS as dependent variable and other parameters as independent variable is given in Eqn. (5.6), with $R^2 = 0.970$. UCS test results of 128 days were used for validation of the predicted equation. Predicted UCS [UCS (P)] values and laboratory

UCS [UCS (L)] values were compared as shown in Figure 5.69. As this equation showed high values of R^2, predicted UCS values have close proximity with experimental data

$$UCS = 55.79-0.25\%BA +0.142D + 12.87CBR \quad (5.6)$$

where, UCS = Unconfined compressive strength (kPa)

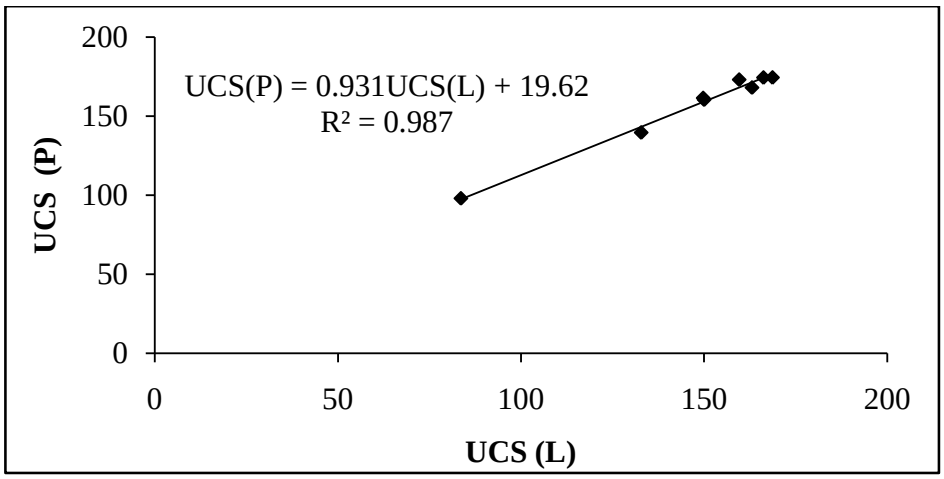

Figure 5.69 Validation of UCS Results for Soil-BA Mixtures

5.4.14.3 Relation between STS & UCS

Relationship has been established between split tensile strength and unconfined compressive strength of BA admixed soil samples from the data of present study. Various models like linear, exponential, polynomial, power and logarithmic were tested, but polynomial relation as shown in Figure 5.70 was best fitted with R^2 = 0.947. Further, the proposed equation was validated using STS laboratory results accrued after 128 days of curing as presented in Figure 5.71

The predicted STS [STS (P)] values and laboratory STS [STS (L)] values were compared and showed excellent relationship as high R^2 values exhibit between them.

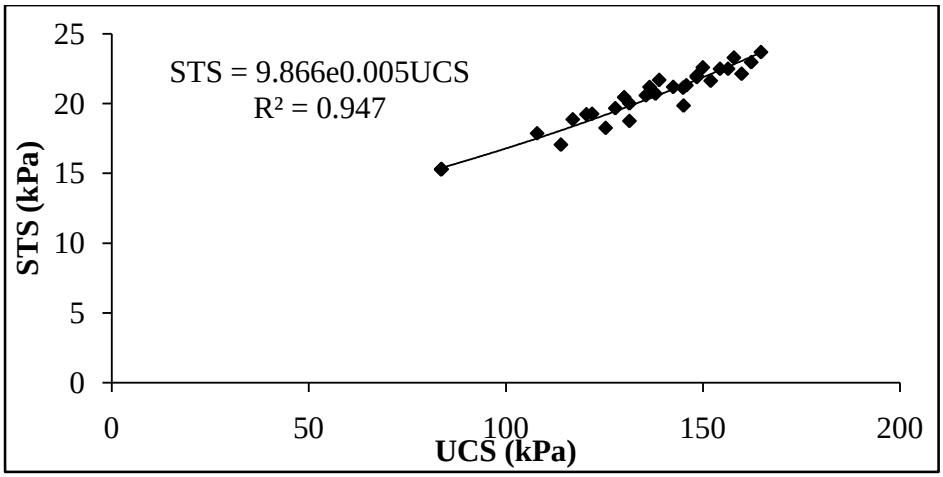

Figure 5.70 Relationship between STS & UCS for Soil-BA Mixtures

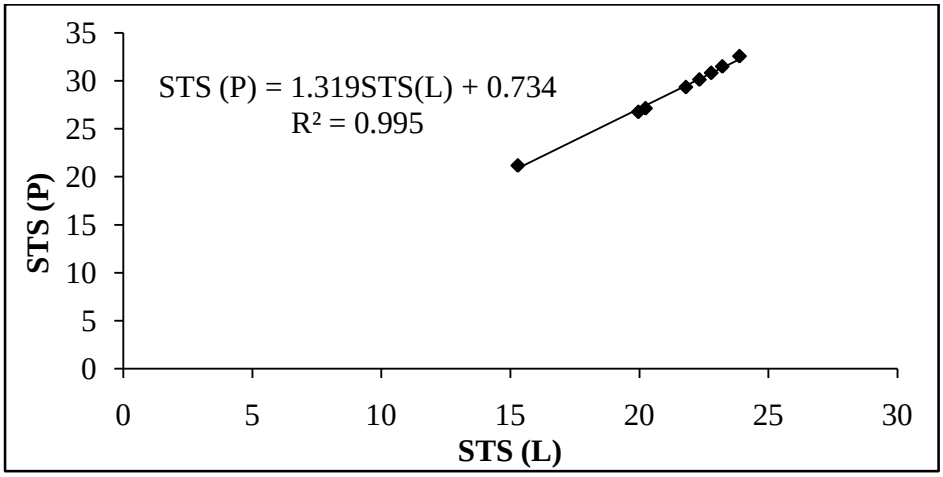

Figure 5.71 Validation Results for STS for Soil-BA Mixtures

5.4.14.4 Relation between M_R & CBR

The cyclic triaxial tests were conducted as per ASTM D5311-11 on natural and treated stabilized specimens with 5%, 10%, 15%, 20%, 25%, 30% and 35% of BA. The tests were conducted at 28 days of curing period. Three levels of σ_3 (50, 100 and 150 kPa) at 0.50 DSL and 0.80 DSL were applied during the test. The correlation was developed between M_R & CBR using regression analysis for each three levels of σ_3 at 0.50 DSL and 0.80 DSL respectively. The results of developed relations are shown in Figure 5.72 (a to f).

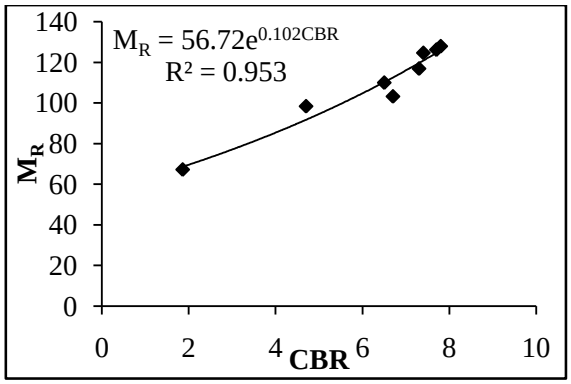

(a) CP 100, DSL 0.5

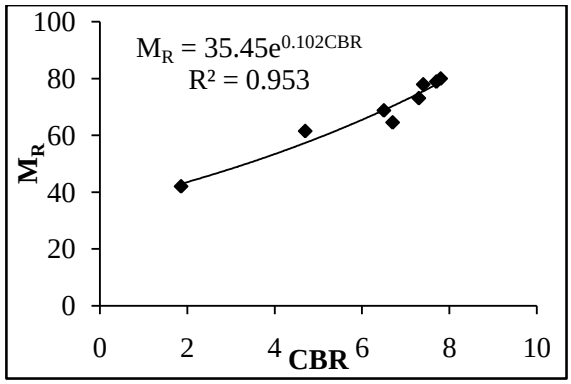

(b) CP 100, DSL 0.8

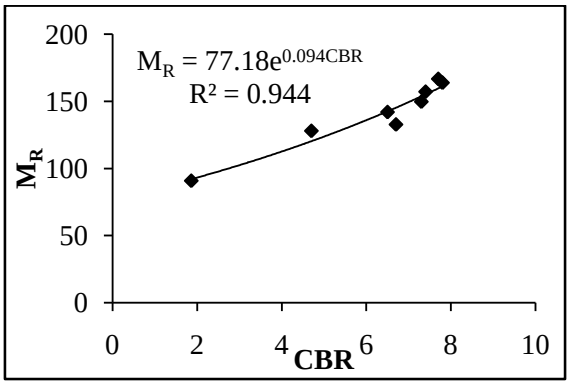

(c) CP 150, DSL 0.5

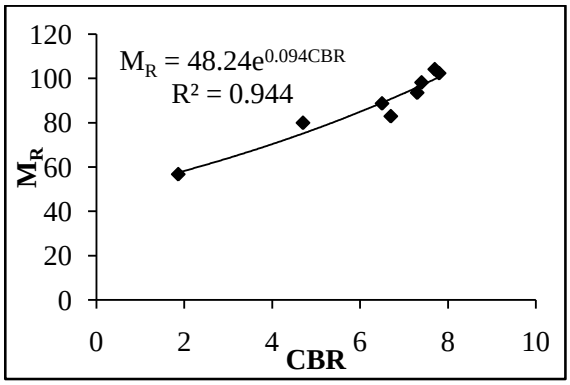

(d) CP 150, DSL 0.8

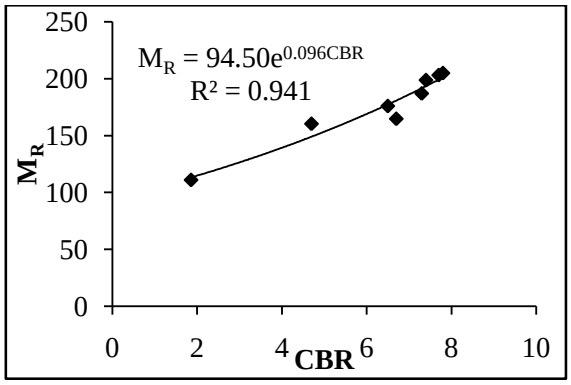

(e) CP 200, DSL 0.5

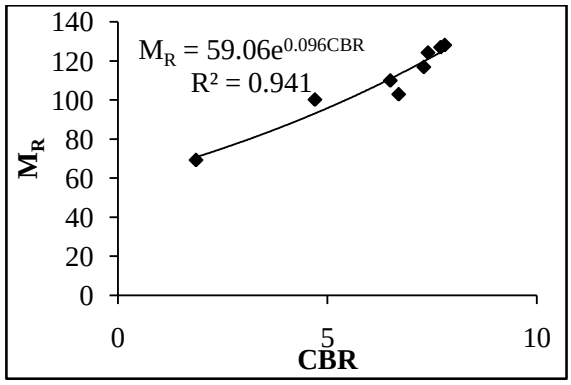

(f) CP 200, DSL 0.8

Figure 5.72 Relation between M_R & CBR for Soil-BA Mixtures

5.5 SOIL-RICE STRAW ASH

5.5.1 Atterberg Limits Test

It can be clearly seen from Figure 5.73 that addition of RSA decreases plasticity index considerably. However, at 20% RSA inclusion level there seems to be slightly ineffective. This may be due to improper mixing of RSA and soil particles. But from 30% RSA inclusion level onwards, marked reduction in PI value was observed. Percentage reduction in PI value was about 1.3 times higher for soil-FA mixtures in comparison to soil-RSA. Hence, it is pertinent to note here that RSA is more effective to control the plasticity of expansive soil as compared to RHA.

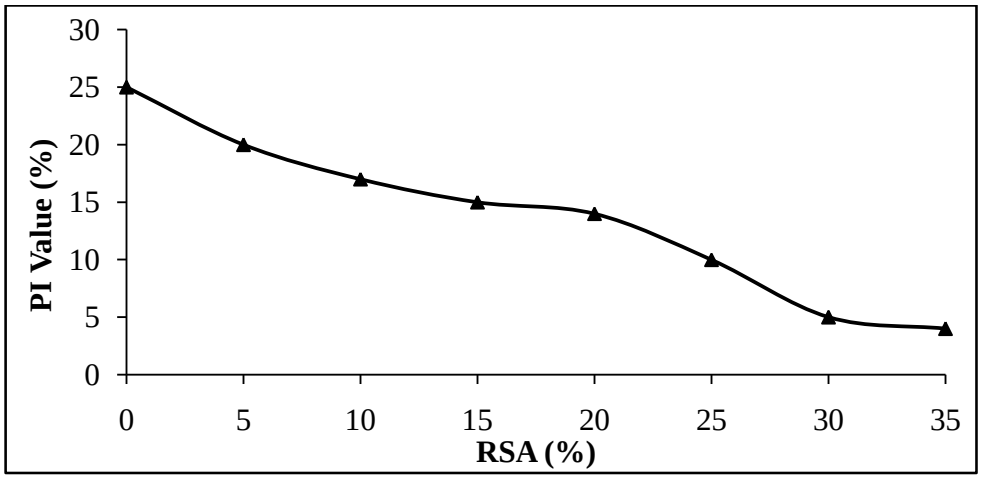

Figure 5.73 Atterberg Limits of Soil-RSA Mixtures

Figure 5.74 clearly depicts that there is a significant impact on shrinkage limit due to addition of RSA to an expansive soil. The increased of shrinkage limits are in the order of 9.2 %, 20.6 %, 26.2 %, 36.6 %, 50.1 %, 59.2 % & 67.42% after admixing RSA @ 5 %, 10 %, 15 %, 20 %, 25 %, 30 % & 35 % respectively. Hence, laboratory results revealed that inclusion of RSA produced about 1.1 times higher SL over RSA.

5.5.2 Free Swelling Index (FSI)

The variation of free swelling index with RSA content is presented in Figure 5.75. Free swelling index decreases with increase in RSA content upto 35%. The trend of decrease in FSI on admixing RSA is very similar to that of FA, RHA and BA. 10.73%, 22.79%, 35.79%,

41.42%, 48.15%, 61.43% and 68.25% are the percentages reduction noted when RSA was substituted @ 5%, 10%, 15%, 20%, 25%, 30% and 35% respectively by weight of dry soil. This analysis strongly suggested that the effectiveness of RSA and FA are almost same as far as FSI test is concerned, as their percentages reduction are very close to each other. Moreover, these two additives are silica rich materials.

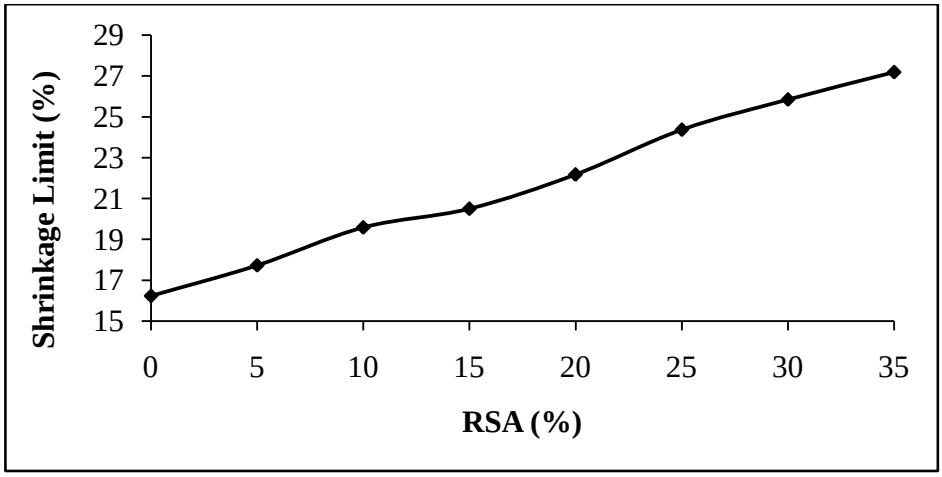

Figure 5.74 Shrinkage Limit of Soil-RSA Mixtures

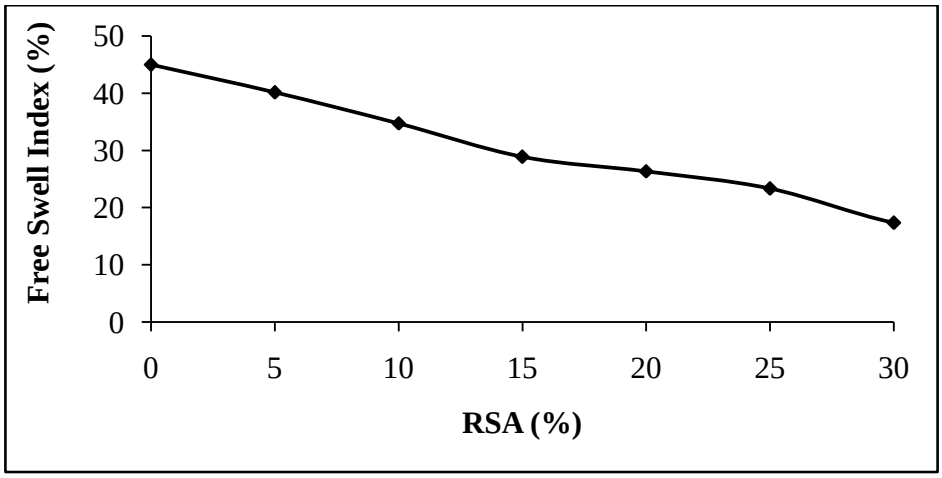

Figure 5.75 Free Swelling Index of Soil-RSA Mixtures

5.5.3 Proctor Test

The effects of RSA addition on OMC of the mixtures are shown in Figure 5.76. The trend of OMC increase is very similar with the case of RHA and BA. The percentages increase of OMC

due to admixing of RSA are 23.5%, 35.3%, 47.1%, 58.8%, 70.6%, 88.2%, 100.6% and 252.9% when RSA was admixed @ 5%, 10%, 15%, 20%, 25%, 30% and 35% respectively with respect to expansive soil. This OMC is about 2.2 and 3.5 times higher than the percentage obtained for BA and FA respectively. Higher water demand is attributed to the porous granular structures of RSA and hydration effect.

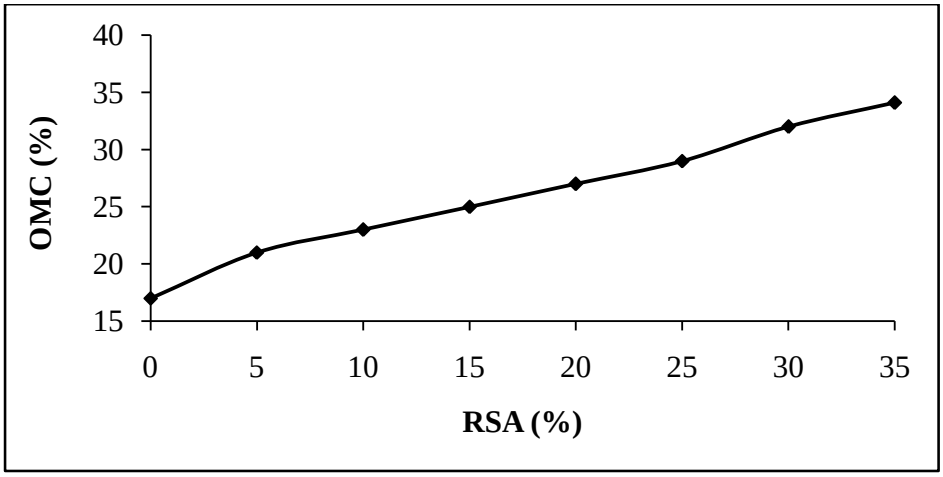

Figure 5.76 OMC of Soil-RSA mixtures

The addition of RSA played an important role in the development of dry density of RSA admixed soils. It is observed that the values of dry density decreases, while increasing the amount of RSA as shown in Figure 5.77. Similar trend has been observed in all the considered soil mixtures. However, the maximum reduction in dry density was observed for RHA admixed soils followed by RSA, FDCS, BA and FA admixed soils. The decrease in dry density of soil and RSA matrix might be due to soil texture admixed with the RSA and its characteristics.

5.5.4 California Bearing Ratio Test

The results of California Bearing Ratio (CBR) Test clearly show that the addition of RSA has influenced the CBR value. It is observed that the CBR value increases, while increasing the amount of RSA irrespective of RSA inclusion levels. Similar trend has been observed in all the other additives. Figure 5.78 clearly depicts that addition of RSA substantially increased CBR value upto 30% inclusion level. Beyond this, no appreciable increase in CBR value is observed. Indeed, CBR value starts declining particularly at 35% RSA inclusion level.

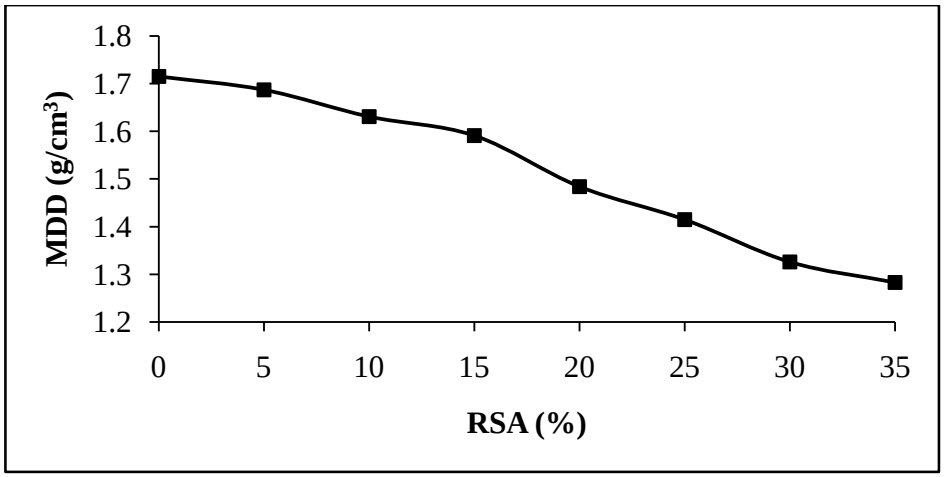

Figure 5.77 MDD of Soil-RSA Mixtures

The percentage increase of CBR value due to admixing of RSA @ 5%, 10%, 15%, 20%, 25%, 30% & 35% are 186.6%, 283.3%, 408.1%, 484.4%, 573.1%, 554.3% & 477.4% respectively with respect to expansive soil. This analysis infers that RSA has excellent efficacy even better than FA, RHA and BA in terms of CBR value. It has also been observed that CBR value increases with the increase of curing time. For 30% RSA inclusion level, the percentage increases in CBR value with respect to 3 days curing are 23.4%, 36.0%, 44.9%, 51.2% & 54.9% respectively for 7, 14, 28, 56 & 128 days. This analysis clearly suggested that there is substantial improvements in CBR value with prolong curing. This effect is mainly because of the growth of the cementitious products that fill the large pores. In overall, the improvement observed on CBR values on admixing of additive was due to the frictional resistance offered by the RSA.

5.5.5 Expansion Ratio

It can be clearly seen from the Figure 5.79 that addition of RSA decreases expansion ratio of expansive soil considerably. Higher reduction in expansion ratio was noticed for higher RSA inclusion levels. The trend of decrease in expansion ratio is cohesive, gradual and very similar to that of FA, RHA, and BA etc. The percentage decrease in expansion ratio due to inclusion of RSA @ 5%, 10%, 15%, 20%, 25%, 30%, and 35%, are 12.5%, 25.0%, 37.5%, 45.0% 50.0% and 55% respective with respect to expansive soil. On average, this increase is about 1.2 times to that of FA. The analysis suggests that RSA can be an effective additive to control expansion ratio over FA.

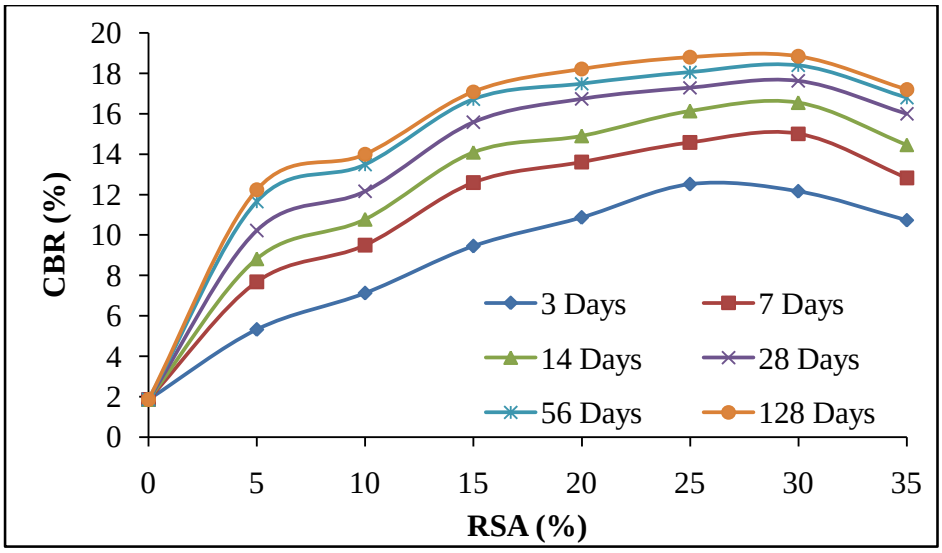

Figure 5.78 CBR of Soil–RSA Mixtures

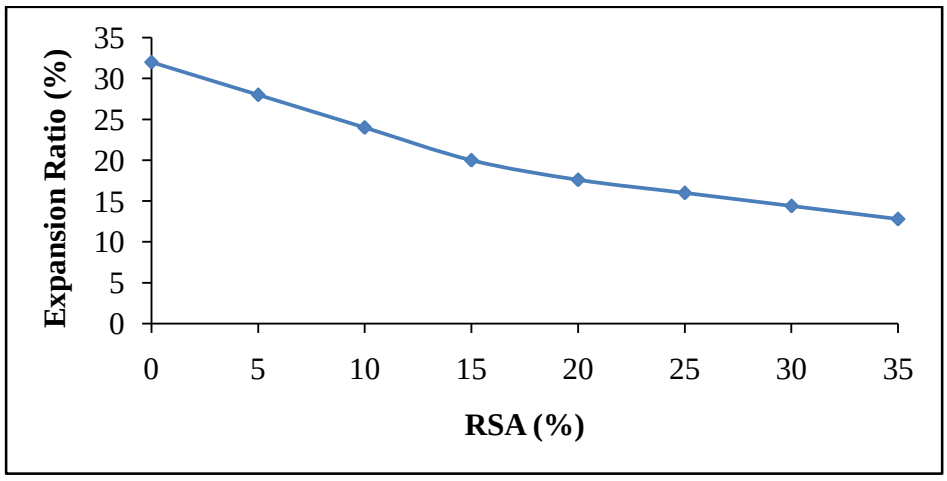

Figure 5.79 Expansion Ratio of Soil-RSA Mixtures

5.5.6 Hydraulic Conductivity Test

The effects of RSA addition on the permeability of the mixtures cured for a period of 7 days is shown in Figure 5.80. Inclusion of RSA reduces permeability considerably as other additives do. The decrease in permeability is more for higher RSA inclusion levels. The trend of decrease of permeability on admixing RSA is gradual. The percentage decreased in permeability on adxing of RSA @ 5%, 10%, 15%, 20%, 25%, 30% & 35% are 33.66%, 45.50%, 55.03%, 58.84%, 70.98%, 74.80% & 77.47% respectively with respect to expansive soil.

This decrease was as a result of the formation of cementitious compounds by calcium and silica and/or alumina from both the soil and RHA as revealed from SEM image. These products could infill the soil voids thereby obstructing the flow of water.

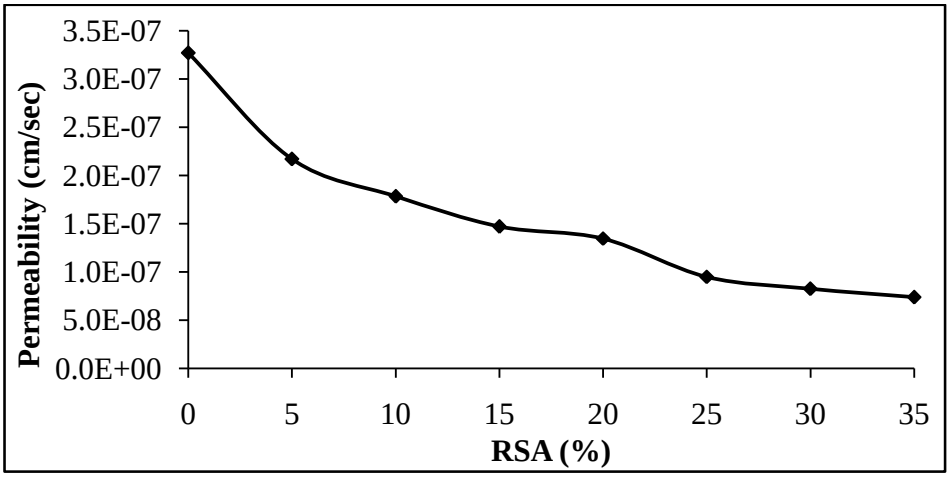

Figure 5.80 Permeability of Soil-RSA Mixtures

5.5.7 Unconfined Compressive Strength Test

UCS value was remarkably improved by admixing of RSA with natural soil sample as shown in Figure 5.81. The percentage increase in UCS on admixing of RSA @ 5%, 10%, 15%, 20%, 25%, 30% & 35% are 56.36%, 77.58%, 91.26%, 102.68%, 111.29%, 112.87% & 90.60% respectively at 7 days with respect to expansive soil. Whereas for 14 days, 28 days, 56 days and 128 days cured samples, these values further increased to 70.39%, 95.94%, 108.06%, 118.82%, 128.32%, 132.37% & 114.90% ; 74.58%, 104.47%, 120.61%, 133.35%, 142.26%, 144.77% & 125.74%; 80.44%, 111.51%, 130.00%, 146.26%, 152.82%, 156.50% & 136.29% ; 92.70%, 121.85%, 138.26%, 152.47%, 158.68%, 162.36% & 144.50% respectively. On average, RSA to FA ratio for curing period of 7, 14, 28, 56 and 128 days are 1.90, 1.92, 2.00, 2.02 and 2.09 respectively. This apparently indicates that RSA has possessed better efficacy for improving compressive strength of admixed soil particular for expansive soil.

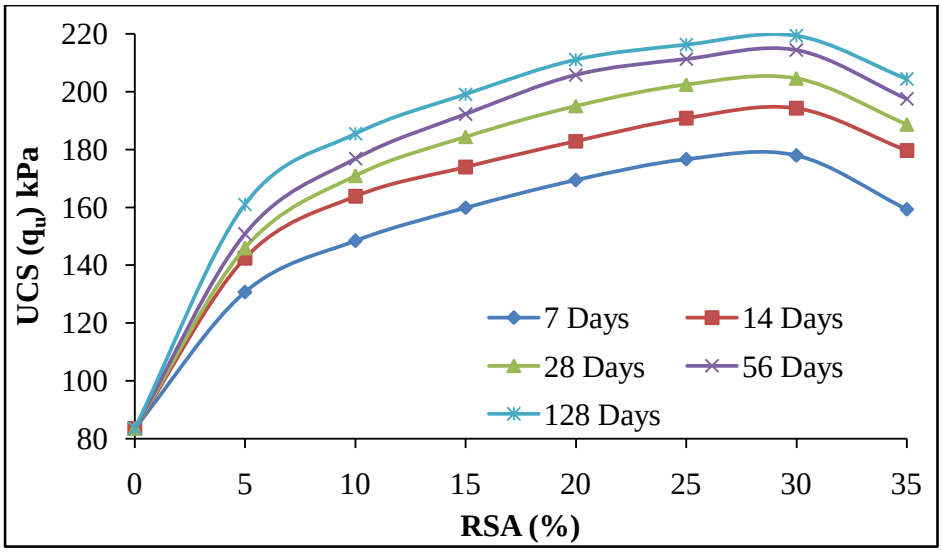

Figure 5.81 UCS of Soil-RSA Mixtures

5.5.8 Split Tensile Strength Test

Figure 5.82 clearly states that admixing of RSA does not increase only compressive strength but also improves tensile strength of admixed soil mixtures considerably. However, tensile improvement is comparatively less in comparison to compressive strength. Steep increase in tensile strength is observed upto 10% RSA inclusion level irrespective of curing time. Beyond this level, the improvements of tensile strength become sluggish. However, maximum tensile strength is read at 30% RSA inclusion level. There is a steep decline in tensile strength beyond 30% inclusion level. Hence, based on the present study the best RSA inclusion level which would produce maximum tensile properties of admixed soil is 30% and if maximum inclusion level is seeking with an intention to utilize waste agricultural by-product in road construction, 30% RSA shall be the maximum inclusion level.

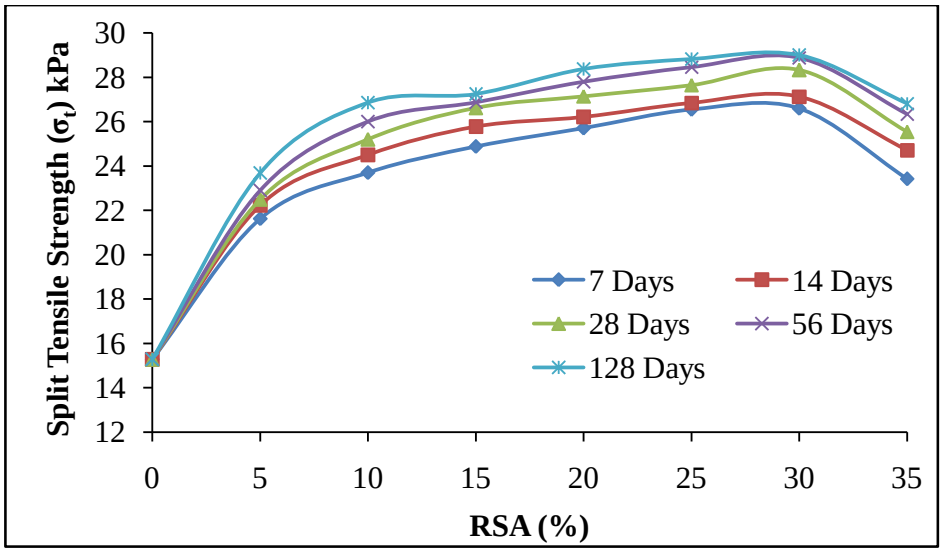

Figure 5.82 Split Tensile Strength of Soil Admixed with RSA

5.5.9 Ratio of Split Tensile to Unconfined Compressive Strength Test

The relative relationship and mobilization between the tensile strength and compressive strength could be discussed by plotting the tensile/compressive strength ratio (σ_t/q_u) versus curing time. Figure 5.83 shows the influence of RSA content on the ratio of split tensile strength and unconfined compressive strength. The results show that unconfined compressive strength and split tensile strengths are closely related. It can be observed that the ratio of split tensile strength and unconfined compressive strength decreased with increase in RSA content, indicating that RSA is more efficient when soil was subjected to compression rather than to tension.

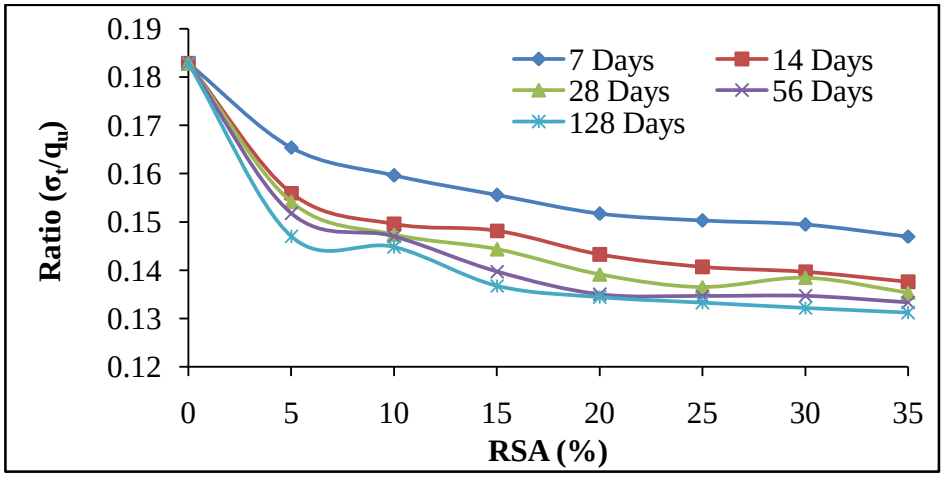

Figure 5.83 σ_t/q_u Ratio of Soil-RSA Mixtures

5.5.10 Triaxial Test

Three different confining stresses such as 100, 150 and 200 kPa were applied on specimens to obtain peak deviator stress as shown in Table 5.4. The range of confining stresses was chosen to obtain more well define and accurate plots of Mohr envelopes to obtain shear strength parameters cohesion (c) and angle of internal friction (φ) of the soils mixed with RSA. The variation of c and φ with admixing RSA are evaluated and results are shown in Figures 5.84 & 5.85 respectively.

Table 5.4 shows deviator stress of RSA admixed soils after 7, 14, 28, 56 & 128 days curing period at three different confining pressures. Higher deviator stresses are observed for higher RSA content irrespective of confining pressure applied and days of curing. However, beyond 30 % RSA content, the deviator stresses starts declining. Admixing of RSA causes increase in cohesion and internal friction angle. Increase in cohesion is more pronounced upto 10% RSA content. The cohesion of soil ranges from 28 to 51.19 kPa and from 28.5 to 63.41 kPa at 7 days and 128 days curing respectively, for RSA contents between 0 & 30%. Improvement on cohesion due to addition of RSA becomes sluggish beyond 10% inclusion level. However, these cohesions are much higher than that of expansive soil. Marked reduction in cohesion is observed beyond 30% BA content. As in the case of cohesion, similar trend of improvement is observed for internal friction angle. The rate of improvement of internal friction angle is rapid for 5% RSA, after which the rate of improvement is gradual. In overall, these internal friction angles are higher than expansive soil irrespective days of curing (Figure 5.85). This improvement may be caused due to the increase of c of the soil upon the ultra fine RSA particles and pozzolanic reaction occurred over a period of time.

Table 5.4 Deviator Stress for RSA Admixed Soil at Different Confining Pressure

% RSA	Confining Pressure (kPa)	Deviator Stress (kPa)				
		7 Days	14 Days	28 Days	56 Days	128 Days
0	100	205.34	206.19	204.83	205.01	204.47
	150	275.91	277.81	276.52	278.17	276.24
	200	337.11	339.77	337.97	338.87	339.18
5	100	326.82	353.29	359.05	368.09	394.71

	150	431.40	462.81	466.76	474.84	505.23
	200	539.25	579.40	585.25	596.31	635.49
	100	366.71	401.35	415.40	426.17	448.85
10	150	480.39	521.75	535.87	545.49	570.04
	200	594.07	646.17	664.65	677.60	709.18
	100	390.16	420.95	442.67	465.34	480.06
15	150	507.21	543.03	566.61	590.98	614.47
	200	632.06	677.73	708.27	739.89	762.09
	100	416.84	446.38	479.93	508.53	523.48
20	150	546.07	589.23	633.51	661.09	680.52
	200	675.29	723.14	772.69	813.65	832.33
	100	438.09	471.48	500.28	519.96	542.84
25	150	560.75	608.21	640.35	670.75	683.98
	200	705.32	759.09	801.69	828.30	857.69
	100	443.14	486.65	511.59	540.40	554.95
30	150	567.22	618.05	644.61	675.50	690.91
	200	713.46	781.08	815.99	853.83	872.93
	100	393.60	441.98	452.00	460.30	479.36
35	150	507.74	565.74	580.82	580.67	620.77
	200	633.70	707.17	721.39	729.57	759.78

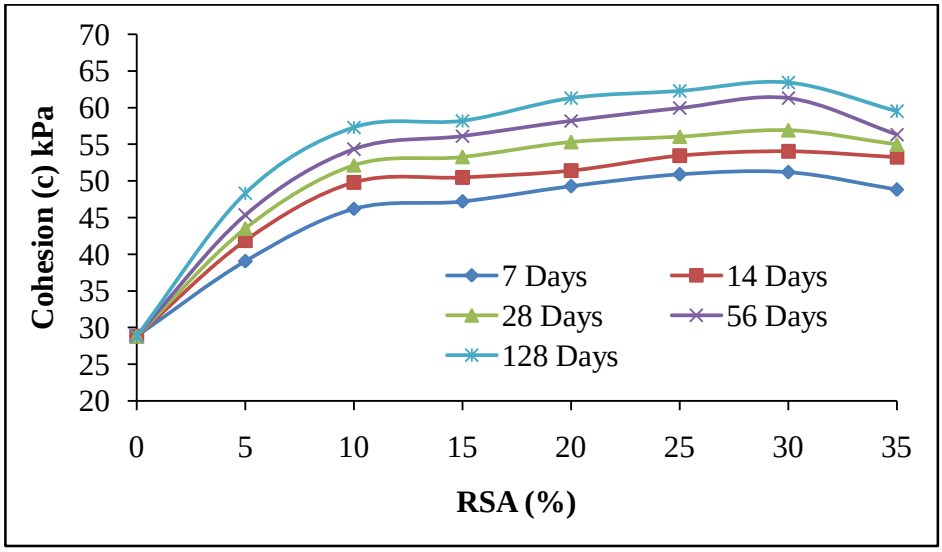

Figure 5.84 Cohesion of Soil–RSA Mixtures

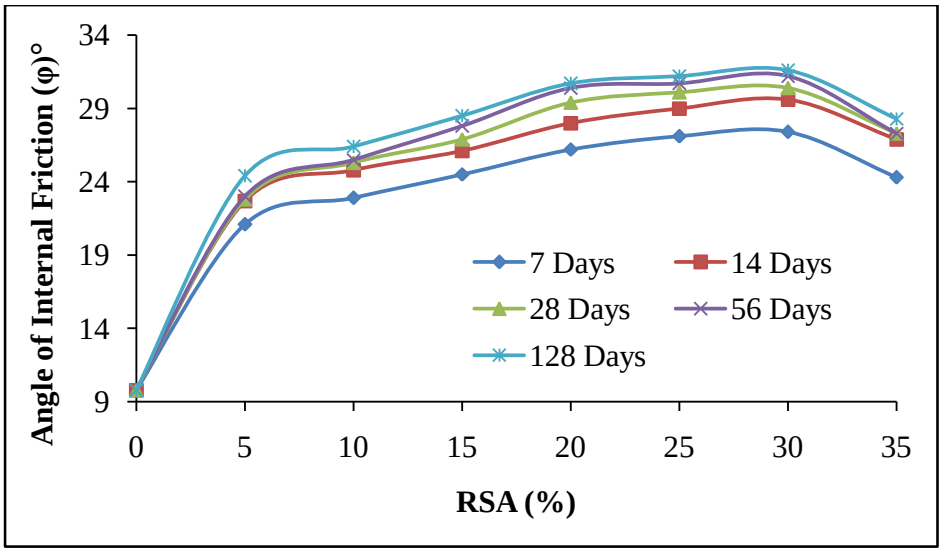

Figure 5.85 Angle of Internal Friction of Soil-RSA Mixtures

5.5.11 Cyclic Triaxial Test

The effects of various percent of RSA and loading cycles on the permanent deformations of the expansive soil and RHA admixed soils were studied. The effects of DSL ratios and confining pressure with number of loading cycles on the permanent deformations were studied for all admixed soil samples. Three confining pressures such as 100, 150 & 200 kPa and two DSL as 0.5 and 0.8 were taken for determination of permanent strain upto 10000 cycles under constant axial loading. The test result was plotted for vertical percent permanent strain as ordinate and number of cycles as abscissa and is presented in Figures 5.86 and 5.87 at DSL 0.5 and 0.8 respectively.

5.5.11.1 Effect of load cycle

Figure shows that rapid increase in deformation of the expansive and RHA admixed soils were observed during the initial approximate hundred cycles of loading and the strain rate was high during this stage in all cases. After few hundred cycles of loading, the increase in deformations was progressive upto 2000 cycles thereafter deformation almost stabilized for RHA admixed soil. But deformation still took place for expansive soil. For RHA admixed soils, the matrix behaves almost elastically under the applied load. The maximum permanent strain of 6.15% was observed for expansive soil at 0.8 DSL for 100 kPa CP and the minimum permanent strain of 1.87% was observed for 30% RSA at 0.5 DSL for 200 kPa CP at 10000 cycles.

5.5.11.2 Effect of confining pressure

Efforts have also been made to study the permanent deformation characteristics of expansive soil and RSA admixed soils at three pre-determined confining pressures. Figures 5.86 [(a) to (c)] and 5.87 [(a) to (c)] illustrate the permanent deformation at the confining pressure of 100, 150 and 200 kPa respectively. Out of this study, the minimum permanent deformation observed after 10000 cycles at 100, 150 and 200 kPa confining pressure are 2.26%, 2.15% & 1.87% respectively at 0.5 DSL . Whereas the permanent deformation for 0.8DSL under the same working condition are 3.2%, 2.9% & 2.5% respectively. Present analysis suggested that permanent deformation decreases with increase in confining pressure irrespective of types of samples. However, least permanent deformation was recorded for 30% RSA inclusion level followed by 35% RSA, 25% RSA, 20%RSA, 15% RSA, 10% RSA, 5% RSA and 0% RSA inclusion levels respectively..

5.5.11.3 Effect of deviator stress level

The permanent strain values obtained at 0.5 DSL for expansive soil and RSA admixed soils are illustrated in Figure 5.86. To appreciate better the effect of σ_d the permanent strain recorded at 0.8 DSL is also presented in Figure 5.87. These different plots have been established considering all the three different confining pressure. Increase of σ_d value signifies improvement in permanent strain. Out of this investigation, the least value of σ_d was observed for 30% RSA admixed soils (1.87%) for 0.5 DSL at 200 confining pressure whereas for 0.8 DSL, 2.5% was observed. This again confirmed that least permanent deformation is offered by 30% RSA inclusion level.

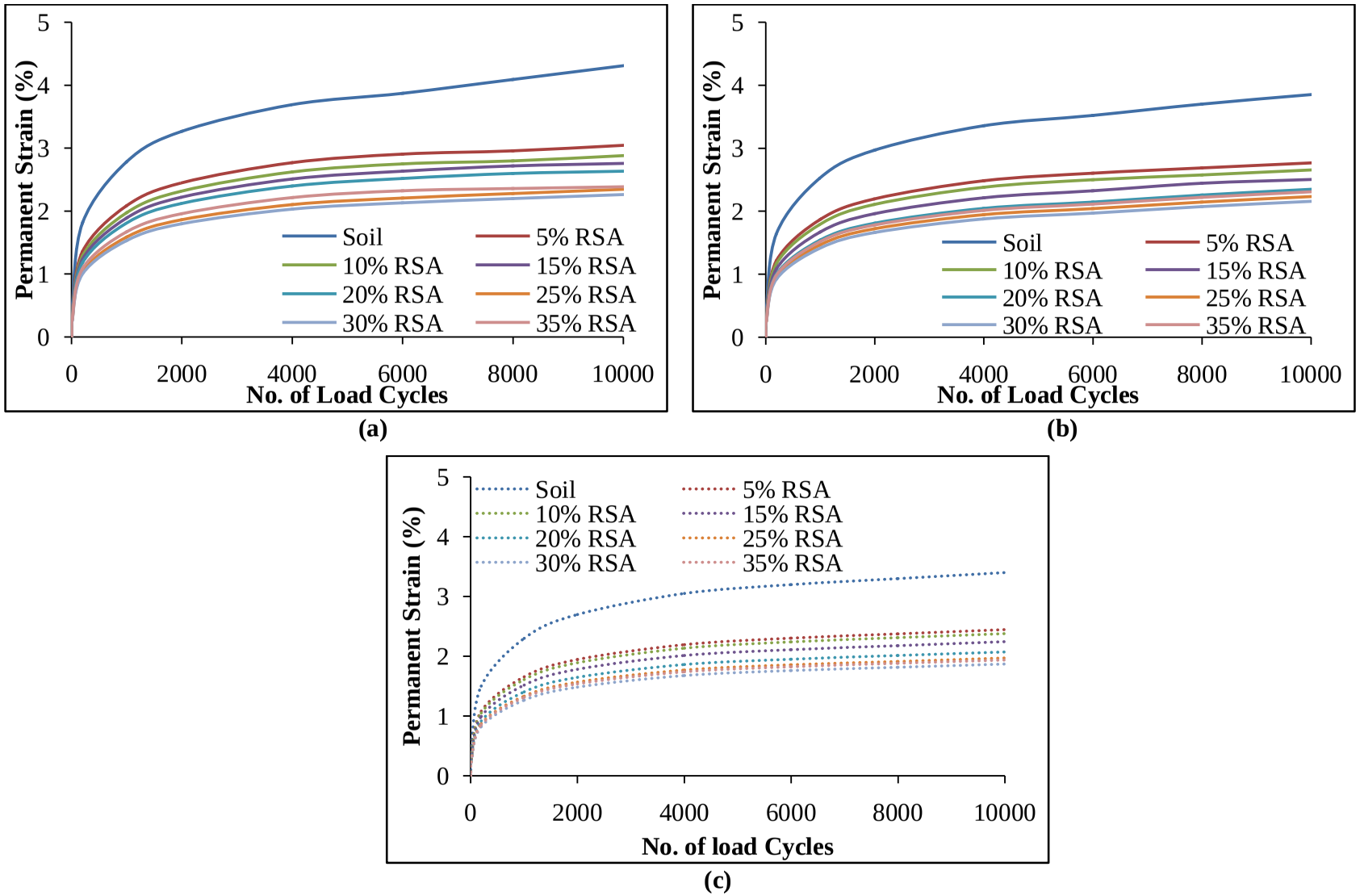

Figure 5.86 Permanent Strain of Soil – RSA Mixtures at 0.5 DSL (a) at 100 kPa CP (b) at 150 kPa CP (c) at 200 kPa CP

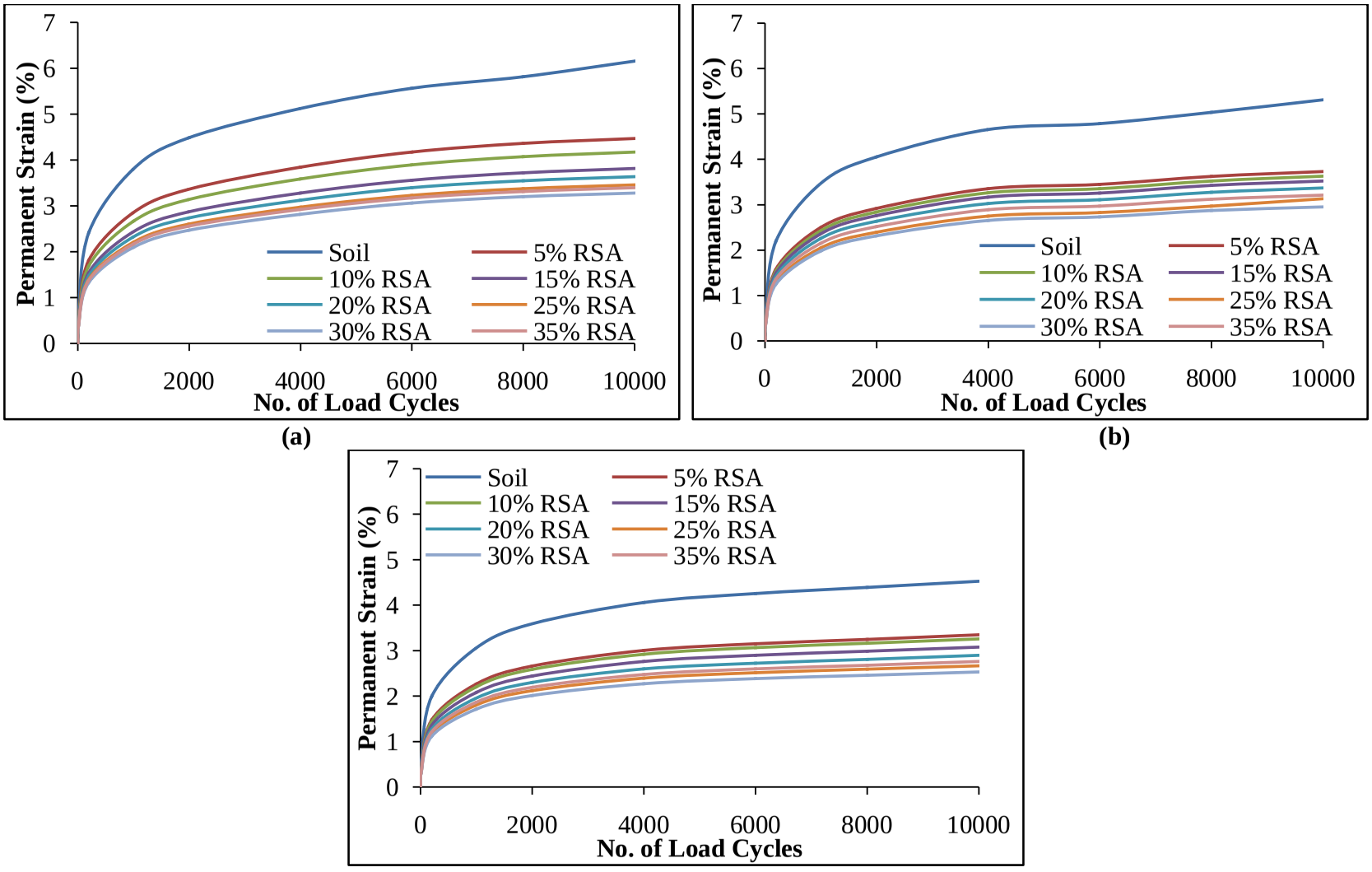

Figure 5.87 Permanent Strain of Soil –RSA Mixtures at 0.8 DSL (a) at 100 kPa CP (b) at 150 kPa CP (c) at 200 kPa CP

For analysis of M_R results, set of six tests were conducted on both expansive soil and RSA admixed soils. Tests were conducted at two pre-determined DSL rates i.e. 0.5 & 0.8. Similarly, three confining pressures of 100, 150 and 200 were chosen for the test. Throughout the test, the aforementioned DSL rates and confining pressures were considered. The main objective of this study was to understand the effects of confining pressure and DSL on expansive soil and RSA admixed soils.

Figure 5.88 reveals that an increase in confining pressure resulted enhancements of M_R of all cases but these value diminish at higher DSL value. M_R values increase with increase in RSA content irrespective DSL and confining pressure. The maximum M_R values observed were 110 MPa & 69 MPa at 0.5 & 0.8 DSL respectively for a constant 200 kPa confining pressure when no admixing was done. But these values increases to 297 & 167 MPa respectively after admixing of 30% RSA. This effect may be attributed to a stiffer soil skeleton structure of admixed soils caused by increased confinement and pozzolanic reactions, which result in a closer bonding of soil particles.

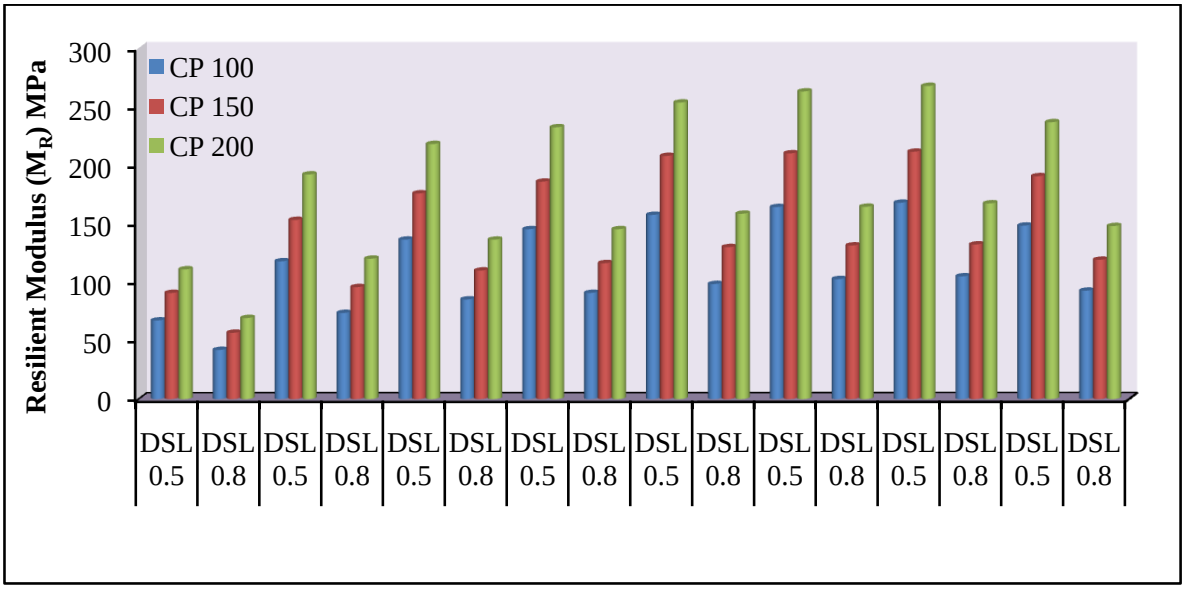

Figure 5.88 Resilient Modulus of Soil-RSA Mixtures

5.5.12 Plate Load Test

The influence of RSA in improving the modulus of subgrade reaction (k) of mixtures was evaluated by comparing the measured k-values for the natural expansive soil and soil-FA mixtures. Inclusion of RSA to expansive soil considerably improved k-value as presented in Figure 5.89. The modulus of subgrade reaction of expansive soil was found to be 17 MPa/m. The rate of improvement of k-value is significant upto 5.0% RSA inclusion level beyond which k-value starts declining. If RSA was reinforced with expansive soils @ 5%, 10%, 15%, 20%, 25%, 30% & 35%, the percentages increase of k-values were 206%, 232.7%, 249.9%, 258.2%, 251.3%, 250.2%, and 246.9% respectively. Based on this analysis, one can clearly say that admixing RSA beyond 10% would give no appreciable improvement in k-value.

The result of modulus of subgrade reaction (k) is shown in Figure 5.89. The modulus of subgrade reaction of soil is 17 MPa/m without any additives. The values of modulus of subgrade reaction enhanced to 58 MPa/m at addition of 15% of RSA contents. It is observed that the modulus of subgrade reaction is increased by increasing BF at 15% and after that almost constant upto 25%. It was slightly decreased after 25% of RSA.

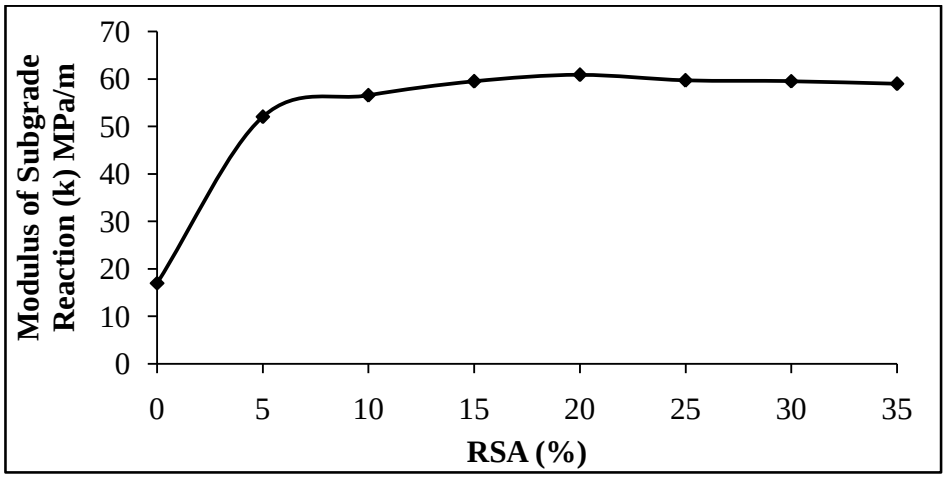

Figure 5.89 Modulus of Subgrade Reaction of Soil Admixed with RSA

Load-settlement curves are plotted with the data obtained from the plate load tests in laboratory. Obtained curves are not well defining the yield point. The ultimate bearing capacity for untreated soil and soil admixed with RSA are found from the tangent intersection of the two

straight portions of the load-settlement curve at the initial straight portion and the steeper straight portion at the end. As shown in figure 5.90 the ultimate load of the untreated soil is found to be 198 kPa. When RSA was admixed at the rate of 5%, 10%, 15%, 20%, 25%, 30% & 35%, ultimate load improvements were 31.3%, 40.4%, 46.5%, 51.5%, 59.1%, 60.6% & 54.5% respectively at 7 days with respect to untreated soil samples. The trend of increase of ultimate load on admixing of RSA was observed upto 30% after which these improvements were decreased. Analysis results revealed that there is substantial improvement in ultimate bearing capacity on admixing of RSA.

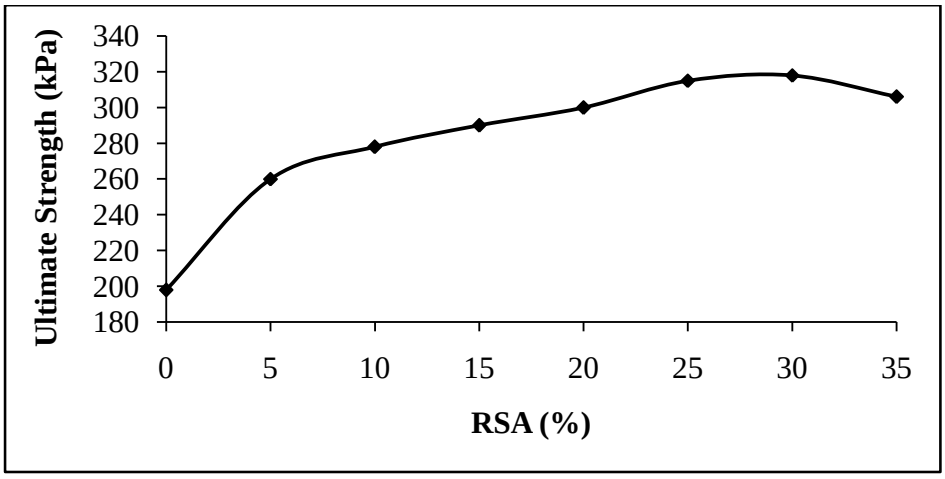

Figure 5.90 Ultimate Strength of Soil-RSA Mixtures

5.5.13 Microstructural Investigation

The microstructure of RSA was investigated by using Scanning Electron Microscope (SEM). The images from Scanning Electron Microscope taken at 500 X magnification are shown in Figures 5.91 (a to d). Like in the case of BA, granular structures of RSA are clearly visible. RSA particles with various sizes and geometry like prismatic, spherical and fibrous were recognized. Formations of important hydration products like C-S-H gel, CAH and $Ca(OH)_2$ are observed from the ground mass. More air voids are observed for 20% & 25% RSA admixed samples in comparison to 30% & 35% RSA admixed samples.

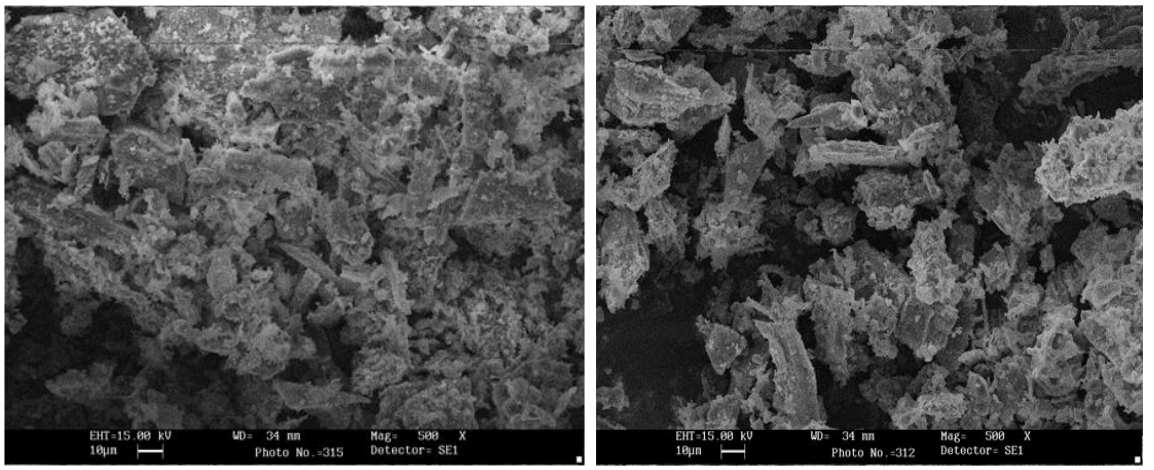

(a) 20 % RSA (b) 25 % RSA

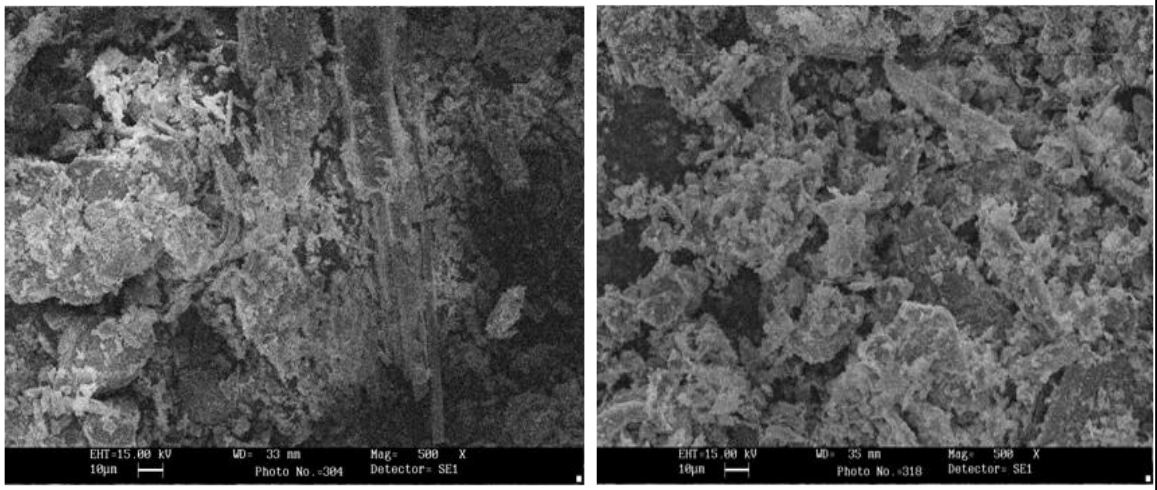

(c) 30 % RSA (d) 35 % RSA

Figure 5.91 SEM Images of Soil-RSA mixtures captured at 500 X magnification

5.5.14 Correlation between different Strength Parameters

5.5.14.1 Relation between CBR, % RSA & Curing Days

The correlation between CBR, RSA and curing days (D) was established using multiple linear regression analysis (MLRA). Test results obtained at 7, 14, 28 & 56 days of curing were considered for the analysis. The developed relation is presented in Eqn. (5.7), with R^2= 0.699. Low values of R^2 show less close proximity to predicted values with experimental data. The validation of the developed relation was done using laboratory CBR values obtained at 128

days of curing. CBR results obtained through predicted equation [CBR (P)] and CBR results accrued from the laboratory [CBR (L)] were compared as shown in Figure 5.92.

$$CBR = 5.04 + 0.344\%RSA + 0.06D \quad (5.7)$$

where, CBR = California bearing ratio, % RSA = percentage rice straw ash, D = number of curing days.

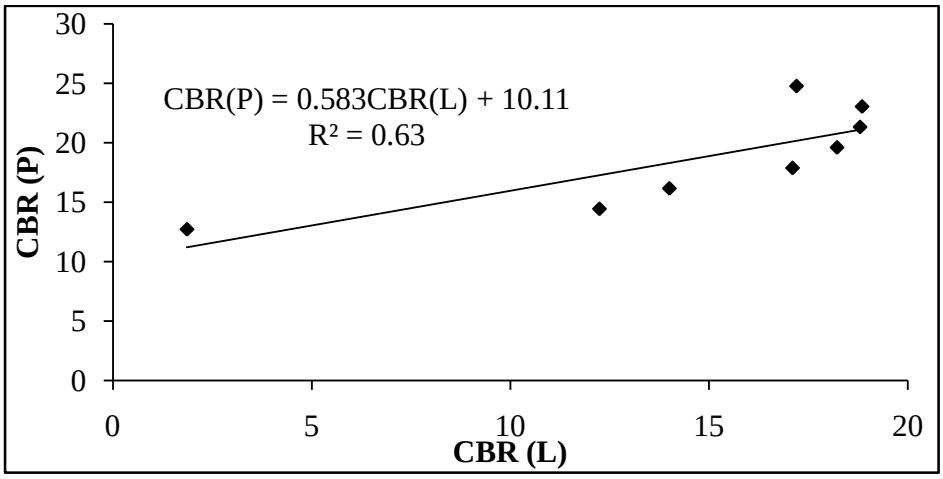

Figure 5.92 Validation of CBR Results for Soil-RSA Mixtures

5.5.14.2 Relation between UCS, CBR, % RSA & Curing Days

The relationship developed between UCS as dependent variable and other parameters as independent variable is given in Eqn. (5.8), with R^2= 0.986. UCS test results of 128 days were used for validation of the predicted equation. Predicted UCS [UCS (P)] values and laboratory UCS [UCS (L)] values were compared as shown in Figure 5.93. As this equation showed high values of R^2, predicted UCS values have close proximity with experimental data.

$$UCS = 69.555 - 0.151\%RSA + 0.019D + 7.781CBR \quad (5.8)$$

where, UCS = Unconfined compressive strength (kPa)

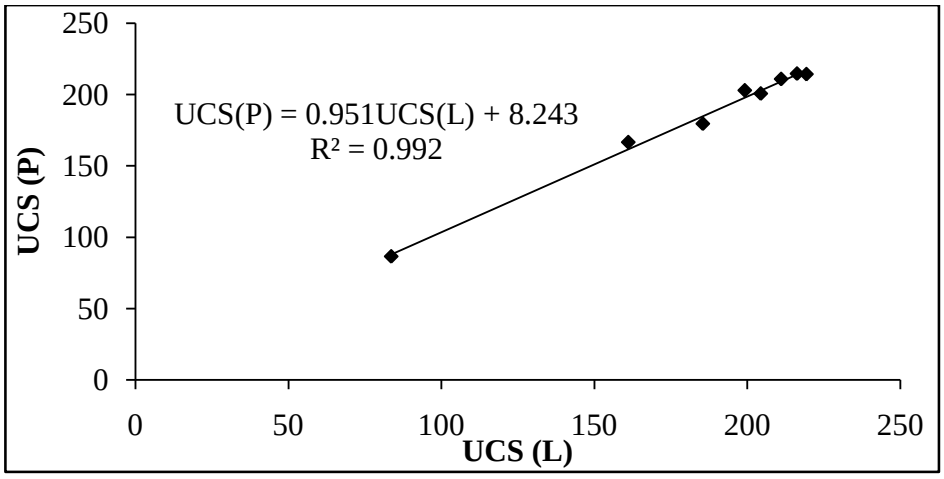

Figure 5.93 Validation of UCS Results for Soil-RSA Mixtures

5.5.14.3 Relation between STS & UCS

Relationship has been established between split tensile strength and unconfined compressive strength of RSA reinforced soil samples from the data of present study. Various models like linear, exponential, polynomial, power and logarithmic were tested, but linear relation as shown in Figure 5.94 was best fitted with R^2 = 0.984. Further, the proposed equation was validated using STS laboratory results accrued after 128 days of curing as presented in Figure 5.95.

The predicted STS [STS (P)] values and laboratory STS [STS (L)] values were compared and showed excellent relationship as high R^2 values exhibit between them.

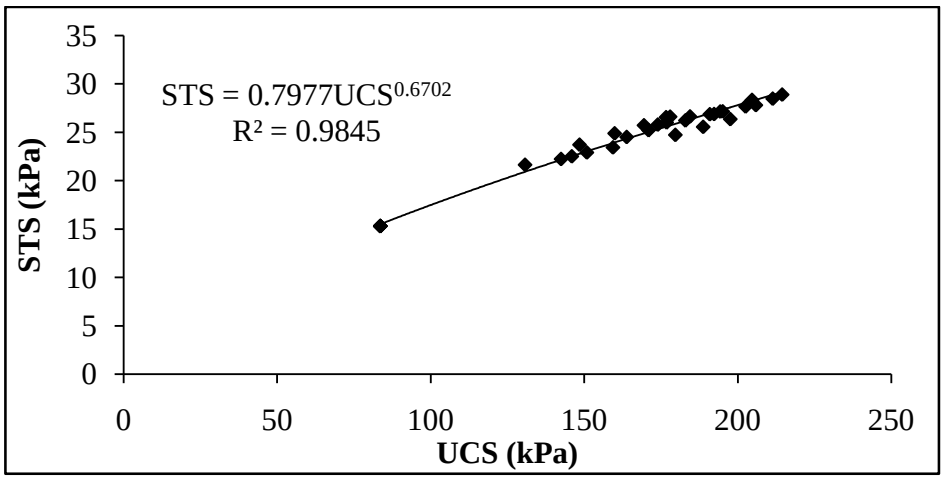

Figure 5.94 Relationship between STS & UCS for Soil-RSA Mixtures

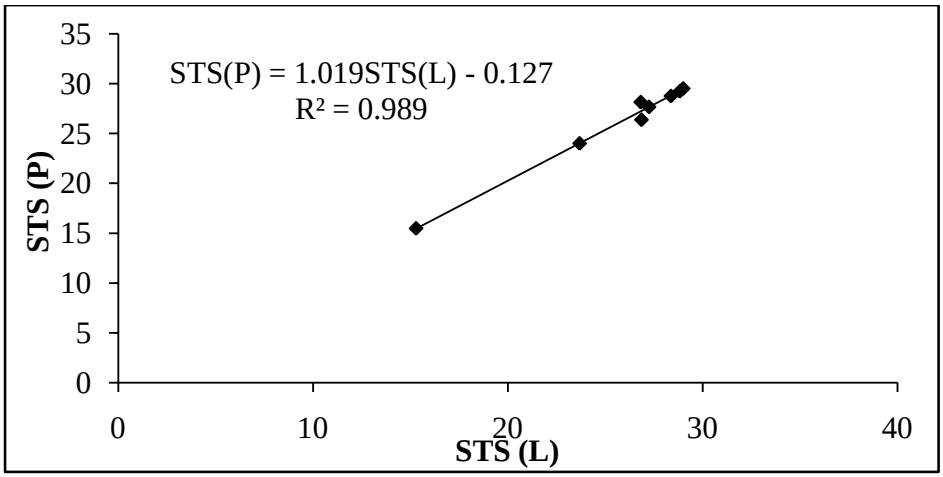

Figure 5.95 Validation Results for STS for Soil-RSA Mixtures

5.5.14.4 Relation between M_R & CBR

The cyclic triaxial tests were conducted as per ASTM D5311-11 on expansive soils and RSA admixed soils. Tests were conducted after the expiry of 28 days curing period. Three levels of σ_3 (50, 100 and 150 kPa) at 0.50 DSL and 0.80 DSL were applied during the test. The main intention behind this effort was to establish correlation between M_R & CBR using regression analysis for each three levels of σ_3 0.50 DSL and 0.80 DSL respectively. Mathematical analysis of data shows good relationship between M_R & CBR described by a power series as presented in Figure 5.96 (a to f).

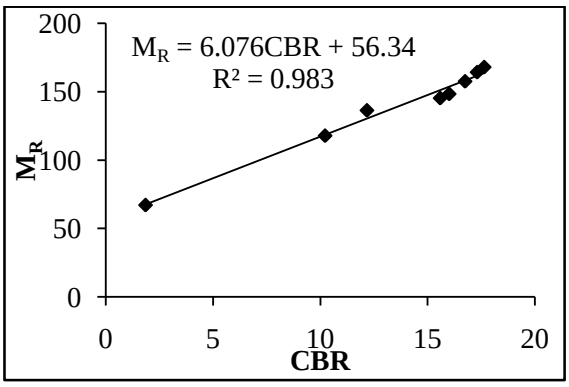

(a) CP 100, DSL 0.5

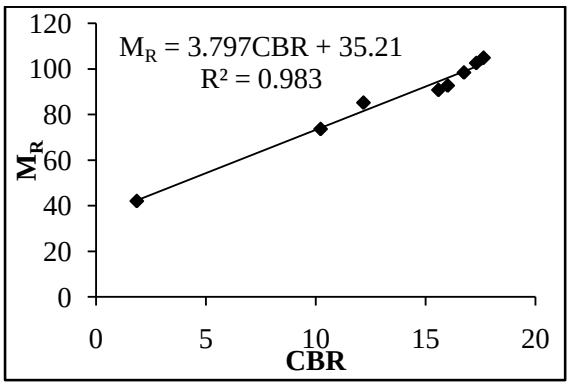

(b) CP 100, DSL 0.8

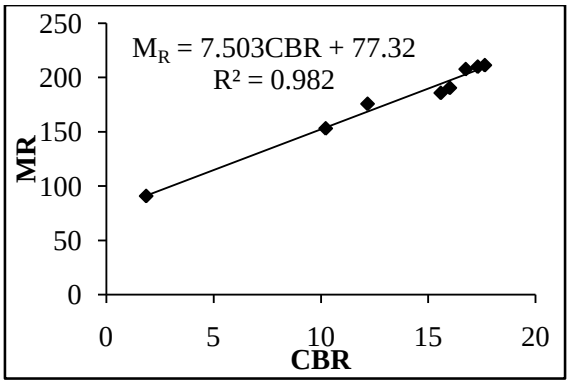

(c) CP 150, DSL 0.5

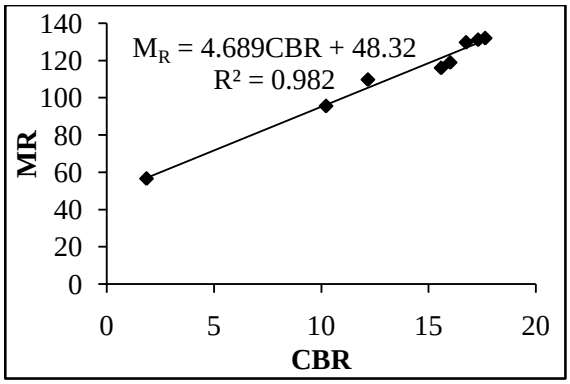

(d) CP 150, DSL 0.8

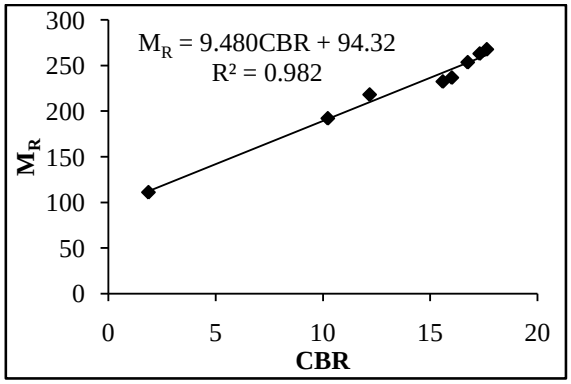

(e) CP 200, DSL 0.5

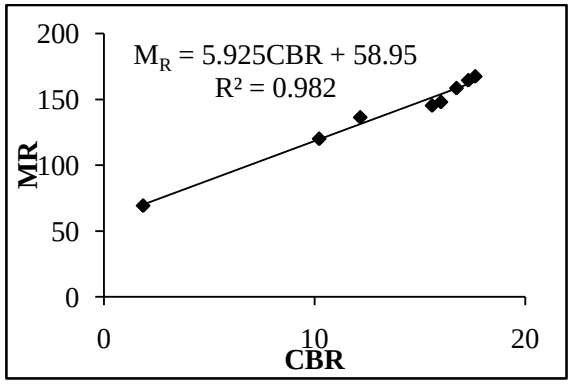

(f) CP 200, DSL 0.8

Figure 5.96 Relation between M_R & CBR for Soil-RSA Mixtures

5.6 SOIL-FINES OBTAINED FROM DEMOLISHED CONCRETE SLAB

5.6.1 Atterberg Limits Test

As it can be seen from Figure 5.97, plasticity index (PI) decreases irrespective of FDCS content of the mixture. The decrease of PI is due to decrease of both liquid limit and plastic limit on admixing of FDCS. The percentage of reduction in PI on admixing of FDCS showed about 1.12 times higher than FA admixed soil samples irrespective of percentage of inclusion. This phenomenon clearly infers that the effect of FDCS addition on PI of the mixtures is more effective than FA addition. Considerable reduction in PI on admixing of FDCS may be attributed to the increase of non-plastic sand & silt particles and remnant cement grains in the matrix. Another possible reason of having marked reduction in PI on admixing of FDCS is, it's

being very fine powder passing 1.18 mm IS sieve size derived from very rich cementing materials; hence, pozzolanic reaction must have been occurred in presence of moisture. However, further investigation is suggested in this regard.

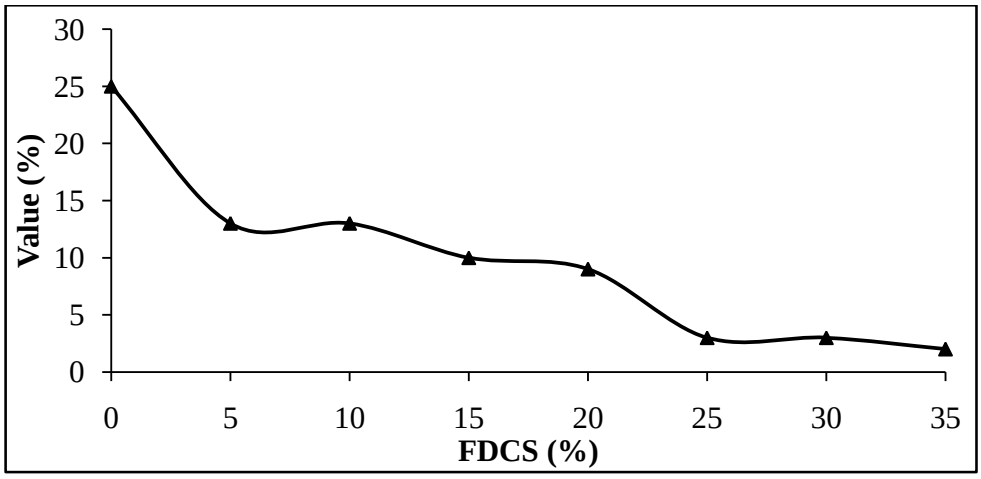

Figure 5.97 Atterbergs Limit of Soil-FDCS Mixtures

It can be seen from the Figure 5.98 that FDCS inclusion increases the shrinkage limit of an expansive soil significantly. The increase of SL is more pronounced at higher substitution levels. About 1.13 times higher SL is offered by FDCS admixed soil mixtures in comparison to FA admixed soil mixtures regardless to substitution levels. This phenomenon is mainly attributed to the flocculation of clay particles caused by the free lime present in the FDCS resulting in the reduction of friction between the particles.

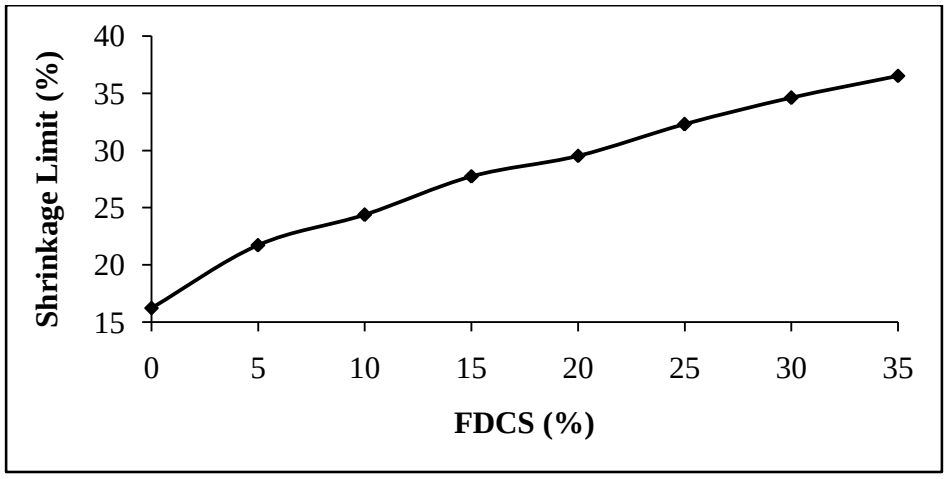

Figure 5.98 Shrinkage Limit of Soil-FDCS Mixtures

5.6.2 Free Swelling Index (FSI)

The effects of FDCS addition on the FSI of the expansive soil is presented in Figure 5.99. As expected, free swelling index decreases with increase in FDCS content upto 35%. 7.41%, 13.13%, 23.27%, 32.54%, 44.94%, 56.33% and 60.56% are the percentages which actually reduced on admixing of FDCS with expansive soil when FDCS was incorporated @ 5%, 10%, 15%, 20%, 25%, 30% and 35% respectively. From this analysis, it is very clear to conclude that the rate of reduction in FSI on admixing FDCS is comparable with other additives like FA, RHA, BA and RSA. This effect is attributed to the increase friction within the matrix upon the action of very fine FDCS and the self-hardening effect related to the presence of free lime.

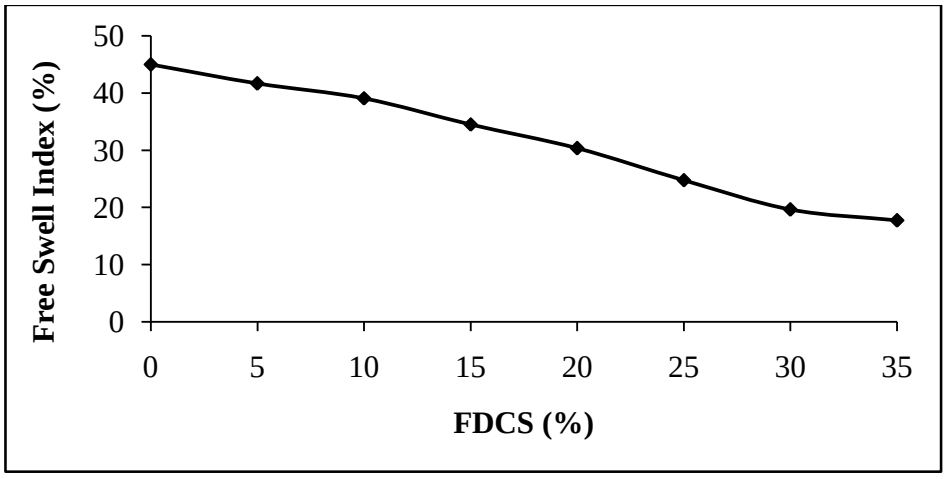

Figure 5.99 Free Swelling Index of Soil-FDCS Mixtures

5.6.3 Proctor Test

The effects of FDCS addition on OMC of the mixtures are shown in Figure 5.100. The trend of OMC increase was very similar with the case of FA, RHA, RSA and BA. However, at 5% FDCS inclusion level, the increase in OMC was slightly pronounced than the rest inclusion levels. This might be due to improper mixing of the materials. The percentage increase in OMC due to admixing of FDCS are 11.8%, 14.7%, 17.6%, 21.2%, 23.5%, 25.9% and 28.2% when FDCS was admixed @ 5%, 10%, 15%, 20%, 25%, 30% and 35% respectively with respect to expansive soil. The increased in OMC on admixing of FDCS was comparable with all the selected additives except RHA admixed soils.

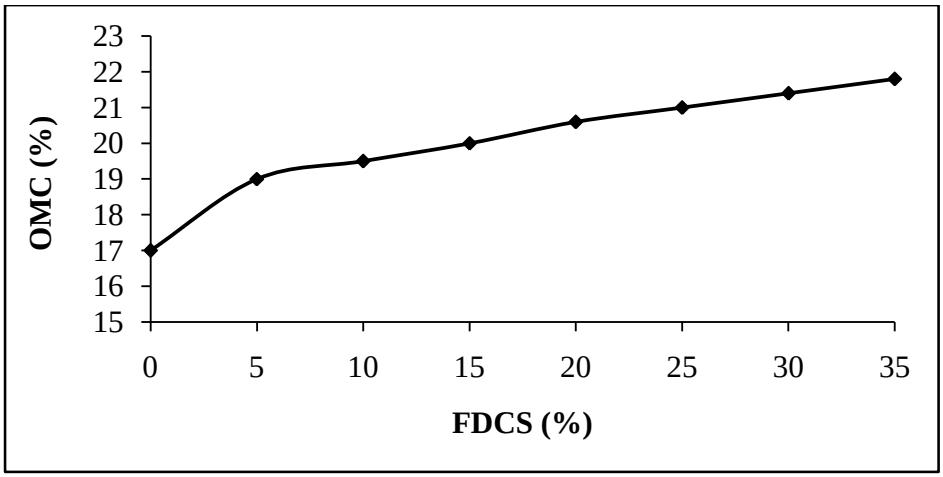

Figure 5.100 OMC of Soil-FDCS Mixtures

The addition of FDCS played an important role in the development of dry density of FDCS admixed soils. It was observed that the values of dry density decreases, while increasing the amount of FDCS like in the case of other additives as shown in Figure 5.77. However, the maximum reduction in dry density was offered by RHA admixed soils followed by RSA, FDCS, BA and FA admixed soils respectively irrespective of inclusion levels. This effect may be attributed to the increase of pozzolanic reaction upon the action of very fine FDCS and the self-hardening effect related to the presence of free lime by virtue of high lime reactivity material.

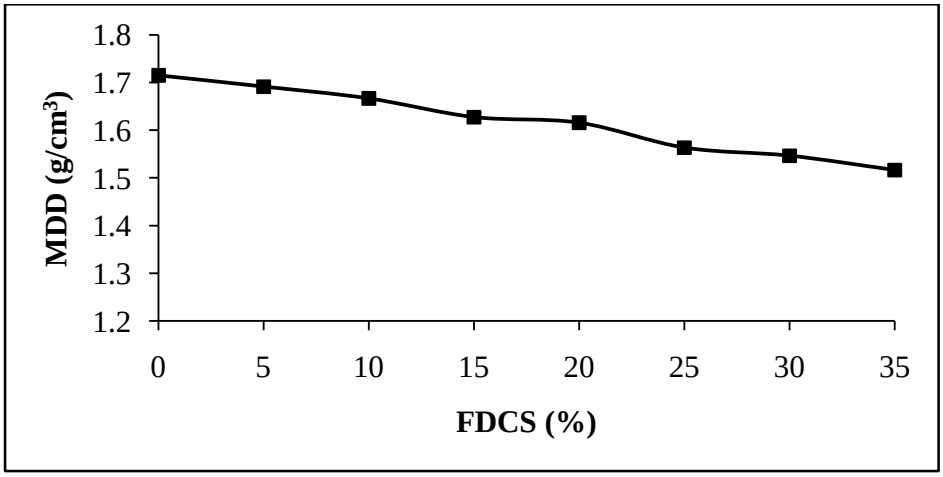

Figure 5.101 MDD of Soil-FDCS Mixtures

5.6.4 California Bearing Ratio Test

The effect of addition of FDCS on CBR value for a period of 3, 7, 14, 28, 56 and 128 days are shown in Figure 5.102. As it was expected, addition of FDCS increases CBR value remarkably. The CBR is increased non-linearly with the increase in FDCS content in soil. The percentage increase of CBR value after admixing FDCS @ 5%, 10%, 15%, 20%, 25%, 30% and 35% are 455.4%, 659.7%, 891.9%, 1022.0%, 1154.8%, 1245.2% & 1307.0% respectively with respect to expansive soils. The improvement of CBR is significant upto 35% FDCS inclusion level irrespective of curing time. However, very slight decrease in CBR value is observed beyond 25% FDCS inclusion level.

It is also found from the laboratory test results that there is an increase in CBR value as the relative humidity curing time increases. These increases are about 10.9%, 16.7%, 20.9%, 23.8% & 25.5% respectively for 7, 14, 28, 56 & 128 days with respect to 3 days curing for 35% FDCS inclusion level. Maximum CBR value was offered by the soil samples kept in humidity condition continuously for 7 days prior soaking. This inference that to elevate maximum strength of admixed soils, test specimen shall be subjected to relative humidity curing for atleast 7 days prior soaking. CBR value improvement on admixing of FDCS is mainly attributed to very fine particles of FDCS which could rearrange better particles distribution of the matrix. The main physical action is that of packing of the FDCS particles at the interface of soil particles. Also due to possibility of having some pozzolanic reaction from unhydrated cement grain presence in FDCS.

5.6.5 Expansion Ratio

The effect of FDCS on expansion ratio of the mixtures is evaluated and the same in presented in Figure 5.103. The pattern of plot connotates decrease of expansion ratio on admixing of FDCS. Reduction in expansion ratio is higher for higher FDCS inclusion level. The rate of decrease in expansion ratio is very significant at 5% FDCS inclusion level. Beyond this level, the rate of ER reduction is gradual upto 35% FDCS content. The percentage reduction in expansion ratio after admixing BA @ 5%, 10%, 15%, 20%, 25%, 30%, and 35% are 27.5%, 35%, 42.5%, 50%, 57.5%, 62.5% and 65% respectively. It is very pertinent to point out here

that amongst all considered additives, the performance of FDCS seems to be the best in controlling ER of expansive soils.

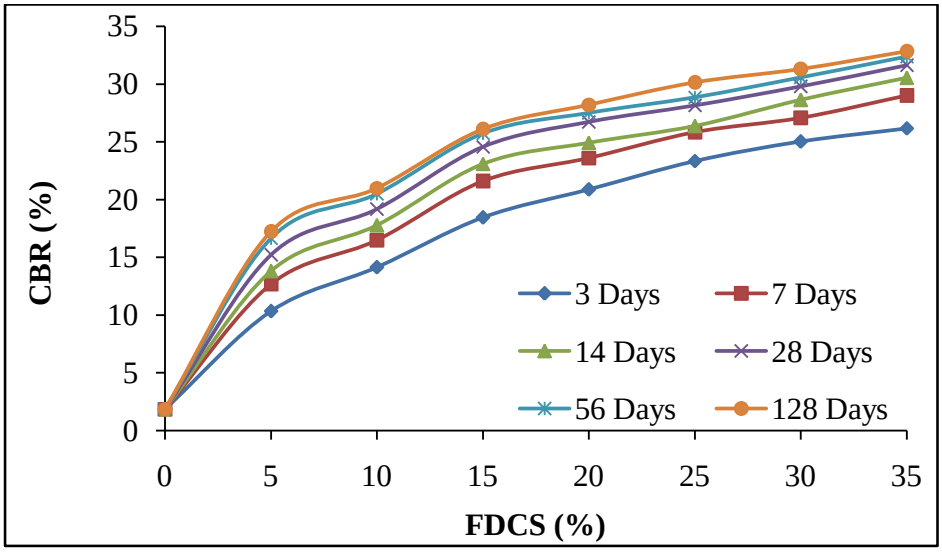

Figure 5.102 CBR of Soil-FDCS Mixtures

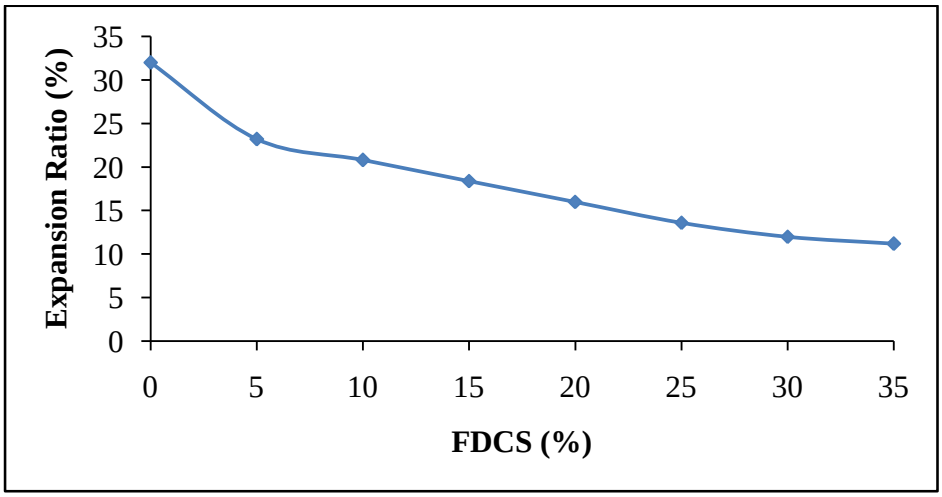

Figure 5.103 Expansion Ratio of Soil-FDCS Mixtures

5.6.6 Hydraulic Conductivity Test

As it can be seen from Figure 5.104, significant amount of coefficient of permeability decreased is observed on admixing of FDCS. Permeability of expansive soil was found to be 3.3×10^{-7} cm/sec. Rate of reduction in permeability of expansive soil on admixing FDCS is gradual as it can be seen for other additives. Higher reduction in permeability is observed for

higher FDCS inclusion levels. The percentage of permeability decrease after admixing FDCS @ 5%, 10%, 15%, 20%, 25%, 30% & 35% are 43.9%, 56.2%, 68.4%, 71.2 %,80.1%, 84.1% & 86.8% respectively. After having this analysis, FDCS once again proved to be that additive, which enables to reduce the coefficient of permeability of expansive soil at maximum.

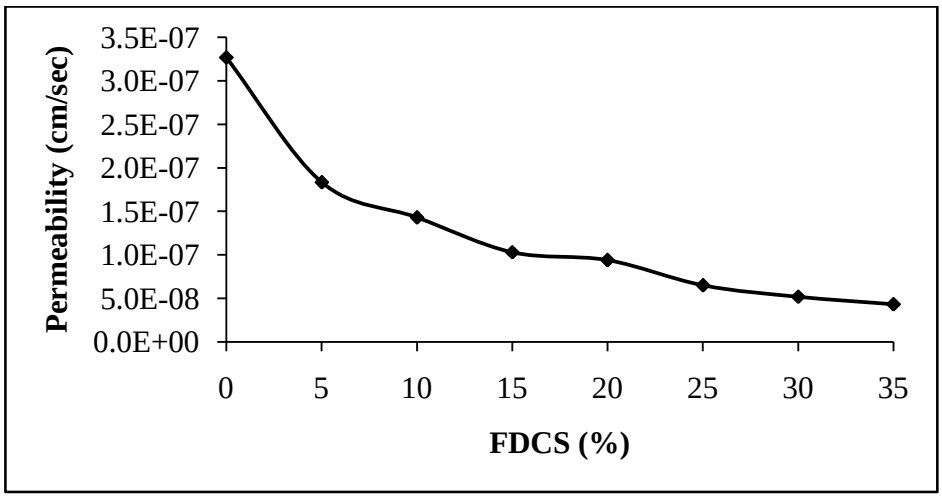

Figure 5.104 Permeability of Soil-FDCS

5.6.7 Unconfined Compressive Strength Test

Admixing of FDCS to expansive soil substantially increased UCS irrespective of days of curing. The maximum increase of UCS is observed at 20% inclusion level. Beyond 20%, the improvement rate of UCS stabilized to a larger extent beyond 30% inclusion levels also as it can be seen from Figure 5.105. Considering overall performance of UCS improvement, the percentage increase of UCS on admixing FDCS @ 5%, 10%, 15%, 20%, 25%, 30% & 35% are 72.00%, 98.89%, 116.12%, 131.05%, 136.64%, 142.67% & 143.97% respectively at 7 days curing with respect to expansive soil. Whereas for 14 days, 28 days, 56 days and 128 days cured samples, these values further increased to 87.43%, 119.45%, 135.11%, 149.46%, 155.71%, 164.90% & 175.07%; 92.03%, 129.01%, 149.29%, 166.02%, 171.33%, 179.03% & 188.94%; 98.49%, 136.89%, 159.90%, 180.73%, 183.16%, 192.41% & 202.46%; and 111.97%, 148.47%, 169.23%, 187.82%, 189.72%, 199.09% & 212.97% respectively. If percentages increase of UCS after admixing of FA, RHA, BA, RSA, FDCS and BF to expansive soil are compared, the performances of additives superior to inferior are listed as follows: BF > FDCS > RSA > RHA > FA respectively.

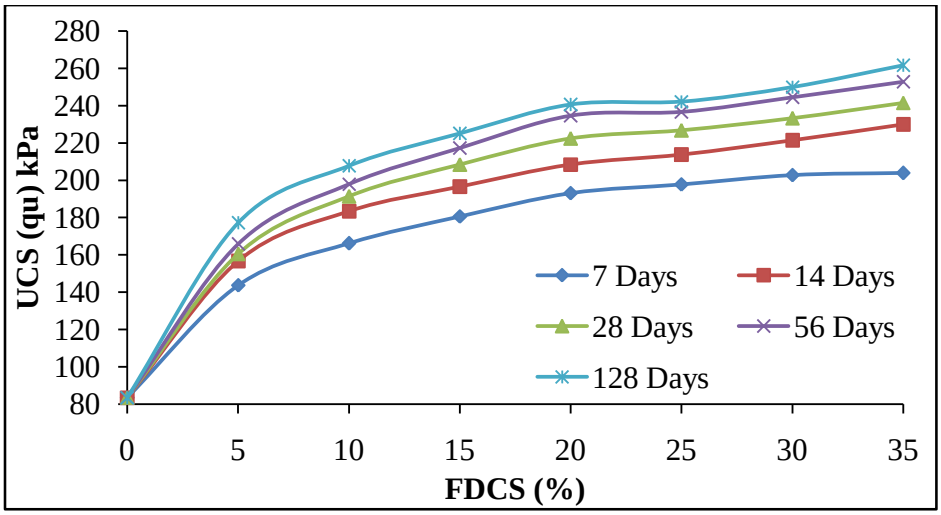

Figure 5.105 UCS of Soil-FDCS Mixtures

5.6.8 Split Tensile Strength Test

Marked improvement in split tensile strength is observed on admixing of FDCS as depicted in Figure 5.106. Maximum tensile strength was observed at 15% FDCS inclusion level. Beyond this level, tensile strength improvement stabilized to large extent beyond 30% FDCS inclusion levels. Therefore, maximum FDCS inclusion level which could produce maximum tensile strength of expansive soil ranges from 15% to 35%. At 35% FDCS inclusion level, about 109.8%, 115.3%, 125.1%, 128.7% & 129.1% improvements on split-tensile strength were observed at 7, 14, 28, 56 and 128 days respectively with respect to expansive soil.

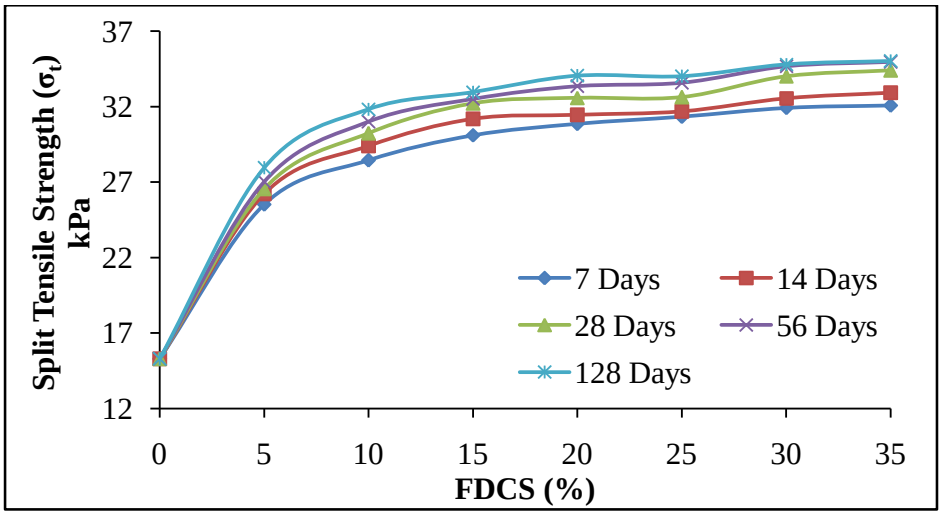

Figure 5.106 Split Tensile Strength of Soil-FDCS Mixtures

5.6.9 Ratio of Split Tensile to Unconfined Compressive Strength Test

The relative relationship and mobilization between the tensile strength and compressive strength could be discussed by plotting the tensile/compressive strength ratio (σ_t/q_u) versus curing time. Figure 5.107 shows the influence of FDCS content on the ratio of split tensile strength and unconfined compressive strength. The results show that unconfined compressive strength and split tensile strengths are closely related. It can be observed that the ratio of split tensile strength and unconfined compressive strength decreased with increase in FDCS content, indicating that FDCS is more efficient when soil was subjected to compression rather than to tension.

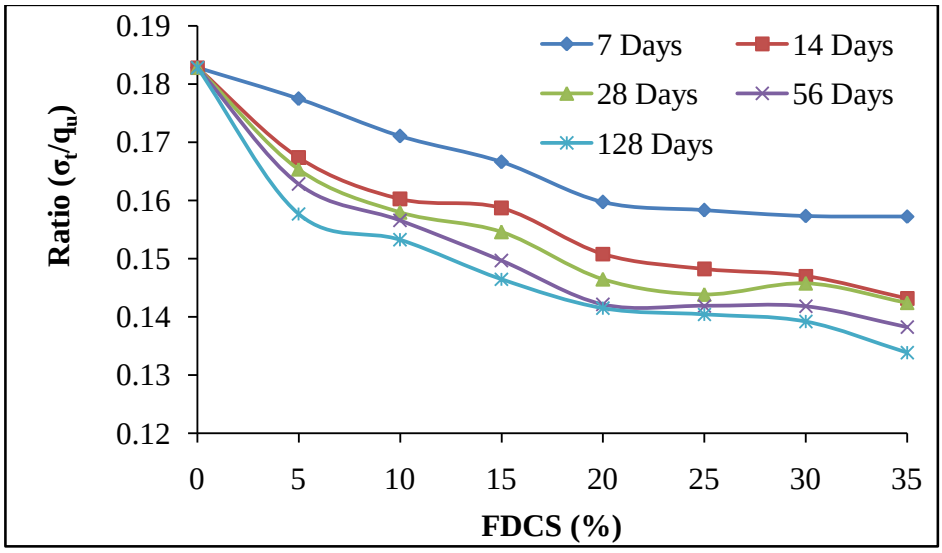

Figure 5.107 σ_t/q_u Ratio of Soil-FDCS Mixtures

5.6.10 Triaxial Test

Three different confining stresses such as 100, 150 and 200 kPa were applied on specimens to obtain peak deviator stress as shown in Table 5.5. The range of confining stresses was chosen to obtain more well defined and accurate plots of Mohr envelopes to obtain shear strength parameters cohesion (c) and angle of internal friction (φ) of the soils mixed with FDCS. The variation of c and φ with admixing FDCS are evaluated and results are as shown in Figures 5.108 & 5.109 respectively.

Table 5.5 shows the deviator stress of soil admixing of FDCS after 7, 14, 28, 56 & 128 days curing period at three different confining pressures. Higher deviator stresses are observed for higher FDCS content irrespective of confining pressure applied and days of curing. Admixing of FDCS causes increase in cohesion and internal friction angle. Increase in cohesion is more pronounced upto 10% FDCS content. The cohesion of soil ranges from 28 to 55.23 kPa and from 28.5 to 67.67 kPa at 7 days and 128 days curing respectively, for FDCS contents between 0 & 35 %. Improvement on cohesion due to addition of FDCS becomes sluggish beyond 10% inclusion level. However, these cohesions are much higher than that of expansive soil. As in the case of cohesion, similar trend of improvement is observed for internal friction angle. The rate of improvement of internal friction angle is rapid for 5% FDCS, after which the rate of improvement is gradual. In overall, these internal friction angles are higher than expansive soil irrespective of days of curing (Figure 5.109). Improvements on cohesion and internal friction angle on admixing of FDCS. Increase of "c" value on admixing may be due to binder effect imparted by ultra fines mortar powder to soil particles and reason for increase of internal friction angle on admixing of FDCS may be due to the fact that the internal friction angle of FDCS is more than that of soil.

Table 5.5 Deviator Stress for FDCS Admixed Soil at Different Confining Pressure

% FDCS	Confining Pressure (kPa)	Deviator Stress (kPa)				
		7 Days	14 Days	28 Days	56 Days	128 Days
0	100	205.34	206.19	204.83	205.01	204.47
	150	275.91	277.81	276.52	278.17	276.24
	200	337.11	339.77	337.97	338.87	339.18
5	100	359.50	388.62	394.95	404.90	434.18
	150	474.54	509.10	513.44	522.32	555.75
	200	593.18	637.34	643.77	655.94	699.03
10	100	410.71	449.51	465.25	477.31	502.71
	150	538.04	584.36	600.18	610.95	638.44
	200	665.36	723.71	744.40	758.92	794.28
15	100	440.88	475.68	500.21	525.83	542.46
	150	573.15	613.62	640.27	667.81	694.35
	200	714.23	765.84	800.34	836.08	861.16
20	100	475.20	508.88	547.12	579.72	596.76

	150	622.51	671.72	722.20	753.64	775.79
	200	769.83	824.38	880.87	927.56	948.86
25	100	490.66	528.06	560.31	582.36	607.98
	150	628.04	681.20	717.20	751.24	766.05
	200	789.96	850.18	897.90	927.70	960.61
30	100	505.18	554.79	583.21	616.05	632.64
	150	646.63	704.58	734.85	770.07	787.64
	200	813.34	890.43	930.23	973.36	995.14
35	100	503.81	565.74	578.56	589.18	613.58
	150	649.91	724.15	743.45	743.25	794.59
	200	811.13	905.18	923.38	933.85	972.52

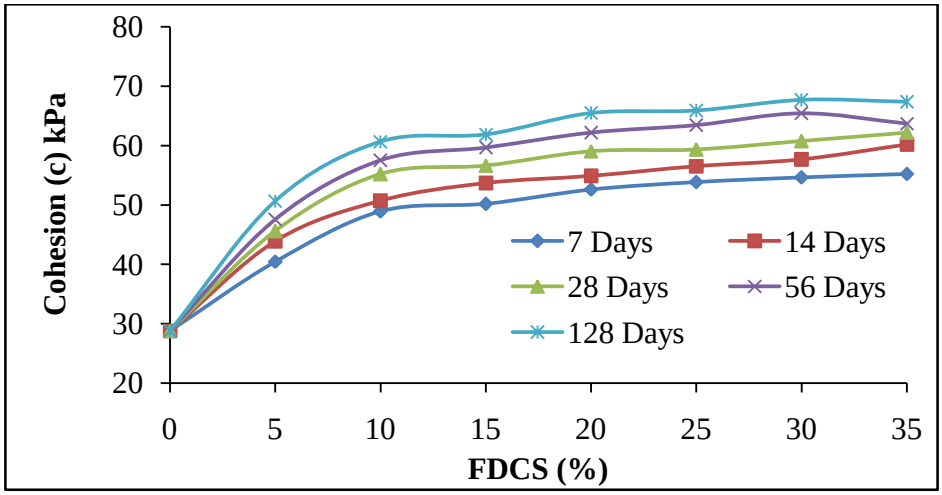

Figure 5.108 Cohesion of Soil-FDCS Mixtures

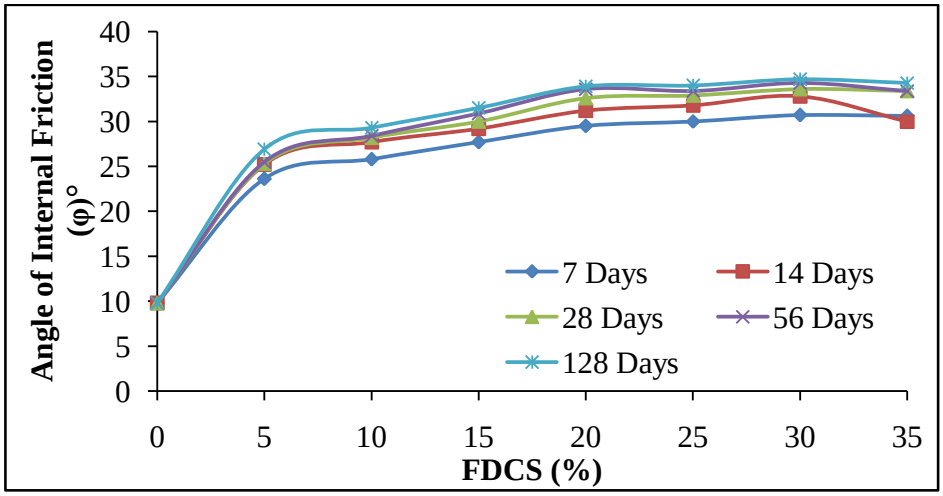

Figure 5.109 Angle of Internal Friction, Soil-FDCS Mixtures

5.6.11 Cyclic Triaxial Test

The effects of various percent of FDCS and loading cycles on the permanent deformations of the expansive soil and RHA admixed soils were studied. The effects of DSL ratios and confining pressure with number of loading cycles on the permanent deformations were studied for all admixed soils. Three confining pressures such as 100, 150 & 200 kPa and two DSL as 0.5 and 0.8 were taken for determination of permanent strain upto 10000 cycles under constant axial loading. The test results are plotted for vertical percent permanent strain as ordinate and number of cycles as abscissa and are presented in Figures 5.110 and Figure 5.111 at DSL 0.5 and 0.8 respectively.

5.6.11.1 Effect of load cycle

Rapid increase in deformation of the expansive soil and FDCS admixed soils were observed during the initial approximate hundred cycles of loading and the strain rate was high during this stage in all cases as shown in Figures 5.110 and 5.111. After few hundred cycles of loading, the increase in deformation was progressively increased upto 2000 cycles thereafter deformation almost stabilized for FDCS admixed soils. But deformation still taken placed for expansive soil. For FDCS admixed soils, the matrix behaves almost elastically under the applied load. The maximum permanent strain of 6.15 % was observed for expansive soil when 0.8 DSL & 100 kPa confining pressure were applied. Consequently, the minimum permanent strain of 1.80% was measured for 35% FDCS inclusion level by applying 0.5 DSL & 200 kPa confining pressure for 10000 cycles.

5.6.11.2 Effect of confining pressure

Effort was made to study the permanent deformation characteristics of expansive soil and FDCS admixed soils at pre-determined three different confining pressures. Figures 5.110 [(a) to (c)] and 5.111 [(a) to (c)] illustrate the permanent deformation at the confining pressure of 100 kPa, 150 kPa and 200 kPa respectively. Out of this study, the minimum permanent deformation observed after 10000 cycles at 100 kPa, 150 kPa and 200 kPa confining pressure are 2.05 %, 2.00 % & 1.80 % % respectively at 0.5 DSL. Whereas, the permanent deformation for 0.8 DSL under the same working condition are 3.03%, 2.64% & 2.35% respectively. Present analysis suggested that permanent deformation decreases with increase in confining

pressure irrespective of types of samples. However, least permanent deformation was recorded for 35% FDCS inclusion level.

5.6.11.3 Effect of deviator stress level

The permanent strain values measured at 0.5 DSL for expansive soil and FDCS admixed soils are illustrated in Figure 5.110. To appreciate better the effect of σ_d the permanent strain recorded at 0.8 DSL is also presented in Figure 5.111. These different plots have been established considering all the three different confining pressure. Increase of σ_d value signifies improvement in permanent strain. Out of this investigation, the least value of σ_d was observed for 30% FDCS admixed soils (1.80%) for 0.5 DSL at 200 confining pressure. Whereas for 0.8 DSL, 2.35% was observed. This again confirmed that least permanent deformation is offered by 30% FDCS inclusion level.

For analysis of M_R results, set of six tests were conducted on both expansive soil and FDCS admixed soils. Tests were conducted at two pre-determined deviator stress level i.e. 0.5 DSL & 0.8 DSL. Similarly, three confining pressures of 100 kPa, 150 kPa and 200 kPa were chosen for the test. Throughout the test, the aforementioned DSL rates and confining pressures were maintained. The main objective of this study was to understand the effects of confining pressure and DSL on expansive soil and RSA admixed soils.

Figure 5.112 reveals that an increase in confining pressure resulted enhancements of M_R of all cases but these value diminish at higher DSL value. M_R values increase with increase in FDCS content irrespective DSL and confining pressure. The maximum M_R values observed were 110 MPa & 69 MPa at 0.5 & 0.8 DSL respectively for a constant 200 kPa confining pressure when no admixing was done. But these values increase to 297 & 167 MPa respectively after admixing of 30% FDCS. This effect may be attributed to a stiffer soil skeleton structure of admixed soils caused by increased confinement and pozzolanic reactions, which result in a closer bonding of soil particles.

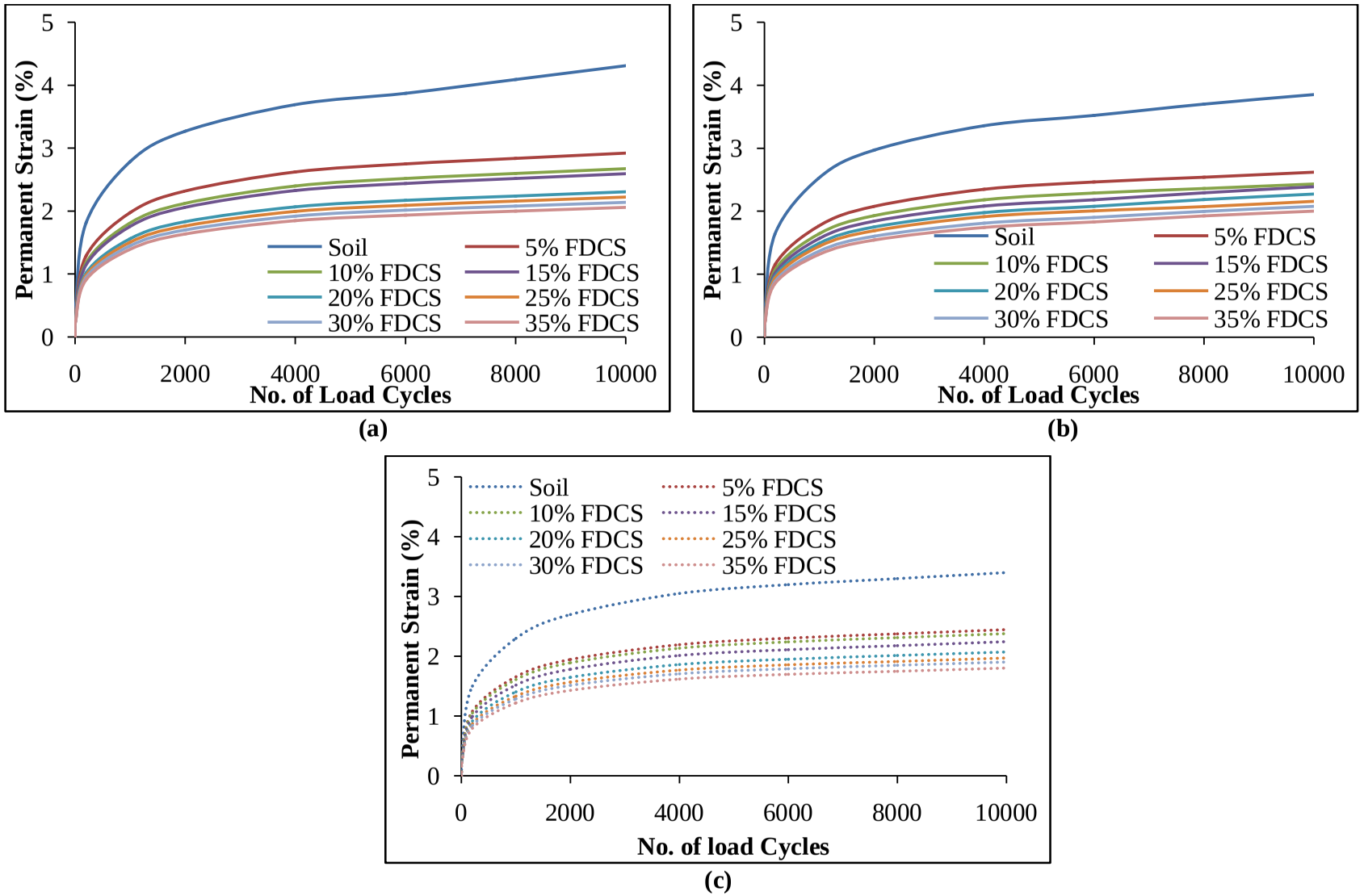

Figure 5.110 Permanent Strain of Soil-FDCS Mixtures at 0.5 DSL (a) at 100 kPa CP (b) at 150 kPa CP (c) at 200 kPa CP

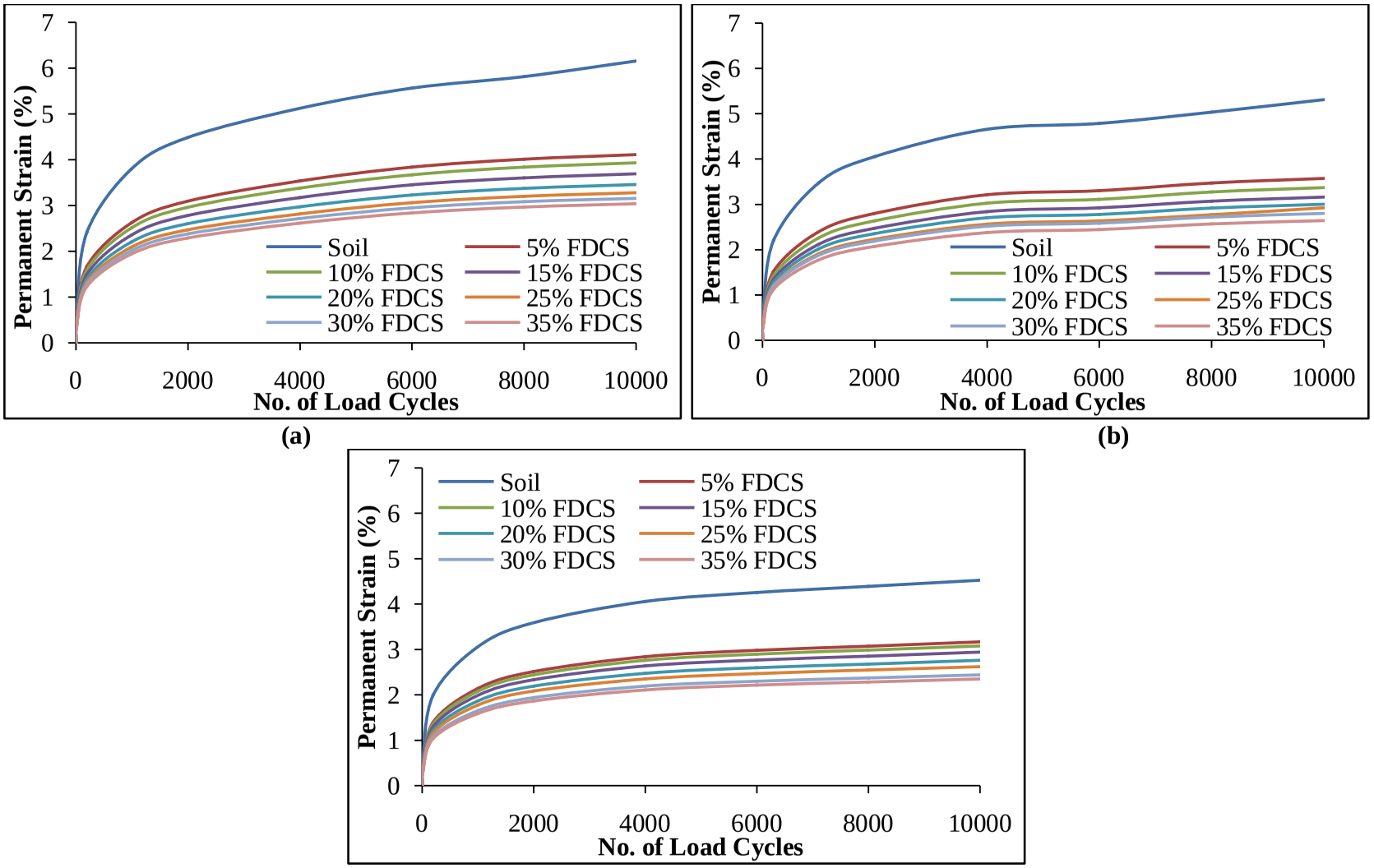

Figure 5.111 Permanent Strain of Soil-FDCS Mixtures at 0.8 DSL (a) at 100 kPa CP (b) at 150 kPa CP (c) at 200 kPa CP

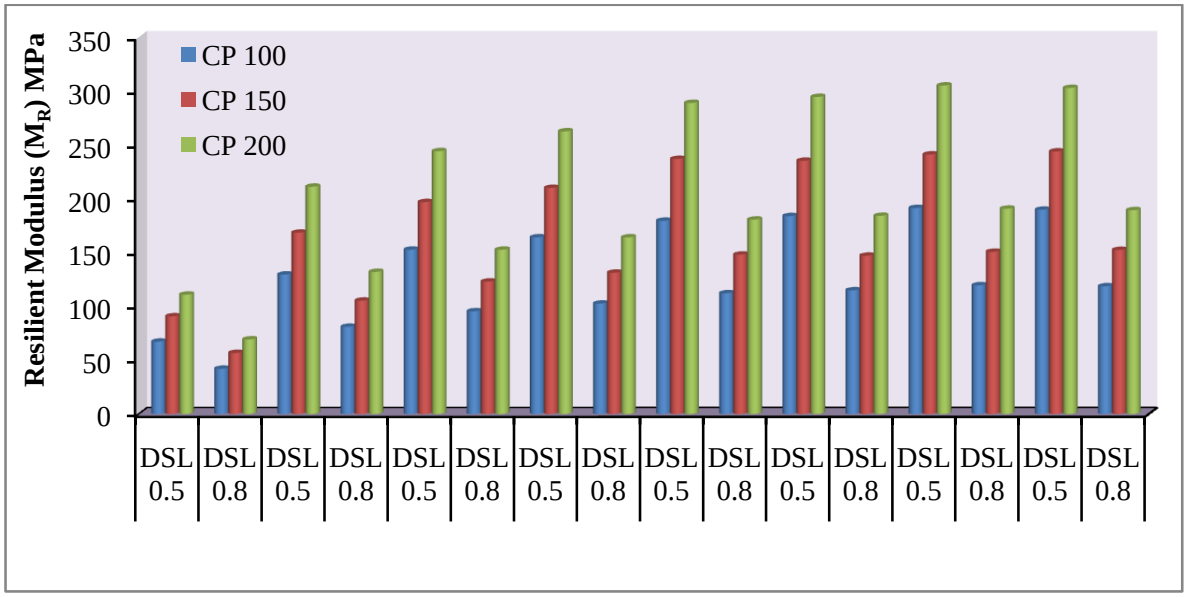

Figure 5.112 Resilient Modulus of Soil-FDCS Mixtures

5.6.12 Plate Load Test

The influence of FDCS in improving the modulus of subgrade reaction (k) of mixtures was evaluated by comparing the measured k-values for the natural expansive soil and soil-FDCS mixtures. Inclusion of FDCS to expansive soil considerably improved k-value as presented in Figure 5.113. The modulus of subgrade reaction of expansive soil was found to be 17 MPa/m. The rate of improvement of k-value is significant upto 5.0% RSA inclusion level beyond which rate of increase of k-value starts declining. If FDCS was admixed with expansive soils @ 5%, 10%, 15%, 20%, 25%, 30% & 35%, the percentages increase of k-values were 243.5%, 307.9%, 358%, 400%, 425.5%, 451.7%, and 470.4% respectively.

Efforts have also been made to obtain load-settlement curves using laboratory data accrued from the plate load tests. As definite yield point could not be obtained from the derived curves, the ultimate bearing capacity for expansive soil and FDCS admixed soils were worked out by extending tangents from the two straight portions of the load-settlement curve one at the initial straight portion and another tangent at the steeper straight portion at the end.

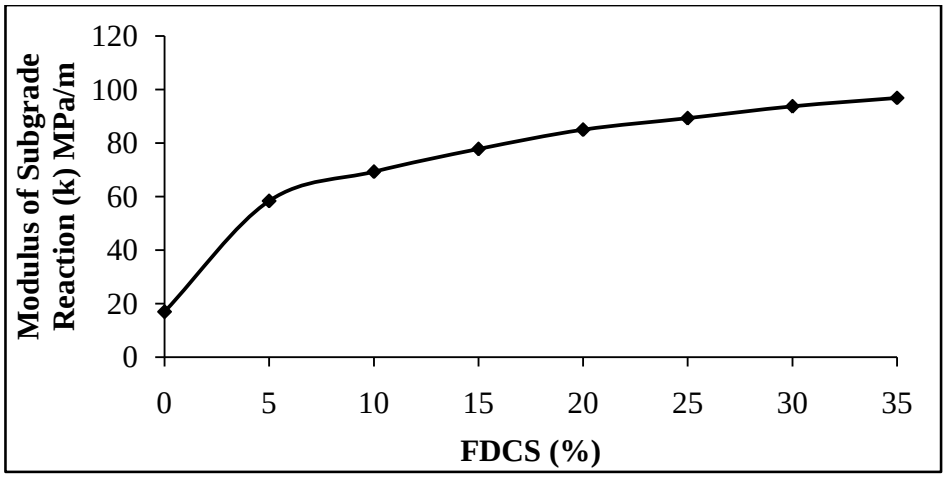

Figure 5.113 Modulus of Subgrade Reaction of Soil-FDCS Mixtures

Figure 5.114 shows the ultimate bearing capacity of soils with or without FDCS. 198 kPa ultimate bearing capacity was noted for natural expansive soil. This capacity improves significantly on inclusion of FDCS and better improvement in bearing capacity was noted for higher FDCS inclusion level. The percentage improvement of bearing capacity at 7 days are 36.4%, 47.5%, 55.6%, 60.6%, 65.7%, 67.7% & 61.6% on admixing of FDCS @ 5%, 10%, 15%, 20%, 25%, 30% & 35% respectively. The increase of ultimate load due to admixing of FDCS is observed upto 30 %, beyond which it starts declining.

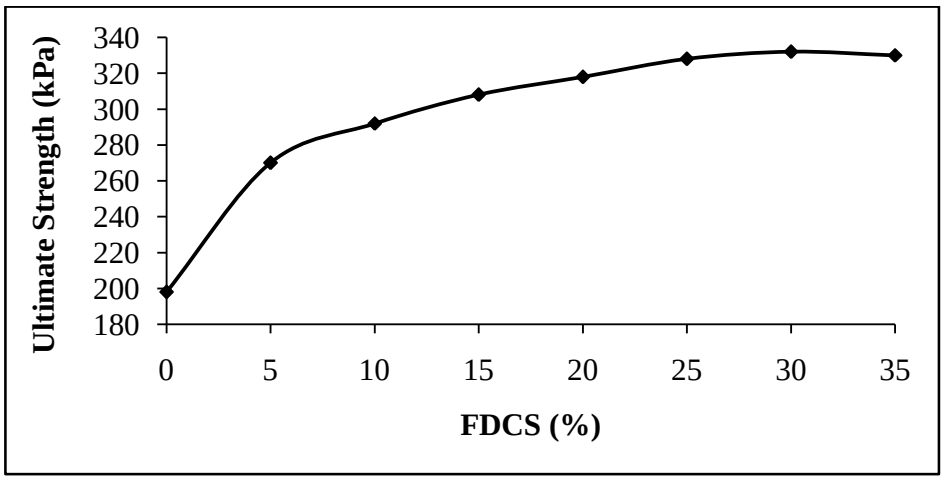

Figure 5.114 Ultimate Strength of Soil-FDCS Mixtures

5.6.13 Microstructural Investigation

The microstructure of FDCS obtained tested concrete cube was investigated by using Scanning Electron Microscope (SEM). The images from Scanning Electron Microscope taken at 500 X magnification are shown in Figures 5.115 (a to d). Granular structures of FDCS are prominently observed in all the SEM images. Few remnant cement grains could also be noticed. SEM images 1.115 (b) & (d) are strongly suggestive of formations of C-S-H gels, ettringite and $Ca(OH)_2$ hydrated compounds. However, TEM study is suggested to digest better about the formations of these compounds. But one thing is very clear that matrix is densely packed and there is a great tendency to develope a strong interaction between soil particles and FDCS. Particles with various sizes and geometry like prismatic, spherical and fibrous have figured out. Few of them may be of SiO_2 compound particular prismatic structures.

5.6.14 Correlation between Different Strength Parameters

5.6.14.1 Relation between CBR, % FDCS & Curing Days

The correlation between CBR, %FDCS and curing days (D) was established using multiple linear regression analysis (MLRA). Test results obtained at 7, 14, 28 & 56 days of curing were considered for the analysis. The developed relation is given in Eqn. (5.9), with $R^2 = 0.851$. High values of R^2 show close proximity to predicted values with experimental data. The validation of the developed relation was done using laboratory CBR values obtained at 128 days of curing. CBR results obtained through predicted equation [CBR (P)] and CBR results accrued from the laboratory [CBR (L)] were compared as shown in Figure 5.116. The equation has acceptable values of R^2 suggesting closeness of predicted values with the experimental data.

$$CBR = 7.17 + 0.723\%FDCS + 0.061D \quad (5.9)$$

where, CBR = California bearing ratio, % FDCS = percentage fine obtained from demolished concrete slab, D = number of curing days.

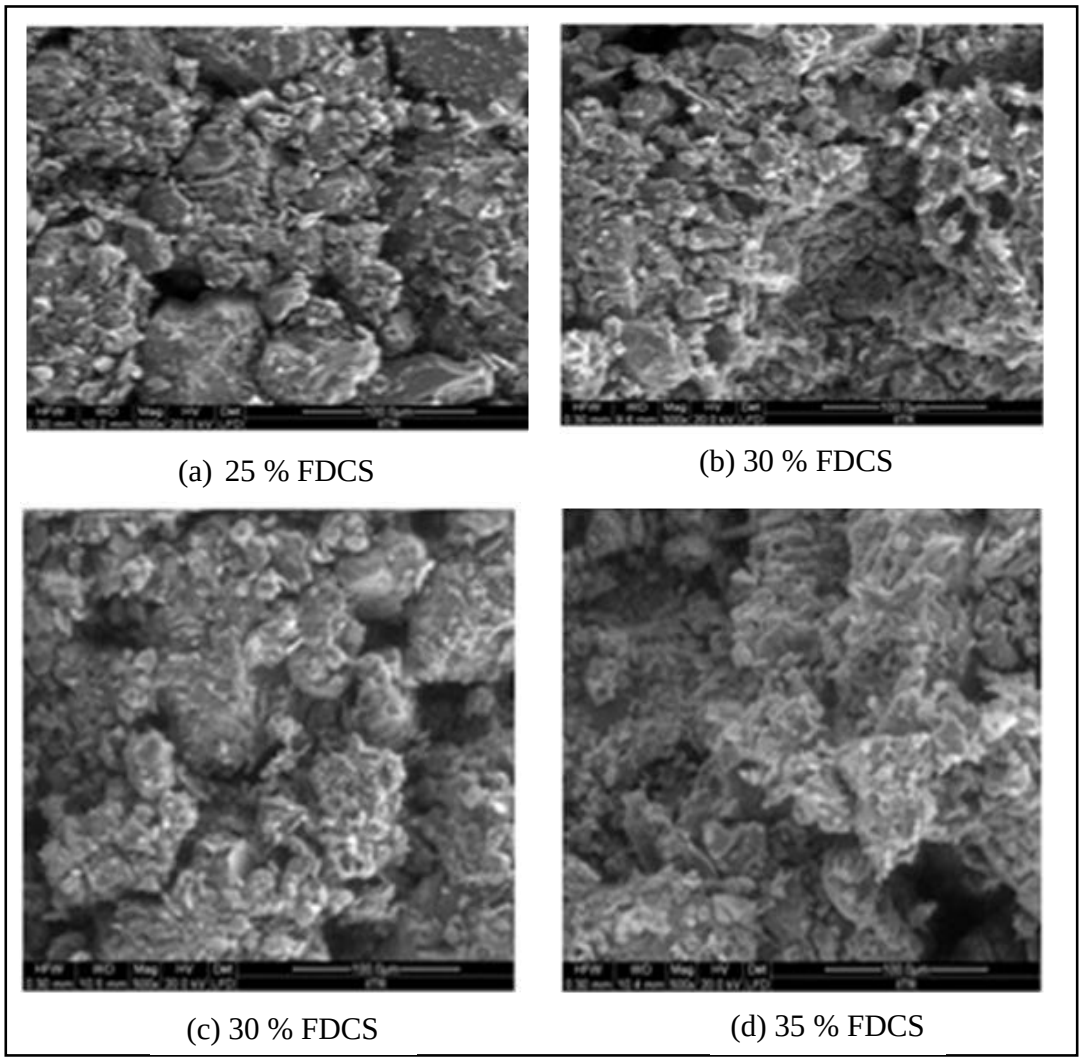

Figure 5.115 SEM Macrographs of Soil-FDCS Mixtures

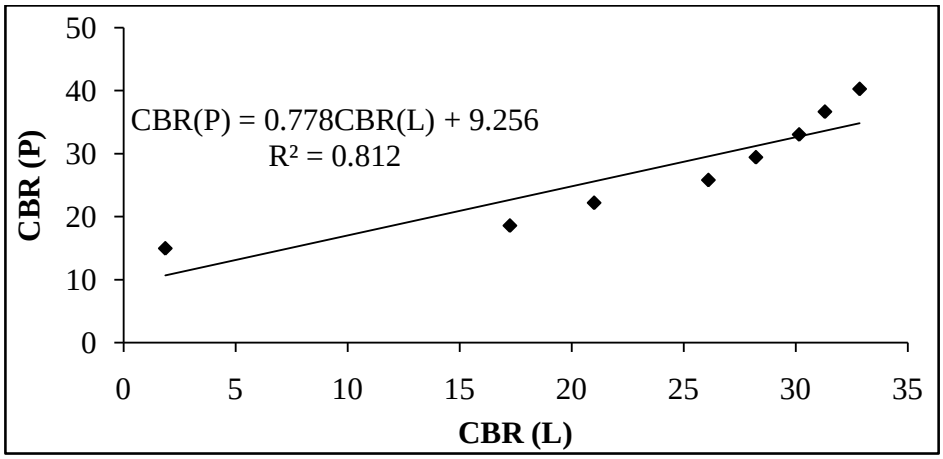

Figure 5.116 Validation of CBR Results for Soil-FDCS Mixtures

5.6.14.2 Relation between UCS, CBR, % FDCS & Curing Days

The relationship developed between UCS as dependent variable and other parameters as independent variable is given in Eqn. (5.10), with R^2= 0.986. UCS test results of 128 days were used for validation of the predicted equation. Predicted UCS [UCS (P)] values and laboratory UCS [UCS (L)] values were compared as shown in Figure 5.117. As this equation showed high values of R^2, predicted UCS values have close proximity with experimental data.

$$UCS = 66.69-0.97\%FDCS + 0.201D + 6.27CBR \quad (5.10)$$

where, UCS = Unconfined compressive strength (kPa)

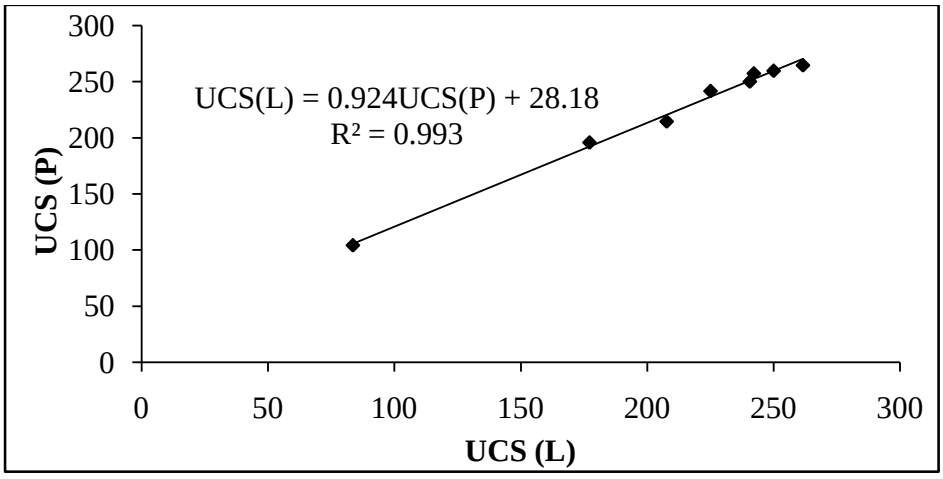

Figure 5.117 Validation of UCS Results for Soil-FDCS Mixtures

5.6.14.3 Relation between STS & UCS

Relationship has been established between split tensile strength and unconfined compressive strength of FA admixed soil samples from the data of present study. Various models like linear, exponential, polynomial, power and logarithmic were tested, but polynomial relation as shown in Figure 5.118 was best fitted with R^2 = 0.994. Further, the proposed equation was validated using STS laboratory results accrued after 128 days of curing as presented in Figure 5.119. The predicted STS [STS (P)] values and laboratory STS [STS (L)] values were compared and showed excellent relationship as high R^2 values exhibit between them.

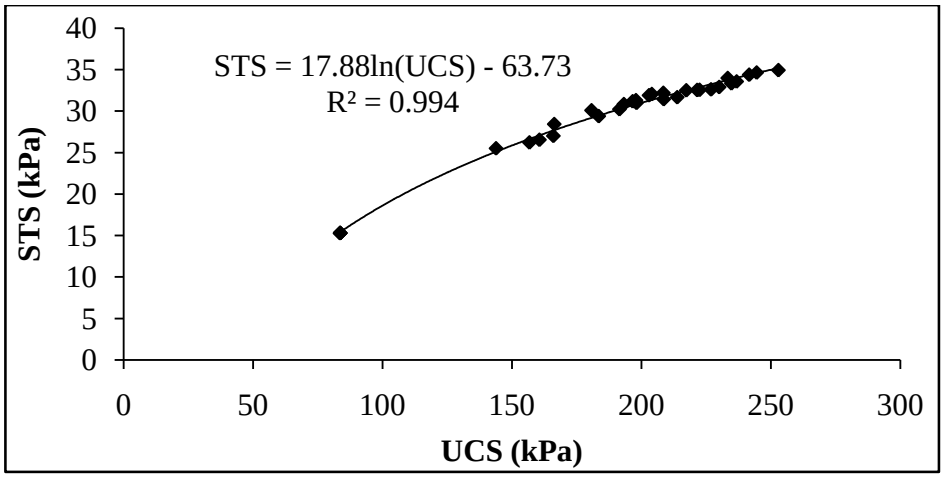

Figure 5.118 Relationship between STS & UCS for Soil-FDCS Mixtures

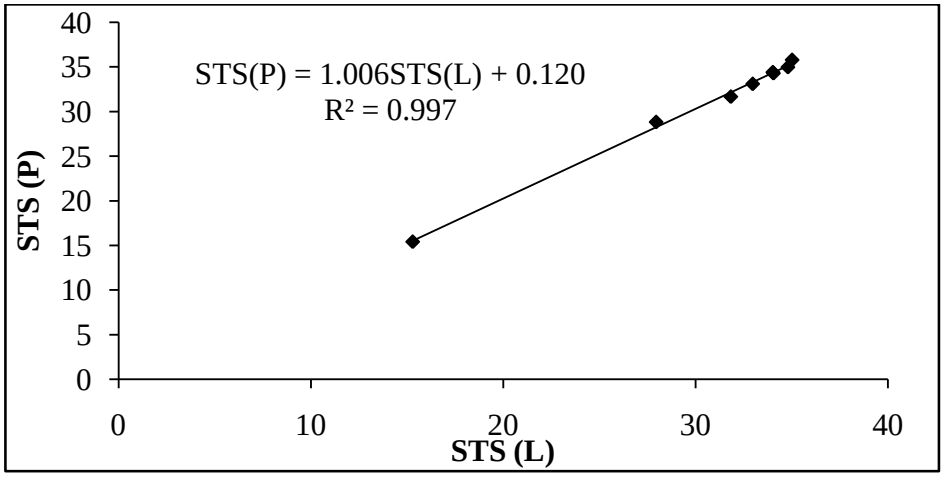

Figure 5.119 Validation Results for STS for Soil-FDCS Mixtures

5.6.14.4 Relation between M_R & CBR

The cyclic triaxial tests were conducted as per ASTM D5311-11 on natural expansive soil and FDCS admixed soil samples. Tests were conducted after the expiry of 28 days curing period. Three levels of σ_3 (50, 100 and 150 kPa) at 0.50 DSL and 0.80 DSL were applied during the test. The main intention behind this effort was to establish correlation between M_R & CBR using regression analysis for each three levels of σ_3 0.50 DSL and 0.80 DSL respectively. Mathematical analysis of data shows good relationship between M_R & CBR described by a power series as presented in Figure 5.120 (a to f).

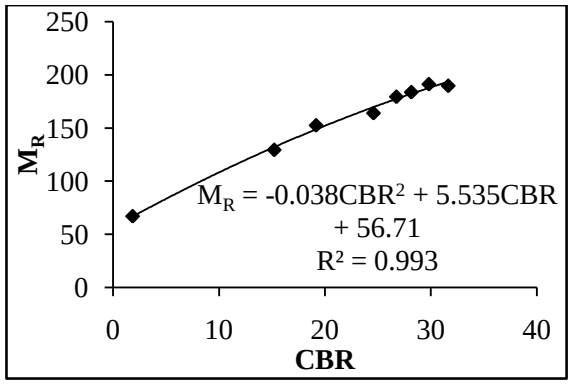

(a) CP 100, DSL 0.5

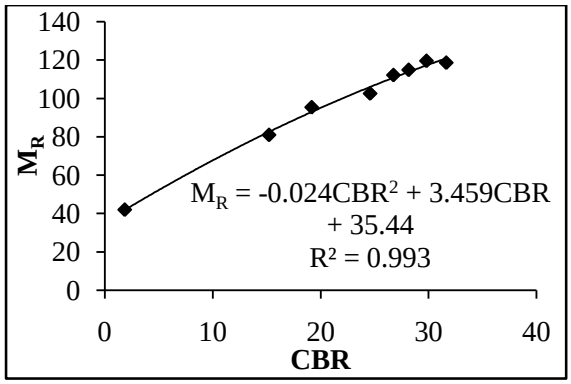

(b) CP 100, DSL 0.8

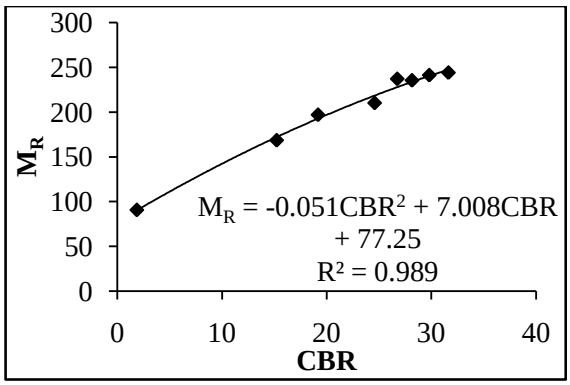

(c) CP 150, DSL 0.5

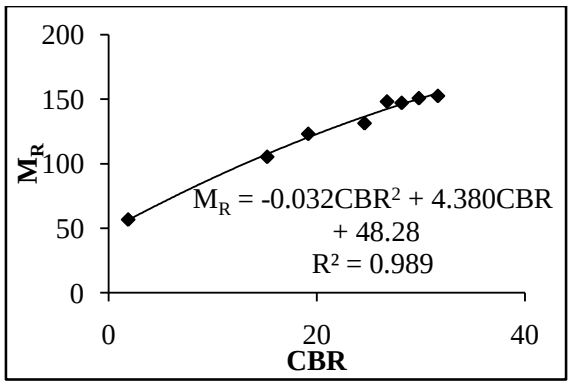

(d) CP 150, DSL 0.8

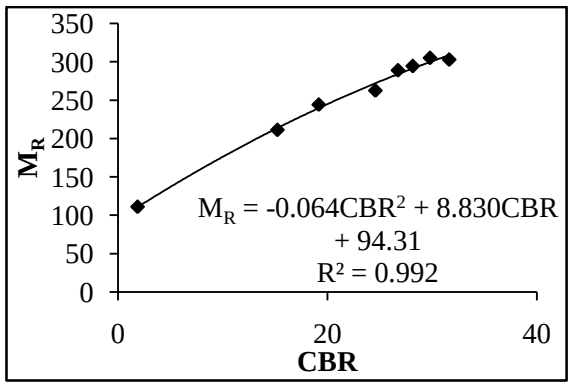

(e) CP 200, DSL 0.5

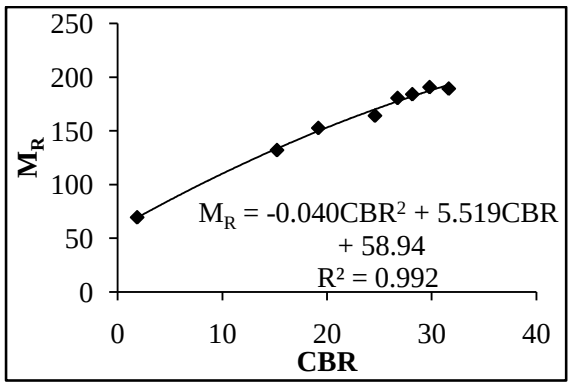

(f) CP 200, DSL 0.8

Figure 5.120 Relation between M_R & CBR for Soil-FDCS Mixtures

5.7 SOIL-BAGASSE FIBER

5.7.1 Proctor Test

Figure 5.121 shows the increasing trend of OMC for soil when percentage content of BF increases. About 5.9%, 10.0%, 18.8%, 25.9% 29.4%, 37.1% and 41.2% OMC increments were observed when BF was incorporated @ 0.5%, 1.0%, 1.5%, 2.0%, 2.5%, 3.0% and 3.5% respectively by weight of dry soil. This phenomenon was mainly due to high water absorption characteristics of BF, it's being cellulose material and porous in nature.

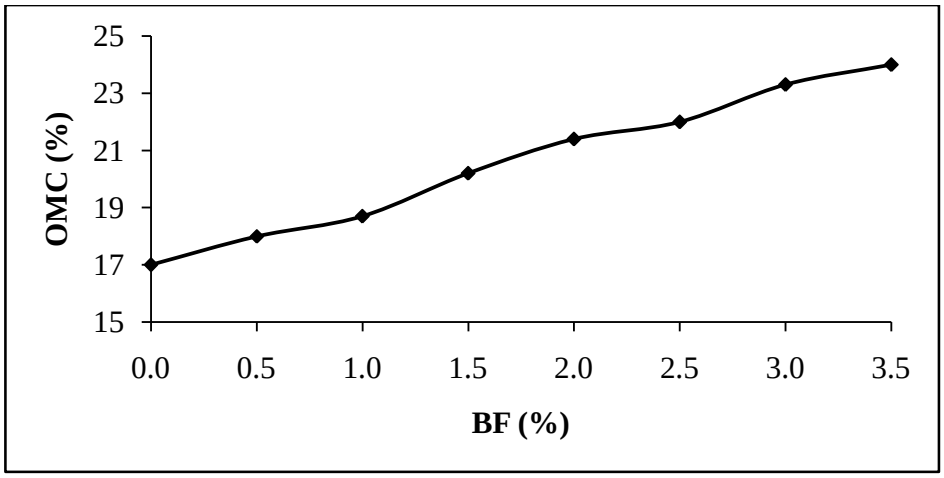

Figure 5.121 OMC of BF Reinforced Soils

As it can be seen from Figure 5.122, the dry density decrease with BF content irrespective of inclusion levels. The trend of decrease in dry density is similar to FA admixed soils. Maximum dry density reduction was noted at 2.5% BF inclusion level. This effect may be attributed to the lighter unit weight of BF than soil particles. Marandi et al. (2008) had studied on the behavior of silty sand soil by admixing palm fiber in it and they have suggested that incorporation of palm fiber increased OMC and decreased dry density of the matrix.

5.7.2 California Bearing Ratio Test

The results of CBR test clearly show that incorporation of BF has influenced CBR value. The improvement of soil strength in CBR due to the incorporation of BF is the function of soil and BF reinforcing effect. Figure 5.123 shows the CBR values of soil admixed with different percentages of BF. The CBR value of natural expansive soil was 1.86; by incorporating upto

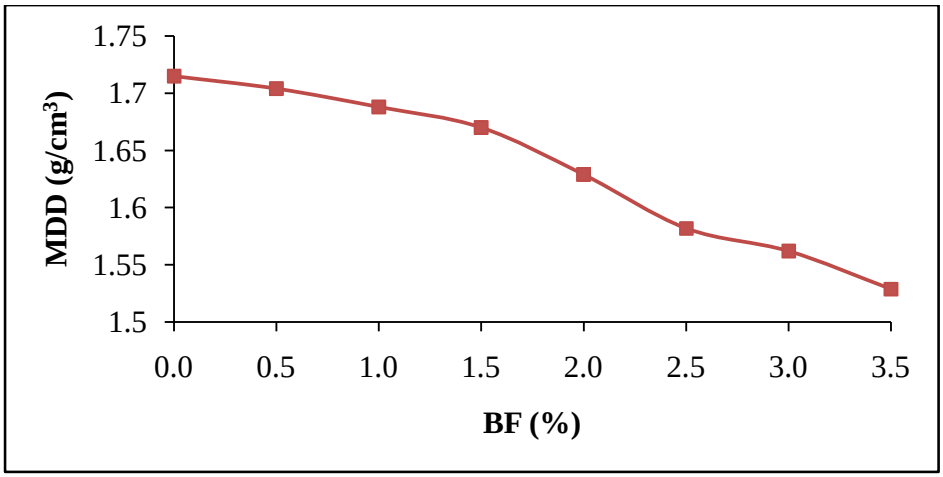

Figure 5.122 MDD of BF Reinforced Soils

3.5% by weight of dry soil, the maximum CBR value noted was 5.4 at 3.0% BF inclusion level. Beyond 3.0% inclusion of BF, there is no appreciable increase in CBR. This analysis suggests that the effect of BF addition on CBR at inclusion level below 3.0% is relatively low for road construction purpose. No appreciable increased in CBR values were observed with the curing period.

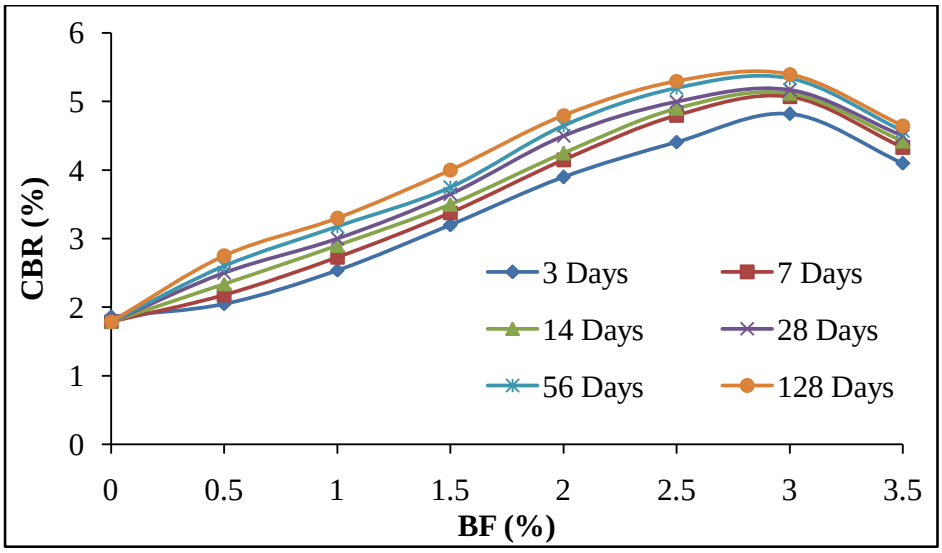

Figure 5.123 CBR of BF Reinforced Soils

5.7.3 Expansion Ratio

Expansion ratio decreases with the addition of BF increase as shown in Figure 5.124. By addition of BF upto 3.5%, ER for soil reinforced reduced to 18.4% from 32%. The rate of ER reduction maintained almost linear relationship with BF inclusion levels. This reduction is attributed to reinforcing effect imparted by BF within the matrix.

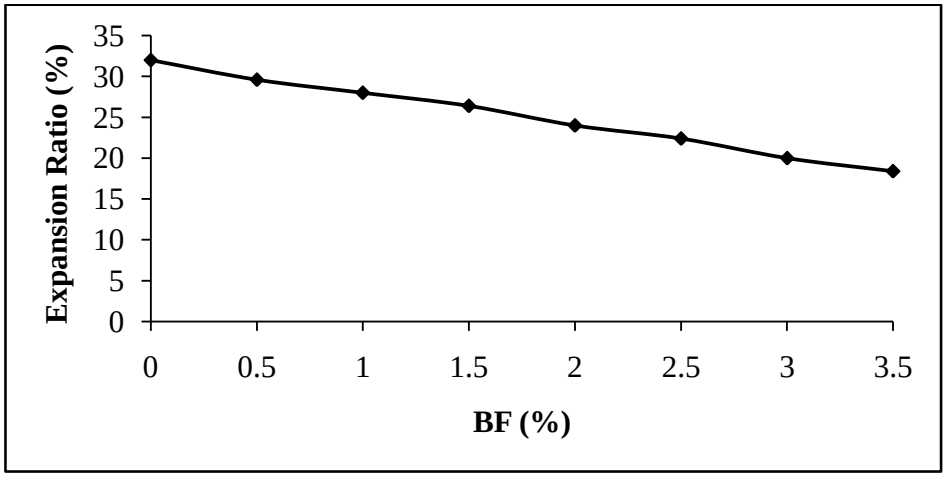

Figure 5.124 Expansion Ratio of BF Reinforced Soils

5.7.4 Hydraulic Conductivity

The variation of hydraulic conductivity of soil with the addition of BF at their respective maximum dry density and optimum moisture content is shown in Figure 5.125. Permeability of unreinforced soil is 3.3×10^{-7} cm/sec. When soil admixed with BF, permeability of soil increases upto 3.5 %. The permeability increases were 16.73%, 22.32%, 31.50%, 43.73%, 52.91%, 59.02% & 65.14% on addition of BF @ 0.5%, 1.0%, 1.5%, 2.0%, 2.5%, 3.0% & 3.5% respectively. The change in the fabric of the expansive soil; causes change in the pore system. Water flow in soil depends on the pore space. In the case of BF, increase in permeability is due to the media presented by BF to flow water in the matrix. This finding is in agreement with Ozkul (2007) who worked on rubber fiber with clayey soil.

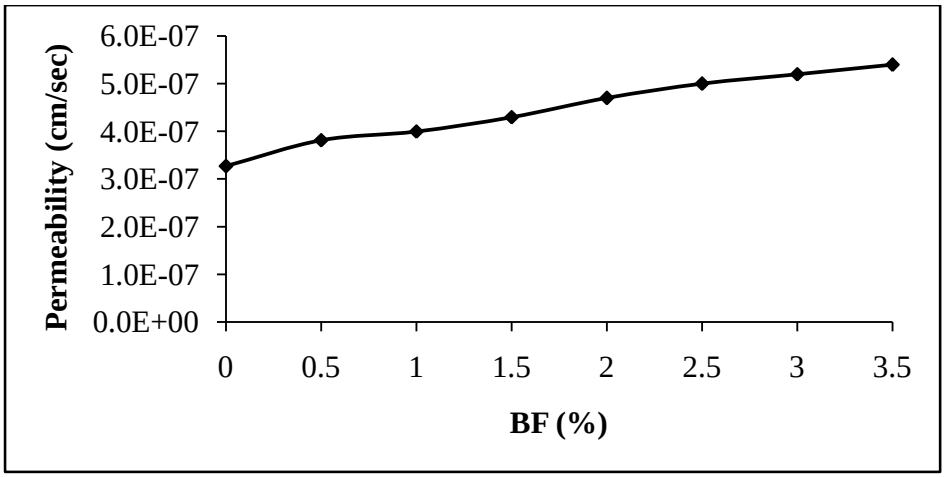

Figure 5.125 Permeability of BF Reinforced Soils

5.7.5 Unconfined Compressive Strength Test

UCS value was remarkably improved by inclusion of BF to expansive soils. The trend of increased of UCS on inclusion of BF is presented in Figure 5.126. When the BF was reinforced @ 0.5%, 1.0%, 1.5%, 2.0%, 2.5%, 3.0% & 3.5%, the improvements observed on UCS were 106.92%, 133.76%, 164.02%, 204.13%, 239.05%, 230.70% & 216.84% respectively at 7 days curing with respect to unreinforced soils. Similarly, 119.18%, 160.90%, 190.00%, 223.50%, 255.82%, 242.40% & 222.61% improvements were observed at 14 days for same BF content. Further improvements on UCS, observed for higher curing periods of 28, 56 and 128 days were 138.18%, 183.17%, 218.45%, 239.29%, 266.58%, 248.52% & 234.14%; 159.89%, 206.65%, 239.88%, 275.30%, 284.86%, 267.39% & 243.59% ; 167.83%, 220.07%, 247.57%, 280.54%, 290.15%, 280.81% & 248.64% respectively. Present analysis clearly suggested that maximum UCS is being offered by sample containing 2.5% BF. Beyond this inclusion level no appreciable increase in UCS was observed.

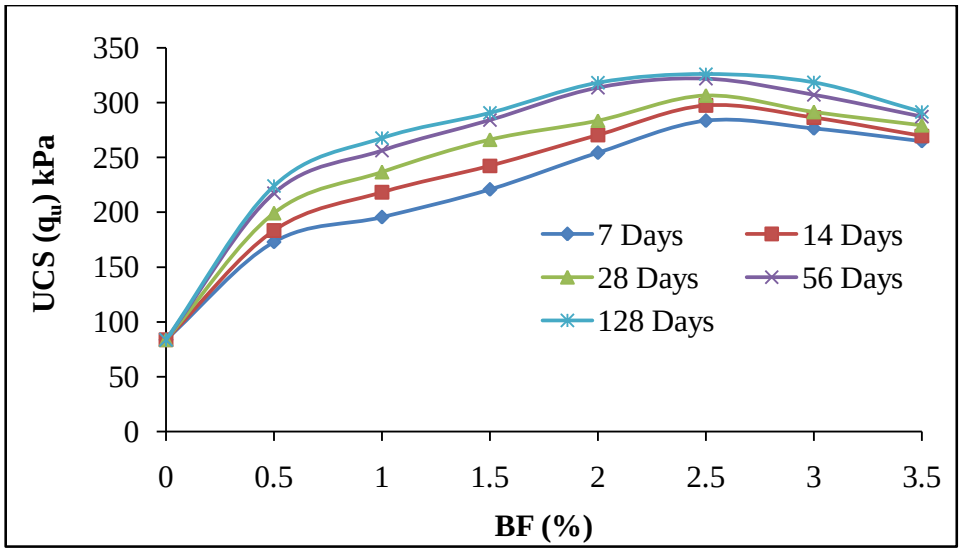

Figure 5.126 UCS of BF Reinforced Soils

5.7.6 Split Tensile Strength Test

The effect of inclusion of BF on split tensile strength for different days of curing time is presented in Figure 5.127. As it was expected, BF inclusion increased the tensile strength of expansive soil. The increase of split tensile strength is pronounced upto 2.5% BF inclusion level. The increment is higher for higher BF inclusion levels. However, Beyond 2.5% inclusion level, no appreciable improvement in tensile strength was observed. Significant improvement in tensile strength was observed for prolong curing. For 2.5% BF reinforced samples, about 549.6%, 572.6%, 597.8% & 614.2% improvements on split-tensile strength were observed at 7, 14, 28, 56 and 128 days respectively when compared to unreinforced soils. This effect may be attributed to the better reinforcing effect of BF as evident from SEM study hence, better clutching of inter-soil particle is made possible thereby interfacial zone of soil particles improved.

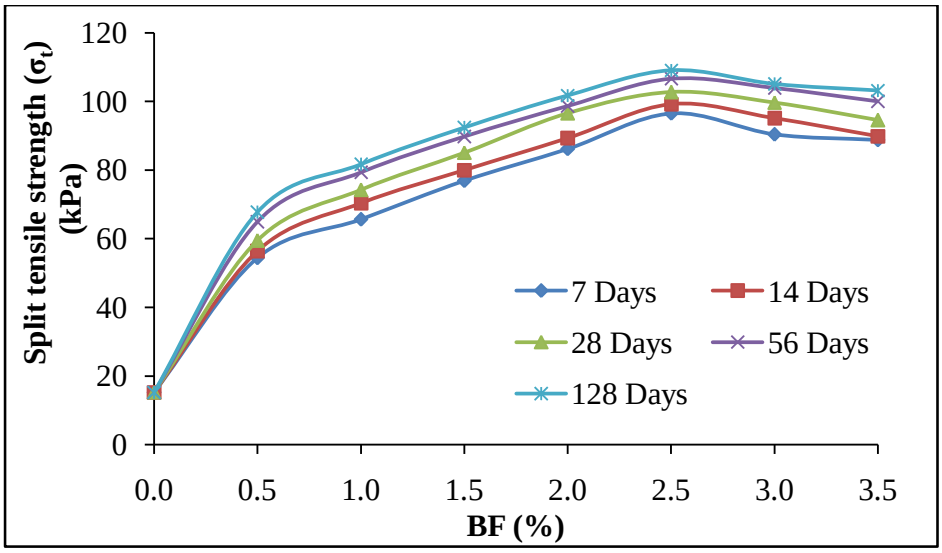

Figure 5.127 Split Tensile Strength of BF Reinforced Soils

5.7.7 Ratio of Split Tensile to Unconfined Compressive Strength Test

The relative relationship and mobilization between the tensile strength and compressive strength could be discussed by plotting the tensile/compressive strength ratio (σ_t/q_u) versus curing time. Figure 5.128 shows the influence of BF content on the ratio of split tensile strength and unconfined compressive strength. The results show that unconfined compressive strength and split tensile strengths are closely related. It can be observed that the ratio of split tensile strength and unconfined compressive strength increased with increase in BF content, indicating that BF is more efficient when soil was subjected to tension rather than to compression. This finding is in agreement with Kumar et al. (2007), that ratio of split tensile strength and unconfined compressive strength increases with increase in polyester fibers content.

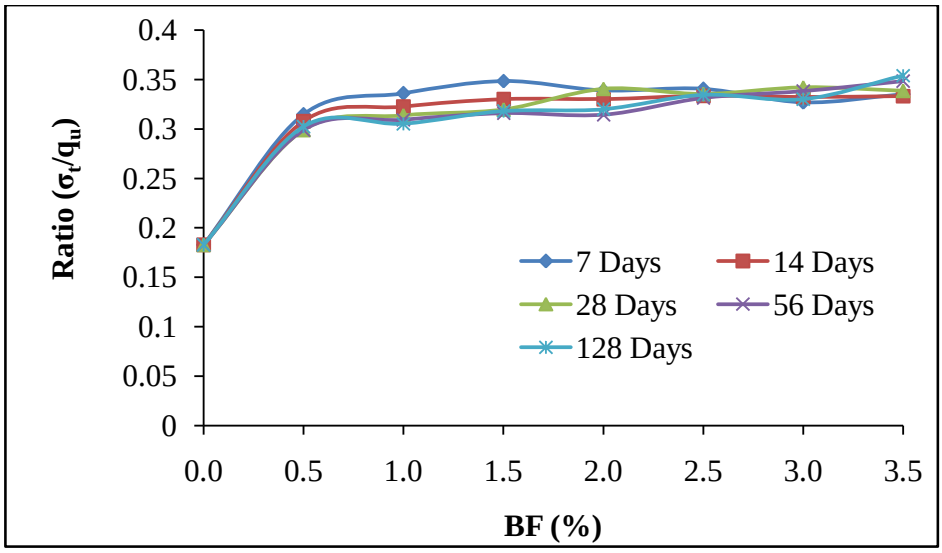

Figure 5.128 σ_t/q_u Ratio of BF Reinforced Soils

5.7.8 Triaxial Test

Three different confining stresses as 100, 150 and 200 kPa were applied on specimens to obtain peak deviator stress as shown in Table 5.6. The range of confining stresses was chosen to obtain more well defined and accurate plots of Mohr envelopes to obtain shear strength parameters cohesion (c) and angle of internal friction (φ) of the soils mixed with BF. The variation of c and φ with admixing BF are evaluated and results are as shown in Figures 5.129 & 5.130 respectively.

Table 5.6 shows the deviator stress of soil admixing of BF after 7, 14, 28, 56 & 128 days curing period at three different pressures. Higher deviator stresses are observed at 2.5 % BF content irrespective of confining pressure applied and days of curing. Admixing of BF causes increase in cohesion and internal friction angle. Increase in cohesion is more pronounced upto 2.5% BF content. The cohesion of soil ranges from 28 to 64.44 kPa and from 28.5 to 76.43 kPa at 7 days and 128 days curing respectively, for BF contents between 0 & 2.5%. Improvement on cohesion due to addition of BF becomes sluggish beyond 2.5%. However, these cohesions are much higher than that of unreinforced soil. As in the case of cohesion, similar trend of improvement is observed for internal friction angle. The rate of improvement of internal friction angle is rapid for 0.5 % BF, after which the rate of improvement is gradual. In overall, these internal friction angles are higher than untreated soil irrespective days of curing (Figure

5.130). BF admixed with soil behaves like strain hardening fiber reinforcement in case of also large deformation. Consoli et al. (2003) also suggested that such behavior of fiber reinforced soil can apposite application in shallow foundation embankment over soft soils, and other earthworks that may suffer excessive deformations. Improvements on cohesion and internal friction angle on admixing of BF is mainly by reinforcing of soft soil when it comes in contact with soil particles.

Table 5.6 Deviator Stress for BF Admixed Soil at Different Confining Pressure

% BF	Confining Pressure (kPa)	Deviator Stress (kPa)				
		7 Days	14 Days	28 Days	56 Days	128 Days
0	100	205.34	206.19	204.83	205.01	204.47
	150	275.91	277.81	276.52	278.17	276.24
	200	337.11	339.77	337.97	338.87	339.18
0.5	100	432.50	454.46	489.85	530.16	548.61
	150	570.90	595.34	636.81	683.90	702.22
	200	713.62	745.31	798.46	858.86	883.26
1.0	100	482.72	534.41	575.29	617.86	647.58
	150	632.37	694.74	742.12	790.87	822.42
	200	782.01	860.41	920.46	982.40	1023.17
1.5	100	538.59	586.75	638.98	687.66	700.31
	150	700.16	756.91	817.90	873.33	896.40
	200	872.51	944.66	1022.37	1093.38	1111.75
2.0	100	625.50	659.92	697.80	775.01	789.01
	150	819.40	871.09	921.10	1007.51	1025.71
	200	1013.31	1069.07	1123.46	1240.01	1254.53
2.5	100	702.99	734.79	757.00	791.52	818.73
	150	899.83	947.88	968.96	1021.07	1031.60
	200	1131.82	1183.01	1213.10	1260.90	1293.59
3.0	100	688.44	717.10	728.44	774.04	805.49
	150	881.20	910.72	917.83	967.55	1002.83
	200	1108.39	1150.94	1161.86	1222.98	1267.03
3.5	100	654.29	663.51	669.06	680.80	683.53
	150	844.03	849.29	859.74	858.83	885.17
	200	1053.40	1061.61	1067.82	1079.06	1083.39

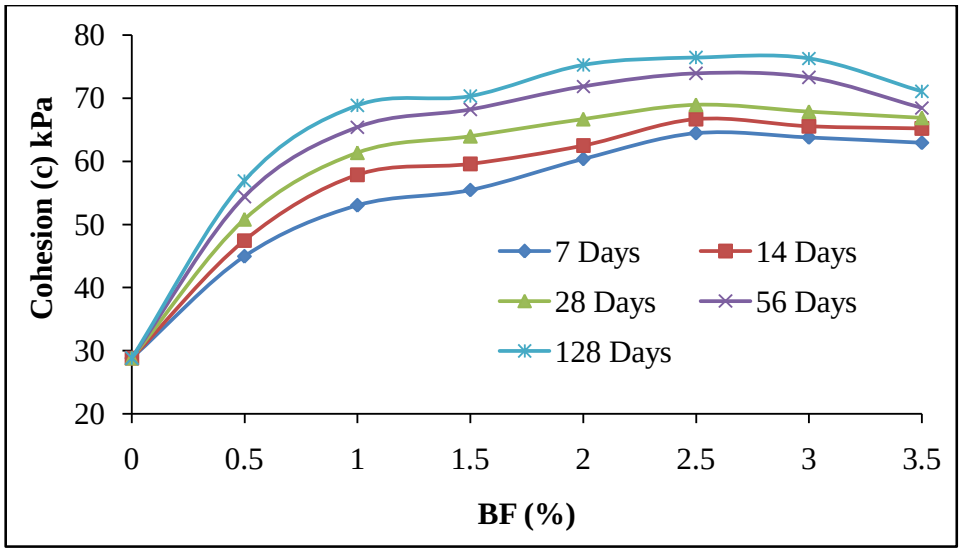

Figure 5.129 Cohesion of BF Reinforced Soils

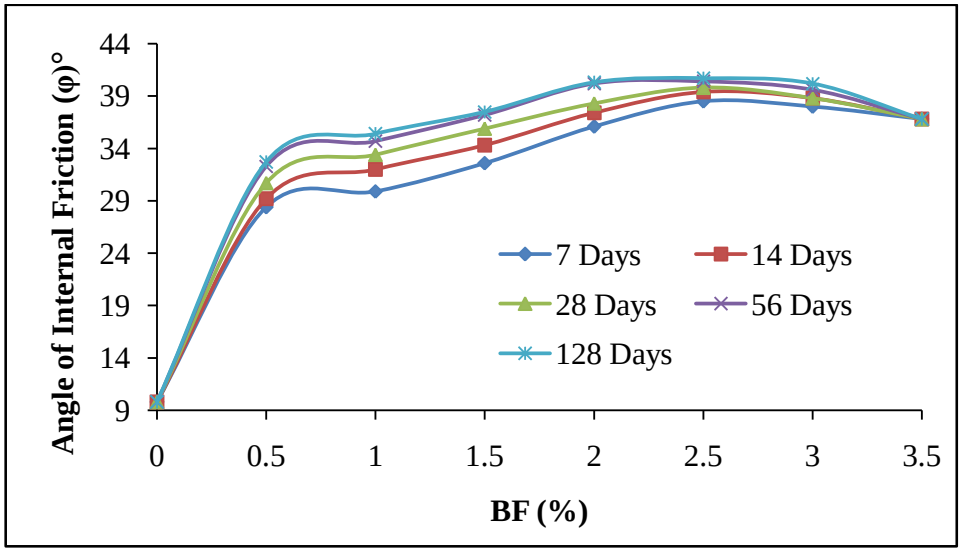

Figure 5.130 Angle of Internal Friction of BF Reinforced Soils

5.7.9 Cyclic Triaxial Test

Cyclic triaxial test was performed at three confining pressures i.e. 100, 150 & 200 kPa and two DSL as 0.5 and 0.8 were selected for determination of permanent strain upto 10000 cycles under constant axial loading for various percentage of BF. The test results were plotted to obtain vertical percent permanent strain with respect to number of cycles and they are presented in Figures 5.131& 5.132 for 0.5 DSL and 0.8 DSL respectively.

5.7.9.1 Effect of load cycle

Figures 5.131 & 5.132 show that rapid increase in deformation of the reinforced and unreinforced soils were observed during the initial approximate hundred cycles of loading and the strain rate was high during this stage in all cases. After few hundred cycles of loading, the increase in deformations was progressively upto 2000 cycles thereafter deformation stabilized (reach approximately almost a constant value), this phenomenon infers that the material behaves almost elastically under the applied load. The maximum permanent strain of 6.15 % was observed for unreinforced soil at 0.8 DSL for 100 kPa confining pressure and the minimum permanent strain of 2.10% was observed for 2.5% BF inclusion level at 0.5 DSL & 200 kPa confining pressure for 10000 cycles.

5.7.9.2 Effect of confining pressure

Permanent deformations for unreinforced soil and reinforced soil were also dependent on confining pressure. Figures 5.131 [(a), (b) and (c)] and 5.132 [(a), (b) and (c)] present the permanent deformation at three confining pressure 100, 150 and 200 kPa respectively. The minimum permanent deformation after 10000 cycles observed were 2.34% & 2.10% at 2.5 % BF inclusion level for 0.5 DSL and 3.69 %, 3.15% & 2.66% for 0.8 DSL at 100, 150 & 200 kPa confining pressures. This analysis reveals that permanent deformation decreases with increase in confining pressure. This finding is in agreement with Chauhan et al. (2008) as they had observed decrease in permanent strain with increase in confining pressure.

5.7.9.3 Effect of deviator stress level

To study the effects of BF on permanent strain and σ_d at 0.5 DSL and 0.8 DSL respectively by incorporating BF to expansive soils Figures 5.131 & 5.132 are presented. Test results gathered at all three confining pressures were used while preparing the graphical plots. Decrease of σ_d implies improvement in permanent strain for both reinforced or unreinforced soils. The minimum value of σ_d observed was 2.10% at 0.5 DSL and 200 confining pressure, whereas for 0.8 DSL for 200 confining pressure, it was 2.66% .

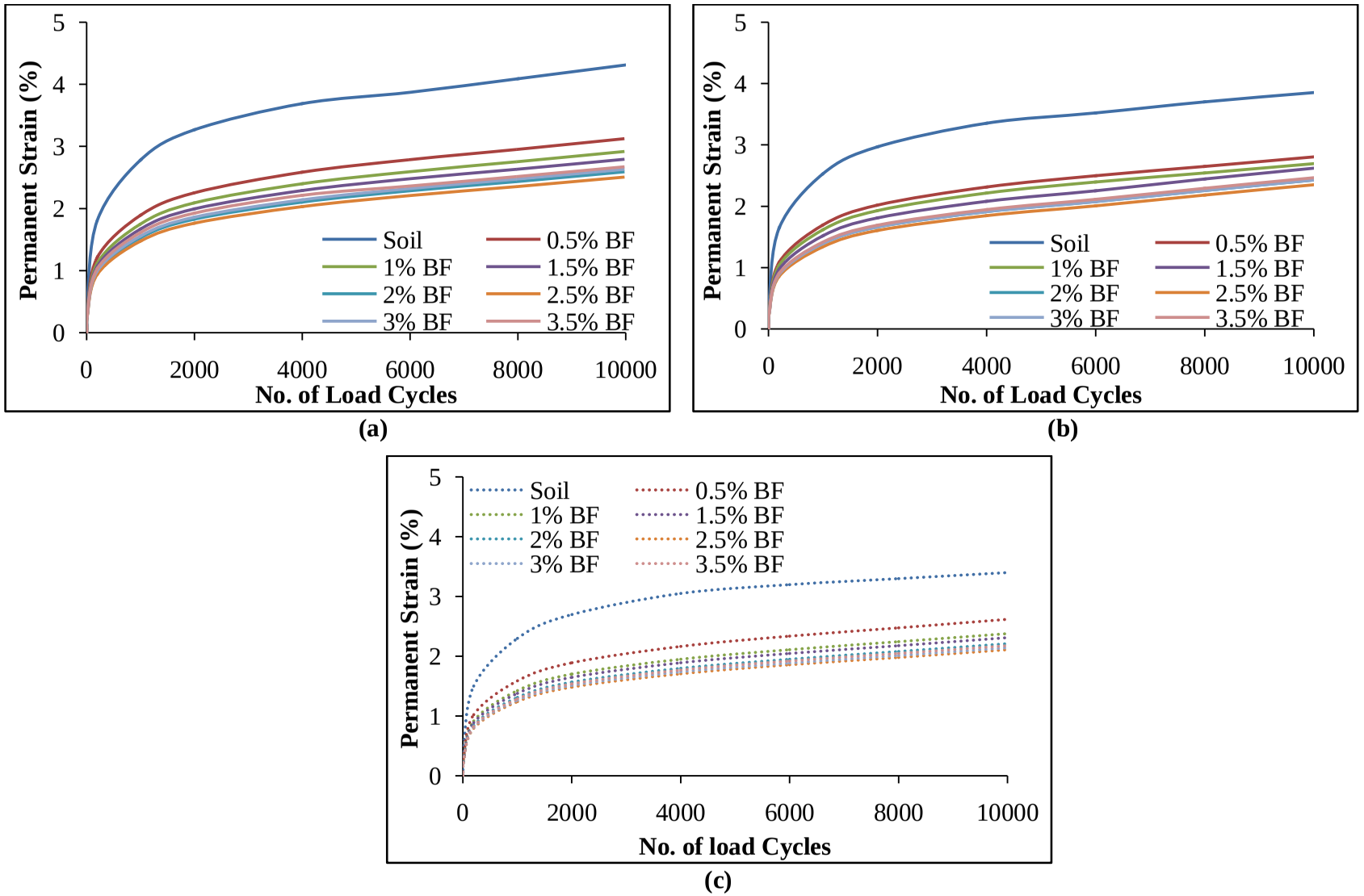

Figure 5.131 Permanent Strain of BF Reinforced Soils at 0.5 DSL (a) at 100 kPa CP (b) at 150 kPa CP (c) at 200 kPa CP

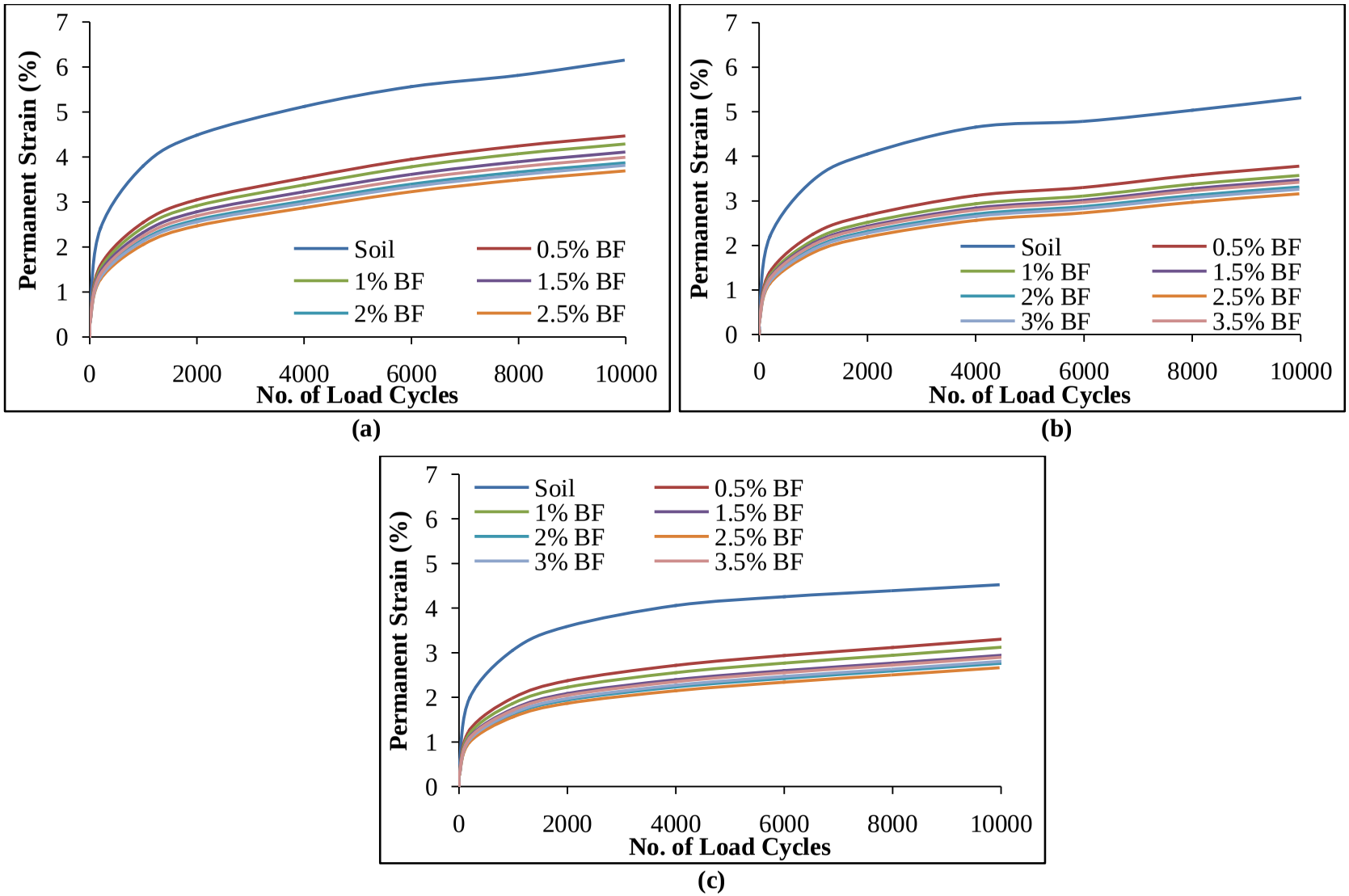

Figure 5.132 Permanent Strain of BF Reinforced Soils at 0.8 DSL (a) at 100 kPa CP (b) at 150 kPa CP (c) at 200 kPa CP

In the analysis of M_R results, a set of six tests was conducted on both reinforced and unreinforced soils with BF. All M_R tests were conducted at two DSL 0.5 & 0.8 along with the three confining pressure 100, 150 & 200 kPa as presented in Figure 5.133. The main motive behind analyzing M_R test results in the present study was to draw information with respect to effects of confining pressure and DSL on soil-BF mixtures.

Figure 5.133 reveals that an increase in confining pressure resulted enhancements of M_R of all cases but these value diminish at higher DSL value. M_R values increase with increase in BF content for every DSL and along with confining pressure. The maximum M_R values observed were 110 MPa & 69 MPa at 0.5 & 0.8 DSL respectively at 200 kPa confining pressure, whereas for 2.5% BF reinforced samples, these values were 397 & 248 MPa. The increase of M_R on inclusion of BF may be due to fiber reinforcing the loose soil particles firmly.

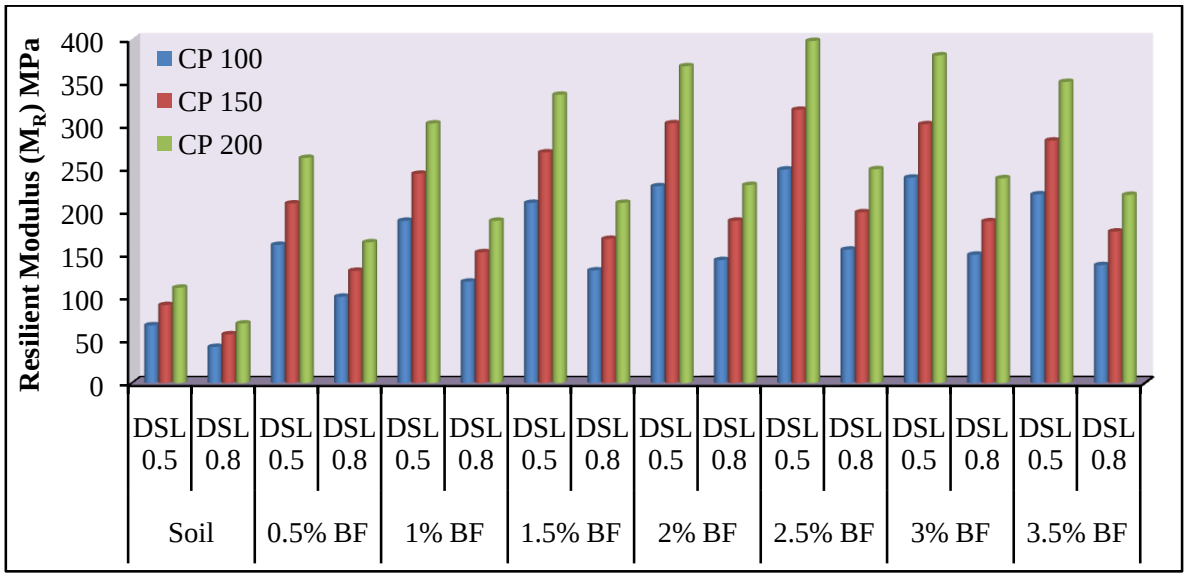

Figure 5.133 Resilient Modulus of BF Reinforced Soils

5.7.10 Plate Load Test

The influence of BF in improving the modulus of subgrade reaction (k) of mixtures was evaluated by comparing the measured k-values for the natural expansive soil and soil-FA mixtures. Inclusion of BF to expansive soil considerably improved k-value as presented in Figure 5.134. The modulus of subgrade reaction of expansive soil was found to be 17 MPa/m.

The rate of improvement of k-value is significant upto 3.0% BF inclusion level beyond which k-value starts declining. If BF was reinforced with expansive soils @ 0.5 %, 1.0 %, 1.5%, 2.0%, 2.5%, 3.0% & 3.5%, the percentages increase of k-values were 32.34%, 55.36%, 82.48 %, 113.47%, 129.49%, 134.58% & 113.47% respectively. Based on the present study, BF can be ideally reinforced @ 2.5% to draw maximum possible k-value.

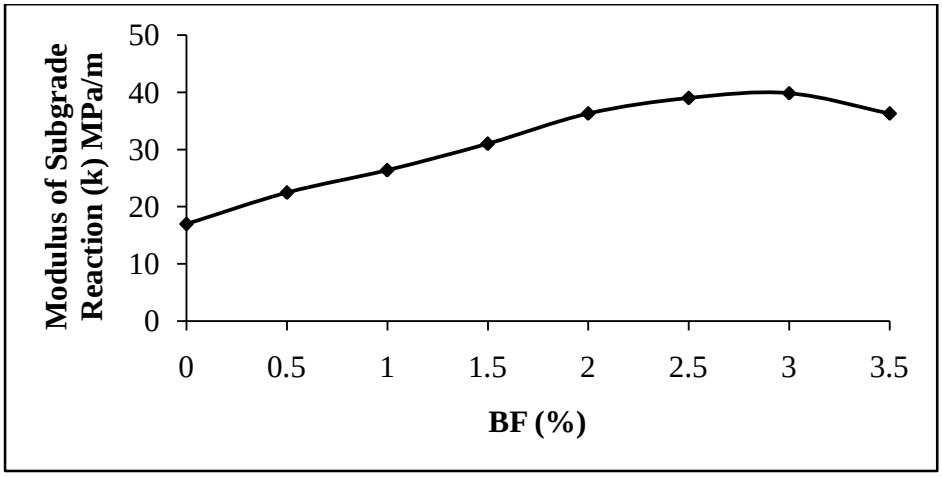

Figure 5.134 Modulus of Subgrade Reaction of BF Reinforced Soils

Efforts have also been made to obtain load-settlement curves using laboratory data accrued from the plate load tests. As definite yield point could not be obtained from the derived curves, the ultimate bearing capacity for unreinforced and BF reinforced soils were worked out by extending tangents from the two straight portions of the load-settlement curve one at the initial straight portion and another tangent at the steeper straight portion at the end.

Figure 5.135 shows the ultimate bearing capacity of soils with or without BF. 198 kPa ultimate bearing capacity was noted for natural expansive soil. This capacity improves significantly on inclusion of BF and better improvement in bearing capacity was noted for higher BF inclusion level. The percentage improvement of bearing capacity are 11.1%, 15.2%, 18.7%, 21.7%, 23.7 %, 25.3% & 22.2% on inclusion of BF @ 0.5%, 1.0%, 1.5%, 2.0%, 2.5%, 3.0% & 3.5% respectively. It was also noted that inclusion of BF 3.0% led to reduction in bearing capacity substantially. Based on the above analysis, the optimal inclusion level for BF is between 2.5%

and 3.0% but ideally 2.5% BF inclusion level shall be preferred if expansive soil is to be stabilized.

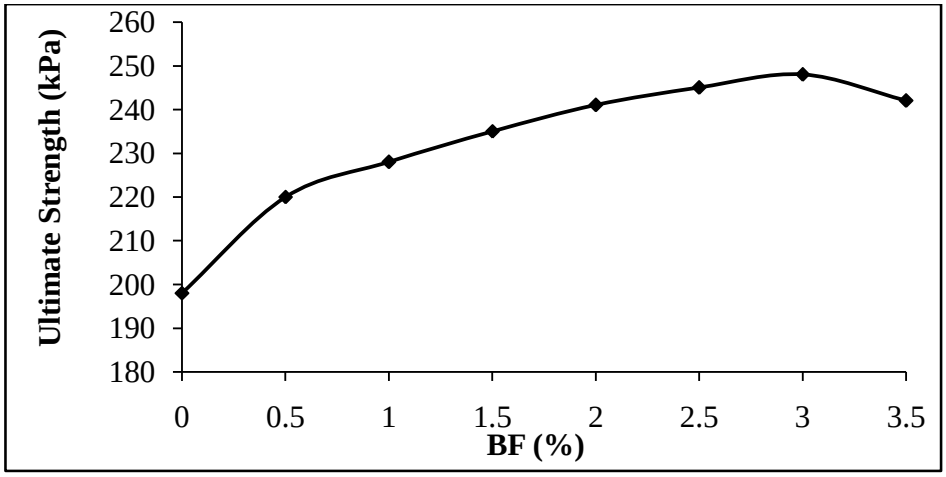

Figure 5.135 Ultimate Strength of BF Reinforced Soils

5.7.11 Microstructural Investigation

Figures 5.136 (a to d) depict the scanning electron microscopy images of soil-BF mixtures. Bagasse fiber embedded within the soil mass is clearly visible from all the images irrespective of percentage of fiber inclusion. Fibers in bagasse consist mainly of cellulose, pentosan and lignin. Cellulose is highly crystalline regardless of the source. The cross section of bagaase fiber is irregular and they are randomly distributed. The bagasse fiber bundles consist of several to hundreds of ultimate fiber cells. Excellent reinforcing effect between soil particles and bagasse fibes is also observed.

5.7.12 Correlation between Different Strength Parameters

5.7.12.1 Relation between CBR, % BF & Curing Days

The correlation between CBR, BF and curing days (D) was established using multiple linear regression analysis (MLRA). Test results obtained at 7, 14, 28 & 56 days of curing were considered for the analysis. The developed relation is presented in Eqn. (5.11), with R^2= 0.858. High values of R^2 show close proximity to predicted values with experimental data. The validation of the developed relation was done using laboratory CBR values obtained at 128

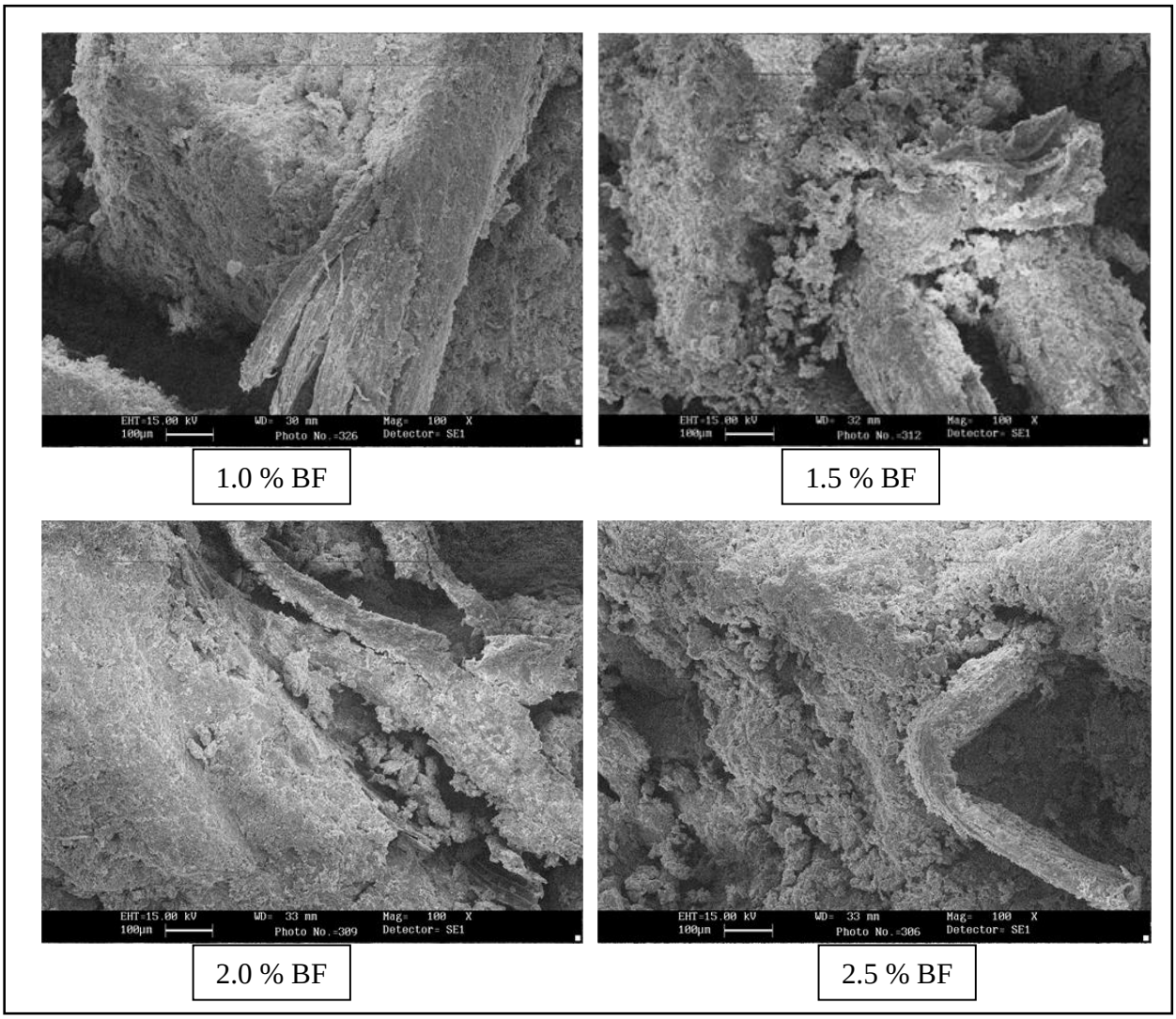

Figure 5.136 SEM Images of Soil-BF mixtures captured at 500 X magnification

days of curing. CBR results obtained through predicted equation [CBR (P)] and CBR results accrued from the laboratory [CBR (L)] were compared as shown in Figure 5.137. The equation has high values of R^2 suggesting closeness of predicted values the experimental data.

$$CBR = 1.905 + 0.937\%\ BF + 0.0063\ D \quad (5.11)$$

where, CBR = California bearing ratio, % BF = percentage bagasse fiber, D = number of curing days.

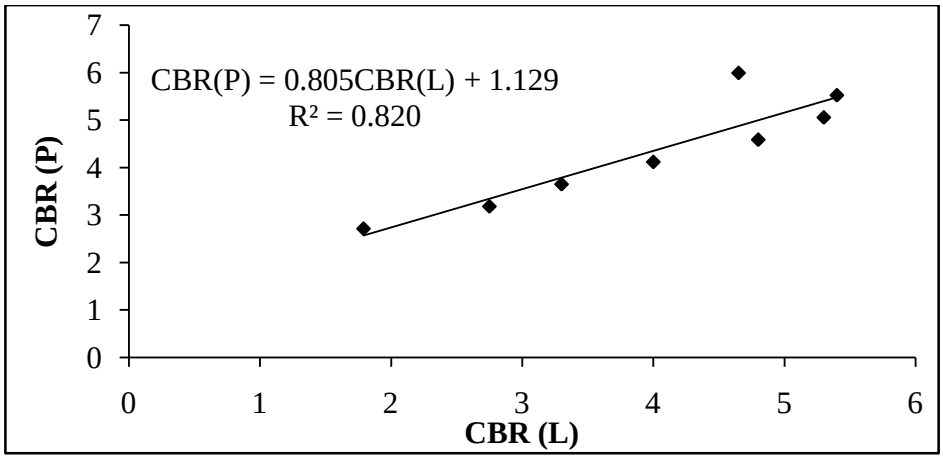

Figure 5.137 Validation of CBR Results for BF Reinforced Soils

5.7.12.2 Relation between UCS, CBR, % BF & Curing Days

In a very similar way, as in the case of CBR, % BF and curing days relationship; UCS values obtained from the laboratory for BF reinforced soil samples cured for 7, 14, 28, 56 & 128 days were considered for establishing general equation to compute predicted UCS value. The relationship developed between UCS as dependent variable and other parameters as independent variable is given in Eqn. (5.12), with R^2= 0.852. UCS test results of 128 days were used for validation of the predicted equation. Predicted UCS [UCS (P)] values and laboratory UCS [UCS (L)] values were compared as shown in Figure 5.138. As this equation showed high values of R^2, predicted UCS values have close proximity with experimental data.

$$UCS = 13.78 - 10.38\%\ BF + 0.122D + 64.45\ CBR \quad (5.12)$$

where, UCS = Unconfined compressive strength (kPa)

5.7.12.3 Relation between STS & UCS

Relationship has been established between split tensile strength and unconfined compressive strength of BF reinforced soil samples from the data of present study. Various models like linear, exponential, polynomial, power and logarithmic were tested, but linear relation as shown in Figure 5.139 was best fitted with R^2 = 0.987. Further, the proposed equation was validated using STS laboratory results accrued after 128 days of curing as presented in Figure 5.140

The predicted STS [STS (P)] values and laboratory STS [STS (L)] values were compared and showed excellent relationship as high R^2 values exhibit between them.

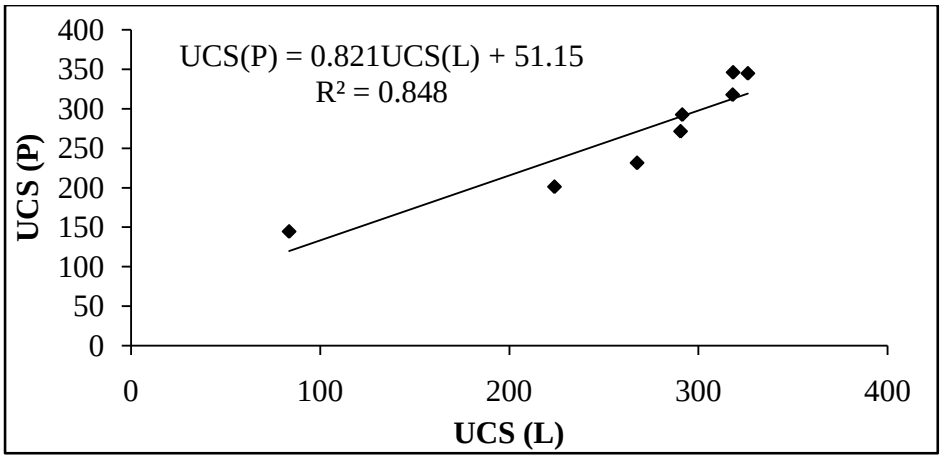

Figure 5.138 Validation of UCS Results for BF Reinforced Soils

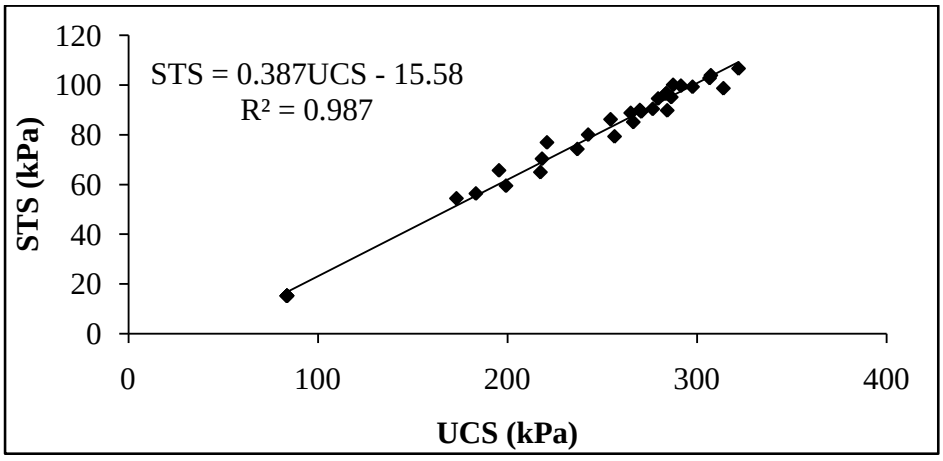

Figure 5.139 Relationship between STS & UCS for BF Reinforced Soils

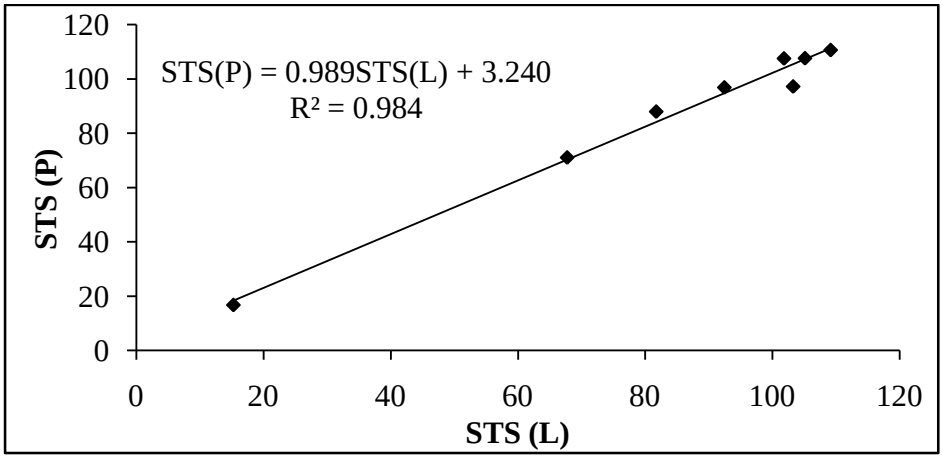

Figure 5.140 Validation of STS Results for BF Reinforced Soils

5.7.12.4 Relation between M_R & CBR

The cyclic triaxial tests were conducted as per ASTM D5311-11 on expansive soil and BF reinforced soil specimens. Tests were conducted after the expiry of 28 days curing period.

Three levels of σ_3 (50, 100 and 150 kPa) at 0.50 DSL and 0.80 DSL were applied during the test. The main intention behind this effort was to establish correlation between M_R & CBR using regression analysis for each three levels of σ_3 0.50 DSL and 0.80 DSL respectively. Mathematical analysis of data shows good relationship between M_R & CBR described by a power series as presented in Figure 5.141 (a to f).

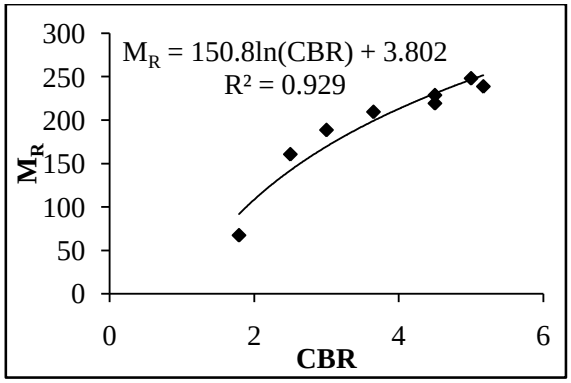

(a) CP 100, DSL 0.5

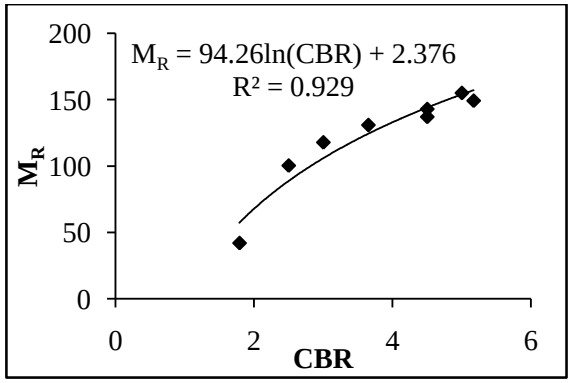

(b) CP 100, DSL 0.8

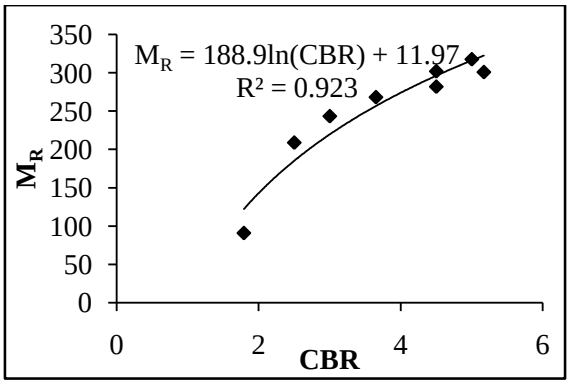

(c) CP 150, DSL 0.5

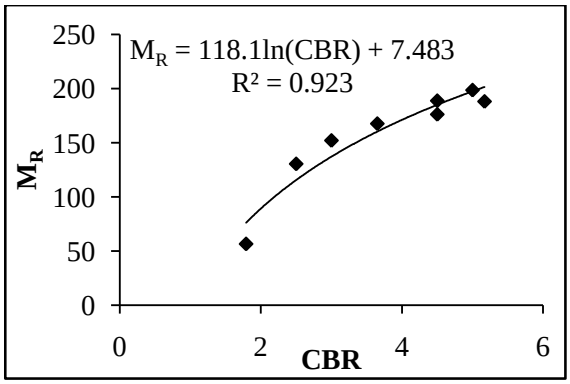

(d) CP 150, DSL 0.8

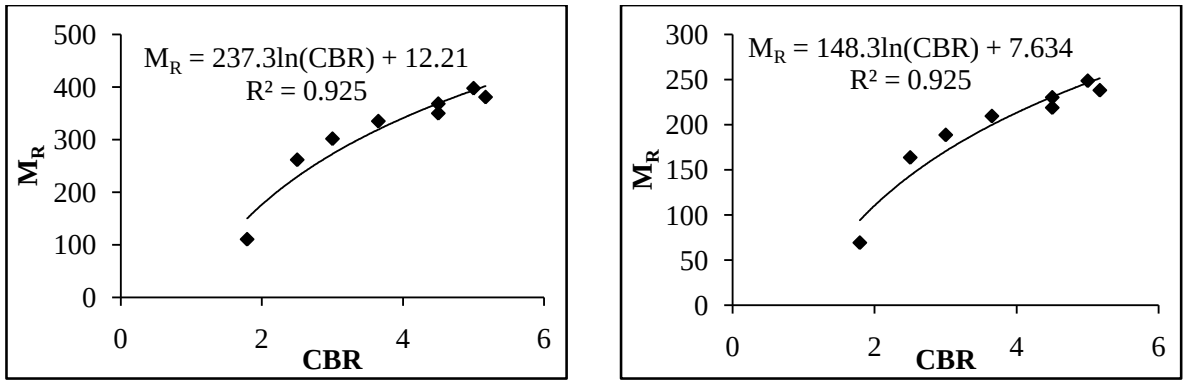

(e) CP 200, DSL 0.5 (f) CP 200, DSL 0.8

Figure 5.141 Relation between M_R & CBR for BF Reinforced Soils

5.8 SUMMARY

This Chapter presents the results of laboratory investigations done to study the behavior of geotechnical properties of Soil admixed with various additives like FA, RHA, BA, RSA, FDCS and BF. The additives were mixed with natural soil in different proportions from 0%, 5%, 10%, 15%, 20%, 25%, 30% & 35% for FA, RHA, BA, RSA, FDCS and from 0%, 0.5%, 1.0%, 1.5%, 2.0%, 2.5%, 3.0% & 3.5% for BF for the present study. The interpretations for various test results were discussed and optimum content of each additive were suggested for future use. The results showing optimum values of various engineering properties for different materials are given in Table 5.7.

Table 5.7 Optimum Values of Various Properties for Different Waste Materials

Materials (Optimum %)	PI	SL (%)	FSI	OMC (%)	MDD (g/cm^3)	CBR# (%)	ER#	Permeability (cm/sec)	UCS* (kPa)	STS* (kPa)	c* (kPa)	φ* (°)	k* (MPa/m)	$M_R$$
Soil (100)	25	16	45.0	17	1.71	1.86	32	3.3E-07	86	15	28.8	10	17.0	42.0
FA (25)	5	28.89	20.8	21	1.63	7.8	19.2	1.3E-07	123	19	42.5	18	51.5	65.7
RHA (25)	9	30.65	17.7	34	1.34	11.15	16.8	1.1E-07	145	23	46.1	22	57.0	83.7
BA (25)	6	26.27	19.0	23	1.51	6.4	17.6	1.2E-07	139	21	45.1	21	49.8	80.0
RSA (30)	5	25.84	17.3	32	1.32	12.17	14.4	8.2E-08	178	26	51.1	27	59.5	104.8
FDCS (35)	2	36.52	17.7	22	1.52	26.17	11.2	4.3E-08	204	32	55.2	38	96.9	118.6
BF (2.5)	-	-	-	22	1.58	2.25	22.4	5.0E-07	283	96	64.4	31	22.8	155.1

3 Days humidity curing and 96 hours soaking
* 7 Days humidity curing
$ 0.8 DSL at 100 kPa confining pressure

CHAPTER 6

PAVEMENT ANALYSIS BY MODEL TANK TEST AND KENPAVE

6.1 GENERAL

Pavement design methods are mainly based either on empirical or on mechanistic-empirical methods. Mechanistic design approach offers many advantages over the empirical methods. Empirical method is generally based on observed performance, without any concern of theoretical performance but in case of mechanistic-empirical design method, the mechanical properties of material are correlated with the observed performance of pavement. The mechanistic-empirical method of design is based on the mechanics of pavement materials such as modulus of elasticity, poison ratio, wheel load etc. for pavement response, as output of stress or strain.

In a mechanistic-empirical pavement study, flexible pavement responses are generally determined due to traffic loading with an analytical program either based on a finite element model or a linear elastic multi-layer model. Generally a finite element model gives better response for various type of loading conditions and can be configured to practical characterization of pavement responses as compared to a elastic multi-layer model. But the major difficulty of using a finite element model is that it takes more time of computation of results. Apart from this, a linear elastic multi-layer model gives fast computation results more easily and efficiently to determine stress and strain since it is more user-friendly.

Boussinesq (1885) and Burmister (1943) gave standard solutions for structural analysis of pavement systems. Based on two standard theories, many solution techniques have been developed for the mechanistic evaluations. Among these, Multi layer theory of Burmister was more accurate than one layer theory of Boussinesq when compared to critical pavement responses. To analyse the layer theory for pavement based on Burmister's layered theory, several linear elastic computer programs have been developed to reduce the complex computation for obtaining stresses, strains, and displacements using mechanistic solutions.

Some computer programs like CHEV, DAMA, BISAR, ELSYM5, PDMAP, SAPIV, ILLI-PAVE, KENPAVE is available to analyse the pavement responses. Warren and Dieckmann (1963) introduced CHEV program only for linear elastic materials which was modified to DAMA program by Hwang and Witczak (1979) to account for nonlinear elastic granular materials. BISAR (De Jong et al., 1973) approached both vertical loads and horizontal loads which were better simulated in highway design sectors. For elastic five-layer systems under multiple wheel loads, ELSYM5 was developed by Kopperman et al. (1986). The KENPAVE program (by Huang, 1993) provided the solution for an elastic multilayer system under a circular loaded area for both flexible as well as rigid pavements. For this study KENLAYER (part of KENPAVE for flexible pavement) is used to check the responses of pavement system.

The behaviour of pavement under repeated load has been studied by model tank test. Strength and flexibility of pavement are usually determined from pavement deformation data which are obtained under the application of standard load. Pavement deformation values can be converted into pavement strength by using different relationships (Piyatrapoomi, N., 2003). The total deflection on surface of specimen was determined and the vertical stress was evaluated at each interface of layers and bottom to better understand the dynamic behaviour of a portion of natural soil subgrade and treated soil subgrade by LVDT and pressure cell as described in chapter 3. In same arrangement the vertical stresses at each interface of layer and bottom of subgrade were calculated by KENLAYER. For model test tank, three magnitudes of pressure are shown in figure 6.1which were applied to check the responses of different layers.

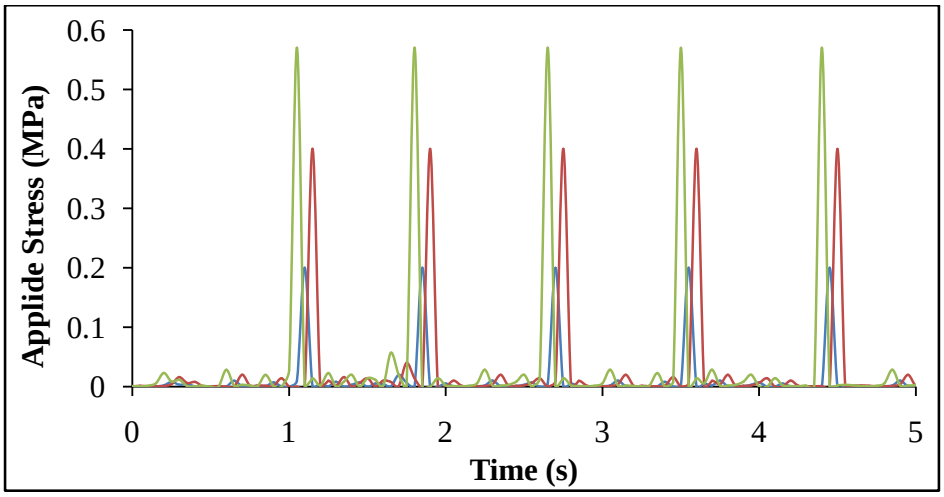

Figure 6.1 Variation in Stress Application during Model Tank Test

6.2 MODEL TANK TEST

Model tank test was conducted in laboratory to determine the surface deformation and vertical stresses at different layers under static loading condition as well as under dynamic loading condition. As stated in chapter 3, the pavement structure of different layers with natural soil was tested in model tank. In case of admixed soil only BA and FDCS at its optimum content were taken as subgrade and other all layers like BC, DBM, WMM and sub-base layer were kept same for the test to validate the KENLAYER analysis. Other admixed soil like FA, RHA, RSA and BF were analysed by KENLAYER.

6.2.1 Vertical deformation

Vertical deformation on top surface of model tank with respect to the no. of load cycles is shown in Figure 6.2. Efforts have been made to draw the permanent deformation characteristics of compacted subgrade prepared with or without waste materials (additives) at pre-determined pressures of 200 kPa, 400 kPa and 570 kPa considering half of single axle load to simulate the actual field conditions. At 570 kPa applied load, the total deformation at surface was more in case of natural soil subgrade as compared to subgrade of BA or FDCS admixed soil. Total deformation, a measure of pavement strength, increased with increase in load cycle (Piyatrapoomi, N, 2004). The increase was rapid upto 200 cycles, after that increase was gradual upto 5000 cycles and then almost constant in case of admixed soil,. But in case of natural soil the increase was prolonged after 5000 cycles. It was also observed that total deformation also increased with increase in applied pressure as shown in figure 6.2 (a), (b) and (c).

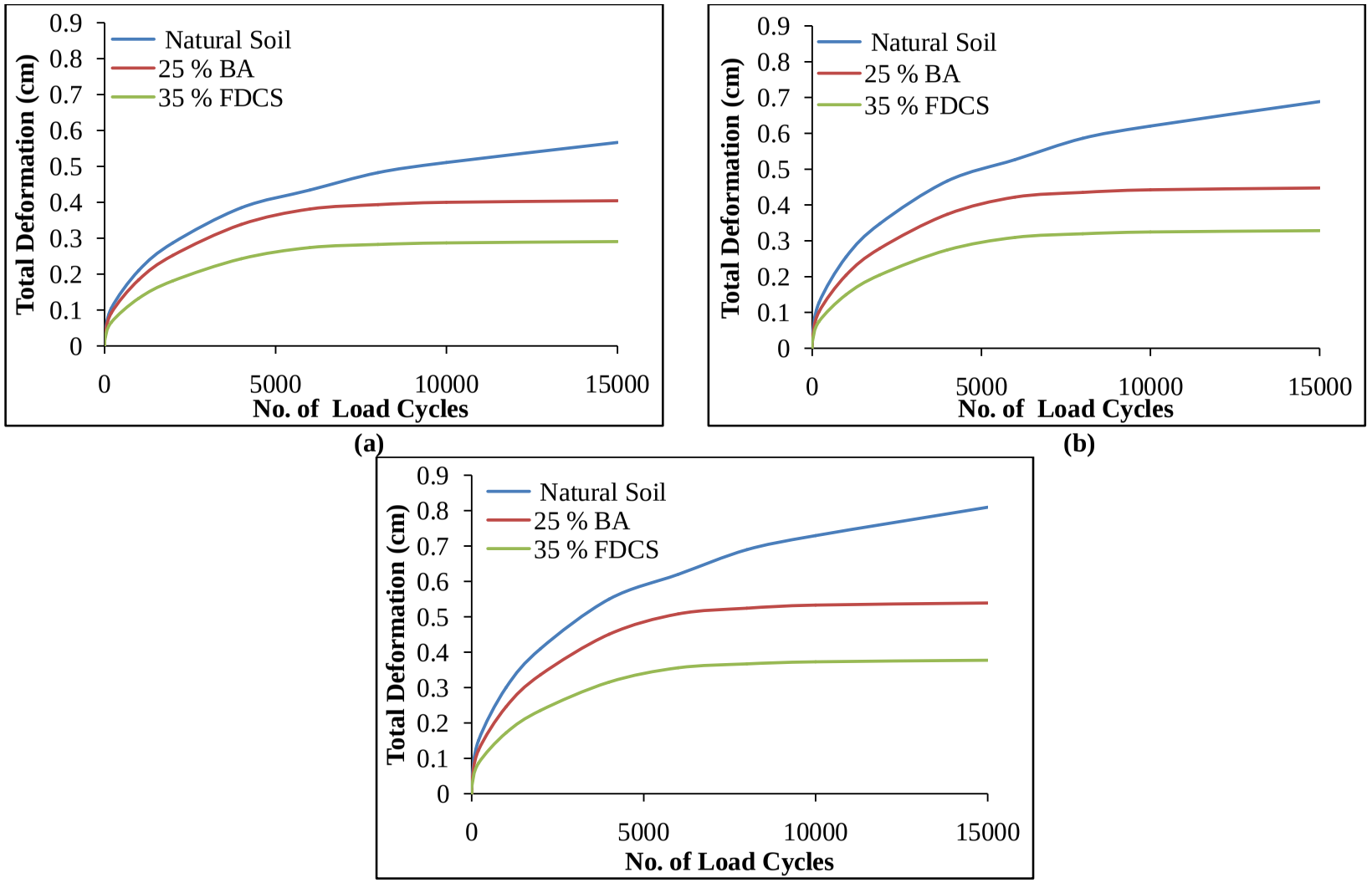

Figure 6.2 Total Deformation with no. of Load Cycles at (a) 200 kPa CP (b) 400 kPa CP (c) 570 kPa vertical pressure

6.2.2 Vertical stress

Vertical stress was determined at each interface and bottom of subgrade of pavement system by pressure cell (as shown in Figure 3.17) at three different applied pressure. The magnitude of vertical stresses is shown in Figure 6.3, 6.4 and 6.5 for natural soil, BA admixed soil and FDCS admixed soil subgrade of pavement system respectively. When pressure was applied on 150 mm radius at surface of pavement, vertical stress decreased with increase in depth for all loading condition. Stress was decreased by 9%, 16.5%, 19.3%, 18.8% & 29.1 % at the depth of 4 cm, 9 cm, 20 cm, 30 cm & 60 cm respectively for natural soil subgrade at 570 kPa as shown in Figure 6.3. When the subgrade soil (bottom layer of pavement) was replaced by 25% BA admixing soil keeping the remaining layers same, then the vertical stress changed in every layers and decreased by 5.2%, 14.3%, 20.8%, 22% & 28.7% at the depth of 4 cm, 9 cm, 20 cm, 30 cm & 60 cm respectively at 570 kPa as shown in Figure 6.4. Again the change in subgrade soil by admixing of 35% FDCS and keeping other layers to be same, the vertical stress again changed in every layer and decreased by 3.9%, 13.3%, 19.1%, 22.3 % & 31.9% at the depth of 4 cm, 9 cm, 20 cm, 30 cm & 60 cm respectively at 570 kPa as shown in Figure 6.5.

From this analysis it was observed that improvement of subgrade soil affects the stresses in all layer. As subgrade soil improve (in strength), the distribution of vertical stress increased at every interface of pavement.

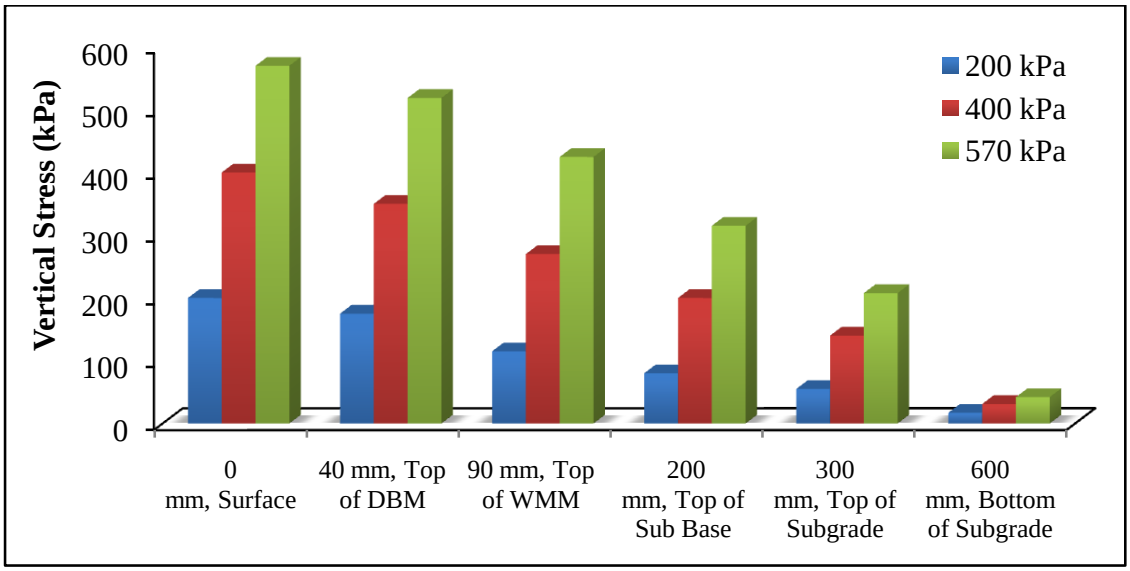

Figure 6.3 Vertical Stress at different layers for Natural Soil Subgrade

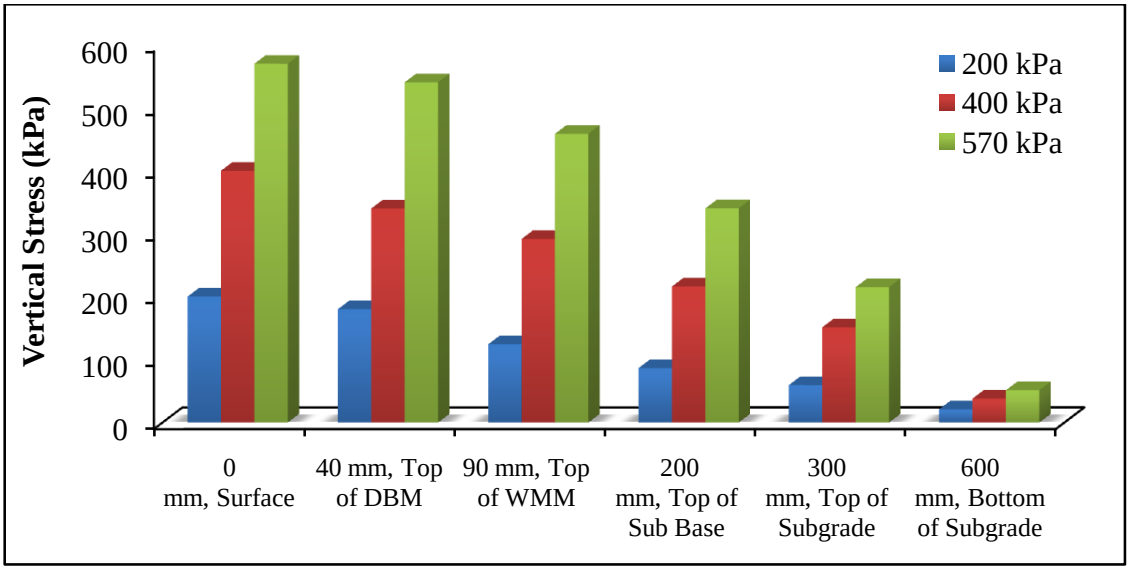

Figure 6.4 Vertical Stress at Different Layers for BA Admixed Soil Subgrade

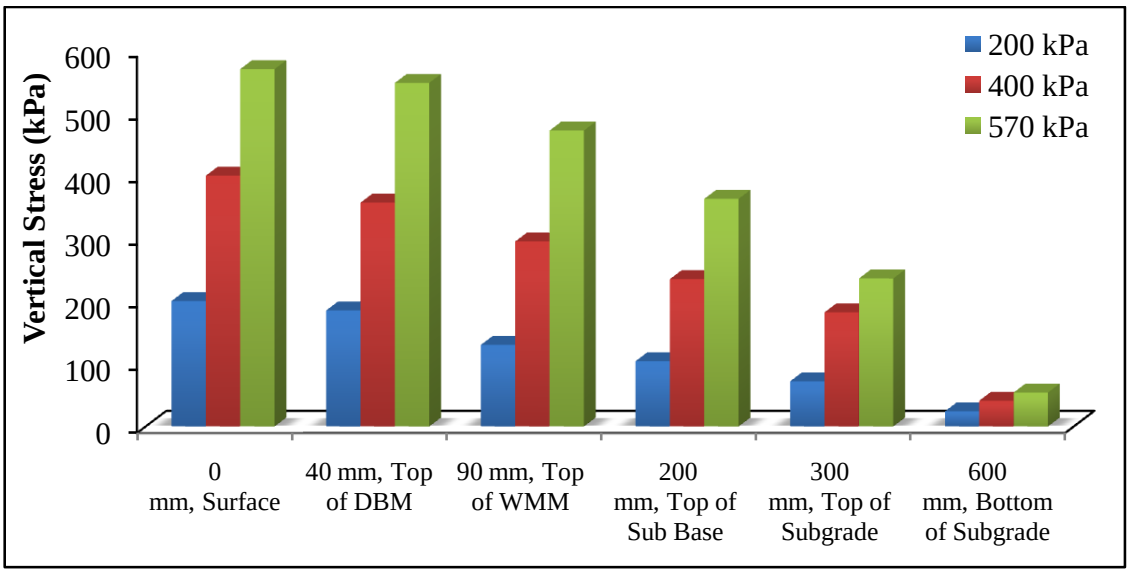

Figure 6.5 Vertical Stress at Different Layers for FDCS Admixed Soil Subgrade

6.3 KENLAYER ANALYSIS

KENLAYER analysis is basically based on the Burmister's layered elastic theory system under a circular loaded area. For this study, load was applied to layered systems under single wheel. Linear elastic behavior of layers were assumed and stress and strain values were determined at different positions throughout the depth of the pavement for all the types of subgrade as natural soil, FA admixed soil, RHA admixed soil, BA admixed soil, RSA admixed soil, FDCS admixed soil and BF admixed soil. The behaviour of pavement system with different subgrade modulus was analyzed by measuring vertical deflection, vertical stress and vertical strain under different traffic loading. The modulus of elasticity of subgrade soil was 19 MPa and increased upto 152 MPa with admixed of FDFC upto 35%. Poisson's ratio is difficult to determine and has relatively minor influence on the design compared to other parameters. Therefore, standard values of Poisson's ratio and modulus of elasticity are used as per IRC 37: 2012. Modulus of elasticity and poison ratio of different layers are shown in Table 6.1. Many researches like Ameri et al. (2012), Sadrnejad et al. (2011), Lav et. al. (2005), Arshad (2007) etc. had also used KENLAYER to determine the vertical deflection, vertical stress and vertical strain for analysis the flexible pavement response.

Table 6.1 Input Data for KENLAYER Analysis

Layer	**Thickness (cm)**	**Modulus of Elasticity (E) MPa**	**Poisson Ratio (υ)**
BC	4	1450	0.35
DBM	5	1400	0.35
WMM	100	400	0.40
Sub-Base	110	370	0.40
Subgrade	300		0.45
Natural Soil		19	
Soil-FA		65	
Soil-RHA		85	
Soil-BA		60	
Soil-RSA		100	
Soil-FDCS		152	
Soil-BF		50	

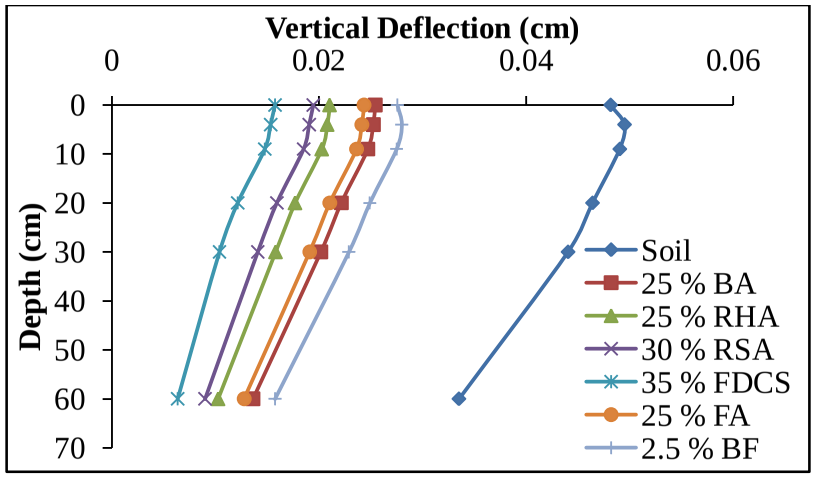

(a) At 200 kPa

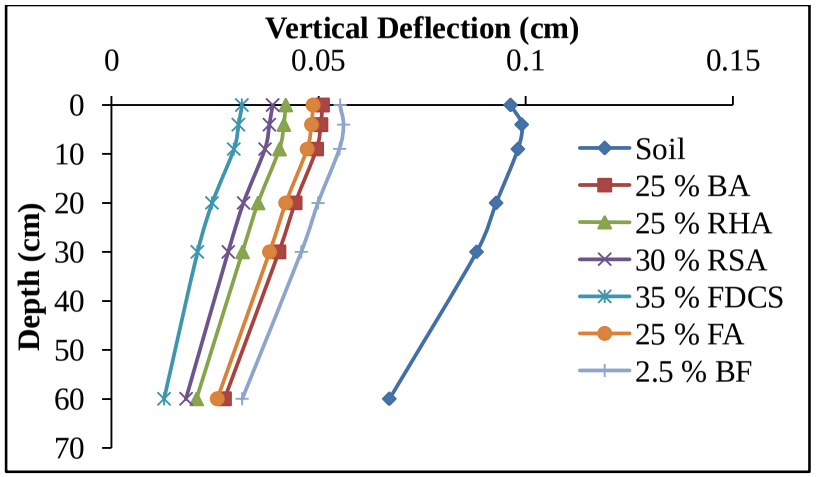

(b) At 400 kPa

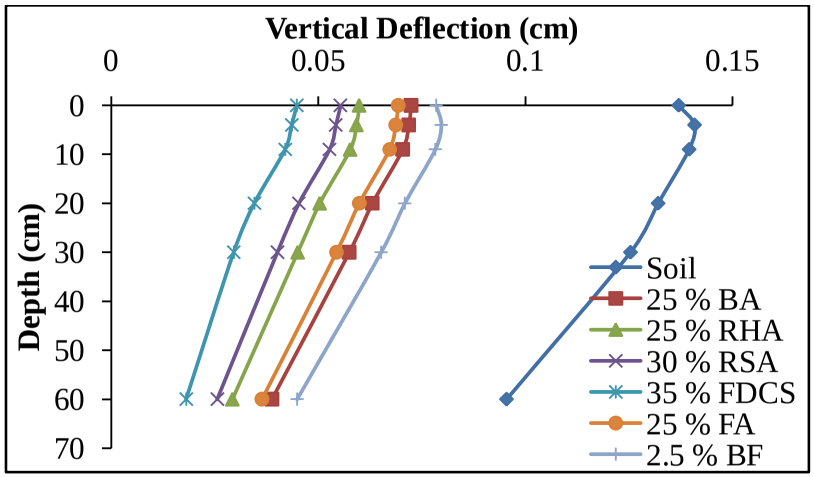

(c) At 570 kPa

Figure 6.6 Vertical Deflections at Different Depth with Different Vertical Pressure

6.3.1 Vertical Deflection

Vertical deflection was determined at different layers by KENLAYER for different admixed soil subgrade at three different applied pressure 200, 400 and 570 kPa as shown in figure 6.6 (a), (b) and (c) respectively. Figure 6.6 (a) shows the comparison between the vertical deflection in pavement of different admixed soils like soil-FA, soil-RHA, soil-BA, soil-RSA, soil-FDCS and soil-BF subgrade with natural soil subgrade at 200 kPa. The curve shows that the vertical deflection decreases with respect to the depth except on top layer (Huang, 2004). In case of admixed soil vertical deflection was reduced as compared to natural soil. Maximum reduction was found 67% and 81% at top and 60 cm depth for combination containing 35% FDCS subgrade soil. The same trend was observed at 400 kPa and 570 kPa pressure.

6.3.2 Vertical Strain

Figure 6.7 shows the vertical strain of pavement system at different applied pressure. At all applied pressures the vertical strains generally increased with increase in depth upto 30 cm and then decreased, and are in fact tensile (negative) in the immediate top layer of pavement surface because of the effect of the horizontal stresses and the Poisson's ratio. Also from the vertical strain profile, the marked influence of the Poisson’s ratio on the thin and intermediate surfacing is evident (Walubita, 2000). For lesser thickness of pavement, the strain of bottom of BC layer turns out to be compressive. The reason behind this may be the failure of the thin layer in shear rather than in flexure. As thickness increases, the pavement starts taking load inducing flexure properties to the bituminous layer. Vertical strain was also influenced by different type of subgrade soil in pavement system. As shown in figure 6.7 (a), the vertical strain decreases due to admixed soil as compared to natural soil. The minimum vertical strain was observed in case of 35% FDCS mixed subgrade soil and reduction was 78% and 68% at top and 60 cm depth. The same pattern was found at applied pressure 400 kPa and 570 kPa.

6.3.3 Vertical Stress

Vertical stress distribution at different layers of pavement have been determined in lab for natural, BA and FDCS admixed soil and by KENLAYER for all admixed soil subgrade as shown in Figure 6.7 (a), (b) and (c) at three different applied pressure 200 kPa, 400 kPa and

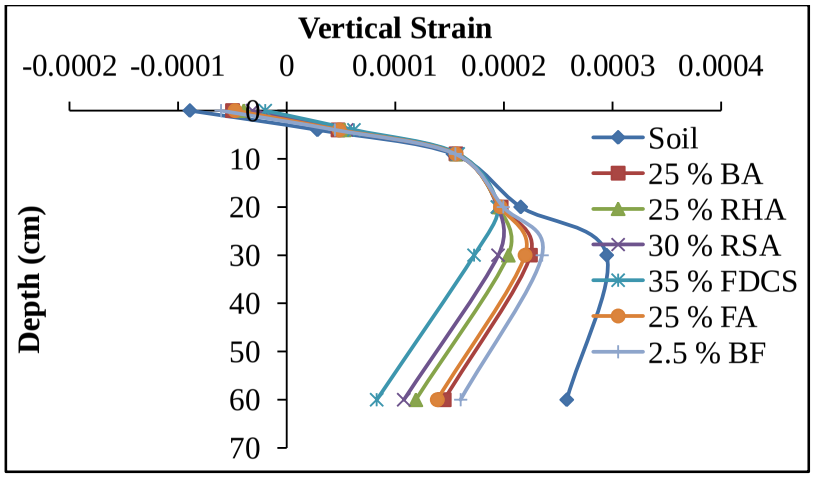

(a) At 200 kPa

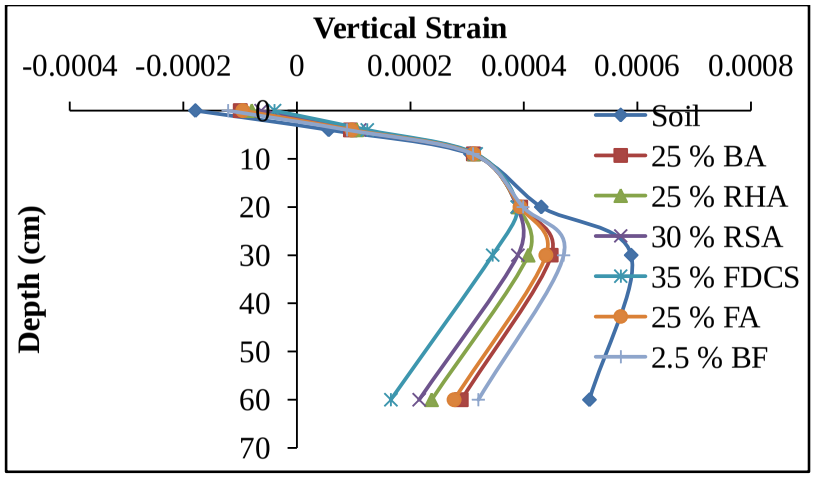

(b) At 400 kPa

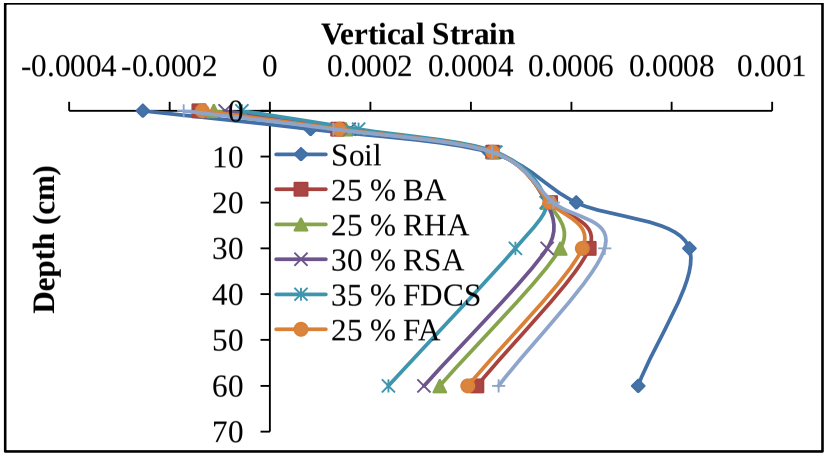

(c) At 570 kPa

Figure 6.7 Vertical Strain Distribution at Different Depths with Different Vertical Pressure

570 kPa respectively. From Figure 6.7 (a), it was observed that the vertical stresses decrease with depth by both analyses like KENLAYER as well as lab data. Vertical stresses of pavement which were determined by lab data followed the same pattern as compared to KENLAYER plots but slightly more in magnitude for every admixed soil and all applied pressures. The vertical stress decreases more upto 30 cm depth and after that the decrease was not prominent. It means higher vertical load is thus transferred to the upper underlying surfacing.

In the thin surfacing layers the vertical stress significantly decreased with depth, and is in fact reduced by about 10% from 200 kPa at the top to about 180 kPa at 4 cm depth, also reduction was 25.2%, 42.4%, 17% & 2.7% at 9, 20, 30 & 60 cm depth respectively in case of natural subgrade soil. When subgrade soil was admixed with 25% FA, the vertical stresses decreased 9.4%, 23.5%, 39%, 16.7% & 6.6% at the depth of 4, 9, 20, 30 & 60 cm respectively for applied pressure of 200 kPa. Like this, vertical stresses decreased by 9.5%, 23.6%, 39.3%, 16.7% & 6.3% for 25% BA; 9.2%, 22.9%, 38.1%, 16.6% & 7.9% for 25% RHA; 9.1%, 22.6%, 37.4%, 16.5% & 8.8% for 30% RSA; 8.8%, 21.7%, 35.6%, 16.4% & 11.1% for 35 % FDCS and 9.6%, 23.9%, 39.9%, 16.8% & 5.5% at the depth of 4, 9, 20, 30 & 60 cm for applied pressure of 200 kPa. The same pattern was found at applied pressure of 400 kPa and 570 kPa as shown in Figure 6.8 (b) & (c) respectively.

From these analyses, it was noticed that if upper layer is much stiffer than the lower layer, it absorbs most of the stress. If stiffness of lower layer is increased, the stress is transferred more in lower layer. At different loading conditions, the ratio of stress transfer was almost same in this study.

6.4 SUMMARY

Mechanistic-emprical design of flexible pavement has been discussed in this chapter. For this, first the stress, strain and surface deflection of model pavement section were found by model tank test and then compared these results were compared with the results of KENPAVE software. Model pavement section consist of subgrade, sub base, WMM, DBM and BC layers. Stresses were determined by pressure cell at each interface layer of model pavement section for only three types of subgrade soil viz., natural soil, BA admixed soil & FDCS admixed soil to validate the KENLAYER analysis and other admixed soil like FA, RHA, RSA and BF were analysed by KENLAYER.

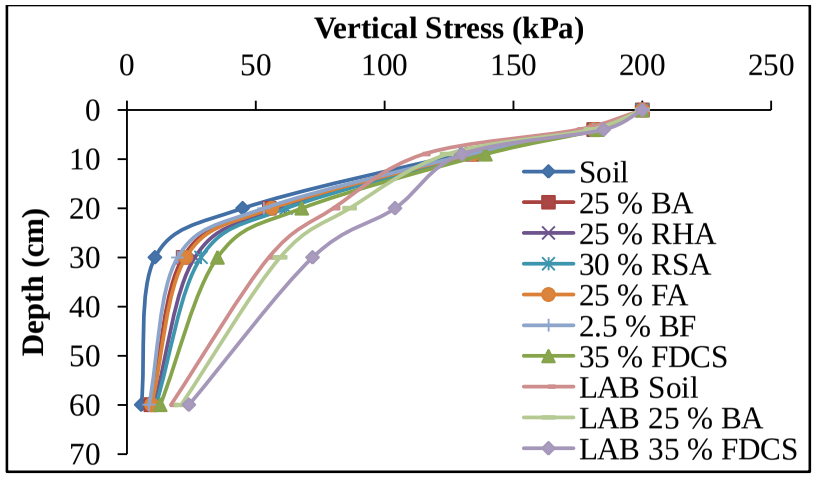

(a) At 200 kPa

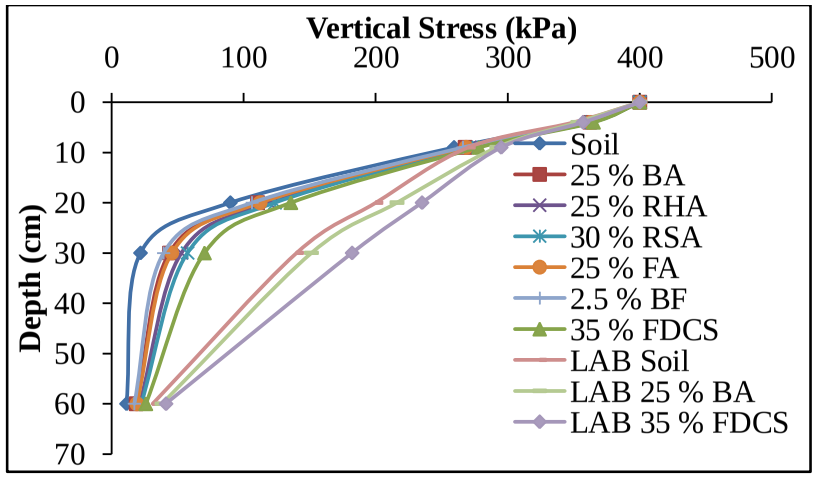

(b) At 400 kPa

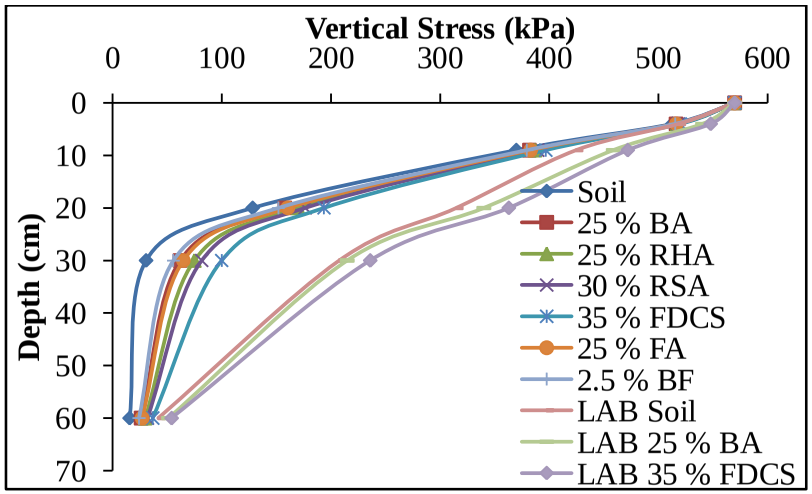

(c) At 570 kPa

Figure 6.8 Vertical Stress Distribution at Different Depths with Different Vertical Pressure

CHAPTER 7

COST ANALYSIS

7.1 GENERAL

Cost analysis of road construction with non-conventional materials, should justify the proposal in terms of cost incurred and benefits derived. In order to achieve the stated objective in Chapter 2, it is required to study the geotechnical properties of the expansive soil and the effects of stabilizers i.e. by adding different types of waste material such as FA, RHA, BA, RSA, FDCS and BF on the properties of expansive soil, especially CBR behavior as describe in Chapter 5. Based on the CBR value it has been studied and the comparative cost analysis is carried out between the stabilized and non-stabilized subgrade soil flexible pavement from the economic point of view.

7.2 COST ANALYSIS

For the cost benefit analysis of the stabilized soil by different types of additives, it is necessary to evaluate the pavement thickness reduction in different layers besed on its CBR value. As per recommendation of IRC:37-2012, the design thickness is given for minimum 3% CBR value of subgrade material of cumulative traffic 2 to 150 million standard axle (msa). Since the used soil has CBR value of 1.86% only which cannot be accepted for pavement construction. The admixing of different types of waste materials increased the value of CBR from 1.86% to 8%, 6.94%, 12.09%, 15.02%, 29.09% & 5.07% on the admixing of optimum content as stated FA, BA, RHA, RSA, FDCS & BF respectively in chapter 5. The increase in CBR value shows the thickness reduction in different layers as resulting in cost reduction of pavement. IRC: 37-2012 gives the different plates for thickness of different layer with respect the different traffic conditions from 2 msa to 150 msa based on CBR value of 3% to 15% for subgrade soil so, the account of thickness for this study CBR value was taken minimum 3% and maximum 15%. According to CBR values of natural soil and soil admixed with optimum content of different additives, the total thickness of pavement excluding subgrade is shown in Figure 7.1 as per IRC: 37-2012. The total thickness of pavement was 805 mm in case of natural subgrade soil

and minimum value was 555 mm after admixing of FDCS and RSA. Table 7.1 shows the thickness of various layers. This reduction in thickness indicates the reduction in cost. From economic point of view the selected waste material is available free of cost from different sources and are widely available across the India, so the cost of stabilizer can be neglected.

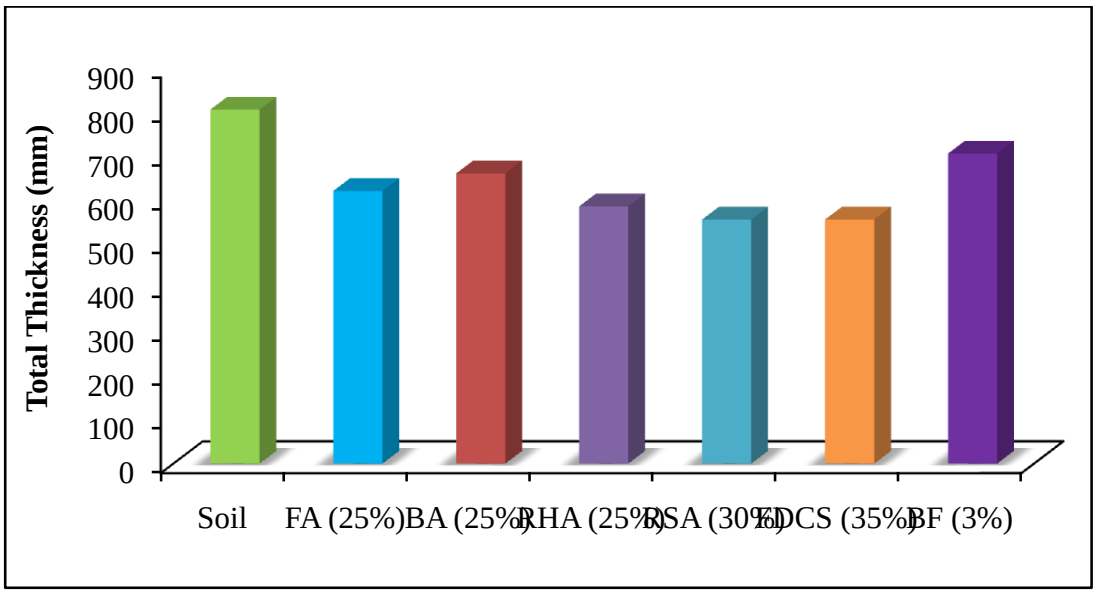

Figure 7.1 Total Thickness of Pavement for Different Admixed Subgrade Soil

As per the schedule rates of 2012, Government of Uttar Predesh, India, the cost of stabilized and unstabilized soil subgrade pavement per km per lane of pavement for cumulative traffic of 50 msa in Indian Rupees has been calculated as shown in Table 7.2. The total cost of pavement was 136.08 lakh/km/lane when subgrade soil was natural soil but it reduced to 106.77 lakh/km/lane by admixing 25% FA subgrade soil. The total cost saving was 21.56% after admixing of FA.

Table 7.1 Various Components of Layers and CBR of Subgrade

S.N.	Subgrade Materials	CBR of Subgrade Materials (%)	Thickness of Various Layers (mm)				
			Sub base	Base Layer I	Base Layer II	DBM	BC
1	Natural soil	1.86	380	150	100	135	40
2	FA	8	200	150	100	100	40
3	BA	6.94	230	150	100	120	50
4	RHA	12.09	200	150	100	95	40
5	RSA	15.02	200	150	100	65	40
6	FDCS	29.09	200	150	100	65	40
7	BF	5.07	300	150	100	115	40

Table 7.2 Cost Analysis of Pavement Containing Natural and Admixed Subgrade Soil per km per Lane

Natural Soil Subgrade		
Description	***Thickness (mm)***	***Cost Per km (lakh)***
Earth Work	500	7.35
Granular Sub-base	380	35.06
Wet Mix Macadam		
For 53 mm maximum size	150	15.32
For 45 mm maximum size	100	9.99
Prime coat		1.35
Tack coat		0.76
Dense Graded Bituminous Macadam	135	49.03
Tack coat		0.76
Bituminous Concrete	40	16.48
	Total Cost	**136.08**
Soil Admixed with 25% FA Subgrade		
Description	***Thickness (mm)***	***Cost Per km (lakh)***
Earth Work	500	7.35
Granular Sub-base	200	18.45

Wet Mix Macadam		
For 53 mm maximum size	150	15.32
For 45 mm maximum size	100	9.99
Prime coat		1.35
Tack coat		0.76
Dense Graded Bituminous Macadam	100	36.32
Tack coat		0.76
Bituminous Concrete	40	16.48
	Total Cost	**106.77**
	Total Saving (%)	**21.54**
Soil Admixed with 25% BA Subgrade		
Description	***Thickness (mm)***	***Cost Per km (lakh)***
Earth Work	500	7.35
Granular Sub-base	230	21.22
Wet Mix Macadam		
For 53 mm maximum size	150	15.32
For 45 mm maximum size	100	9.99
Prime coat		1.35
Tack coat		0.76
Dense Graded Bituminous Macadam	120	43.58
Tack coat		0.76
Bituminous Concrete	50	20.60
	Total Cost	**120.92**
	Total Saving (%)	**11.14**
Soil Admixed with 25% RHA Subgrade		
Description	***Thickness (mm)***	***Cost Per km (lakh)***
Earth Work	500	7.35
Granular Sub-base	200	18.45
Wet Mix Macadam		
For 53 mm maximum size	150	15.32
For 45 mm maximum size	100	9.99
Prime coat		1.35
Tack coat		0.76
Dense Graded Bituminous Macadam	95	34.50
Tack coat		0.76
Bituminous Concrete	40	16.48

	Total Cost	**104.95**
	Total Saving (%)	**22.88**
Soil Admixed with 30% RSA Subgrade		
Description	***Thickness (mm)***	***Cost Per km (lakh)***
Earth Work	500	7.35
Granular Sub-base	200	18.45
Wet Mix Macadam		
For 53 mm maximum size	150	15.32
For 45 mm maximum size	100	9.99
Prime coat	1	1.35
Tack coat	1	0.76
Dense Graded Bituminous Macadam	65	23.61
Tack coat	1	0.76
Bituminous Concrete	40	16.48
	Total Cost	**94.05**
	Total Saving (%)	**30.89**
Soil Admixed with 35% FDCS Subgrade		
Description	***Thickness (mm)***	***Cost Per km (lakh)***
Earth Work	500	7.35
Granular Sub-base	200	18.45
Wet Mix Macadam		
For 53 mm maximum size	150	15.32
For 45 mm maximum size	100	9.99
Prime coat	1	1.35
Tack coat	1	0.76
Dense Graded Bituminous Macadam	65	23.61
Tack coat	1	0.76
Bituminous Concrete	40	16.48
	Total Cost	**94.05**
	Total Saving (%)	**30.89**
Soil Admixed with 2.5% BF Subgrade		
Description	***Thickness (mm)***	***Cost Per km (lakh)***
Earth Work	500	7.35
Granular Sub-base	300	27.68
Wet Mix Macadam		
For 53 mm maximum size	150	15.32

For 45 mm maximum size	100	9.99
Prime coat		1.35
Tack coat		0.76
Dense Graded Bituminous Macadam	115	41.77
Tack coat		0.76
Bituminous Concrete	40	16.48
	Total Cost	**121.44**
	Total Saving (%)	**10.76**

Figure 7.2 shows the total cost of pavement per km per lane for different soil subgrades as natural soil, soil-FA, soil-RHA, soil-BA, soil-RSA, soil-FDCS and soil-BF at its optimum content. Total cost of pavement was 136.08 lakh, 106.77 lakh, 109.53 lakh, 104.95 lakh, 94.05 lakh, 94.05 lakh & 121.44 lakh /km/lane when subgrade soil was natural soil, FA, BA, RHA, RSA, FDCS & BF admixed soil respectively. There the total percent reduction of cost was 21.56%, 19.53%, 22.90%, 30.90%, 30.90% & 10.78% for different subgrade soil admixed with FA, BA, RHA, RSA, FDCS & BF respectively as shown in Figure 7.3. It was seen that all waste materials used for subgrade soil at its optimum content of admixing not only improve the strength but also reduce the total cost of pavement.

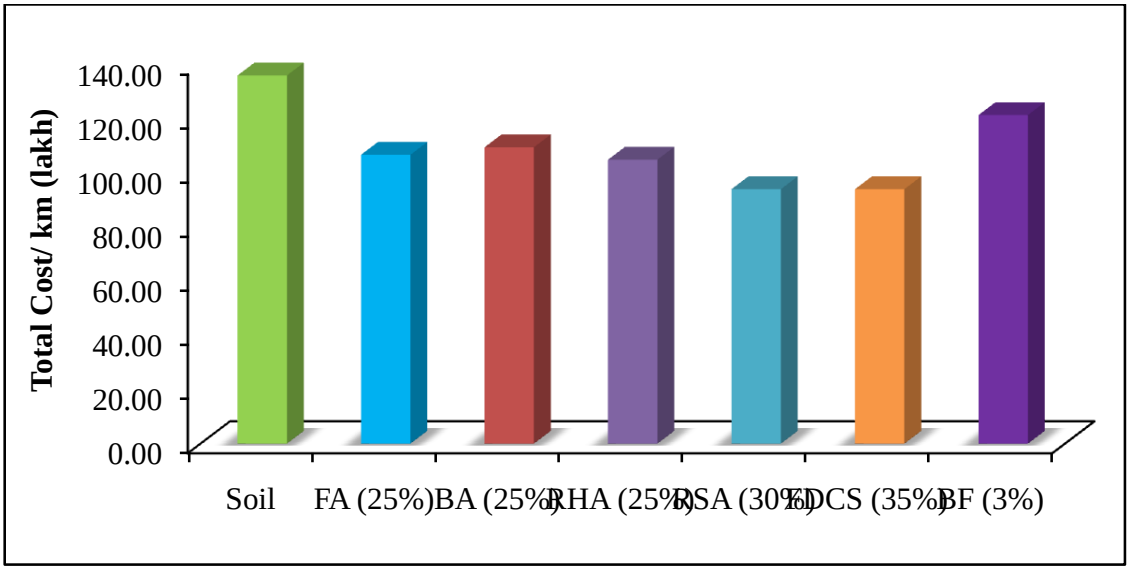

Figure 7.2 Total Cost of Pavement for Different Admixed Subgrade Soil

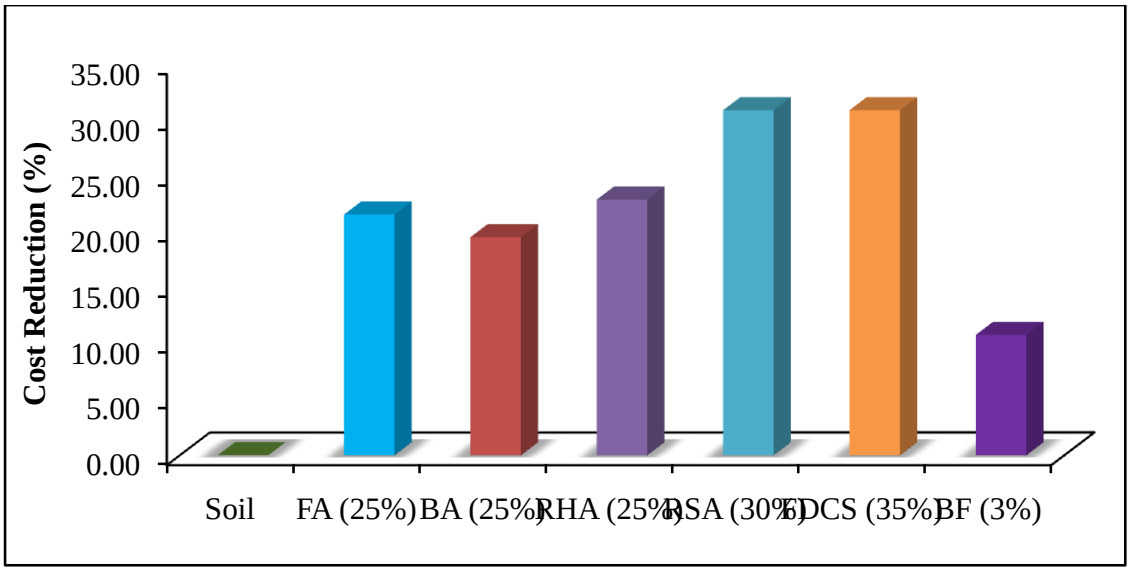

Figure 7.3 Total Cost Reduction of Pavement for Different Admixed Subgrade Soil

7.3 SUMMARY

Cost analysis was conducted to determine the total cost of pavement per km per lane for different soil subgrades as natural soil, soil-FA, soil-RHA, soil-BA, soil-RSA, soil-FDCS and soil-BF admixed at their optimum content. CBR values were changed by admixing of different waste materials which affects the total costs of pavement. According to CBR values, the thickness of different layers was determined by IRC: 37-2012 and thickness of subgrade was kept same as 500 mm. The total thickness of pavement was 805 mm in case of natural subgrade soil and minimum 555 mm at admixing of FDCS and RSA. As per the schedule rates of 2012, Government of Uttar Predesh , India, the cost of different layers was determined per km per lane for cumulative traffic of 50 msa and then total cost was calculated for stabilized and unstabilized soil subgrade pavement. It was seen that all waste materials used for subgrade soil at their optimum content reduce the total cost of pavement and comparatively more reduction was observed for FDCS and RHA admixed soil subgrade.

CHAPTER 8

CONCLUSIONS AND RECOMMENDATIONS

8.1 CONCLUSIONS

Based on the studies conducted in the present research work, following conclusions have been drawn:

8.1.1 TGA and Physical Properties

From TGA curve, it is learnt that mass loss for fly ash (FA) and rice husk ash (RHA) were found to be in the range of 1.0-1.7% after heating to a high temperature of 650^0 C. Whereas for bagasse ash (BA) and rice straw ash (RSA), the mass loss was in the range of 8-11%. This analysis elucidates that collected waste materials content no appreciable amount of carbon substance. Hence, in their present form itself, they can be utilized as additives (stabilizers) for improving the properties of expansive subgrade soil.

8.1.2 Atterberg limits

Adding FA, RHA, BA, RSA & FDCS to the expansive soil causes a decrease in plasticity index parameter. Decrease of plasticity index was due to the decrease in both liquid limit and plastic limit. However, maximum percentage decrease in PI was offered by FDCS followed by FA, BA, RHA and RSA respectively irrespective of inclusion levels. Laboratory results elucidate that FDCS is the most suitable additives amongst all selected additives from plasticity index point of view. Considerable decrease in PI on admixing of FDCS may be attributed to the increase of non-plastic sand & silt particles and remnant cement grains in the matrix. Also, FDCS being ultra fine cementing material, there might have been pozzolanic reaction of cement grain with Portlandite to form additional calcium silicate hydrates.

8.1.3 Free Swelling Index

Substantial decrease in free swelling index was observed after admixing of FA, RHA, BA, RSA and FDCS to an expansive soil irrespective of inclusion levels. Free swelling index of expansive soil was found to be 45. Whereas this value decreased to 13.82, 10.89, 12.15, 14.29 & 17.75 when FA, RHA, BA, RSA and FDCS were admixed with expansive soil. From free swelling index point of view, RHA apparently proves to be the most effective additive followed by BA, RSA, FA and FDCS respectively.

8.1.4 Compaction Analysis

Increasing the amount of FA, RHA, BA, RSA, FDCS and BF causes an increase in optimum moisture content. Optimum moisture content increased with increasing additives content. The rate of optimum moisture content increase was almost linear with additives content. This increase was maintained upto 35% inclusion level for FA, RHA, BA, RSA and FDCS. Whereas for BF, it was upto 3.5%. Optimum moisture content for FA, RHA, BA, RSA, FDCS admixed soils and BF reinforced soil are 23.0%, 42.0%, 25.5%, 34.1%, 21.8% and 24% respectively. The increase of optimum moisture content on admixing of additives may be due to the activation of pozzolan reaction of soil and free lime presence in FA, RHA, BA, RSA and FDCS. Whereas for BF, this phenomenon was mainly due to high water absorption characteristics of BF, being cellulose material and porous in nature.

Increasing the inclusion level of FA, RHA, BA, RSA, FDCS and BF to expansive soil makes soil lighter. Therefore, increasing the amount of FA, RHA, BA, RSA, FDCS and BF causes a decreasing rate in dry density. Maximum reduction in dry density was observed at 35% inclusion level for FA, RHA, BA, RSA and FDCS admixed soils. Whereas for BF, it was observed at 3.5% inclusion level. Maximum dry density of expansive soil was found to be 1.72 g/cm^3 and this MDD decreases to 1.59 g/cm^3, 1.23 g/cm^3, 1.42 g/cm^3, 1.28 g/cm^3, 1.52 g/cm^3 & 1.53 g/cm^3 after admixing FA, RHA, BA, RSA, FDCS and BF respectively.

8.1.5 California Bearing Ratio and Expansion Ratio

There is a considerable increase in CBR value on admixing of FA, RHA, BA, RSA, FDCS and BF to expansive soil. From CBR value point of view, the maximum CBR value recorded for

FA, RHA, BA, RSA, FDCS and BF are at 25%, 25%, 25% 30%, 35% and 3.0% mixing respectively irrespective of curing period. Substantial improvement in CBR value was observed for admixed soil samples subjected to relative humidity curing for 7 days continuously. Admixing of BF 3.0% could elevate CBR value upto 5.4 from 1.86. Higher CBR value for higher inclusion levels of FA, RHA, BA and RSA are mainly because of the growth of the cementitious products that fill the large pores. In overall, due to the frictional resistance offered by the additives (FA, RHA, BA and RSA). CBR value improvement on admixing of FDCS is mainly attributed to ultra fine particles of FDCS which could rearrange particles distribution of the matrix. As a result of which dense packing of the FDCS particles at the interface of soil particles occurred. It may also be due to pozzolanic activity of FDCS. However, further investigation is sincerely suggested in this regard.

No appreciable increased in CBR value was observed with the increasing curing period for BF reinforced soils. This clearly advocates that BF is an inert substance for expansive soil.

8.1.6 Hydraulic Conductivity

Incorporation of FA, RHA, BA, RSA & FDCS to expansive soil reduces permeability considerably. Whereas for BF reinforced soils, permeability increases. The decrease of permeability was more pronounced upto 20 % inclusion levels for FA & RHA admixed soils; 25% & 15% inclusion levels for RSA and BA admixed soils respectively. Higher reduction in permeability is observed for higher FDCS inclusion levels. When soil was admixed with BF, permeability of soil increases upto 3.5 % inclusion level. The percentage increase of permeability after admixing of BF @ 0.5 %, 1.0 %, 1.5 %, 2.0 %, 2.5 %, 3.0 % & 3.5 % are 16.73 %, 22.32 %, 31.50 %, 43.73 %, 52.91 %, 59.02 % & 65.14 % respectively with respect to expansive soil. The change in the fabric of the expansive soil; causes change in the pore system. Water flow in soil depends on the pore space. In the case of BF, increase in permeability is due to the media presented by BF to flow water in the matrix. The decrease of permeability on admixing of FA, RHA, BA and RSA may be due to the partial dissociation of the calcium hydroxide in samples. The calcium ions combined with the reactive silica or alumina, or both, which obstructed flow through the soil voids.

8.1.7 Unconfined Compressive Strength and Split Tensile Strength

Admixing of FA, RHA, BA, RSA, FDCS & BF increased the unconfined compressive strength of the soil considerably. Maximum improvements were observed at 30% inclusion level for FA & RHA admixed soils. Similarly, for BA and FDCS admixed soils, maximum unconfined compressive strength was observed at 35% inclusion level. Whereas for bagasse fiber reinforced soil, maximum unconfined compressive strength was recorded at 2.5% inclusion level. If percentage increase of UCS after admixing of FA, RHA, BA, RSA, FDCS and BF to expansive soil are compared, the performance of these additives superior to inferior are in the order of BF > FDCS > RSA > RHA > FA respectively. Significant improvement in unconfined compressive strength for reinforced bagsse fiber is mainly due to excellent reinforcing effect of fiber. However, further study in this regard is sincerely recommended particularly for long term performance as bagsse fiber is biodegradable material. Prolong curing showed significant impact on unconfined compressive strength particularly for admixed soils.

Substantial improvement in split tensile strength was observed for admixed soils irrespective of inclusion levels. Highest tensile strength was recorded at 30% inclusion level for FA admixed soils. Similarly, highest tensile strengths were recorded at 25%, 30%, 35%, and 2.5% inclusion levels for RHA, BA, RSA, FDCS and BF admixed soils respectively. Beyond these inclusion levels, unconfined compressive strength starts declining. Significant improvement in tensile strength was observed for prolong curing.

Ratio of split tensile strength to unconfined compressive strength decreased with increase in FA, RHA, BA, RSA, & FDCS content, indicating that these additives are more efficient when soil was subjected to compression rather than to tension. But ratio of split tensile strength and unconfined compressive strength increased with increase in BF content, indicating that BF is more efficient when soil was subjected to tension rather than to compression.

8.1.8 Triaxial Test

Three different confining stresses i.e. 100, 150 and 200 kPa were applied on specimens to obtain peak deviator stress. Higher deviator stresses are observed for 30% FA, 25% RHA, 25%

BA, 30% RSA 35% FDCS & 2.5% BF content irrespective of confining pressure applied and curing period but beyond this inclusion levels, the deviator stress starts declining gradually.

Admixing of these additives causes increase in cohesion and internal friction angle. Cohesion of soil increases from 28.83 kPa to 42.99, 46.12, 45.15, 51.19, 55.23 & 64.44 kPa after admixing of FA 30%, RHA 25%, BA 25%, RSA 30% FDCS 35% & BF 2.5% respectively. As in the case of cohesion, similar trend of improvement is observed for internal friction angle. The rate of improvement of internal friction angle is rapid upto 5% inclusion level for all the cases but beyond this level, the rate of improvement of internal friction angle is slightly sluggish and this largely extend beyond optimum inclusion levels and thence, internal friction angle reduced significantly. Improvements in cohesion and internal friction angle on admixing of FA, RHA, BA, RSA and FDCS may be due to pozzolanic activity and also may be due to the fact that internal friction angle of these additives are more than that of expansive soil. Whereas in the case of BF reinforced soil, reinforcing bagasse fiber soil behaves like strain hardening fiber reinforcement. Consoli et al. (2003) also suggested that such behavior of fiber reinforced soil can apposite application in shallow foundation embankment over soft soils.

8.1.9 Cyclic Triaxial Test

Rapid increase in deformation of the expansive soil and admixed soils were observed during the initial approximate hundred cycles of loading and the strain rate was high during this stage in all cases. After few hundred cycles of loading, the increase in deformations was progressively increased upto 2000 cycles thereafter deformation almost stabilized for admixed soils. But deformation was still taking place for expansive soil. For admixed soils, the matrix behaves almost elastically under the applied load. The maximum permanent strain of 6.15 % was observed for expansive soil when 0.8 DSL and 100 kPa confining pressure were applied. Consequently, the minimum permanent strain of 2.21 %, 2.04%, 2.1%, 1.87%, 1.80% and 2.10% respectively for FA 30%, RHA25%, BA 25%, RSA 30%, FDCS 35% and BF 2.5% under 0.5 DSL at 200 kPa for 10000 cycles. From permanent strain point of view, the least permanent strain is offered by FDCS admixed soil followed by RSA, RHA, BA & BF and FA respectively.

It is also learnt that permanent deformation decreases with increase in confining pressure irrespective of types of samples. However, least permanent deformation was recorded for 35% FDCS inclusion level amongst all additives. 30%, 25%, 25%, 30% , 30%, 35% and 2.5% are the respective inclusion levels at which minimum permanent deformations occurred after admixing of FA , RHA, BA, RSA, FDCS and BF respectively.

On other hand, decrease of deviator stress (σ_d) value signifies improvement in permanent strain. The minimum value of (σ_d) observed for 30% FA admixed soil was 2.21% by applying 0.5DSL & 200 kPa. Whereas for 0.8DSL, 2.94% was observed.
Similarly minimum value of σ_d for 25% RHA , 30BA%, 30%RSA, 30% FDCS and 2.5% BF were 2.04%, 2.4%, 1.87%, 1.80% and 2.10% respectively under 0.5DSL & 200 kPa. Whereas these values for 0.8DSL & 200 kPa are 2.35%, 2.70%, 2.5%, 2.35% and 2.66% respectively for RHA, BA, RSA, FDCS and BF admixed soils.

Resilient modulus (M_R) values increase with increase in additives content irrespective of DSL & confining pressure. The maximum M_R values observed were 110 MPa & 69 MPa at 0.5 & 0.8 DSL respectively for a constant 200 kPa confining pressure when no admixing was done. These values increased to 171 & 107 MPa, 214 & 134 MPa , 205 & 128 MPa, 205 & 128 MPa, 297 & 167 MPa and 397 & 248 MPa after admixing 30% FA, 25% RHA, 25%BA, 30% RSA, 35% FDCS and 2.5% BF respectively for the same working condition. Improvement in resilient modulus of expansive soil on admixing of additives may be due to a stiffer soil skeleton structure of FA , RHA, BA, RSA and FDCS, caused by increased confinement and pozzolanic reactions, which result in a closer bonding of soil particles.

8.1.10 Plate Load Test

It was observed that modulus of subgrade reaction (k) was increased upto 25% FA, 25% RHA, 25% BA, 30% RSA, 35% FDCS & 3% BF inclusion levels. Beyond this levels, k value decreases. The modulus of subgrade reaction value of expansive soil was found to be 17 MPa/m^3. This value increased to 51.57, 57.08, 49.83, 59.52, 96.92 & 39.86 MPa/m^3 respectively after admixing FA, RHA, BA, RSA, FDCS & BF to expansive soil. Highest k-

value was offered by FDCS admixed soil followed by RSA, RHA, FA, BA and BF respectively.

Similarly, there is substantial improvement in ultimate strength capacity of expensive soil on admixing of FA, RHA, BA, RSA, FDCS & BF. Initial k-value of expansive soil was 198 kPa and this value increased to 293, 308, 300, 318, 330 & 248 kPa respectively on admixing of FA 30%, RHA 25%, BA 25%, RSA 30% FDCS 30% & BF 3% respectively.

8.1.11 Microstructural Investigation

Upon inclusion of fly ash (FA), substantial formations of Calcium Silicate Hydrate (C-S-H) gel, Portlandite [Ca (OH_2)] along with presence of ettringite compound are seen from SEM images. Interestingly, ettringite was formed using fly ash spheres as nucleation site. These are the few hydrated compounds which basically mobilized to generate pozzolanic reaction and infill voids better. Fly ash used was amorphous in nature. Rice husk ash (RHA) is of cellular shape and possessed larger surface area caused by microstructural shape like cubes of cellular beehives. Presence of cellular shape of RHA could increase water absorption capacity.

Bagasse fibers are uniformly distributed over the soil matrix as evident from SEM image. Presences of abundant granular structures of BA are also distinctly visible from the ground mass. The chemical compositions shown in Table 4.9 in chapter 4, reveal that BA can be assigned as class N pozzolana as prescribed by ASTMC 618. BA particles with various sizes and geometry like prismatic, spherical and fibrous were recognized. The result of SEM suggests that prismatic particles consist mainly of silica. **G**ranular structures of RSA are clearly visible from SEM image. RSA particles with various sizes and geometry like prismatic, spherical and fibrous were detected. Formations of important hydration products like C-S-H gel, CAH and $Ca(OH)_2$ are observed from the ground mass.

Granular structures of FDCS are prominently observed in all the SEM images. Few remnant cement grains could also be noticed. SEM images strongly suggests formations of C-S-H gels, ettringite and Ca ($OH)_2$ hydrated compounds. However, TEM study is suggested to digest better about the formations of these compounds. But one thing is very clear that matrix is densely packed and there is a great tendency to develope a strong interaction between soil

particles and FDCS. Particles with various sizes and geometry like prismatic, spherical and fibrous have figured out. Few of them may be of SiO_2 compound particular prismatic structures.

Fibers in bagasse consist mainly of cellulose, pentosan and lignin. Cellulose is highly crystalline regardless of the source. The cross section of bagaase fiber is irregular and they are randomly distributed. The bagasse fiber bundles consist of several to hundreds of ultimate fiber cells. Excellent reinforcing effect between soil particles and bagasse fibes is also observed.

8.1.12 Correlation Between Different Strength Parameters

It was observed that the relationship between CBR value (CBR in %) and additives content (FA, RHA, BA,RSA, FDCS & BF in %) has strong correlation with curing time (D ≥ 3 days) described by a linear equation as given below:

For soil-FA mixtures

$$CBR = 2.559+0.172\ \%FA+0.0144\ D; \qquad R^2= 0.849 \qquad (8.1)$$

For soil-RHA mixtures

$$CBR = 4.072 +0.266\%RHA +0.025D; \qquad R^2 = 0.739 \qquad (8.2)$$

For soil-BA mixtures

$$CBR = 3.45+0.117\%BA +0.02D; \qquad R^2= 0.555 \qquad (8.3)$$

For soil-RSA mixtures

$$CBR=5.04+0.344\%RSA+0.06D; \qquad R^2=0.699 \qquad (8.4)$$

For soil-FDCS mixtures

$$CBR = 7.17 +0.723\%FDCS + 0.061D; \qquad R^2 =0.851 \qquad (8.5)$$

For soil-BF mixtures

$$CBR = 1.905 +0.937\%\ BF +0.0063\ D \qquad R^2=0.699 \qquad (8.6)$$

Similarly, CBR (CBR in %), UCS value (UCS in %) and additives content (FA, RHA, BA,RSA, FDCS & BF in %) have strong correlation with curing time (D ≥ 3 days) described by a linear equation as given below:

For soil-FA mixtures

$$UCS = 67.8233 - 0.73\%FA+0.05D+9.88CBR; \quad R^2= 0.964 \quad (8.7)$$

For soil-RHA mixtures

$$UCS = 65.07 -1.18\%RHA +0.16D +9.51CBR; \quad R^2= 0.965 \quad (8.8)$$

For soil-BA mixtures

$$UCS = 55.79-0.25\%BA +0.142D + 12.87CBR; \quad R^2= 0.970 \quad (8.9)$$

For soil-RSA mixtures

$$UCS = 69.555-0.151\%RSA +0.019D +7.781CBR; \quad R^2= 0.986 \quad (8.10)$$

For soil-FDCS mixtures

$$UCS = 66.69-0.97\%FDCS + 0.201D + 6.27CBR; \quad R^2= 0.986 \quad (8.11)$$

For soil-BF mixtures

$$UCS = 13.78 -10.38\% BF +0.122D+64.45 CBR; \quad R^2= 0.852 \quad (8.12)$$

High values of R^2 show close proximity to predicted values with experimental data.

8.1.13 Model Tank Test and KENPAVE Analysis

Vertical deformation characteristics recorded for pre-determined pressures of 200 kPa, 400 kPa and 570 kPa considering the half of single axle load to simulate the field conditions revealed that total deformation at surface was more in case of expansive soil as compared to BA & FDCS admixed soils. It was also observed that total deformation of pavement system increased with increase in load cycle. The increase was rapid upto 200 cycles, after that increase was gradual upto 5000 cycles for all cases. Whereas for admixed soils, this increase was almost stabilized after 2000 cycles but for expansive soil, total deformation continued even after 5000 cycles.

Similarly, vertical stresses were determined at each interface and bottom of subgrade pavement system at three different pressures. It was observed that vertical stress decreased with increase in depth for all loading conditions. The vertical stress decreased at the depth of 4cm, 9cm, 20 cm, 30 cm & 60 cm are 9%, 16.5%,19.3%,18.8% & 29.1% respectively when subgrade layer was prepared with expansive soil for a given pressure of 570 kPa. When BA admixed soil was

used in liu of expansive soil in the subgrade layer, the vertical stress decreased at the depth of 4cm, 9cm, 20 cm, 30 cm & 60 cm are 5.2%, 14.3%,20.8%,22.0% & 28.7% respectively. These decrease for FDCS admixed soil subgrade are found to be 3.9%, 13.3%, 19.1%, 22.3% and 31.9% respectively for the same working conditions.

From KENLAYER analysis, it was also observed that the vertical deflection decreases with respect to the depth except on top layer. Lesser deflection was observed for admixed soil as compared to expansive soil. Of all the considered admixed soils, FDCS admixed soil subgrade offered the maximum reduction in deflection under the same working conditions. Maximum reductions recorded were 67% at top and 81% at 60 cm. Similarly, the minimum vertical strain was recorded for FDCA admixed soils at 35% inclusion level amongst the admixed soils. Vertical strain reduction at top was 78% and 68% at 60 cm depth (bottom).

8.1.14 Cost Comparison

Cost comparison made based on CBR values of expansive soil and admixed soils suggest that total cost of pavement without any additives for a lane having 3.5 m would be Rs. 136.08 lakh/km/lane exclusively for materials. But if admixing is done with FA, RHA, BA, RSA, FDCS and BF, there would be a cost saving of about 21.56%, 19.53%, 22.90%, 30.90%, 30.90% & 10.78% respectively. In this way, the maximum cost saving is offered by FDCS & RSA followed by BA, FA, RHA and BF respectively.

8.2 RECOMMENDATIONS

Based on the studies carried out in the present research work, following recommendations are being made:

1. For the properties investigated in this study, the expansive soil can be stabilized satisfactorily with 25% to 30% of Dadri fly-ash in its present form without further treatment.
2. Admixing of rice husk ash (RHA), bagasse ash (BA), rice straw ash (RSA), fines obtained from demolished concrete slab (FDCS) and bagasse fiber (BF) substantially improved engineering properties of expansive soil. Based on their efficacies while admixing with

expansive soil, the following inclusion levels are recommended for stabilizing expansive soil in road construction industry:

(i) Rice husk ash (RHA) – 25% by weight of dry soil.
(ii) Bagasse ash (BA) – 25% -30% by weight of dry soil
(iii) Rice straw ash (RSA) – 30% by weight of dry soil.
(iv) Fines obtained from demolished concrete slab (FDCS) -35% onwards.
(v) Bagasse fiber (BF) – between 2.5- 3.0% by weight of dry soil.

3. Admixing of FA, RHA, BA, RSA, FDCS and BF with expansive soil not only improved soil engineering properties but also considerably reduced the cost of road construction. In addition to that, recycling of these waste materials can benefit our community and the environment. Hence, use of these waste materials is strongly recommended if available near the work site.

8.3 SCOPE FOR THE FUTURE RESEARCH

1. The present study entails with specific condition (as received state) of waste materials (additives). Study for conditions other than as received state of material can be pursued.

2. In the present study, characterization of waste materials (additives) and performance related tests and mixtures performance tests for a short-term have only been addressed due to paucity of time. Therefore, long-term performance tests are strongly recommended particularly for bagasse fiber (BF) as this material is biodegradable.

REFERENCES

1. Aigbodion, V. S., Hassan, S. B., Ause, T. and Nyior, G.B. (2010), "Potential Utilization of Solid Waste (Bagasse Ash)", Journal of Minerals & Materials Characterization & Engineering, Vol. 9 (1), 67-77.
2. Alhassan, M. (2008), "Potentials of Rice Husk Ash for Soil Stabilization", A.U. J.T., Vol. 11(4), 246-250.
3. Al-Mukhtar, M., Lasledj, A. and Alcover, J. F. (2010), "Behavior and Mineralogy Changes in Lime-Treated Expansive Soil at 20°C", Applied Clay Science, Vol. 50 (2), 191-198.
4. Altun, S. and Goktepe, A.B. (2008), "Effects of Freezing and Thawing Processes on the Mechanical Behavior of Silty Soils Stabilized with Fly Ash", Advances in Transportation Geotechnics, Taylor & Francis Group, London, UK, 635-641.
5. Ameri, M., Salehabadi, E. G., Nejad, F. M. and Rostami, T. (2012), "Assessment of Analytical Techniques of Flexible Pavements by Final Element Method and Theory of Multi-Layer System", Journal of Basic and Applied Scientific Research, Vol. 2(11), 11743-11748.
6. Arnold, G. K. (2004), "Rutting of Granular Pavements", PhD Thesis, University of Nottingham, UK.
7. Arshad, A, K. (2007), "Flexible Pavement Design: Transitioning from Empirical to Mechanistic-Based Design Methods", JURUTERA Cover Story, July, 14-19.
8. ASTM C 618, (2001) "Standard Specification for Coal Fly Ash And Raw or Calcined Natural Pozzolan for Use as a Mineral Admixture in Concrete, ASTM Standards, 310-313.
9. ASTM D 1632, (2007), "Standard Practice for Making and Curing Soil-Cement Compression and Flexure Test Specimens in The Laboratory", ASTM International, United States.
10. ASTM D 3967 (2008), "Standard Test Method for Splitting Tensile Strength of Intact Rock Core Specimens", ASTM International, United States.

11. ASTM D 5311, (2011), "Standard Test Method for Load Controlled Cyclic Triaxial Strength of Soil", ASTM International, United States.
12. Awanti, S. S.; Amarnath, M. S. and Veeraragavan, A. (2008), "Laboratory Evaluation of SBS Modified Bituminous Paving Mix", Journal of Materials in Civil Engineering, Vol. 20(4), 327–330.
13. Bagasse Cogeneration Global Review and Potential (2004), World Alliance Fordecentralized Energy, Scotland, UK.
14. Baghdadi, Z. A., Fatani, M.N. and Sabban, N.A., (1995), "Soil Modification by Cement Kiln Dust", Journal of Materials in Civil Engineering, ASCE, Vol. 7(4), 218 – 222.
15. Bairagi, N. K., Vidyadhara, H. S., and Ravande, K. (1990), "Mix Design Procedure For Recycled Aggregate Concrete", Construction & Building Materials, Vol. 4(4), 188-193.
16. Basha, E.A., Hashim, R., Mahmud, H.B. and Muntohar, A.S. (2005), "Stabilization of Residual Soil with Rice Husk Ash and Cement", Construction and Building Materials, Vol. 19, 448–453.
17. Basic Road Statistics of India (2012), "Government of India, Ministry of road transport and highways", Transport research wing, New Delhi, India.
18. Basu, G., Roy, A.N., Bhattacharyya, S.K. and Ghosh, S.K. (2009), "Construction of Unpaved Rural Road Using Jute–Synthetic Blended Woven Geotextile – A Case Study", Geotextiles and Geomembranes, Vol. 27, 506–512.
19. Behaka, L. and Nunezb, W. P. (2013), "Effect of Burning Temperature on Alkaline Reactivity of Rice Husk Ash with Lime", Road Materials and Pavement Design, http://dx.doi.org/10.1080/14680629.2013.779305.
20. Blengini, G. A. (2009), "Life Cycle of Buildings, Demolition and Recycling Potential: A Case Study in Turin, Italy", Building and Environment, Vol. 44, 319– 330.
21. Boussinesq, J. (1885), "Application des potentials a l'etude de l'equilibre et du Mouvement des Solids Elastiques, Gauthier-Villars, Paris, France
22. Bowles, J., (1992), "Engineering Properties of Soil and Their Measurements", McGraw-Hill Boston, 4th Edition.
23. Brooks R. M. (2009), "Soil Stabilization with Flyash and Rice Husk Ash", International Journal of Research and Reviews in Applied Sciences, Vol. 1(3), 209-217.

24. Brooks, R., Udoeyo, F. F. and Takkalapelli, K. V. (2011), "Geotechnical Properties of Problem Soils Stabilized With Fly Ash and Lime Stone Dust In Philadelphia", Journal of Materials in Civil Engineering, ASCE, Vol. 23 (5), 711-716.
25. Brown, S. F., (1996), "36th Rankine Lecture: Soil Mechanics in Pavement Engineering Geotechnique", Vol. 46(3), 383–426.
26. Brown, S. F., (2004), "Design Considerations for Pavement and Rail Track Foundations", Proceeding International Seminar on Geotechnics in Pavement and Railway Design and Construction, Athens, 61–72.
27. Burmister, D. M. (1943), "The Theory of Stresses and Displacements in Layered Systems and Applications to the Design of Airport Runways", Transportation Research Record, No. 23, 126-144.
28. Burmister, D. M. (1949), "Principles and Techniques of Soil Identification", Proceeding of Annual High Research Board Meeting, National Research Council, Washington, D.C. Vol. 29, 402-433.
29. Central Electricity Authority, (2011), "Report on Fly Ash Generation at Coal/Lignite Based Thermal Power Stations and its Utilization in the Country for the Year 2010-11", New Delhi, India.
30. Chandra, S., Kumar, S. and Anand, R. K. (2005), "Soil Stabilization with Rice Husk Ash and Lime Sludge", Indian Highways, Indian Roads Congress, Vol. 33 (5), 87-98.
31. Chandra, S., Viladkar, M. N., and Nagrale P. P. (2008), "Mechanistic approach for fiber-reinforced flexible pavements, Journal of Transportation Engineering", ASCE, Vol. 134(1), 5–23.
32. Charaverty, A. and Kaleemullah, S. (1991), "Production of Amorphous Silica and Combustible Gas from Rice Straw", Journal of Materials Science, Vol. 26, 4554-4560.
33. Chen, F. H. (1988), "Foundations on Expansive Soils", Elsevier Publication, Amsterdam.
34. Choobbasti, A. J., Ghodrat, H., Vahdatirad, M. J., Firouzian, S., Barari, A., Torabi, M. and Bagherian, A. (2010), "Influence of Using Rice Husk Ash in Soil Stabilization Methodwith Lime", Front. Earth Sci. China, Vol. 4(4), 471–480.
35. Chusilp, N., Jaturapitakkul, C., Kiattikomol, K. (2009), "Effects of LOI of Ground Bagasse Ash on the Compressive Strength and Sulfate Resistance of Mortars", Construction and Building Materials, Vol. 23, 3523–3531.

36. Collins, R. J. and Ciesielski, S. K. (1993), "Recycling and Use of Waste Materials and Byproducts in Highway Construction", NCHRP Synthesis of Highway Practice 199, Transportation Research Board, Washington, DC.
37. Consoli, N. C., Casagrande, M. D. T., Prietto, P. D. M. and Thome, A. (2003), "Plate Load Test on Fiber-Reinforced Soil", Journal of Geotechnical and Geoenvironmental Engineering, Vol. 129 (10), 951-955.
38. Consoli, N. C., Prietto, P. D. M., Carraro, J. A. H., and Heineck, K. S. (2001). "Behavior of Compacted Soil-Fly Ash-Carbide Lime-Fly Ash Mixtures", Journal of Geotechnical and Geoenvironmental. Engineering., Vol. 127, 774–782.
39. Consoli, N. C., Rosa, F.D., Fonini, A. (2009), "Plate Load Tests On Cemented Soil Layers Overlaying Weaker Soil", Journal of Geotechnical and Geoenvironmental Engineering, Vol. 135(12), 1845-56.
40. Consoli, N. C., Schnaid, F., Milititsky, J. (1998), "Interpretation of Plate Load Tests On Residual Soil Site", Journal of Geotechnical and Geoenvironmental Engineering, Vol. 124(9), 857-67.
41. Consoli, N. C., Vendruscolo, M. A., Prietto, P. D. M. (2003), "Behavior of Plate Load Tests on Soil Layers Improved With Cement and Fiber", Journal of Geotechnical and Geoenvironmental Engineering, Vol.129 (1), 96-101.
42. Cordeiro, G. C., Filho, R. D. T. and Fairbairn, E. M. R. (2010), "Ultrafine Sugar Cane Bagasse Ash: High Potential Pozzolanic Material for Tropical Countries", IBRACON Structures and Materials Journal, Vol. 3(1), 50 – 67.
43. Cordeiro, G.C., Toledo Filho, R.D., Fairbairn, E.M.R. (2009), "Effect of Calcinations Temperature on the Pozzolanic Activityof Sugar Cane Bagasse Ash", Construction and Building Materials, Vol. 23, 3301–3303.
44. Das, B. M., (2010), "Principles of Geotechnical Engineering", 7th Edition, Cengage Learning, United States of America.
45. De Jong. D. L., Peatz, M. G. F., and Korswagen, A. R. (1973), "Computer Program Bisar, Layered Systems under Normal and Tangential Loads, Konin Klijke Shell-Laboratorium, Amsterdam, External Report, AMSR.0006.73.

46. Department of Urban Development , Solid Waste Management, Chapter – 12, Govt. of Delhi, http://ccsindia.org/ccsindia/pdf/Ch12_Solid%20Waste%20Management.pdf, Assessed on November 2011.
47. Dhawan, P. K., Swami, R. K., Mehta, H. S., Bhatnagar, O. P., and Murty, A. V. R. S. (1994), "Bulk Utilization of Coal Ashes from Road Works", Indian Highways, Indian Roads Congress, Vol. 22(11), 21-30.
48. Dongxing, X., Houben, L., Molenaar, A. and Zhonghe, S. (2010), "Cement Treated Recycled Demolition Waste as a Road Base Material", Journal of Wuhan University of Technology-Mater, Vol. 25, 696-699.
49. El-Sayed, M. A. and El-Samni, M. T. (2006), "Physical and Chemical Properties of Rice Straw Ash and Its Effects on the Cement Paste Produced from Different Cement Types", J. King Saud Univ., Vol. 19(1), 21-30.
50. FAOSTAT, http://faostat.fao.org/, Accessed on 10 September, 2012.
51. Ferguson, G. (1993), "Use of self-cementing fly ashes as a soil stabilization agent", Fly ash for soil improvement, Geotechnical Special Publication, No. 36, ASCE, New York, 1–14.
52. Franklin associates, 1998, http://www.fal.com/solid-waste-management.html#municipal. Assessed on February 2012.
53. Furlonge, R. J. (1996), "Road Fatality Modeling in Trinidad and Tobago", Waste Indian Journal of Engineering, Vol. 19 (1), 10-15.
54. Fwa, T. F., Tan, S. A. and Zhu, L. Y. (2004), "Rutting Prediction of Asphalt Pavement Layer Using C – φ Model", Journal of Transportation Engineering, Vol. 130 (5), 675–683.
55. Ganesan, K., Rajagopal, K. and Thangavel, K. (2007), "Evaluation of Bagasse Ash as Supplementary Cementitious Material", Cement & Concrete Composites, Vol. 29, 515–524.
56. Geiman, C. M., Filz, G. M. and Brandon, T. L. (2005), "Stabilization of Soft Clay Subgrades in Virginia", Phase I Laboratory Study Virginia Transportation Research Council.
57. Ghaman, R. S., Owen, L., Zhang, L., VanGorder, R. and Liu, K. (2004), "Advanced Traffic Research Laboratory Development", in the proceedings of IEEE Intelligent Transportation Systems Conference Washington, D.C., USA Conference.

58. Gosavi M., Patil K. A., Mittal S. and Saran S. (2004), "Improvement of properties of black cotton soil subgrade through synthetic reinforcement," IE (I) Journal-CV, Vol. 84, 257-262.
59. Govindarao, V. M. H. (1980), "Utilization of Rice Husk - A Preliminary Analysis", Journal of Science and Industrial Research, Vol. 39(6), 495-515.
60. Hadi, N. A. R. A., Khoury, H. N., Suliman, M. R. (2008), "Utilization of Bituminous Limestone Ash from EL-LAJJUN Area for Engineering Applications", Acta Geotechnica, Vol. 3 (2), 139-151.
61. Han, Y.W. and Anderson, A.W. (1974), "The Problem of Rice Straw Waste: A Possible Feed through Fermentation", Oregon Agricultural Experiment Station, Technical Paper No. 3713.
62. Haque, A., Mujtaba, I. M. and Bell, J. N. B. (2000), "A Simple Model for Complex Waste Recycling Scenarios in Developing Economics", Waste Management, Vol. 20, 625–631.
63. Head, K. H., (1992), "Manual of Soil Laboratory Testing", Vol. 2: Permeability, Shear Strength and Compressibility Tests, New York: Halsted Press, 2nd Edition.
64. Holtz, R.D. (2001), "Geosynthetics for Soil Reinforcement", 9th Spencer J. Buchanan Lecture.
65. Horpibulsuk, S., Rachan, R., Raksachon, Y., Suddepong, A., Chinkulkijniwat, A. (2010), "Analysis of Strength Development in Cement-Stabilized Silty Clay Based on Microstructural Considerations. Construction and Building Materials, Vol. 24, 2011–2021.
66. http://www.docstoc.com/docs/3765459/GEOGRAPHY-Outline-Political-Map-of-India-Identification-only-Major-soil
67. Huang, Y. H. (2004), "Pavement analysis and Design", Second edition, Pearson Prentice Hall, USA.
68. Huang, Y. H., (2004), "Pavement Analysis and Design" Pearson Prentice Hall, Second Edition.
69. Hwang, D., and Witczak, M. W. (1979), "Program DAMA User's Manual, Department of Civil Engineering", University of Maryland, MD.
70. ICAR, Indian Council of Agricultural Research (2010), http://geographyias.blogspot.in/2010/12/indian-soils.html

71. Indian Institute of Sugarcane Research, http://www.iisr.nic.in/services-facilities/statnew.htm. Accessed on date October 2012.
72. Indiana Department of Transportation, (2008), "Design Procedure for Soil Modification and Stabilization".
73. IRC 37 (2001), "Guidelines for the Design of Flexible Pavement", Indian Roads Congress, New Delhi.
74. IRC 37 (2012), "Guidelines for the Design of Flexible Pavement", Indian Roads Congress, New Delhi.
75. IRC: SP: 58 (2001), "Guidelines for Use of fly Ash in Road Embankments", Indian Roads Congress, New Delhi.
76. IS : 2720 (Part 16), (1987), "Methods of Test For Soils, Laboratory Determination of CBR", Reaffirmed 1997, Bureau of Indian Standards, New Delhi.
77. IS : 2720 (Part 40), (1977), "Methods of Test for Soils, Determination of Free Swell Index of Soils", Reaffirmed 1997, Bureau of Indian Standards, New Delhi.
78. IS : 2720 (Part 5), (1985), "Methods of Test for Soils, Determination of Liquid and Plastic Limit", Reaffirmed 1995, Bureau of Indian Standards, New Delhi.
79. IS : 2720 (Part 6), (1972), "Methods of Test for Soils, Determination of Shrinkage Factors", Reaffirmed 1995, Bureau of Indian Standards, New Delhi.
80. IS : 2720 (Part 8), (1983), "Methods of Test for Soils, Determination of Water Content-Dry Density Relation Using Heavy Compaction", Reaffirmed 1995, Bureau of Indian Standards, New Delhi.
81. IS 3812 (1981), "Specification for Fly Ash for Use as Pozzolana and Admixture", Reaffirmed 1999, Bureau of Indian Standards, New Delhi.
82. IS: 1888, (1982), "Method of load test on soils", Reaffirmed 1997, Bureau of Indian Standards, Manak Bhavan, 9 Bahadur Shah, Zafar Marge, New Delhi.
83. IS: 2720 (Part 10), (1991), "Methods of Test For Soils, Determination of Unconfined Compressive Strength", Reaffirmed 1995, Bureau of Indian Standards, New Delhi.
84. IS: 2720 (Part 11), (1993), "Methods of Test For Soils, Determination of Unconfined Compressive Strength", Reaffirmed 1997, Bureau of Indian Standards, New Delhi.
85. IS: 2720 (Part 17) (1986), "Methods of Test for Soils, Laboratory Determination of Permeability", Reaffirmed 1997, Bureau of Indian Standards, New Delhi.

86. IS: 2720 (Part 3) (1980), "Methods of Test for Soils, Determination of Specific Gravity", Reaffirmed 1997, Bureau of Indian Standards, New Delhi.
87. IS: 2720 (Part 4) (1985), "Methods of Test for Soils, Grain Size Analysis", Reaffirmed 1995, Bureau of Indian Standards, New Delhi.
88. Jain, P. K., Chandra, S., and Verma, R. K. (2004), "CBR Values of Stabilized Fly Ash", Indian Highways, Indian Roads Congress, Vol. 32 (9), 15-20.
89. Jha, J. N. and Gill, K. S. (2006), "Effect of Rice Husk Ash on Lime Stabilization", Journal of the Institution of Engineers (India), Vol. 87, 33-39.
90. Justiz-Smith, N. G., Virgo, G. J. and Buchanan, V. E. (2008), "Potential of Jamaican Banana, Coconut Coir and Bagasse Fibres as Composite Materials", Materials Characterization, Vol. 59, 1273-1278.
91. Kamel, M. A., Ali, M. El. and Ajmi, H. M. El. (2011), "Procedure for Quantification and Optimization of Stabilized Subgrade Pavement Materials", International Journal of Advanced Engineering Sciences and Technologies, Vol. 2 (1), 25–35.
92. Kaniraj, S. R. and Havanagi, V. G. (1999), "Compressive Strength of Cement Stabilized Fly Ash-Soil Mixtures", Cement and Concrete Research, Vol. 29, 673–677.
93. Kar, R. K., Pradhan, P. K., Naik, A. (2012), "Plate Load Test on Fiber-Reinforced Cohesive Soil", EJGE, Vol. 17, 633-49.
94. Khobklang, P., Nokkaew, K. and Greepala, V. (2009), "Effect of Bagasse Ash on Water Absorption and Compressive Strength of Lateritic Soil Interlocking Block", Excellence in Concrete Construction through Innovation – Limbachiya & Kew (eds.), Taylor & Francis Group, London, 181-185.
95. Kolias, S., Rigopoulou, V. K., Karahalios, A. (2005), "Stabilisation of Clayey Soils with High Calcium Fly Ash and Cement", Cement & Concrete Composites, Vol. 27 (2), 301–313.
96. Kopperman, S., Tiller, G., and Tseng, M. (1986), "ELSYM5, Interactive Microcomputer Version: User's Manual", Federal Highway Administration, Washington, D.C.
97. Kumar, A., Walia, B. S. and Bajaj, A. (2007), "Influence of Fly Ash, Lime, and Polyester Fibers on Compaction and Strength Properties of Expansive Soil", Journal of Materials in Civil Engineering, Vol. 19(3), 242–248.

98. Kumar, P. and Singh, S. P. (2008), "Fiber-Reinforced Fly Ash Subbases in Rural Roads", Journal of Transportation Engineering, ASCE, Vol. 134 (4), 171-180.
99. Lav, A. H., Lav, M. H. and Goktepe, A. B. (2005), "Analysis and Design of a Stabilized Fly Ash as a Pavement Base Material" World of Coal Ash (WOCA) April 11-15, Lexington, Kentucky, USA.
100. Leite, F. C., Motta, R. S., Vasconcelos, K. L., and Bernucci, L. (2011), "Laboratory Evaluation of Recycled Construction and Demolition Waste For Pavements", Construction and Building Materials, Vol. 25, 2972–2979.
101. Maheshwari, K. V., Desai A. K. and Solanki, C. H. (2011), "Performance of Fiber Reinforced Clayey Soil", Electronic journal of geotechnical engineering EJGE, Vol. 16, 1067-1082.
102. Mahmud, H. B, Chia B. S., Hamid N.B.A.A., (1997), "Rice Husk Ash- an Alternative Material in Producing High Strength Concrete", Proceedings of International Conference on Engineering Materials, Ottawa, Canada, 275-284.
103. Malekzadeh M. and Bilsel H. (2012), "Effect of Polypropylene Fiber on Mechanical Behaviour of Expansive Soils", EJGE, Vol. 17, 55-63.
104. Mallela, J., Quintus, H. V. and Smith, K. (2004), "Consideration of Lime-Stabilized Layers in Mechanistic-Empirical Pavement Design", The National Lime Association.
105. Mandal J. N. and Joshi A. A. (1996), "Centrifuge Modelling of Geosynthetic Reinforced Embankments on Soft, Ground, Geotextiles and Geomembranes", Vol.14, 147-155.
106. Mandey, S. (2011), The Energy and Resource Institute, New Delhi, India.
107. Mantohar, A. S. and Hantoro, G. (1999), "Behavior of Engineering Properties on the Clay Blended with LRHA (Lime Rice Husk Ash)", Research Report for Grant 1999 Muhammadiyah University of Yogyakarta, Indonesia.
108. Marandi, M., Bagheripour, M.H., Rahgozar, R. and Zare, H. (2008), "Strength and Ductility of Randomly Distributed Palm Fibers Reinforced Silty-Sand Soils", American Journal of Applied Sciences, Vol. 5(3), 209-220.
109. Muhanna, A. S., Rahman, M. S., and Lambe, P. C. (1999), "Resilient Modulus Measurement of Fine-Grained Subgrade Soils", Transportation Research Record, No.1687, 3-12.

110. Muntohar, A. S. (2002), "Ultilization of Uncontrolled-Burnt Rice Husk Ash In Soil Improvement", Dimensi Teknik Sipil, DTS, Vol. 4 (2), 100-105.
111. Muntohar, A.S (2011), "Effect of Specimen Size on the Tensile Strength Behavior of the Plastic Waste Fiber Reinforced Soil – Lime – Rice Husk Ash Mixtures", Civil Engineering Dimension, Vol. 13(2), 82-89.
112. Nelson, J. D. and Miller, D. J. (1992), "Expansive Soils, Problems and Practice in Foundation and Pavement Engineering," John Wiley & Sons, Inc, USA.
113. Nicholson P., Kashyap V., & Fuji C. (1994), "Lime and Fly Ash Admixture Improvement of Tropical Hawaiian Soils", Transportation Research Record, No. 1440, 71-78.
114. Noor, M. J. M. M., Aziz, A. A. and Suhadi, R. U. R. (1993), "Effect of Cement-Rice Husk Ash on Compaction, Strength and Durability of Melaka Series of Lateritic Soil", The Professional Journal of the Institution Of Surveyors Malaysia, Vol. 28(3), 61-67.
115. Nunes, M. C. M. and Dawson, A. R. (1997), "Behavior of Some Pavement Foundation Materials Under Repeated Loading", Transportation Research Record, No.1577, 1-9.
116. Ola, S. A. (1975), "Stabilization of Nigeria lateritic soils with cement, bitumen and lime", Soil Mechanics and Foundation Engineering, Proceeding 6th Reg. Confrence Africa, Durban, South Africa, 145-152.
117. Olawale, O. and Oyawale, F. A. (2012), "Characterization of Rice Husk via Atomic Absorption Spectrophotometer for Optimal Silica Production", International Journal of Science and Technology, Vol. 2(4), 210-213.
118. Osinubi, K. J. (1998), "Permeability of Lime-treated Lateritic Soil", Journal of Transportation Engineering, Vol. 124, 465-469.
119. Osinubi, K. J. and Katte, V. Y. (1997), "Effect of Elapsed Time After Mixing on Grain Size and Plasticity Characteristics; Soil Lime Mixes", Nigeria Soc. Engin. Tech. Trans., Vol. 32 (4), 65-76.
120. Osinubi, K. J.; Amadi, A. A.; and Eberemu, A. O. (2006), "Shrinkage Characteristics of Compacted Laterite Soil-fly Ash Mixtures. NSE Technical transaction, Vol. 41, 36-48.
121. Osinubi, K.J., Bafyau, V, and Eberemu, A.O. (2009), "Bagasse Ash Stabilization of Lateritic Soil", Appropriate Technologies for Environmental Protection in the Developing World, Springer, 271-280.

122. Osinubi, K.J., Ijimdiya, T.S., and Nmadu, I. (2009), "Lime Stabilization of Black Cotton Soil Using Bagasse Ash as Admixture", Advanced Materials Research, Vol. 62-64, 3-10.
123. Ozkul, Z. H. and Baykal, G. (2007), "Shear Behavior of Compacted Rubber Fiber-Clay Composite in Drained and Undrained Loading", Journal of Geotechnical and Geoenvironmental Engineering, Vol. 133 (7), 767-781.
124. Pal, M. (2012), "Effect of Rice Husk Ash on Unconfined Compressive Strength of Soil", International Journal of Engineering Research and Technology, Vol. 5 (2), 191-196.
125. Panda, M. and Mazumdar, M. (1999), "Engineering Properties of EVA-Modified Bitumen Binder for Paving Mixes", Journal of Materials in Civil Engineering, Vol. 11(2), 131-137.
126. Pappua, A., Saxenaa, M. and Asolekar, S. R. (2007), "Solid Wastes Generation in India and their Recycling Potential in Building Materials", Building and Environment, Vol. 42, 2311–2320.
127. Pateriy, I.K. and Patil, K. A. (2006), "Stabilization of Soil Subgrade with Polypropylene Fibres", Grameen Sampark Prdhanmantri Gram Sadak Yojana, 22-26.
128. Petkovic, G., Engelsen, C. J., Haoyad, A. O., and Breedveld, G. (2004), "Environmental Impact from the Use of Recycled Materials in Road Construction: Method for Decision-Making In Norway", Resources, Conservation and Recycling, Vol. 42, 249–264.
129. Phanikumar, B. R., and Radhey, S. S. (2004), "Effect of Fly Ash on Engineering Properties of Expansive Soil", Journal of Geotechnical and Geoenvironmental Engineering, Vol. 130 (7), 764-767.
130. Piyatrapoomi, N., Kumar, A., Robertson, N. and Weligamage, J. (2004), "Reliability of optimal intervals for pavement strength data collection at the network level", In: The 6th International Conference on Managing Pavements, 19-24 October, Brisbane, Australia.
131. Piyatrapoomi, N., Kumar, A., Robertson, N. and Weligamage, J. (2003), "A Probability-Based Analysis for Identifying Pavement Deflection Test Intervals for Road Data Collection", In : the International Conference on Highway Pavement Data Analysis and Mechanistic Design Application, 7-10 September, Columbus.
132. Prabakar, J., Dendorkar, N. and Morchhale, R. K. (2004), "Influence of Fly Ash on Strength Behavior of Typical Soils, Construction and Building Materials, Vol. 18, 263–267.

133. Prasad D.S.V., Kumar M.A. and Raju G.V.R. P. (2010), "Behavior of Reinforced Sub bases on Expansive Soil Sub grade", Global Journal of Researches in Engineering, Vol. 10(1), 2-8.
134. Prasad, D. S. V., Raju, G. V. R. P. and Kumar, A. (2009), "Utilization of industrial waste in flexible pavement construction", Electronic Journal of Geotechnical Engineering EJGE, Vol. 13, 1-12.
135. Prusinski, J. R. and Bhattacharja, S. (1999), "Effectiveness of Portland Cement and Lime in Stabilizing Clay Soils", Transportation Research Record, No. 1652, 215-227.
136. Punith, V. S. and Veeraragavan, A. (2011), "Characterization of OGFC Mixtures Containing Reclaimed Polyethylene Fibers", Journal of Materials in Civil Engineering, Vol. 23 (3), 335–341.
137. Punthutaecha, K. (2002), "Volume Change Behaviour of Expansive Soils Modified with Recycled Materials," Ph.D. Thesis, The university of Texas at Arlington.
138. Puppala A. J. and Musenda C. (2000), "Effects of Fiber Reinforcement on Strength and Volume Change In Expansive Soils," Transportation Research Record, No. 1736, 134-140.
139. Puppala, A, J., Ramakrishna, A. M., and Hoyos, L. R. (2003), "Resilient Moduli of Treated Clays from Repeated Load Triaxial Test", Transportation Research Record, No.1821, 68-74.
140. Ramachandra, T. V. and Saira, V. (2004), "Exploring Possibilities of Achieving Sustainability in Solid Waste Management", Indian Journal of Environmental Health, Vol. 45 (4), 255–64.
141. Ranasinghe and Arjurna, P. (1993), "Use of Rice Straw as Pozzolana", Master Thesis No. St-85-1, Asian Institute of Technology.
142. Rao, V. V. L. K., Lakshmy, P., Senguta, J. B. and Gangopadhyay, S. (2009), "Polyester fiber Waste As Reinforcing And Mixture in Concrete for use in Road works", New Building Material & Construction World, Vol.15, No.6, 174-187.
143. Ravi Shankar, A. U. and Suresha, S. N. (2006), "Strength behaviour of geogrid reinforced shedi soil subgrade and aggregate system", Road Materials and Pavement Design an International Journal (RMPD), 313-330.

144. Ravi Shankar, A.U., Mithanthaya, I. R., Bhavanishankar Rao, N. and Ganesh, C. (2010), "Fatigue Behaviour of Lateritic Soil Stabilized with Enzyme", International Journal for Civil Engineering –Research India Publications, Vol. 5, 2595-2608.
145. Sadrnejad, S. A., Ghanizadeh, A. R. and Fakhri, M. (2011), "Evaluation of Three Constitutive Models to Characterize Granular Base for Pavement Analysis using Finite Element Method", Australian Journal of Basic and Applied Sciences, Vol. 5(7), 778-786.
146. Sahoo, U. C., Reddy, K. S. and Pandey, B. B. (2006), "Structural Evaluation of a Concrete Filled Cell Pavement", IJPEAT, UK, Vol. 7 (1), 1-10.
147. Schroeder, R. L. (1994), "The Use of Recycled Materials in Highway Construction", Federal Highway Administration, Public Roads, Vol. 58(2).
148. Seco, A., Ramirez, F., Miqueleiz, L. and Garcia, B. (2011), "Stabilization of Expansive Soils for Use in Construction", Applied Clay Science, Vol. 51, 348–352.
149. Seed, H.B., Chan, C.K., (1966), "Clay strength under earthquake loading conditions", Journal of Soil Mechanics and Foundry Engineering Division, ASCE, Vol. 92, 53–78.
150. Sengupta, J. (2002), "Recycling of Agro-Industrial Wastes for Manufacturing of Building Materials and Components in India. An Over View", Civil Engineering & Construction Review, Vol. 15 (2), 23–33.
151. Senol, A., Edil, T. B., Bin-Shafique, M. S. Acosta and Beason, C. H. (2006), "Soft Subgrade Stabilization by Using Various Fly Ashes", Journal of Resources Conservation and Recycling, Vol. 46 (4), 365-376.
152. Shafique, S. B., Rahman, K., Yaykiran, M. and Azfar, I. (2010), "The Long-Term Performance of Two Fly Ash Stabilized Fine-Grained Soil Subbases", Resources Conservation and Recycling, Vol. 54, 666–672.
153. Sharp, R.W. and Booker, J.R., (1984), "Shakedown of Pavements under Moving Surface Loads", Journal of Transportation Engineering, ASCE, Vol. 110(1), 1–13.
154. Shen, D.H. and Du, J.C. (2004), "Evaluation of building materials recycling on HMA permanent deformation", Construction and Building Materials, Vol. 18, 391–397.
155. Shirazi, H. (1999), "Field and Laboratory Evaluation of the Use of Lime Fly Ash to Replace Soil Cement as a Base Course", Transportation Research Record, No. 1652, 270-275.

156. Show, K. Y., Tay, J. H. and Goh, A. T. C. (2003), "Reuse of Incinerator Fly Ash in Soft Soil Stabilization", Journal of Materials in Civil Engineering, ASCE, Vol. 15 (4), 335-343.
157. Shrivastava, S. and Chini, A. (2009), "Construction Materials and C&D Waste in India", Conference on construction material Stewardship - Lifecycle Design of Buildings System and Material, Conference Proceeding, 72-76.
158. Singh, H.P. Sharma, A.and Chanda, N. (2011), "Study of Strength Characteristics of Coir-Fiber Reinforced Soil", Proceedings of International Conference AMTID, NIT Calicut, 1-9.
159. Singh, N.B., Singh, V.D., Rai S. (2000), "Hydration of Bagasse Ash-Blended Portland Cement", Cement and Concrete Research, Vol. 30, 1485-1488.
160. Sivapullaiah, P. V. (1996), "Pozzolanic Stabilization of Expansive Soils, Expansive Soils: Recent Advances in Characterization and Treatment", Taylor and Francis Group, London.
161. Sobhan, K. and Mashnad, M. (2003), "Mechanical Stabilization of Cemented Soil–Fly Ash Mixtures with Recycled Plastic Strips", Journal of Environmental Engineering, ASCE, Vol. 129(10), 943–947.
162. Soni, D. K. and Jain, A. (2008), "Effect of Freezing-Thawing and Wetting-Drying on Tensile Strength of Lime-Flyash Stabilized Black Cotton Soil", Proc. of 12th International Conference of International Association for Computer Methods and Advances in Geomechanics (IACMAG), Goa, India, 2285-2291.
163. Soutsos, M. N., Tang, K. and Millard, S. G. (2011), "Concrete building blocks made with recycled demolition aggregate", Construction and Building Materials, Vol. 25, 726–735.
164. Srinivasan, R. and Sathiya, K. (2010), "Experimental Study on Bagasse Ash in Concrete", International Journal for Service Learning in Engineering, Vol. 5(2), 60-66.
165. Taneerananon, P. and Somchainuek, O. (2005), "Bus Crash Situation In Thailand: Case Studies", Journal of the Eastern Asia Society for Transportation Studies, Vol. 6, 3617 – 3628.
166. Tishmack, J. K., Peterson, J. R. and Flanagan, D. C. (2001), "Use of Coal Combustion By-Product to Reduce Soil Erosion", International Ash Utilization Symposium, Center for Applied Energy Research, Kentucky.

167. Unnikrishnan, N., Rajagopal, K. and Krishnaswamy, N.R. (2002), "Behaviour of Reinforced Clay under Monotonic and Cyclic Loading", Geotextiles and Geomembranes, Vol. 20, 117–133.
168. Vegas, I., Ibanez, J.A., Cortazar, L. S. and Frías, M. (2011), "Pre-Normative Research On The Use Of Mixed Recycled Aggregates In Unbound Road Sections", Construction and Building Materials, Vol. 25, 2674–2682.
169. Warren, H., and Dieckman, W. L. (1963), "Numerical Computation of Stresses and Strains in a Multiple-Layer Asphalt Pavement System", International Report, Chevron Research Corporation, Richmond, CA.
170. Wattanasiriwech, S., Wattanasiriwech, D. and Svasti, J. (2010), "Production of Amorphous Silica Nanoparticles from Rice Straw with Microbial Hydrolysis Pretreatment", Journal of Non-Crystalline Solids, Vol. 356, 1228–1232.
171. Wayne, A. C., Mohamed, A. O. and El-Fatih, M. A. (1984), "Construction on Expansive Soils in Sudan", Journal of Construction Engineering and Management, Vol. 110 (3), 359-374.
172. Werkmeister, S. (2003), "Permanent Deformation Behaviour of Unbound Granular Materials in Pavement Constructions", Doctor Thesis, Technical University of Dresden, Germany.
173. Winterkorn, H. F. and Pamukcu, S. (1990), "Soil Stabilization and Grouting", Foundation Engineering Handbook, 2nd Edition, Van Nostrand Reinhold, New York.
174. Xuan, D. X. L., Houben J. M., Molenaar, A. A. A. and Shui, Z. H. (2011), "Mixture Optimization Of Cement Treated Demolition Waste With Recycled Masonry And Concrete", Materials and Structures, Vol. 3, 57-62.
175. Yadu, L., Singh, D. and Tripathi, R. K. (2011), "Strength Characteristics of Rice Husk Ash Stabilized Black Cotton Soil", Proceedings of International Conference on Advances in Materials and Techniques for Infrastructure Development, NIT Calicut, India, 1-6.
176. Yoshizawa, S., Tanaka, M. and Shekdar, A. V. (2004), "Global Trends in Waste Generation. In: Recycling, Waste Treatment and Clean Technology", TMS Mineral, Metals and Materials Publishers, Spain, 1541-1552.
177. Zaharieva, R. H., Dimitrova, E., Bodin, F. B., (2003), "Building Waste Management in Bulgaria: Challenges and Opportunities", Waste Management, Vol. 23, 749–761.

178. Zhang, M. H. and Malhotra, V. M. (1996), "High Performance Concrete Incorporating Rice Husk Ash as a Supplementary Cementing Material", ACI Mater J., Vol. 93 (6), 629-636.

179. Zia, N. and Fox, P. J. (2000), "Engineering Properties of Loess–Fly Ash Mixtures for Road Base Construction", Transportation Research Record, No. 1714, 49-56.

LIST OF PUBLICATIONS

INTERNATIONAL JOURNAL

1. **Aditya Kumar Anupam**, Praveen Kumar and G. D. Ransinchung R. N. (2012). "Analysing the suitability of Waste Materials for Road Construction" International Journal on Science and Technology Review (IJSTR), Vol. 1, No. 1, pp 69-75.

2. G. D. Ransinchung R. N., Chauhan Arun Prakash, **Aditya Kumar Anupam** and Praveen Kumar (2012). "Influence of moisture content on use of recycle aggregate in PQC" International Journal of Global Technology Initiatives, Issue 1, pp A8-A15.

3. **Aditya Kumar Anupam**, Praveen Kumar and G. D. Ransinchung R. N. "Performance Evaluation of Structural Properties for Soil Stabilized Using Rice Husk Ash" Road Materials and Pavement Design, Taylor & Francis, (Accepted).

4. **Aditya Kumar Anupam**, Praveen Kumar and G. D. Ransinchung R. N. "Evaluation of Strength Characteristics of Clayey Soil Modified Using Bagasse Ash for Subgrade Pavement Construction" Journal of Civil Engineering and Management, Taylor & Francis, SCEM-2013-0205 (Communicated).

NATIONAL JOURNAL

1. G. D. Ransinchung R.N., Praveen Kumar, **Aditya Kumar Anupam** and Pooja Sharma, "Evaluation of Efficacy of Fines Obtained from Demolished Concrete Slab as a Soil Stabilizer". The Indian Road Congress (IRC), (Revised Manuscript Submitted).

2. G. D. Ransinchung R.N., Praveen Kumar, Brind Kumar, **Aditya Kumar Anupam** and Arun Prakash Chauhan, "Laboratory Evaluation for the Use of Moorum and Ganga Sand in Wet Mix Macadam Unbound Granular Base Course" The Indian Road Congress (IRC), (Revised Manuscript Submitted).

3. **Aditya Kumar Anupam**, Praveen Kumar and G. D. Ransinchung R. N. "Laboratory Study on Performance of Various Agricultural and Industrial Waste Materials in Road Construction" Indian Road Congress (Communicated).

4. Praveen Kumar, G. D. Ransinchung R. N., and **Aditya Kumar Anupam, "**Use Of Fine Grained Waste Materials in Highway Construction – A Review." Indian Road Congress (Communicated).

5. Shashi Kant Sharma, G.D. Ransinchung R.N., Praveen Kumar and **Aditya Kumar Anupam**, "Fiber Reinforced Cement Composites-A Review" The Indian Road Congress (IRC), (Revised Manuscript Submitted).

INTERNATIONAL CONFERENCE

1. Praveen Kumar and G. D. Ransinchung R. N., **Aditya Kumar Anupam** "Laboratory Evaluation to Study the Engineering Behavior of Slag Cement for Soil Subgrade" International Conference on 2nd NUiCONE Institute of Technology, 8-10 December, 2011, Nirma University, Ahmedabad.

2. **Aditya Kumar Anupam**, Praveen Kumar and G. D. Ransinchung R. N. **"**A Comparative Study Of Sugar Cane Bagasse Ash & Fly Ash For Use In Pavement Construction" International Conference on Highway Engineering April 18-20, 2012, Bangkok, Thailand.

3. **Aditya Kumar Anupam**, Praveen Kumar and G. D. Ransinchung R. N. **"**Permeability study on fly ash and rice husk ash admixes with subgrade soil for pavement construction" International conference on advance in architecture and civil engineering, AARCV, June 21-23, 2012, Bangalore.

4. **Aditya Kumar Anupam**, G. D. Ransinchung R. N., and Praveen Kumar **"**Influence of recycled fines obtained from demolished concrete slabs for use in pavement quality concrete construction" 25th ARRB Conference – Shaping the future: Linking policy, research and outcomes, Perth, Australia 2012.

5. **Aditya Kumar Anupam**, Praveen Kumar and G. D. Ransinchung R. N. **"**Influence of rice husk ash and fly ash on strength behaviour of subgrade soil for pavement construction" International conference on transportation planning & implementation methodologies for developing countries, December 12-14, 2012, Indian Institute of Technology Bombay.

6. **Aditya Kumar Anupam**, Praveen Kumar and G. D. Ransinchung R. N. **"**Laboratory Study on Permanent Deformation Behaviour of Soil Admixed with Bagasse Ash under Repeated Triaxial Loading" Indian geotechnical conference (IGC-2012) Advances in Geotechnical Engineering, 13 - 15 December, 2012, Indian Institute of Technology Delhi New Delhi, India.

7. **Aditya Kumar Anupam**, Praveen Kumar and G. D. Ransinchung R. N. "Application of Fiber as Reinforcement for Pavement Construction- A Critical Appraisal" 2nd International Conference on Evolution In Science & Technology & Eyne On Educational Methodologies (ESTEEM), March 3-4, 2013, PPIMT Hisar, India.

8. **Aditya Kumar Anupam**, Praveen Kumar and G. D. Ransinchung R. N. "Influence Of Time Variation On Admixed Soil Swelling Properties" 2nd International Conference on Emerging Trends in Engineering and Technology, April 12-13, 2013, TMU Moradabad, India.

NATIONAL CONFERENCE:

1. **Aditya Kumar Anupam**, Praveen Kumar and G. D. Ransinchung R. N. "Stabilizing the subgrade soil with slag cement – A laboratory study" Advances in Mechanics and Materials RAMM-2012, 25-26 February 2012 VSS University of Technology, Burla, Odisha, India.

2. Praveen Kumar, G. D. Ransinchung R. N., and **Aditya Kumar Anupam** "Application of industrial and agricultural waste materials for highway construction" Twenty Eight National Convention of Civil Engineers, 12-14th October 2012, Institution of Engineers, Roorkee Local Centre.

3. **Aditya Kumar Anupam**, Praveen Kumar and G. D. Ransinchung R. N. "Improvement of Soil Swelling Potential Using Fly Ash And Rice Husk Ash." National Conference on Geotechnical and Geoenvironmental Aspects of Wastes and Their Utilization in Infrastructure Projects GGWUIP, February 15 – 16, 2013, GNE college and IGS Ludhiana Chapter, Ludhiana, India.

4. Praveen Kumar, G. D. Ransinchung R. N., and **Aditya Kumar Anupam** "Waste Materials - An Alternative to Conventional Materials in Rural Road Construction" Workshop on Non-Conventional Materials/ Technologies, CRRI New Delhi, National Rural Roads Development Agency, Ministry of Rural Development, Government of India, 18th February, 2012.